A Matrix Theory of Constrained Network Flow for Sustainability Assessment: Case Study of Waiheke Island Water Resource

Sungsoo Koh

A thesis submitted in fulfillment of the requirements

for the degree of Doctor of Philosophy

Department of Civil and Environmental Engineering

University of Auckland, September 2014

ABSTRACT

This thesis developed a matrix based, mathematical theory for constrained network flow for a novel sustainability assessment metric. The predominant environmental modelling frameworks discussed in industrial ecology, namely footprint analysis, input-output analysis, and LCI, share a common mathematical structure. These frameworks, which aim to establish quality databases, can accurately calculate the total environmental impact of a regional system or industrial process in terms of the quantity of resource extraction and waste/pollutant emissions. This thesis explores an alternative use for these frameworks, by introducing the concept of constraints to the established computation methods. Abovementioned framework can be generalised to a matrix based system of linear inequations, which is similar to linear programming. In contrast to the usual linear programming problems, such as trying to find the optimal solution, the framework focusses on the geometry and volume of the feasible space enclosed by sustainability constraints. In this thesis, the volume of the feasible space is conceptually connected to Bossel's (1999) accessibility space and can define a metric to express sustainability. Collecting data in regard to the sustainability constraints is the key driver for the proposed theory and has to be accumulated from external studies of physical and social models. Case studies of constraints found in various components of the water resources system in Waiheke Island provided the demonstration of the matrix based constrained network theory and the sustainability metric. The case study showed that the water resource carrying capacity for the island using current infrastructure setting with RWH, aquifer pumping, onsite wastewater treatment is 21300, with land use being limiting factor. Introduing greywater reuse to the island increased the carrying capacity to 31900 and introduction of SWRO did not have large impact on the carrying capacity but provided flexibility on water resource management and thus improved optimal population level from 14000 to 20000.

ACKNOWLEDGEMENT

I would like to express thanks to my main supervisor, Dr. Carol Boyle for all the guidance and encouragements. Throughout my Ph.D. years, my family was there for me with patience. Especially my wife, Jiyun, I cannot thank enough. My parents and parents in law supported me with prayers and words of advice. I am indebted to them greatly. I will not forget the financial help from parents of both families in the time of needs.

My senior in our research group, Gaya helped me with proofreading the manuscript. Reginald Samuel in Auckland Council helped me getting necessary GIS data and have access to the Council resource consent files hidden deep in the archives.

Abbreviations

ARC Auckland Regional Council
BEA U.S. Bureau of Economic Analysis
DEM Digital Elevation Model
EEIO Environmentally Extended Input-Output Analysis
EF Ecological Footprint
EIO-LCA Economic Input-Output Life Cycle Assessment
EXIOPOL Environmental Accounting Framework Using Externality Data and Input-Output Tools for Policy Analysis
FFD First Flush Diverter
GDP Gross Domestic Product
GHG Greenhouse Gas
GIS Geographical Information System
IO Input-Output
IOT Input-Output Table
LCA Life Cycle Analysis
LCC Life Cycle Cost
LCI Life Cycle Inventory
MFA Material Flow Analysis
MRIO Multi-Regional Input-Output
NAMEA National Accounting Matrix with Environmental Accounts
NPISH Non-Profit Institutions Serving Households
NPP Net Primary Production
NZ New Zealand
PIOT Physical Input-Output Table
RWH Rainwater Harvest System
SAM Social Accounting Matrix
SEEA System of Environmental-Economic Accounting
SNZ Statistics New Zealand
SUT Supply-Use Table
SWRO Seawater Reverse Osmosis
TDML Total Daily Maximum Load
TN Total Nitrogen
WF Water Footprint
YAS Yield-After-Spillage

Table of Content

Chapter 1 Introduction

1.1 Rise of Quantitative Sustainability Models

1.1.1 Global Sustainability Challenge

Humans have become a natural force that influences both the physical and biochemical dynamics of the surface of the earth. Human society now appropriates 23% of the world bioproduction (Haberl et al., 2007) and 30% of the accessible flow of water (Postel, Daily, & Ehrlich, 1996). Forests are being cleared at a rate of 130,000 km^2 per year for the last 15 years, and 15% of ocean fish stocks were depleted in the same period (Galli et al., 2012). Every day, 400 TWh equivalent of primary energy is being consumed (BP, 2014; IEA, 2013), 100 million tonnes of CO_2 are being emitted to the atmosphere (Olivier, Janssens-Maenhout, Muntean, & Peters, 2013), and 190 million tonnes of material is being extracted from the environment (Giljum, Dittrich, Lieber, & Lutter, 2014). With 7 billion people living and increasing, the influence of human species will only increase further if the current lifestyle continues.

Evidence for a planet-wide destruction of the ecosystem is compelling. With massive natural resources appropriation away from ecosystem and habitat modification, we are witnessing the greatest rate of species' extinction in history (UNEP, 2007). The destruction and degeneration of the environmental system will ultimately harm human society. The human society is embedded in the ecosystem and the natural environment in terms of material and energy flow. Our daily lifestyles and the industrial systems that support them assume stable environmental conditions. Many of the primary industries and livelihood of communities rely on many

ecological services such as pollinations, climate regulation, and food regeneration (Costanza et al., 1997). With the decline of the capacity of ecological services, it is likely that the human society will suffer the consequences. The reduction of fish catch, global warming, the change of habitat, alteration of habitat through development, loss of topsoil, air and water quality degradation and loss of biodiversity are just a few example of such evidences. There are many reported cases of sudden, non-linear, tipping point responses of ecosystems to a gradual increase in environmental pressure (i.e. sudden regime shift following gradual response). The ecosystem responses are difficult to predict and adapt to (Lade, Tavoni, Levin, & Schlüter, 2013; Lenton & Williams, 2013; Scheffer, Carpenter, Foley, Folke, & Walker, 2001).

Above mentioned environmental concerns resulted in environmentalism and the sustainability movement; two distinct but similar movements. Environmentalism (a.k.a. the Green movement) and sustainability both advocate the conservation of natural systems but have different ultimate goals. Natural Habitats (2009) contrasts the difference between the two: "Environmentalism consists of a social movement regarding environment conservation and preservation that strives to persuade or induce the political acceptance process by lobbying, activism as well as education for protecting natural resources and eco-systems. It aims to control pollution and protect biodiversity by focusing on balancing the various natural systems by becoming more earth friendly." On the other hand, "Sustainability, in contrast to the environmentalism, represents the idea that human society should operate by utilizing industrial and biological processes that can be sustained indefinitely." The ultimate focus of environmentalism is the conservation of the natural environmental system itself, but the focus of sustainability is in maintaining the operation of human society indefinitely. Current industrial processes rely heavily on depletable non-renewable resources, and its renewable ecological resource pools

are becoming exhausted due to heavy exploitations. Both resource pools will become exhausted if the current industrial business-as-usual practices are to continue. Because human society relies on the environmental system, the goals of environmentalism become necessary strategic steps in order to sustain the operation of human society. However, human society has to undergo a severe transformation to depart from the current trajectory of environmental destruction. Despite its anthropogenic reasons, environmental protection is the best option for our society to ensure its well-being in a long term.

1.1.2 Quantitative Sustainability Models

There were several quantitative models that tried to address key sustainability issues. Quantitative models describe the relationships between the underlying variables of the human society-environmental system and they can also be used to predict the behaviours of the systems. These predictions can help form strategies towards the sustainability goal, which is to transform the human society to be operated and maintained indefinitely and harmoniously with the environmental base system.

The simplest one is the IPAT equation (Ehrlich & Holdren, 1971). IPAT equation is a conceptual equation trying to describe the factors determining the total environmental impact of human society. It states that the total environmental impact is the multiplication of population, affluence, and technology, where affluence is a measure of the material standard of living, and technology is the environmental efficiency to achieve such material standard for the population. This model provides the basis for three strategies to reduce the environmental impact, associated with reducing three controlling factors respectively; the reduction of population, lowering material requirement per person, and improving technological efficiency are all valid

strategies in reducing the total environmental impact of human society.

Another interesting model, the World3, was developed by Meadows (1972), following the Malthusian conceptualisation of the population. It utilised a time-dependent simulation framework called system dynamics, developed by Forrester (1969). It modeled the world as five main interacting subsystems; population, non-renewable resources, agriculture, industry, and pollution. Each subsystem had a number of interacting variables, which are conceptualised as linked stock-flow variables and are represented as a system of ordinary differential equations. The parameters were calibrated to the actual statistics at the time of development. The model predicted the famous overshoot and collapse pattern of the population, agriculture, and industry, sometime in the mid-21st century. It raised many interests and critiques regarding the issues of overpopulation and resource depletion problems. One critique was the assumption of constant technology, which assumed that the industry relied only on non-renewable resources. The model was revised 30 years later (Meadows, Randers, & Meadows, 2004) to include updated statistics, newly developed recycling technology, and the global climate change. The characteristic overshoot and collapse pattern persisted in the updated model, demonstrating that the pattern is essential in the current industrial-agricultural-population system arrangement that is embedded in the finite world.

Another quantitative modeling paradigm is the indicator framework. Indicators are the selection of variables that represents the state and orientation of the system. Indicators are often used as a guide for policy decisions to identify the trend and effectiveness of policy implementations. There is no one-fits-all indicator set, and the choice of indicators depends on the interests of the users (e.g. analyst, policy makers, grassroots group, the general public). The indicator sets are used to track the trend of the critical variables for reporting purposes.

Within the field of sustainability indicators, there was an interesting concept proposed, called choice space (Potschin & Haines-Young, 2008), and it formed a conceptual basis for the theory presented in this thesis. Among the different types of indicators (e.g. 5 types of indicators defined in DPSIR frameworks, as outlined in Hák, Moldan, & Dahl (2007)), state variables provide information about the condition of the system at a given time. The indicators provide critical information on the historical evolution and the future projection of critical variables. This information can be used to support evidence-based decision-making process and provide the basis for environmental accounts (UNEP, 2012).

What is more important than a simple projection of the indicator values is the value judgement of whether the projection is an acceptable one. The determination of judgement criteria called limits, are determined from the scientific recognition of system behaviours, public consensus, or precautionary guideline for minimum safety standard. They are in place so that the danger of collapse or significant damage is not extreme, given the presence of uncertainty and environmental variability (Potschin & Haines-Young, 2008). These limits form acceptable ranges of the state of environments and society conditions. Potschin & Haines-Young (2008) named the region of acceptable environmental and social condition sustainability choice space, because the region acts as a "room that we have for manoeuvre in designing our different policy options." (Potschin & Haines-Young, 2008). These acceptable ranges for the variables were proposed to change over time depending on the external condition of the environment, and the acceptable ranges of the variables appear in a region in a time-series graph (Figure 1.1). If the trajectory of the critical variables wanders beyond the boundary of the sustainability choice space, the trajectory is classified as unsustainable. They argue that management policies have to be changed if the trajectory is to to move outside the sustainability choice space.

Unfortunately, this idea was only described in qualitative terms and no concrete quantitative analysis was conducted.

This idea is fundamental to the idea of sustainability, and independent authors came up with the same idea in different literatures. In the discussion of the multi-disciplinary quantitative indicator system, Mayer (2008) briefly mentions a similar conceptual diagram with the indicator trajectory (Figure 1.2). In Mayer's diagram, the region of sustainability is defined in a higher dimensional variable-time space, and if the trajectory moves beyond the boundary of acceptable variable values, the trajectory is classified as not sustainable.

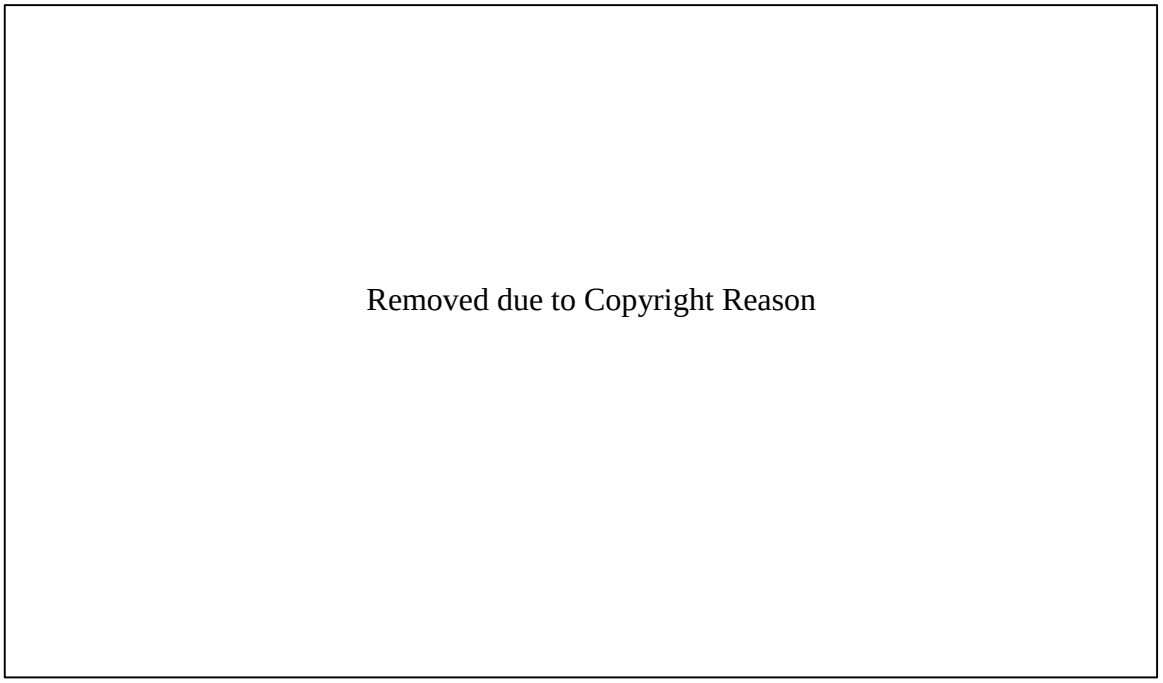

Figure 1.1 Sustainability Choice Space Model from Potschin & Haines-Young (2008).

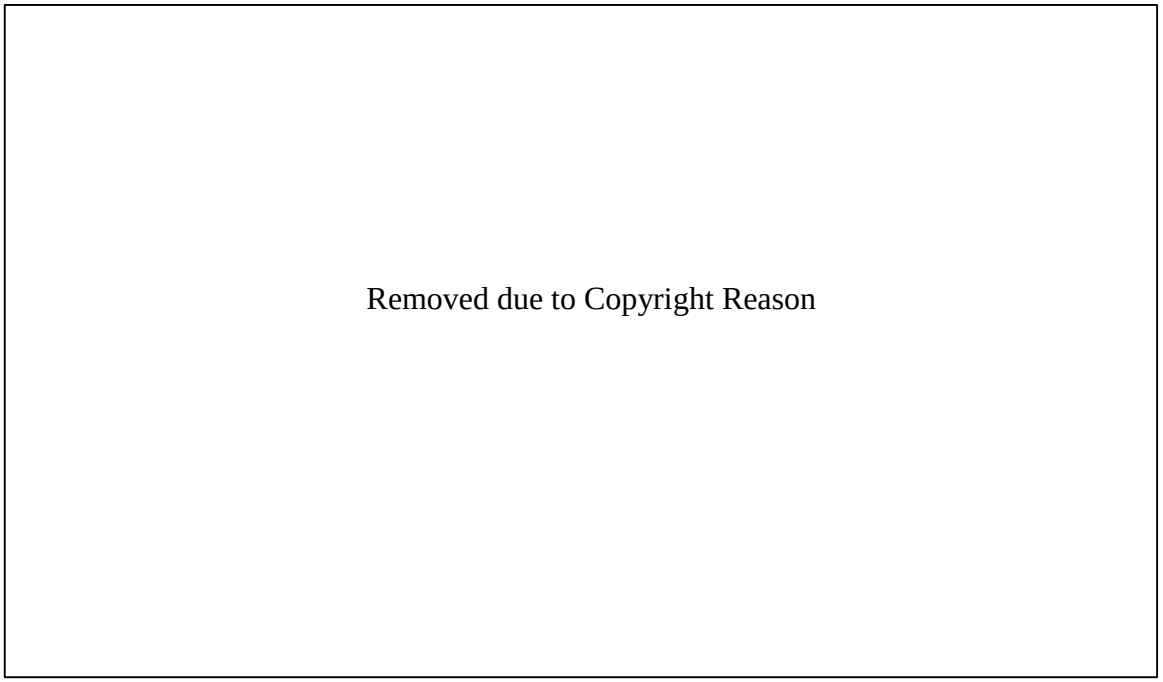

Figure 1.2 Sustainable State Indicator Trajectory depicted by Mayer (2008).

Gallopín (2003) presented a phase space diagram for dynamic critical state indicator sets for the human-environmental system. He defined "safe ranges" as the acceptable region of sustainability indicators, in a box-shaped region in the phase space. An example of an unacceptable region in phase space ("incompatible with life") is depicted in Figure 1.3. The focus of his work was on the dynamic nature of the society-environment system. Some regions in the phase space will have repulsive dynamics resulting in inaccessible domains, where the laws of dynamics of the society-environment system simply keeps the systems off from the phase space region. On the other hand, some regions in the phase space have attractive dynamics resulting in metastable regions. The natural systems are known to be homeostatic and tend to stay within certain environmental variable ranges; this is an example of the so-called attractive region. When human intervention is large enough to push away the system

coordinate outside the boundary of the attractive region, the system coordinate will stray away from the previous region. Thus he names the attractive regions “catastrophic domains”. As a concept, once the dynamic regions on the phase space is known, it is possible to plan ahead so that human interventions does not lead to environmental destruction. The difficulty is identifying the systems of dynamic equations itself, which is the most challenging problem for complex society-environmental systems. Again this framework conceptually suggests the existence of acceptable/unacceptable regions of the system conditions.

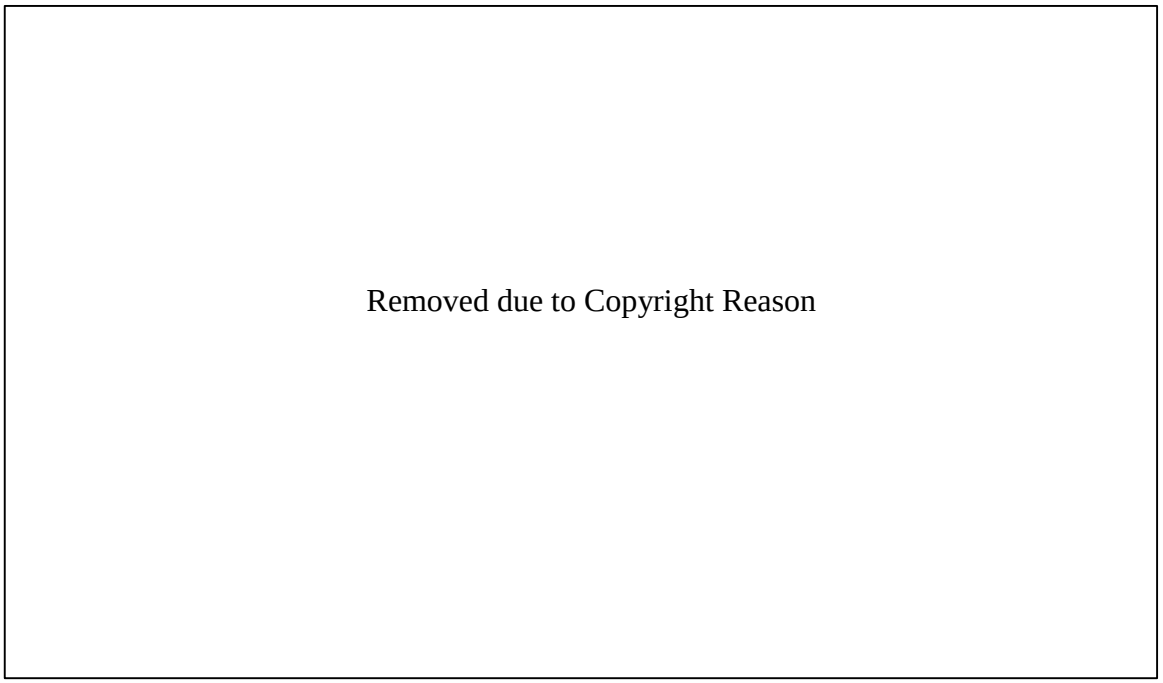

Figure 1.3 Phase Space Diagram for Sustainability Indicators by Gallopín (2003). The vertical and horizontal axis represents human and natural system variables respectively. The figure was taken directly from the literature. The vertical axis represents the conceptual aggregate of variables associated with human systems and the horizontal axis represents the conceptual aggregate of the variables associated with natural environmental systems.

Bossel (1999) also introduced the idea of an accessible space of indicators in his discussion about the systematic method of choosing appropriate variables for sustainability indicator sets. The time trajectory of these indicators represents the evolution of the society and its natural habitat. In the discussion, Bossel identifies nine types of constraints that may define the course of society development. They are:

- **Laws of nature** Laws of nature create restrictions in what dynamics the system can take. For example, the minimum nutrient requirements for plant growth, or the maximum energy efficiencies of thermal processes provide the basis of the restrictions for the system development from an initial condition.
- **Physical environment** The limitations of the global planetary environment such as available space; waste absorption capacity of soils, rivers, oceans, atmosphere; availability of renewable and non-renewable resources; soil fertility and climate provide constraints for human society growth.
- **Solar energy flow and Material resource stocks** Ultimately, renewable energy is limited by the rate of solar energy flux that can be captured and used by plants and technology. All material resources are limited as stocks but will be limited by the rate of recycling.
- **Ecological Carrying capacity** This constraint is related to the appropriation of the ecological carrying capacity by human. In the long term, it is limited by the photosynthetic productivity of a region, which is determined by the resource (nutrient, water, light) that is 'in the minimum' (Liebig's Law; limiting factor). Humans can partially, and only temporarily, overcome the carrying capacity of a region by bringing

in critical resources from other regions. Eventually, as the resource becomes scarcer in other regions, this transfer would have to stop.

- **Human actors Human capital** The fifth set of constraints is related to the capacity of human creativity and ingeneity. Societies which are more innovative, have a better educated and trained population, provide a diverse and open-cultural environment, thus have a greater accessibility space left than others. Society with more human capital will experience freedom of choice in terms of how they can innovate and how they can adapt to the changes.
- **Human organisations, culture, technology** This constraint is related to the capability of the society as a whole because of their arrangement and technological implementation. Existing human organizations, cultural and political systems, available and possible technology and its systems, constrain the accessibility space.
- **Ethics and value** Ethical standards, behavioural or cultural values, and norms of a given society limit the choices that it can take. This introduces the seventh set of constraints.
- **Role of time** This constraint is related to the lagging time of any changes made by society. For example, building infrastructure, or introducing a new technology, or cleaning water in groundwater passage, or restoring soil fertility, or stopping population growth, all takes time.
- **Role of evolution** Sustainable development implies constant evolutionary, self-organizing, and adaptive change. This constraint is related to the adaptive capacity of the human system by having diversity. Lack of diversity and alternative options mean

a higher chance of catastrophic failure in the time of sudden pressure. The available spectrum of diversity is the ninth set of constraints identified by Bossel.

These nine types of constraints were represented as c1 to c9 in the Figure 1.4. He recognised that there are numerous constraints that restrict societal development and these constraints "reduces the total range of future theoretical possibilities, leaving only a limited, potentially accessible set of options", which he called the accessibility space (Bossel, 1999). In the end, two most constraining constraints bind the accessibility space (Figure 1.4). The location of constraints changes over time, and the constraints that bind the accessibility space may change to different ones.

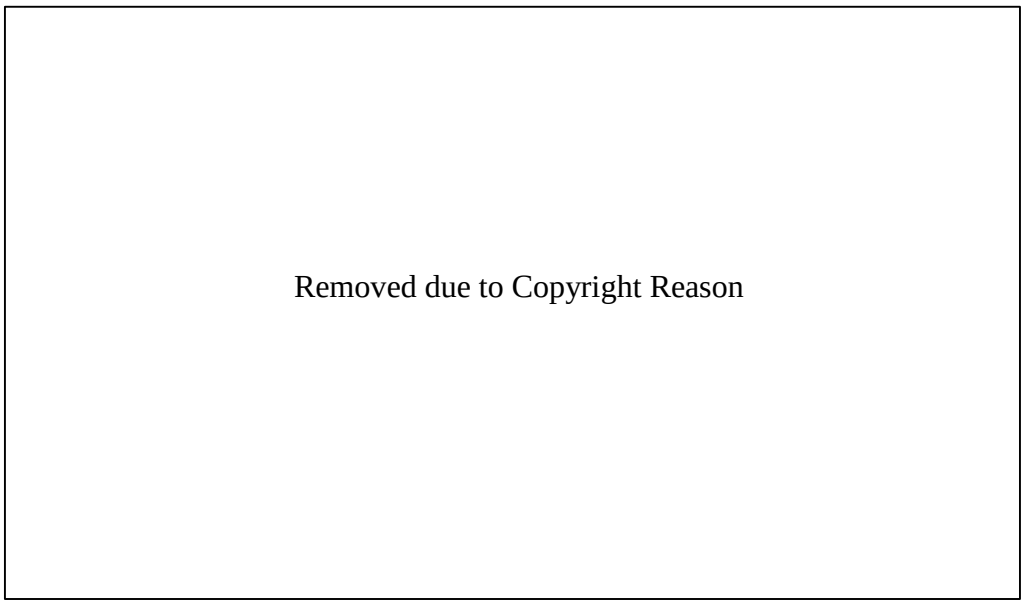

Figure 1.4 Accessibility space concept in Bossel (1999).

The common attributes of the abovementioned literature, regardless of their independent development, is that they are all defined on an axis. The authors all had a quantitative implication of the concepts. The problem was that the application of the concept is very difficult,

being a quantitative intensive procedure - sustainability concepts are very broad and requires lots of data accumulation for the concept to work in reality.

The abovementioned literature on sustainability space, defined as acceptable state variable ranges, are left with a conceptual framework only (or proposals for further research). The main trend in the sustainability research field has shifted away from the quantitative approach to implement the sustainability range space concepts. The probable reason for this may be due to the difficulty of establishing the scientific ground of the limits of the quantitative indicators that support the concepts. The concept has great potential; in order for the concept to work, there is a need to understand the specific application area and the estimation procedures for the constraint work. The abovementioned conceptual frameworks do not refer to the specific application of the concept, and thus there is no mention of the spatial and temporal extent of the systems - they are only abstract ideas only. This thesis begins from this gap in the literature by exploring how these concepts could be applied in a real life situation. Thus the key contribution is the concrete mathematical framework that implements the abovementioned concept, and a real life application to demonstrate the use of the framework.

1.1.3 Data-driven Models for Sustainability

Recently, a large number of publications in the areas of data-intensive modeling of society-wide metabolism and material flows have appeared (Fischer-Kowalski et al., 2011; Kennedy et al., 2010; Kenway, Gregory, & McMahon, 2011; Niza, Rosado, & Ferrao, 2009). Progress in material flow modeling is staggering, both in terms of the amount of data and the refinements made to methodologies in the empirical society-environment system modeling frameworks. The coupled empirical society-environmental models are possible because of the similarity

between the two systems - they have many components exchanging material and energy where the exchanges are represented by networks of flows (Suh, 2005). These models are created and reported as a national or regional dataset so that they can be used as the underlying model for creating extended models that answer the specific interests of analysts.

The prominent modeling frameworks intensely developed over the last two decades are a family of footprints, Environmentally Extended Input-Output (EEIO) Analysis and Life Cycle Analysis (LCA). Their methodologies are in the process of integration (Suh et al., 2004; Tukker et al., 2009; Wiedmann, 2009b) for complementarity and completeness. These studies now derive their dataset from national statistics and extension specific environmental databases that are intended for technical level modeling. The scope of the studies range from a local, factory level case studies to regional, national, and international level. These models can comprehensively account for the total material flows at detailed disaggregated levels in terms of the industry and commodity types. These models are promising tools that can enhance the science of sustainability with the support of extensive empirical data and concrete methodologies at a greater depth and detail. This thesis will use the mathematical framework these tools provide to build the matrix based theory.

1.1.4 Delineating the Constraints Quantitatively

Among the many issues involved in sustainability, the biophysical constraint for society's growth is the oldest, and the most important issue (Graedel & Voet, 2010; Rockström et al., 2009). The finiteness of resource for human society was initially investigated under the term, carrying capacity (Daily & Ehrlich, 1992). Its definition is taken from the field of ecology, which is the maximum population that can be supported by nutrient availability and

environmental conditions.

The concept of carrying capacity is one of the core themes of sustainability. However, it cannot be computed directly because of the complexity in the material-energy exchange between human society and the environment. The operation of human society requires the import of various material goods and energy, which are harvested from the environment, and its operation creates unavoidable waste emissions to the environment. Expressing the capacity or environmental constraint using a single variable called carrying capacity is an over-simplification. Each type of resources and waste emission category will have its capacity or limits. Constraints on the critical resources, such as land area, biocapacity, energy, water, mineral resources, and pollutant assimilation capacity have been studied case by case until the emergence of recent research initiatives that investigate the interaction and combined effect of these critical constraints towards the society (Graedel & Voet, 2010). More detailed review of the studies of constraints is made in Chapter 2.

1.2 Research Motivation and Approach

Quantitative studies of sustainability reviewed in the previous section are parts of a jigsaw puzzle that show particular aspects of sustainability. These fields have been developed independently, but the trend in integrated modeling is emerging in the sustainability research field. There is a huge research opportunity, and the gap waiting for the outlined concepts above to be integrated into a single coherent framework.

1.2.1 Integrating Multicommodity Flow Network and Constraints

Society draws multiple resources from the environment and there already exists tools that

model multi-resource flows in the coupled society-environmental system (Section 1.1.3 and Section 2.3). There have been many empirical works done that estimate various types of constraints for the society and the environmental systems (Section 1.1.4 and Section 2.2).

Although the society resource flow modeling frameworks provide a way to describe detailed interlinks among compartments of the society and the environmental systems, traditionally, these material and energy flow models were used to calculate the magnitude of the total environmental impact that the society creates to maintain its economic throughput. The calculated environmental impacts are usually used to compare the environmental performance of alternative policy strategies or product designs promoting the reduction in environmental impact per service (Section 2.3).

A new approach to the way the calculated environmental impacts from the material flow models is proposed in this thesis. The calculation results can be compared with the sustainability constraints to gain insight into how close the current situation is to the environmental capacity to support our society.

These environmental capacities or sustainability constraints are estimated in different fields, reported independently from one system and another. There has been no particular coordination on the decision of which system or what flow quantity should be investigated (Section 2.2). The material flow models can act as an integration framework for organising the constraints, not only as a repository for collecting constraints for a database, but also as a system-level model that identify how these constraints estimated in different disciplines interact. This concept is visualised in Figure 1.5. The material flow model for the society represents the environmental impacts in terms of the quantity of extracted/utilised primary resources, and

waste emission to the environment (Section 2.3). The material flow models account for the multiple types of resources and emissions concurrently, using a matrix formulation that will be described in Chapter 3.

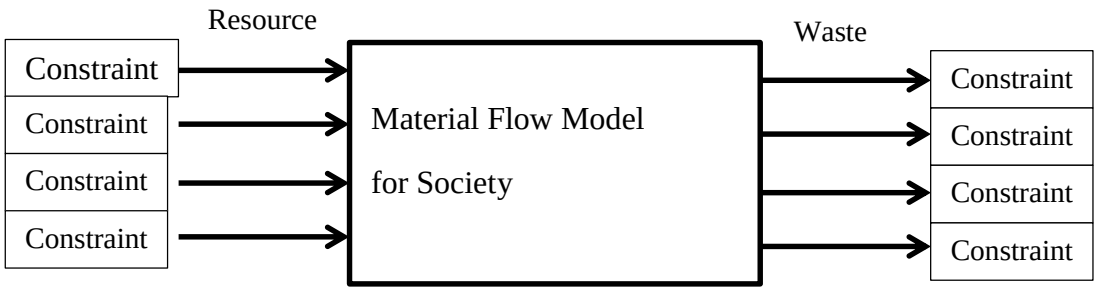

Figure 1.5. Integration of Material Flow Models and Constraints Concept. Multicommodity flow models can organise the results of individual environmental constraint studies by binding them using flow quantities.

1.2.2 Defining Sustainability Measure

Comparing the environmental impact to the known environmental constraints quantitatively gives a measure of absolute sustainability (Faber, Jorna, & Van Engelen, 2005). Absolute sustainability is a term used in contrast to relative sustainability. The absolute sustainability concept was one of the fundamental ideas in the early years of sustainability literature. However, because of the difficulty in estimating the constraints, an alternative approach, the relative sustainability concept was created. The contrast between the two is related to the goal of sustainable development (Faber et al., 2005). While relative sustainability aims to *improve* the society-environmental system with respect to key performance indicators, absolute sustainability aims to *operate* the society-environmental system *within acceptable bounds* (as discussed in Section 1.1.2). Gradual improvements in environmental performance promoted

by the relative sustainability concept have been important contributors towards the vision of achieving sustainability, they do not necessarily achieve the goal of sustainability, which can only be defined by the absolute sustainability concept (Benn, Dunphy, & Griffiths, 2006; Jerneck & Olsson, 2008; Kemp & Rotmans, 2005; Moors, 2006).

One of the purposes of developing the proposed theory was to create a measure for absolute sustainability, which is the "distance" between the coordinate of current system condition and the space of unsustainability (see Figure 1.1 – 1.4 for visual context). This measure of absolute sustainability can determine if a given system is sustainable without reference to its historic paths. A snapshot of the system orientation is all the information the measure will need in order determine if the system is in a sustainable orientation.

1.4 Study Scope.

The application of the theoretical framework was scoped to estimate the supportable population for Waiheke Island. There are many other constraining aspects that may prohibit the infinite growth of the population and economy on the island. However due to limitation in expertise, only the water resources constraints are investigated to demonstrate the use of the theoretical development. Further constraints can be added to refine the results identified in the thesis. One of such example is given by comparing the effect of different constraints giving rise to a different estimation of the maximum population supported within the resource endowed on the island.

1.5 Thesis Outline

The thesis consists of two parts. The first part, consisting of Chapters 2 to 3, develops the

mathematical theory of the constrained multi-commodity flow network. The second part, consisting of Chapter 4 to 6, is the application of the theory, which is a case study of the growth potential of the water resource in Waiheke Island.

Chapter 2 reviews two fields of active research, which are to be incorporated into the unifying mathematical frameworks; they are constraint science and industrial ecology (the research field where material flow modeling is studied) as they were introduced in Section 1.1.4 and 1.1.3 respectively. In the constraint science section, the origins of various sustainability constraints and quantitative works of sustainability constraints are reviewed. In the industrial ecology section, the mathematical structure underlying three similar network based methods are reviewed. The lack of interdisciplinary studies between these two fields is pointed out, which the thesis aims to fill (Section 2.4).

Chapter 3 develops the matrix theory of the constrained multi-commodity flow network. The multi-commodity flow network models the society-environmental system as a network of numerous agents that exchange multiple types of commodities. Each agent is a process that takes in multiple commodity flows and outputs different multiple commodity flows. These agents are modeled as a node in the network. The theory of multi-commodity network adopts the open system, a modularised approach for an easy extension for the future development of the model. The theory development begins with a simple model which gradually becomes complex. At the end of the chapter, the core analysis tool for the absolute sustainability is proposed; a metric for options space volume. This metric measures how much freedom is available in organising the multi-commodity network. Losing the ability to sustain the flow network, otherwise called sustainability, is depicted as losing options. As constraints become more strict (e.g. losing biodiversity or the depletion of resources), the arrangement options for

the flow network gets reduced to the point where no arrangement of the network agent will give a sustainable flow arrangement. Therefore, if there is evidence for the decrease in the freedom of choice, it can be considered that the system is heading towards unsustainability. This metric also gives an idea of how close the system is to the point of unsustainability.

Chapter 4 begins the application of the case study. It provides an overview of the water resource issues for Waiheke Island and also the conceptual network model for the island. It furthermore provides the estimation of the technical coefficients. This estimation is later used to formulate the final model in Chapter 6.

Chapter 5 provides the rationale for the constraints estimation that is used in Chapter 6. The constraint factors for growth of the five technologies are considered; (1) roof-top rainwater harvest systems, (2) groundwater bores, (3) onsite wastewater capacity, (4) greywater potential and (5) seawater reverse osmosis. Several other factors of production, such as land area, electricity and financial capacity are also considered in this chapter.

Chapter 6 collects the total estimation of constraints from Chapter 4 and 5 and combines them into the matrix framework of the multi-commodity flow network. It demonstrates how the matrix framework may be used in real-life case studies. It showcases two important tools to analyse the sustainability measure: the size and orientation of the sustainability option space.

Chapter 7 is the concluding chapter; it outlines the limitations of the model and the developed theory, along with future directions.

Chapter 2 Literature Review

2.1 Introduction

The key element of sustainability explored in this thesis is the concept of constraints and their interdependence. Human society must operate within the acceptable boundaries that safeguard its continued operation. However, both the needs of human society and the dynamics of the environment evolve over time; thus it has been strongly suggested that the understanding of complex systems is needed in order to define the constraints or limits of the systems involved properly. The central methodological approach to understanding complex systems is the systems approach that considers the entire complex system as interactions of smaller systems.

Human society utilises numerous resources for industrial production, involving multiple types of primary extractive industries and emissions across almost every activity ranging from production to consumption. The field of industrial ecology focusses on quantitative flow-based models among economic and industrial agents in society, and provide valuable integration tools for systems involving multiple types of resources and sinks. Industrial ecology tools have been the driving force behind the improvement in environmental efficiency by providing measures of environmental performance of interlinked industrial systems in the form of detailed databases and structured assessment models (Ayres & Ayres, 2002). The databases and assessment tools have been very valuable in increasing the efficiency of production and waste management systems in terms of fostering cleaner production and recycling strategies. Nevertheless, these tools do not explicitly address the issue of constraints.

This review chapter is structured into three parts, each dedicated to the respective research

questions:

(1) What is the current level of development in methodologies and theories for sustainable constraints imposed on human society? What are the gaps in research directions?
(2) What is the state of the science in the industrial ecology modelling tools? How can they be utilized to address the shortcomings found in the constraints-based carrying capacity concept?
(3) Were there previous efforts to investigate the constraints in the networked system? Are the results of these efforts suitable for the sustainability analysis involving multiple resource constraints?

Section 2.2 overviews the science of sustainability constraints, with respect to the types of constraints found in the society-environmental system in particular. How and where the sustainability constraints arise are discussed, along with the directions of previous research and the difficulties faced in the field. This is a preliminary effort in forming systematic feeds into the proposed theory of constrained network theory in Chapter 3, considering that the theory needs to be multidisciplinary, providing a way to join data from different disciplines.

Section 2.3 reviews three industrial ecology tools that provide the mathematical basis of the proposed constrained network theory. These include footprint, input-output analysis and Life Cycle Inventory Model (LCI). In the recent years, more and more cross-disciplinary research is produced across these three analysis tools, one of which is used to fill in the data gaps in others (B. R. Ewing et al., 2012; Finnveden et al., 2009). This is natural because they share similar mathematical frameworks which are based on the matrix computation that will be discussed in the review. The reason they share the similarity in the computation is that they all

represent a material or energy flow among networked agents and networks, which are best represented using matrices. The common features of computational structure are summarised in this section and further developed in chapter 3 for the proposed theory.

2.2 Constraints Science

The fundamental issue of sustainability is the imbalance between the basic physiological and psychological requirement of humanity, defined as needs, and the availability of resources to meet those requirements, otherwise known as capacities. This issue has been captured in the famous definition of sustainable development: ″the development that meets the needs of current generation while not compromising the ability of future generations to meet their own needs″ (WCED, 1987). This statement lies upon an implicit precondition that the finite nature of the environmental and physical resources, if over-exploited to satisfy the current generation′s needs and desires, will eventually diminish the future generations′ share of finite resources. This is particularly true for non-renewable resources, where consumptive production would eventually mean the exhaustion of the resources. It is obvious that the tapping of the renewable resources have to be well managed so that their renewal capacity is not compromised.

2.2.1 Types of Constraints

The most pessimistic sustainability argument shares the philosophical thoughts of Malthus, who noted that the exponential growth of population cannot be supported by the growth of agricultural yields. This was derived from the observations of food shortages in his era, which was overcome by the green agricultural revolution of 20th century. Many are still concerned if the human race is going to face catastrophic carrying capacity issues.

Humans share a common resource pool with the rest of the ecological system. The notion of carrying capacity based on food supply gained popularity again in late 20th century (Daily & Ehrlich, 1992). Many works were trying to conceptualise what carrying capacity was (Goodland & Daly, 1996). Daly (1996) proposed a criteria for environmental sustainability in terms of renewable and non-renewable resource pools as (Goodland, 2002):

(1) Harvest rates of renewable resources (e.g. forestry, fishery, agriculture) must be kept within the regenerative capacities of the natural system;
(2) Waste emissions should be kept within the assimilative capacity of the local environment, without unacceptable degradation of its future waste absorptive capacity or other important services; and
(3) Depletion rates of non-renewable resources should be set below the historical rate at which renewable substitutes were developed by human invention and investment according to the Serafian quasi-sustainability rule.

This definition is based on the material flow rates of the resources, i.e. the extraction rates and emission rates. Indeed, the quantitative determinations of the rate based constraints are most frequently found in literature. However, there are two more classes of constraints found in literature – they are stock constraints, mostly dealing with the non-renewable stocks estimated to be remaining, and condition constraints which are based on the state variable of the environments. Thus, there are three classes of constraints found in the literature.

2.2.1.1 Flow-based Constraints

The human society requires multiple types of resources for its operation, and thus one way of defining its operating space is through a study of its resource availability (Graedel & Voet,

2010). The material flows from the environment to the human society gives some guide to which materials and what quantity are currently sustaining the human society operation. The material flow analysis studies done over the past decade or so have now established the country-by-country database globally (Behrens, Giljum, Kovanda, & Niza, 2007; Schandl & Eisenmenger, 2006). For example, the global extraction of the material was estimated at 55 billion tons in 2002 with the percentage share of 29%, 42%, 10%, 19% for fossil fuels, metals, other minerals and biomass respectively (Behrens et al., 2007). There is abundant information in regard to the resource constraints of the valuable resources.

Fossil fuels and other mineable minerals have a high economic value, and their production is sensitive to the economy. There is evidence of peak oil which is caused by the cost rise to extract oil from the ground (Sorrell, Speirs, Bentley, Brandt, & Miller, 2010). However, there is a technological response to the rise of costs and also the venture towards employing new technology is becoming profitable. For example, the exploration and extraction of shale gas and fracking is gaining attention as a new source of oil but they are associated with number of social and environmental problems that limits its application (Hutton, 2012). The utilisation of fossil fuel is restricted by another constraint, greenhouse gas emission. The point here is that the determination of the minable resources requires economic considerations − more on the stock constraint estimation for depletable resources.

The constraints for the harvest of biomass is considered with two measures; net primary production and ecological footprint. Net primary production (NPP) is a measure of photosynthesis by the plant species and it is estimated globally that human appropriation of the net primary production was estimated to exceed 23% (Haberl et al., 2007). In some regions of

the world, human appropriate more than 100% of NPP, meaning the biomass stocks are being depleted in these areas. For the regions with appropriation exceeding 100% of NPP, the existing amount of the biomass (e.g. forest mass) form a stock constraint and the dynamics will follow similar pattern as non-renewable mineral resources. In the period of 1913 to 2005, the appropriation of NPP has doubled and in the worst-case scenario, it is projected that the NPP appropriation may rise to 44% by 2050 (Krausmann et al., 2013). By then, more regions will be devastated by such high proportion of extraction. Ecological footprint is another measure of the human use of the planetary regeneration capacity, which is measured in terms of the effective land and sea areas to support biological production. It initially began with the attempt to measure the land area needed for food production (Rees, 1992), but soon expanded its scope to general types of land use appropriation for human purposes. It was attempted to expand to cover all types of produced goods and human activities but later found that some of the human necessities do not strictly relate to land areas and thus the scope of the ecological footprint has been limited to land use categories only (Kitzes & Wackernagel, 2009). There is debate on the validity of the double counting of land area as carbon sinks and vegetation growths. These led to the development of additional types of footprints, namely carbon and water footprints. These footprints provide a way to compare human activity and the natural capacity.

The potential of individual energy sources is being investigated and reported; for example, hydropower potential (H. Huang & Yan, 2009), solar power potential (Fluri, 2009; Hang, Jun, Xiao, & Junkui, 2008), wind power potential (Archer & Jacobson, 2005), and geothermal potential (Balat, 2006; Bertani, 2012) are being studied. Photovoltaic cell is constrained by not on the availability of sunlight or the area needed for the installation, but by the costs, environmental impact, and the availability of the material needed to create PV cells (Fthenakis,

2009). The limitation of conventional photovoltaic cells was known to be bound by the availability of the rare earth elements rather than the abundantly available solar energy (Andersson, Azar, Holmberg, & Karlsson, 1998; Fthenakis, 2009). In the world of renewable energy, the installed capacity and the potentials play two critical constraints for the energy production of a particular technology. Expanding the installed capacity would require significant investment and is associated with environmental impact. Geothermal power potential depends on the geological activity of the areas, and there are existing methodologies to estimate for specific world regions (Balat, 2006). There are established statistics for the deployment of geothermal energy in world regions as well (Bertani, 2012). While the estimates for the installed capacity are well tracked ~~of~~, the information about the potential for different energy types is uncertain because of the economic nature of the energy infrastructure development.

In addition to resource constraints, the dataset for emission limits and threshold studies are also well established. The studies into emission limits are organised by chemical species. For example, Sheppard (2002) discusses the ecotoxicity thresholds for atmospheric ammonia. The total maximum daily load (TMDL) is another framework that provides estimates of the tolerable amount of pollutants for a given water basin (Benham et al., 2006; Borah et al., 2006; Miller, 2002; Wang & Keller, 2009). However, these studies require in-depth modelling of the target environment and datasets established by the accumulation of case-studies.

2.2.1.2 Stock-based Constraints

The constraints of non-renewable resource availability are better defined as remaining stock quantities than flow quantities. Many metal minerals reserves are defined as stock availability. Tolerable soil erosion (Verheijen, Jones, Rickson, & Smith, 2009) is another stock type

environmental constraint. The production limits of non-renewable resources are accounted using the concept of peak resources, following the increase of the cost of production. The economic control makes the identification of limits for non-renewable difficult. The ongoing discovery of new sources and processes to enlarge the reserves of minerals and fossil fuels continues to fan the inconclusive debate on when the depletion of non-renewable resource will happen.

Recycling technology improves the conditions of non-renewable resources sustainability. It increases the availability of the mineable minerals for society by reusing the existing materials for production. This includes rubber, plastics, and metals, which are used for durable goods. The stocks within the society are defined and estimated to be the potential for the resources. New concepts are being developed to understand the potential of the available usable stocks and the economic viability for the recovery of used stocks. Urban mining looks for electronic devices that have a higher concentration of precious metal than the raw ores found in mines (Brunner, 2011) - this is because the natural mine is being exhausted. Landfill recovery for material is another effort. Recycling and reuse are incorporated in estimating the resource available for society. Even though the recycling initially works as a supplementary resource that alleviate the requirement for the stock resource mining of non-renewable mineral, it is expected that the output of the recycling mineral will become dominant over the mining of the minerals. The constraints that define the throughput of the recycling technology are the installation level of the recycling facility and the collection efforts.

What is interesting is that the distinction between the stock and flow constraints becomes blurred when the recycling becomes more dominant over raw mined mineral uses. In the regime where the dominant source of mineral is non-renewable mining sources, the recycling is only

a supplementary and the society is considered stock constrained. As the recycling process become more prevalent (which is the case in today) and the proportion of the recycled material usage becomes larger, the society becomes more reliant on the resource flow generated by the recycling facility and collection capability. This dual source problem cannot be addressed using traditional concept of stock and flow based constraint. This is the exactly the case where the system representation of multiple technology becomes useful. This mineral technology can be considered as mix of two distinct technologies, one with stock constraint (mining-refinery technology) and the other with flow constraint (collection-recycle technology). The interaction of these different constraints through the network of resource flow is the exact topic that is going to be addressed by the framework that is going to be developed in this thesis.

2.2.1.3 State-based Constraints

More recent advancements include comparing the global ecological footprint to the biocapacity of the planet, (Moore, Cranston, Reed, & Galli, 2012; Niccolucci, Tiezzi, Pulselli, & Capineri, 2012) and estimating the human appropriation of natural resources compared to the total natural resource endowment (Haberl et al., 2007; A. Y. Hoekstra, 2009; Postel et al., 1996).

An earlier and widely adopted way of quantifying sustainability is the indicator framework, as promoted by Agenda21 (UN, 1992) and subsequently utilised in Global Environmental Outlook (GEO)-series (the latest versions; UNEP, 2007, 2012). The indicator framework was created to support policy decision making and awareness building (Ness, Urbel-Piirsalu, Anderberg, & Olsson, 2007; Singh, Murty, Gupta, & Dikshit, 2009), hence they are aimed to provide science-based quantitative narratives. The choice and interpretations of the indicator

values are often subjective to the investigators and publishers, and there is no standard method of determining if the given indicator values indicate sustainability. Typical uses of indicators include spatial comparisons to identify hotspots, or temporal comparisons to identify the trend of environmental conditions, i.e. to identify whether the system is improving or declining, thus providing information on relative sustainability (for description of relative vs absolute sustainability, see Faber et al., 2005). While relative sustainability information provides illuminating awareness of the situation, more information is needed to guide the policy targets - the absolute sustainability criteria. What is needed is the absolute sustainability criteria that will determine if the given system state is truly sustainable. According to Lancker & Nijkamp (2000), ″a given indicator does not say anything about sustainability unless a reference value such as thresholds is given to it″. This motivates further studies on the thresholds or the targeted acceptable sustainability condition. Progress in studies of correct target thresholds will improve how indicators are used to make decisions to safeguard the society from an unsustainability collapse.

2.2.2 Nature of Constraints in Complex Systems

A sudden regime shift in the ecological condition after an increase in stress is a well-known phenomenon (Scheffer et al., 2001). The environmental system is resilient; it tries to restore back to the previous condition when an external force is applied to push it from the original condition. Degradation of the environment accumulates over time; the accumulation occurs not on the apparent condition but to the capacity of the underlying mechanism that provides the reduction in resilience. When there is a shock to the system that lacks a resilience property, a

sudden shift of regime occurs. Once the dynamic quality of the ecological system has shifted to another condition, the resilience condition now tries to be at the new metastable condition (Holling, 1996). According to the catastrophe theory, a non-linear S-shaped bifurcation separation curve develops in the space between the pressure and response variables. This creates a sudden drop in the response variable, even though the pressure variable was increased incrementally. This contrasts with the current managerial dose-response paradigm of ecological management adopted by many governmental agencies. From observations that indicate many complex systems have evolved and organised to operate at homeostasis, Holling′s resilience theory focuses on the ability of the adaptive system to absorbs external shocks. This property is called resilience where external disturbances may change some variables, but the overall qualitative dynamics stay unchanged in such systems.

Instances of tipping point behaviours are well-documented at a local and regional scale (Scheffer et al., 2001), but it is still debated if a similar pattern will be followed at global scale (Lenton & Williams, 2013). Tipping point is formally defined as ″a point at which a small perturbation can cause a qualitative change in the future state of a system″ (Lenton et al., 2008). In order for a global level tipping behaviour to occur, the transition from local to global tipping must be explained. For this to happen, various tipping elements must have strong enough connectivity forming a network so that they can produce ″domino dynamics″ (Lenton & Williams, 2013). The research in this direction is novel with ongoing debate and theoretical progression. Of course global-level tipping point events have occurred in the past but they were rare. For example, the ″Great Oxidation″ of the atmosphere occurred 2.4 billion years ago, and glaciations occurred 720 million and 640 million years ago (Lenton & Williams, 2013).

Further research is called for to examine the connectivity of the economic trade links, physical links and adaptation/evolutionary processes in a complex ecosystem and planetary geo-processes.

The general pattern of the tipping point is a build-up followed by a collapse, thus called tipping, along with evidence of these events happening in the ecosystem (Schellnhuber, 2010), economic systems (Baharumshah & Lau, 2007), and a combination of both (Lade et al., 2013). A proposal of the measure of the early warning signal to collapse based on the catastrophe theory (Scheffer et al., 2009) is gaining the recognition.

Rockström et al. (2009) popularised the notion of the planetary boundary for human operation space − they renewed attention to the global sustainability problems associated with human appropriation and tolerable emission limits at a global level. These are defined as the tolerable level to prevent ecological collapses and tipping point behaviours.

Such cascade collapse and interactions among collapsible agents are being addressed in literature. Regional-level ecological collapses are reported in literature, but a global-scale collapse has not yet been seen. Current argument lies in the strength of the connectivity among the regional ecoregions, and on how strongly they are related in the event if one ecoregion fails. This strength is yet unknown and is subject to open research.

Scientific studies such as coupled climate models often involve highly sophisticated integrated models requiring vast computational resources, which creates a barrier to development. Research and modelling of dynamic linkages among economic, industrial and environmental systems are still being carried out, although the need for research was recognised as early as

the 1970s (e.g. Meadows, 1972).

Abstract mathematical models, both hypothetical and applied, which create these collapse patterns, are being proposed. For example, the cascading effect that leads to the catastrophic shifts is considered (Kinzig et al., 2006) and integrated ecological threshold behaviour is modelled and studied in a ecological-human coupled system (Horan, Fenichel, Drury, & Lodge, 2011).

Flow and stock-based constraints are typically determined by the resource availability. On the other hand, state-based constraints and complex system thresholds are typically associated with the environmental assimilation capcity of waste and pollutant emissions. Determination of resource availability is relatively easier than determination of the environmental assimilation capacity of pollutants. This is because the response dynamics of the environmental system is complex and only elaborate predictive models can provide when and how the threshold behaviours will occur. For example, the earth climate models designed to determine target levels of CO_2 emission are complex and difficult to work with. Estimation of state-based constraints, emission based constraints will be more difficult than resource availability constraints because the investigators must understand how the system evolves including identification of threshold points of the system. Estimating constraints for the emissions will always involve the modelling of the response dynamics of the environmenal systems, which are largely complex. The case studies appearing at chapter 5 demonstrated this difficulty, where constraints were estimated from elaborate models.

2.3 Industrial Ecology Material Flow Models

Industrial ecology has been developed with the goal of quantifying the flow relationship among industrial bodies, following the analogies of the ecological system (Ayres & Ayres, 2002). The industrial bodies can range from individual processes to economic sectors, depending on the scopes and purposes of the studies. The society-environmental material and energy exchange flows can be modelled by multi-commodity flow network, with the links representing the flow of commodities of different types, and the nodes representing the economic and environmental processes that consumes and transforms the commodities.

Industrial ecology modelling tools provide an excellent foundation for integrating the interactions between multiple resources, processes and trade interactions. They feature tools that explicitly model the flows and stocks of society, supported by structured databases of coefficients. Among many tools developed in the field of industrial ecology, input-output analysis, footprint analysis and Life Cycle Inventory (LCI) address the multi-commodity flows and can be reduced down to a common matrix based mathematical structure. This common matrix-based structure forms the basis of our thesis′ theory development.

2.3.1 Footprints

Footprint accounting estimates the quantity of primary resource and total emission required to create a particular product or to sustain a lifestyle of an average person in a country. There are a number of footprint accounts developed so far (Wiedmann, 2009a), with the names designating the final impacts, which can be the total quantity of the resources or emissions. Other footprints are water, carbon, energy and footprints of various air emission chemicals

(Wiedmann, 2009a). Ecological, water and carbon footprints have standard methodologies for international comparison and data compilation (B. Ewing, Reed, Galli, Kitzes, & Wackernagel, 2010; Arjen Y. Hoekstra, Chapagain, Aldaya, & Mekonnen, 2011; ISO, 2013).

The computed total primary resources/emissions are to be compared with estimates of the resource-specific capacities, in the case of ecological and water footprints, so that the level of human appropriation can be recognised. Footprint account has two components: footprint account and capacity account. The most famous tool that addresses the carrying capacity is the footprints. Ercin & Hoekstra (2012) expresses the research needs in estimating the maximum allowable GHG concentration, freshwater availability and waste assimilation capacity per catchment areas, which are designed to supplement various footprint accounts. They also recommended constructing a way to translate the global-scale capacity to carbon and water footprint**.**

The core data required for a footprint account are the conversion factors from the various consumption activities of human society, to the amount of primary resources and emission required. For example, the ecological footprint relies on the agricultural yield data from FAOSTAT, which is a conversion factor for the amount of food production in tonnes to land areas in ha (Galli et al., 2007). Carbon footprint utilises the studies of annual carbon capture potentials for various land types (Cucek, Klemes, & Kravanja, 2012); and water footprint utilises the accumulated studies of water uses of various crops (Arjen Y. Hoekstra & Mekonnen, 2012).

There is recent effort made to integrate the footprint families in a single analysis, using regional input-output framework (B. R. Ewing et al., 2012), which is essentially a network framework

which will be reviewed in Section 2.3.4. The approach taken by Ewing et al. (2012) is similar to the proposed matrix model in this thesis (Figure 2.1(a)). Ewing et al. (2012) proposed a theoretical framework to utilise the input-output tables to calculate the national level EF and WF. In order to include information about international trade, 3-dimensional matrix data structures were proposed (Figure 2.1(b)), each layer of table corresponding to the footprint account for each country. In the end, the total amount L^z/Z and W^z/Z provides the ratio of EF and WF required per industry production.

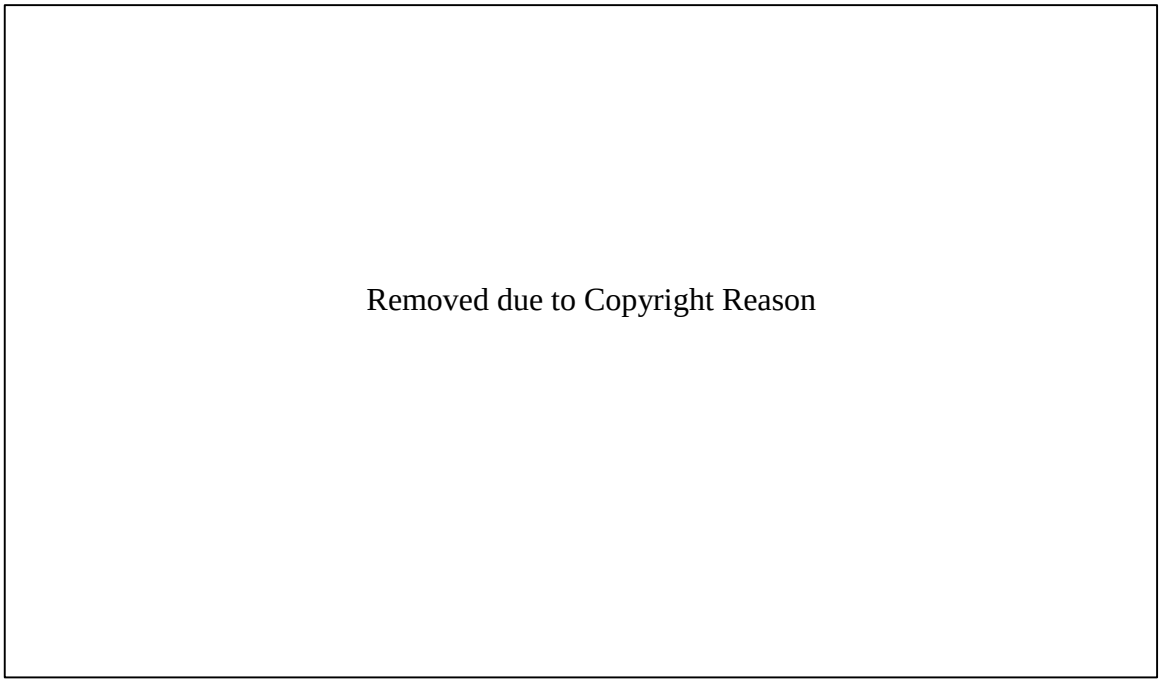

Figure 2.1. Input-output Table Organisation for Footprint Family Framework. (a) Normal IOT used for EF and WF (b) multi-regional IOT for EF and WF. Picture is taken from Ewing et al. (2012). Detailed explanation of the mathematical structure is given in Section 2.3.4. In the input-output framework, the rows (L^z and W^z) underneath the main matrix Z represent the production inputs and the column (Y) on the right of the main matrix Z represents the output

of the economy. The entries of the row vectors L^z and W^z represent the ecoogical and water footprints required for production in each sector of economy.

2.3.2 Input-output Analysis

Input-output analysis was originally developed by Wassily Leontief (1936) to model the circular interdependency of industrial sectors. The strength of input-output analysis lies in its global coverage of the economic system. Input-output tables are now an integral component of the Systems of National Accounts (UN, 2008), which is adopted by most countries in the world. Each year, the trade relations among the economic sectors can be summarised in input-output tables in three different forms. The original IOTs that Leontief developed were symmetric tables showing inter-industry trade volumes, how much goods and services each industry sector sold to another, and the final demand. An observation about IOTs is that the ratio of the product does not change much yearly because of the industrial sector specific formula for production.

The industrial structure of which industry purchases what and how much in order to produce one unit of the final product do not change as quickly, because the short-term event or shock, and the ratio is considered to be constant. Thus IOTs are typically used to predict the short-term indirect ′knock-on′ impact through economic networks arising from disasters, sports events and policy changes, with a tool called economic multipliers (Richardson, 1985). The multiplier-based application of IOT are still being published - the economic impact of disaster events, water shortages and droughts (Perez & Barreiro-Hurle, 2009; Rose & Liao, 2005; Changkuan Zhang, Tang, & Park, 2009), Hurricane Katrina (Hallegatte, 2008); economic impacts of policy changes, Super-city amalgamation of Auckland, NZ (Vaithianathan, 2009), various water policy options (Llop, 2008); economic benefits analysis on infrastructure

improvements, transportation systems (Farooq, Hardy, Gao, & Siddiqui, 2008), river rehabilitation (Sporri, Borsuk, Peters, & Reichert, 2007), and the economic impacts of one-off events such as sports (Dwyer, Forsyth, & Spurr, 2005; Kim, Chon, & Chung, 2003). The typical economic impacts considered are the influence on the Gross Domestic Product (GDP), employment and sector-specific production output.

Inter-industry economic structure is alternatively presented in make-use tables, which is the favoured form in modern input-output economic structure reporting. Make-use tables show intermediate results in the process of summarising the national accounts (Trinh, Kobayashi, & Kim, 2012) − this expresses the economic structure using two tables linking the amount of commodity to the industry. The Make table shows the amount of commodities produced in all the economic sectors along with the imports of commodities. The Use table shows the amount of commodities used by the economic sectors, final demands and exports. It is possible to revert to the rectangular Leontief IOT under either the commodity technology assumption or the industry technology assumption (Trinh et al., 2012). Make-use tables have a formal similarity to an LCI database (Heijungs, 2001), where each column of the LCI database links the primary commodities and emissions associated with the unit industry processes - make-use tables link the economic commodity quantity to unit operation of economic sectors. The most recent published IOTs for New Zealand linked 80 economic sectors to 137 goods and services categories (SNZ, 2007).

Environmentally extended input-output analysis (EEIO) has extended both Leontief and Make-use table forms. While Cumberland (1966), Daly (1968), Leontief (1970) developed the formal extension of symmetric Leontief tables (called industry-industry tables), Victor (1972) and

Isard (1968) developed the extension of Make-use tables (called commodity-industry tables). The make-use tables have more flexibility than the conventional Leontief table when it comes to environmental extension because industrial sectors can be associated with multiple commodity IOs. For example, make-use tables will model an agricultural sector to produce several different types of fruits but Leontief input-output tables will model the agricultural sector to have a single aggregate production output. Essentially, make-use tables portray more detailed information of the internal processes going on in the industry, but lacks explicit information on inter-industry connections. However, information on inter-industry connections can be inferred from the make-use table under the assumptions stated in the previous paragraph.

The construction of Physical Input-Output Tables (PIOTs) at national and global levels have been advocated by numerous researchers (R. Hoekstra & van den Bergh, 2006; Suh & Kagawa, 2005). PIOTs record physical (mass) flow among economic and environmental sectors based on mass balance principles. However, the construction of PIOTs requires extensive mass balance surveys, and it is virtually impossible to create such dataset from actual surveys. Thus, it remains as demonstrative prototypes and has not been utilised widely. While it is not widely applied, the tabular structure can incorporate the constraints just as any other matrix based framework.

Natural resource accounts such as water, land and forestry accounts (e.g. Hubacek & Giljum, 2003; Perrings & Vincent, 2003) which parallel the corresponding evolution in accounting systems such as the Systems of Environmental and Economic Accounts (SEEA) and National Accounting Matrices including Environmental Accounts (NAMEA) (Pedersen & De Haan, 2006) have been developed. Thus footprint estimations based on national and regional input-output models are frequently used (Daniels, Lenzen, & Kenway, 2011; Hubacek & Giljum,

2003; M. Lenzen, Wood, & Wiedmann, 2010; Wiedmann, 2009b).

The input-output model was used to supplement the high data requirement of LCAs since the 1990s. The traditional LCA model was based on process analysis where the collection of data and subsequent modelling at the process level was considered time-consuming, costly and prone to truncation errors (Manfred Lenzen, 2000). Moriguchi et al. (1993) was the first to apply the input-output model in calculating the life cycle of CO_2 emissions of automobiles in Japan. Series of studies under the name of the Environmental Input–Output Life Cycle Assessment (EIO-LCA) substantiated the general application of IO to LCA that began with the work of Lave et al. (1995), who constructed a comprehensive 498 commodity by 498 commodity environmental IO database for use in LCA. The methodology of incorporating IO into LCA has been further refined by the development of hybrid LCA (Suh et al., 2004).

Overall, input-output tables have found a central role in various industrial ecology tools when it comes to representing the economy and environmental system as a whole. It provides the basis for organising the matrix formalism for the network theory of flows in Chapter 3.

2.3.3 Life Cycle Inventory (LCI)

Life Cycle Inventory (LCI) is one of the four phases involved in Life Cycle Analysis (LCA). It concretely models the physical flow among the industrial processes, producing a unit of final good or service called a functional unit. The end outcome is a list of primary resource inputs and airborne/waterborne environmental emissions in physical units. LCA is a systematic approach to evaluating the overall environmental burdens from what is called a reference flow (Heijungs & Suh, 2002). The algorithm involves a series of linear algebra based on the generic

life-cycle inventory database that converts one type of commodity to another.

There are five methodological choices for LCI (Suh & Huppes, 2005). The simplest LCI method used is the process based approach, which traces the upstream and downstream manufacturing/emission processes with manual step-by-step calculations. The most commonly implemented method in the LCI software is the matrix based method, which is capable of dealing with cyclic relations such as recycling (Heijungs & Suh, 2002). While there are three other more advanced methods involving tiered-hybrid approaches, the matrix based LCI is the fundamental form of computational LCI.

Life cycle assessments started with the pragmatic analysis of products from various companies. Thus the methodologies used for each study varied from each other (Boustcad, 1996; Hunt & Franklin, 1996). The first scientific paper for LCA emerged in the 1990s (Guinee & Heijungs, 1993) and the interest in LCA has grown significantly since then. With the collaborative discussion of many, the methodology, comprising of four stages of analysis, has stabilised to the current form; scope, inventory, impact and interpretation (Guinée, 2002; Rebitzer et al., 2004).

Life Cycle Inventory analysis distinguishes between the economic flows and environmental interventions. Heijungs & Suh (2002) utilised the example of electricity generation and fuel production to illustrate the underlying calculation procedure. In order to produce 10kWh of electricity, 2 litres of fuel are needed, and the corresponding emissions of 1kg of CO_2 and 0.1kg of SO_2 are produced. Likewise, in order to produce 100 litres of fuel, 50 litres of crude oil is needed, with 10kg of CO_2 and 2kg of SO_2 being emitted. The unit production vector for electricity generation p_1 and fuel production p_2 are represented as the following: (Heijungs &

Suh, 2002, p. 13):

$$p_1 = \begin{pmatrix} litre\ of\ fuel \\ kWh\ of\ electricity \\ kg\ of\ CO_2 \\ kg\ of\ SO_2 \\ litre\ of\ crude\ oil \end{pmatrix} = \begin{pmatrix} -2 \\ 10 \\ 1 \\ 0.1 \\ 0 \end{pmatrix}, p_2 = \begin{pmatrix} litre\ of\ fuel \\ kWh\ of\ electricity \\ kg\ of\ CO_2 \\ kg\ of\ SO_2 \\ litre\ of\ crude\ oil \end{pmatrix} = \begin{pmatrix} 100 \\ 0 \\ 10 \\ 2 \\ -50 \end{pmatrix} \quad (2.1)$$

Here, the negative numbers represents the input to the production process and the positive numbers represents the output. The process matrix is created by combining the above vectors:

$$P = \left(\begin{array}{cc} -2 & 100 \\ 10 & 0 \\ \hline 1 & 10 \\ 0.1 & 2 \\ 0 & -50 \end{array}\right) = \begin{pmatrix} A \\ \hline B \end{pmatrix} \quad (2.2)$$

The upper two rows, the litre of fuel and kWh of electricity, are the flows created by the modeled industrial production processes. They are termed the economic flows because they are often exchanged via market transactions. The bottom three rows are the environmental interventions, which are the by-products of the industrial processes that are exchanged with environmental systems. The part of matrix P involving coefficients of economic flows and the part involving the environmental intervention coefficient are denoted by matrix A and B respectively for future reference. The output of the industrial processes can be scaled by operating them for longer duration for a given day or by using the larger installation of the same industrial technology, i.e. scaled industrial process. The operation intensities of the production facilities are denoted by $(s_1, s_2)^T$. The final operation vector can then be written as:

$$P \cdot s = \left(\begin{array}{cc} -2 & 100 \\ 10 & 0 \\ \hline 1 & 10 \\ 0.1 & 2 \\ 0 & -50 \end{array}\right) \begin{pmatrix} s_1 \\ s_2 \end{pmatrix} = \begin{pmatrix} f \\ \hline g \end{pmatrix} \quad (2.3)$$

Using linear algebra, the operation intensities that will create desired final output combination can be calculated. For example, if the final output required in the economic system is 1000kWh of electricity with no fuel remaining, the following set of equations can be formed for the economic flow criterion:

$$A = \begin{pmatrix} -2 & 100 \\ 10 & 0 \end{pmatrix} \begin{pmatrix} s_1 \\ s_2 \end{pmatrix} = \begin{pmatrix} 0 \\ 1000 \end{pmatrix} = f \tag{2.4}$$

Solving this equation yields $(s_1, s_2)^T = (100, 2)$. This scaling vector can be used to determine the environmental intervention generated in order to satisfy the economic flow criterion by multiplying it by the process matrix P:

$$f = P \cdot s = \left(\begin{array}{cc} -2 & 100 \\ 10 & 0 \\ \hline 1 & 10 \\ 0.1 & 2 \\ 0 & -50 \end{array}\right) \begin{pmatrix} 100 \\ 2 \end{pmatrix} = \begin{pmatrix} 0 \\ 1000 \\ 120 \\ 14 \\ -100 \end{pmatrix} \tag{2.5}$$

The system of production processes would absorb 100 L of crude oil, emit 120 kg of CO_2 and 14 kg of SO_2 in order to produce 1000 kWh of electricity. Therefore, the basic mathematical formulation of an LCI problem can be represented by the three equations below, where solving the problem involves finding the vectors s and g, given vector f which is called the reference flow vector, to meet the functional unit requirement.

$$P = \begin{pmatrix} A \\ B \end{pmatrix}, A \cdot s = f, B \cdot s = g \tag{2.6}$$

Matrix A and B are assumed to be near constant because they represent the technology used to produce goods and services where technological innovation occurs at a slow pace, of the time frame in the order of decades. These matrix entries are stored in LCI databases (e.g. EcoInvent;

Frischknecht et al., 2005) and invoked in the LCA software. There are a number of other options for LCI databases following a similar format, for example the International Reference Life Cycle Data System (ILCD) is emerging (Finnveden et al., 2009). In a practical LCA application, the number of processes used in the LCI computation will range from several to several hundreds. The matrix size used in the computation will also be large.

2.3.4 Matrix Formalisms

The three industrial ecology modelling frameworks reviewed above can be categorised into three distinct archetypes; commodity-commodity, industry-industry and commodity-industry models, following the notation of input-output models.

2.3.4.1 Commodity-commodity Network

Footprint families and the Bureau of Economic Analysis (BEA) economic structure data table (BEA, 2010) belong to commodity-commodity models, which are expressed in terms of conversion factors. These conversion factors link the amount of raw materials needed to produce the intermediate and final products. They can be described as stoichiometric ratios of the industrial products.

The network representing the calculation of family of footprints can be viewed in Figure 2.2, with a simple 3 product by 3 resource footprint network. Product-level footprint analysis calculates how much of primary resource is needed to produce one unit of such product. The resources in Figure 2.2 can be land area, freshwater quantity, emission, etc. The product level coefficients are typically obtained from LCI studies. The primary resource to the product quantity relation can be expressed with:

$$x_i = A_{ij} \times y_j \quad (2.7)$$

where x_i and y_j denote the vector representing the quantities of resource extraction and product creation; A_{ij} denotes the technical coefficient matrix; and i and j are indices for resource and product respectively. These technical coefficients house the conversion factors evaluated in numerous product-level footprint studies. The quantity measurements for x_i and y_j do not have to be in mass units nor do they have to be the same between x_i and y_j. The unit of technical coefficient matrix rectifies the unit difference.

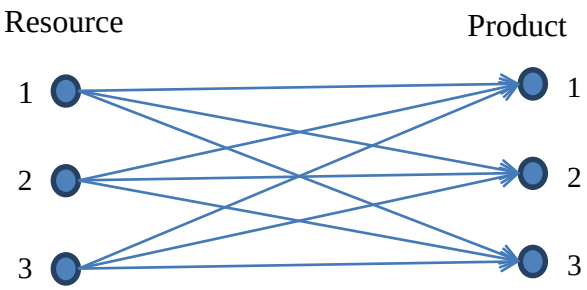

Figure 2.2. 3-by-3 Resource-to-Product network model.

The entries of A_{ij} represent the connection strengths of the network links. There may be cases where a product does not require a type of primary resource at all; this means the resource-to-production network link strength will be zero between these nodes. In real life applications, the network would be much larger, with a N-resource to M-product network, where N and M are the number of types of resources and products handled by the society respectively.

With population and economic growth, the demand for the products will change over time. There are three types of final demands that drive a national economy (UN, 2008) - the residential, government and capital investments. These final demands require a different mix of commodities produced by the industries. In reality, hundreds of commodity categories are

traced (e.g. 190 goods and services categories are traced in supply-use table of New Zealand 2007 (SNZ, 2007)). The mix of items are traced to households, government and capital investment accumulation in the use table. This mixture further extends the network model described in figure 2.2 into a 3-tier model for future projections (figure 2.3).

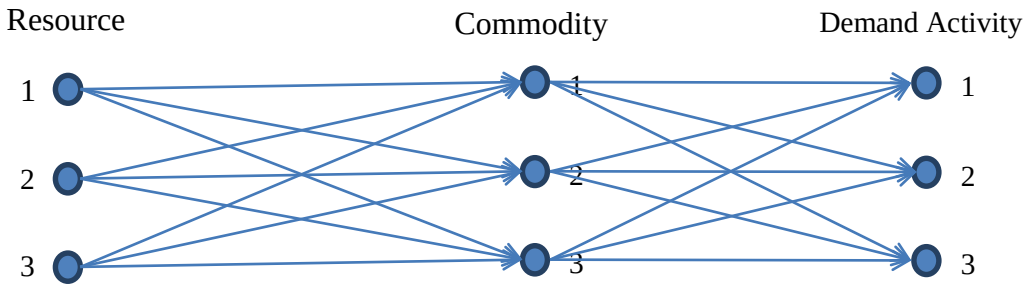

Figure 2.3. 3-tier network model of quantitative sustainability.

The simplest model that connects the final demand commodity quantity and society activity would be a linear relationship, assuming constant economies of scale, for simplicity of the discussion. The matrix relation between the demand commodity and the final demand activity can also be represented by using a matrix equation:

$$y_j = S_{jk} \times z_k \tag{2.8}$$

where y_j and z_k are quantities of commodity and demand activity level respectively. Lifestyle, policy and industrial changes will be reflected in the matrix S_{jk}. Similar to the technological coefficient matrix, the columns of the lifestyle matrix S_{jk} contain the mix of commodities required for each unit increase in the final demand activity. The information about the technological progresses and the lifestyle change will be contained in matrix A_{ij} and S_{jk} in this framework. The growths of the society will be accounted for in the activity vector z_k which is

an external variable for the model.

$$x_i = A_{ij} \times S_{jk} \times z_k \tag{2.9}$$

This equation has the structure similar to the IPAT equation introduced in section 1.1.2. IPAT equation is a conceptual representation of the factors that affect the total environmental impact of a given population. There is a conceptual linkage between the primary resource usage x_i and the impact I; between the technological conversion coefficients A_{ij} and technology T; between lifestyle matrix S_{jk} and affluence A; between final demand activity vector z_k and population P. The equation 2.9 can be considered as a concrete implementation of the IPAT equation, broken down to specific areas of population activity, life-style commodities required to support the population and the technical coefficients that industrial technology network provides to the population.

2.3.4.2 Commodity-industry Network

Make-use input-output analysis and LCI falls into this flow matrix model. The central technical coefficient represents the relationship between the industrial unit process or the industrial sectors. The main matrix P is a combined matrix of A and B where A and B are the flow matrix for economic and environmental commodities. The economic commodities are the ones produced and exchanged within the nodes of the network, and the environmental commodities are those exchanged with an external environment. In matrix A and B, the rows represent the commodities, and the columns represent the economic sectors or industrial processes. The resulting matrix equation is the following:

$$P = \binom{A}{B}, A \cdot s = f, B \cdot s = g \tag{2.10}$$

Given that technology (i.e. the way of production) stays the same, the column ratios of A and B will stay the same. The expansion of the industrial process is described by variable s, which is a scaling factor. With the increase in population and economic development, the amount of final demand (vector f) will increase over time. This increases industrial process scaling factors (vector s) and ultimately results in the environmental interaction flow vector (vector g).

This commodity-industry network representation is the representation that will be developed further in Chapter 3 because it can represent multi-commodity flow networks naturally.

2.3.4.3 Industry-industry Network

Industry-industry network shows the interaction among the production agents. This is in relation to the graph-theoretic representation of a network and is the most typical link to the traditional network analysis.

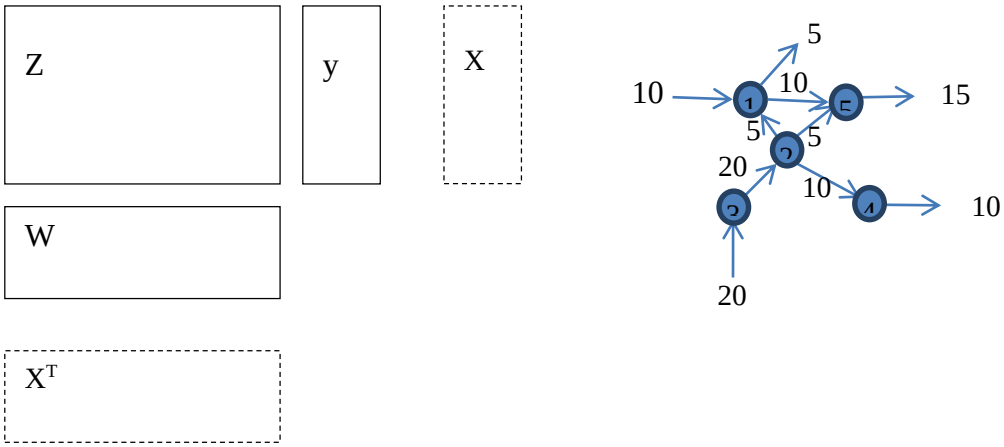

Figure 2.4. Industry-industry Flow Network.

In terms of the flow network, matrix Z represents the flow interaction from the industry to industry, in the same convention of the adjacency matrix of graph theory – these are the

internal flows among the network nodes. The row matrix W and y show the external interactions, where W records the input flows to the network nodes and y records the output flows from the network nodes. The number of rows corresponds to the number of external agents that provide the input flow to the network. In the input-output analysis, no accumulation of flows within the network nodes is assumed. This means that the sum of entries in matrix y and W are equal. Also, the row sum of Z + y and column sum of Z + W are equal, as they are incoming flows and outgoing flows of the network nodes. These row sum and column sums are the total productions of individual sectors or nodes, or it can be considered as the total throughput of the nodes **X**.

The example network shown in the figure above will create the following matrices:

$$Z = \begin{bmatrix} 0 & 0 & 0 & 0 & 10 \\ 5 & 0 & 0 & 10 & 5 \\ 0 & 20 & 0 & 0 & 0 \\ 0 & 0 & 0 & 0 & 0 \\ 0 & 0 & 0 & 0 & 0 \end{bmatrix} \quad y = \begin{bmatrix} 5 \\ 0 \\ 0 \\ 10 \\ 15 \end{bmatrix} \quad X = \begin{bmatrix} 15 \\ 20 \\ 20 \\ 10 \\ 15 \end{bmatrix} \tag{2.11}$$

$$W = [10 \quad 0 \quad 20 \quad 0 \quad 0] \tag{2.12}$$

In an economic system, the future projection of growth in matrix **y** will result in the increase of burdens in W. This is modeled by assuming that the throughputs of the nodes (i.e. the vector **X**) are determined by the output requirement **y**, the ratios of the input-outputs of each node stays constant, and the throughput distributions are expressed as a multiple of X. These assumptions result in the expression, X = Z + y = AX + y, which reduces down to the Leontief′ s equation; y = (I-A)X; $\mathbf{X} = (I-A)^{-1}\mathbf{y}$. Matrix A is the technical coefficient for the network nodes, which describes the ratios between the intakes and outputs of the industry sectors. The burdens for the inputs increase proportionally with variable X. In economic input-output analysis, rows

of W consist of different added-value contributors such as wage for labour, profit, and government taxes. In environmentally extended input-output analysis, the physical inputs for the industry are accounted for in the rows of the W matrix.

2.4 The Knwledge Gap and Potential Research

As was identified in this chapter, there are serious efforts to increase the understanding of environmental constraints and the resource constraints for the society. Human society is facing the resource depletion and degraded capacity of environmental assimilation of pollutants. Although there are progresses in understanding the individual constraints, one by one, there is an absence of integrative framework that can address the combined effect of the constraints. The literature review identified a potential candidate to fill this gap, the industrial ecology framework, which views the society-environment system as a flow network.

The industrial ecology network frameworks only models the networked flows of goods and services among human society. These frameworks comes with consideration of the technical coefficients that describes the conversion ratio from the raw resources to units of goods and services and from the units of goods and services to pollutant emissions. By combining the information of network flow and the technical coefficient, the industrial ecology framework calculates the resource intakes and pollutant emissions for the society, items by items. At this moment in time, the industrial ecology framework does not take into account the effect of environmental constraints.

There is an interesting and important research avenue presented between these two fields of study. The approach is to extend the mathematical framework developed in the field of

industrial ecology so that the quantity of resource requirements and pollutant emission can be compared to the environmental constraints (i.e. resource availability and assimilation capacity). Although it is a natural idea to compare the estimated environmental impacts (i.e. resource requirements and pollutant emission) to the environmental capacity, surprisingly few number of instances compare the environmental impacts to the environmental capacity. Those studies that do compare the requirements and constraints are limited to single types of resources (e.g. land area, ecological footprint-biocapacity, freshwater requirement-availability, minerals reserve, energy reserve).

The present study attempts to addresses multiple resource/goods/services flow concurrently and to compare multiple resource/emission requirements to multiple constraints. This is achieved by utilising the power of multi-commodity network representation developed in the field of industrial ecology. This work is novel to the field of industrial ecology because the tools developed in the field do not consider the effect of the constraints at this point in time.

Thus the work proposed in this thesis is novel to both fields of constraint science and industrial ecology by contributing complementary strengths of these two fields. The power of system-level representation methodology developed in the field of industrial ecology will open up pathways to integrate individual studies made in the constraint science field, from the study proposed in this thesis. Also, knowledge about the constraints on the multi-commodity flow network will provide a basis of the value judgement on the estimated environmental impacts. Essentially, the tool will be able to answer how large the estimated environmental impacts are compared to the known environmental constraints.

Chapter 3 Constrained Networks Theory

3.1 Introduction

Chapter 2 discussed the two primary aspects of the science of sustainability that needs to be combined - interconnectedness and constraints. Society operates within multiple external and internal constraints. These may be of different types such as biophysical, monetary or social constraints. Among these, sustainability science focusses on biophysical constraints, which are related to resource generation and emission assimilation limits in material flows (Goodland, 2002). Resource depletion and the more stringent environmental management constraints are expected to be seen in mid-to-long term future governance. Industrial ecology flow models provide promising frameworks that deal with multiple resource-sink flow relationships and also, a major uptake in accumulation of data that support industrial ecology is observed. At the same time, renewed interest in constraint science was observed in the late 2000s. These two fields of study are now maturing, their combination leading to a new research avenue that may explore the initial question in sustainability science – the absolute sustainability criteria.

This chapter analyses and extends well established industrial ecology models, two variants of input-output analysis (Leontief and Supply-use table) and Life Cycle Inventory (LCI), to include constraints. These frameworks are based on common tabular (or matrix) representations, which are essentially network flows through many nodes resembling the expressions used in graph theory and network science. This is natural because input-output analysis deals with the flows among multiple economic sectors, and LCI deals with the flows among multiple industrial processes. Mathematical framework defines precisely where and

how the constraints are imposed on the matrix framework of the network flows. By formulating the constrained flow network in mathematical terms, several clear measures could be developed that reflect the absolute sustainability at the system level.

Section 3.2 overviews the link between flow networks and matrix formulation. Section 3.3 extends the Leontief input-output framework, which is a single commodity flow network, to include constraints. Section 3.4 extends the LCI and Supply-Use table to include constraints. LCI and Supply-use table essentially have the same mathematical structure, representing multi-commodity network flows. Section 3.5 develops the suite of mathematical measures of absolute sustainability for the constrained network framework. Section 3.7 concludes the chapter.

3.2 Flow Network and Matrix Formulation

Network theory studies the systemic properties of networks as a whole. A network is a collection of nodes which interact with each other using links. The interaction links are defined as the connection strengths between a pair of nodes. Networks are found in many natural and artificial systems. Typical interest of the mathematical network theory has been statistical measures of the entire network such as degrees and clustering coefficients (e.g. Albert & Barabási, 2002). Many engineering applications define and utilise various property measures of a specific networked systems of interest, other than statistical measures. The core strength of a network approach is its comprehensiveness of representation, enabling to formulate a structured calculation concurrently on the properties of networked interactions.

3.2.1 Closed/Open Network Representation

Data structure that describes any given network, the adjacency matrix, is already well

established. Adjacency matrix describes the strength of link connections from the source node (enumerated in row index) to destination nodes (enumerated in column index). Adjacency matrix can represent complete information of flows in a closed network. Consider a 4-node network interacting with an external environment node (Figure 3.1); the exchange is measured in an arbitrary unit (e.g. nutrients measured in calories).

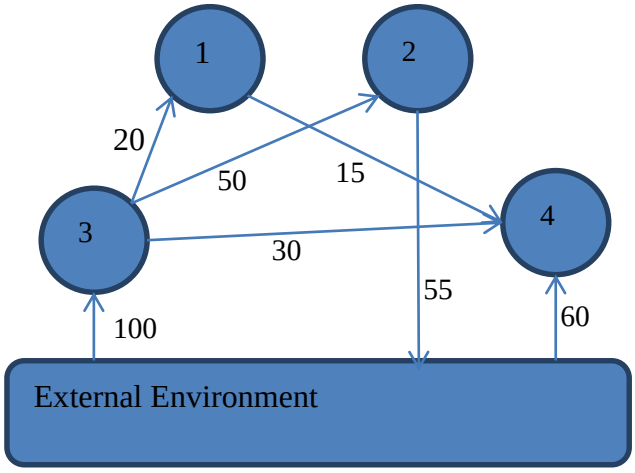

Figure 3.1. An example network.

This example can be considered as a closed 5-node network and is represented using a 5x5 adjacency matrix Z_{ij} as the following, where i = the row index of the source nodes and j = the column index of the destination node:

$$Z_{ij} = \begin{bmatrix} 0 & 0 & 0 & 15 & 0 \\ 0 & 0 & 0 & 0 & 55 \\ 20 & 50 & 0 & 30 & 0 \\ 0 & 0 & 0 & 0 & 0 \\ 0 & 0 & 100 & 60 & 0 \end{bmatrix}$$

The example can also be considered as an open 4-node network. More than one matrix is needed to describe the flow system completely. The four nodes designated by index 1 to 4 are the internal network nodes, the fifth node being the external node. The last row and column of

the matrix Z_{ij} represents the interface flow at the outer fringe of the open network of 4 nodes. When the network is considered separately as an open internal network and external nodes, the links are distinguished into three types: input, output, and intra-network flow. Following this distinction, the 5x5 matrix Z_{ij} is broken down into three compartments (Figure 3.2). The top-left 4x4 compartment (green box) describes the intra-network flow among the 4 internal nodes, while the fifth column and row compartments (red boxes) describe the flow interactions with the external environment. The bottom-left row vector accounts for the input (or provision) from the environment to the respective nodes. The top-right column vector accounts for the output (or extraction) to the environment from the respective nodes.

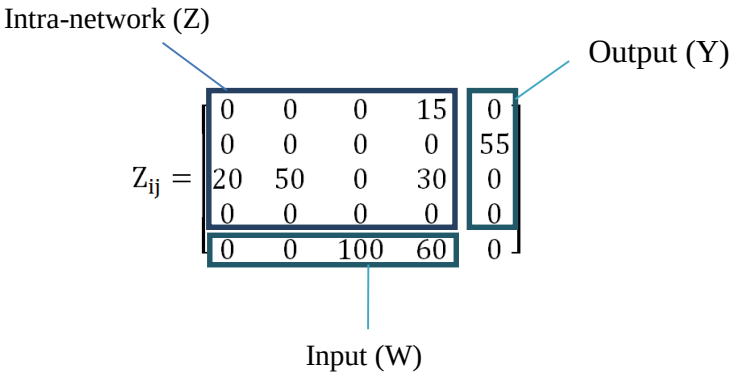

Figure 3.2. Matrix Representation of an Open Network. Three matrices are required to describe an open network.

The necessity of conceptualising a problem using an open network concept is due to several reasons. Firstly, even though it is possible and tempting to create a complete picture of the global network using comprehensive global data coverage, some regions of the network may still have data deficiency. It may be the case that the data deficiency will continue because the benefit of obtaining the data is not worth the effort. For example, in a typical investigation of

the interactions between economic and ecological systems, data on ecological flows is not available at a level that is as detailed as that of economic systems. Often the modelling effort is truncated up to the interface between economic systems and the ecological compartment is considered as external nodes. This type of truncation is also used in national-level or regional-level studies of economic structures, where the rest of the world is treated as the external environment. Secondly, open network modelling enables you to model a part of the global system with a greater level of detail. Thirdly, many people are interested in the implications of having the combined action of the constraints at different scales. Open network approach is capable of answering this call. When constraints are considered in sustainability, they are considered in a closed setup which only exists on a global scale - for example, as in World3 model (Meadows, 1972) or ecological footprints (Rees, 1992). Now, it is desirable to develop a theory that can scale down the global requirements of a regional/local level or system-specific design criteria.

The three industrial ecology models mentioned earlier are formulated from an open network approach, even though they do not explicitly state this. The details of how they achieve this will be explained in the subsequent sections.

3.2.2 Approach to theory development

The theory development will take 3 steps. First, the mathematical structures of the existing network modelling tools are observed. Some frameworks do not explicitly reference networks, but they still represent the flows through networked systems. The frameworks that exist in literature focus on the flows through network nodes. Secondly, the consequences of adding a constraint criteria to the sources and sinks of the networked flow are explored. This is the

original contribution of the present theoretical work. The formulation of the constraints will be general enough to be applied in various contexts. The tools for the analysis will then be introduced. The addition of constraints is a natural extension of the flow network models, and the constrained network model is capable of linking the information about the capacity of individual nodes to the capacity of the overall network. At the end of the chapter, possible application contexts on where and how this theory can be applied will be discussed with some hypothetical examples.

3.3 Single Commodity Network

The simplest flow network is a single commodity network. The convention is that the row indices represent the source nodes, and the column indices represent the destination. The matrix representation of the single commodity flow network has been applied in different contexts; in energy-based ecology (S. L. Huang & Chen, 2009; Ulanowicz, 2004) and industrial energetics. In fact, the means by which common mathematical framework underlies the economic, industrial and ecological network systems is already recognised in literature (Suh, 2005). The common mathematical structure was developed from the Leontief input-output model, which expresses flow quantities among the nodes in single commodity flow networks.

Single commodity network is one of the many alternative ways of modelling real ecological and industrial systems. In principle, ecological and industrial flows involve multiple types of commodity exchange. The key feature of the single commodity network approach is aggregating the flows in terms of a single measurement unit over the entire network; e.g. monetary units in economic networks or energy based units in industrial/ecological networks (of energy, productive land area, CO_2 emission equivalent). Irrespective of the units of

measurement used, the frameworks share the same mathematical structure because they all extend the Leontief's input-output framework.

3.3.1 Leontief Input-output Table

This matrix format is directly comparable with the symmetric Leontief input-output table. Consider a section of the national input-output of the New Zealand economy in 2007 as an example (SNZ, 2012).

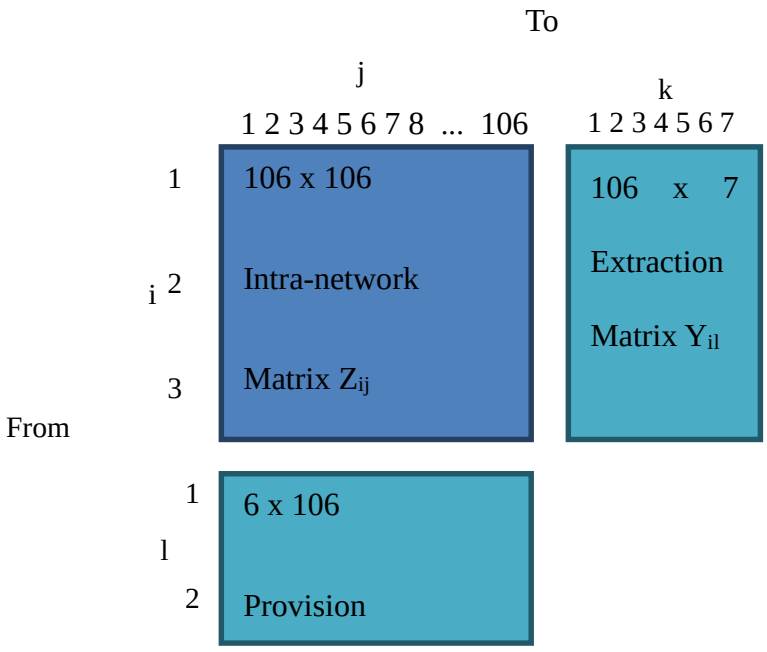

Figure 3.3. Symmetric NZ Input-output Table Structure. This table shows the economic production made from 6 primary inputs (labled with index l), and 7 ultimate consumers of the economic outputs (labeled with index k). The whole network consists of 106+6+7 nodes. The 106x106 matrix Z_{ij} describes the flows among the economic sectors. For example, the numeric entry $Z_{5,7}$ (5^{th} row, 7^{th} column) represent flow quantity from economic sector node 5 to node 7; similarly, the entry $W_{6,45}$ will represent the flow quantity from the 6^{th} primary input node to

economic sector node 45.

The arrangement of the input-output table follows that of the matrix representation of the open network in Figure 3.2. Instead of network flow of 4 nodes as in Figure 3.1 and 3.2, the input-output table represents intra-network flow among 106 productive nodes. Another difference is the size of the input vectors (W) and output vectors (Y). In figure 3.1 and 3.2, there was only 1 environmental node, so the size of the input and output quantities could be represented using vectors. The input-output table of NZ economy utilises matrices for inputs and outputs of the economy. The input matrix W has 6 rows; it means that the NZ economy was modeled to draw inputs from 6 external primary resource entities. The output matrix Y has 7 columns; it means that the NZ economy was modeled to provide outputs to 7 external consumer entities. This is because the open network of the inert-industry economy is embedded within several different external environments. The 6 rows in the provision matrix represent the provision from five entities outside the realm of the industry network; (1) import, (2) government (i.e. taxes), (3) labour, (4) entrepreneurship, and (5) capital. The 7 columns in the extraction matrix represent the extraction of six entities outside of the network; (1) export, (2) households, (3) Non-profit institutions serving households (NPISH), (4) central government, (5) local government, and (6) capital. NPISH include religious services, clubs and NGOs.

Several interesting points are observed by comparing the structure of the input-output table with the modified adjacency matrix representation for the open network. First, the modified matrix representation for the open network can accommodate interactions with multiple external entities. Also, the external entities responsible for provision and extraction do not need to be same. This means that the overall operation of the open network can be directional, proceeding from the provisioning environment to the extractive environment entities. The

second observation is on the role of the monetary transaction record in the economic input-output table. The quantities measured in the provision compartment in the NZ input-output table are the flow of money, which is the counter flow of the usable goods and services provided by the external entities. For example, the provisions of labour and entrepreneurship are measured and named as ″compensations for employees″ and ″operating surpluses″, which are paid amounts for the work done by employees, and the provision of ingenuity and risk bearing operations of entrepreneurs. These items record the flow of money out of the network which is the counter-flow of the physical inflow of goods and services of equal values provided by these external entities. Same counter-flow condition applies to the extraction interface represented in the 106 x 7 extraction matrix; the recorded quantity is the money paid by the external final consumers but at the same time interpreted as the flow of goods and services from industry network to the final consumer destinations. Therefore, the economic input-output network can be interpreted in two ways, either (1) the flow of physical goods and services from the provision environment to the final consumers or (2) the flow of money from the final consumers to the provision environment mediated by the industry network. For the sake of sustainability, the flows and constraints of both physical commodities and money are important.

The force that drives the commodity flow through the industry network is the purchasing power of money, bestowed by the counter-flow generated in the provision matrix interface. The purchasing power is bestowed upon the household and government by the transfer of money as recorded in the provision matrix. The flow of money is augmented and redistributed by financial institutions and the government spending policy, which are described not in this input-output but in an extended framework of the social accounting matrix (SAM). Although it is

possible to establish the mapping of the SAM to the single commodity matrix network framework, considering the SAM still accounts for the comprehensive money flow in a national economy, this mapping exercise is beyond the purpose of demonstrating the structure and capability of matrix-based framework for the single-commodity network flow. Rigorous mathematical treatment of the environmental SAM is provided in de Anguita & Wagner (2014).

3.3.2 Generalisation and Extension

The pictorial description of the input-output flow of the physical goods and services in Figure 3.3 can be expressed mathematically as the following:

i = index of source node

j = index of destination node

k = index of extraction environment node

l = index of provision environment node

Z_{ij} = intra-network flow of commodity from node i to j

Y_{ik} = extraction flow of commodity from node i to k

W_{lj} = provision flow of commodity from node l to j

Z, Y, W are the actual measured flow quantities during a period (e.g. annual, daily)

$\mathbf{w}_l = \Sigma_j W_{lj}$ = row vector of provision flows to all nodes from node l

$\mathbf{y}_k = \Sigma_i Y_{ik}$ = column vector of extraction flows from all nodes to node k;

$\mathbf{s}_i$ = vector of stock of commodity within nodes, in case of long-term commodity or long term assets

$\mathbf{x}_i = \Sigma_j Z_{ij} + \Sigma_k Y_{ik}$ = column vector of commodity produced by node i

$\mathbf{x}_j = \Sigma_i Z_{ij} + \Sigma_l W_{lk}$ = row vector of commodity absorbed by node j

$\Sigma_l \mathbf{w}_l$ = total quantity of provision to the network

3.3.3 Continuity relation

The matrix framework satisfies the continuity relation. $\mathbf{x}_i = \Sigma_j Z_{ij} + \Sigma_k Y_{ik}$ shows that the total production is split into intra-network flow and extractions.

$\mathbf{x}_j = \Sigma_i Z_{ij} + \Sigma_l W_{lj}$ shows that the total absorption are from intra-network flow and provision.

$\mathbf{x}_i = \mathbf{x}_j$, for i = j, if no stock accumulation is allowed within the node.

This means that all commodity flow into the node must flow out at the same rate during the period of observation. Alternatively, this relationship can be called conservation of mass or energy if physical commodity is a concern.

When a node provides storage capacity for the energy or mass, the quantity stored in the nodes are called stock, and the change in the stock will be:

$$\Delta \mathbf{s}_i = \mathbf{x}_j - \mathbf{x}_i \text{ , for all } i = j. \tag{3.1}$$

Stock accumulation has relevance in productive asset accumulation, especially if the commodity has a long shelf life. There are commodities which have a short shelf life duration and have to be consumed before it perishes, such as vegetables. There are commodities which have a long term shelf life but are classified as consumables such as petroleum. They are storable but are consumed along with the disappearance of the commodity. Assets have a long-term shelf life and provide services over time; long-term assets such as furniture or building can be accumulated.

3.3.4 Property of a Node

The operation level of the network is measured by the throughput of the network nodes. In the case of a non-stock network, they can be measured in terms of $\mathbf{x}_i = \mathbf{x}_j$.

Either x_i or x_j determine the operation level of the network node production. The choice is made by the driving factor of the network. If the network is extraction driven, the production vector

$\mathbf{x}_i$ becomes the choice. If the network is provision driven, the $\mathbf{x}_j$ becomes the choice of measurement.

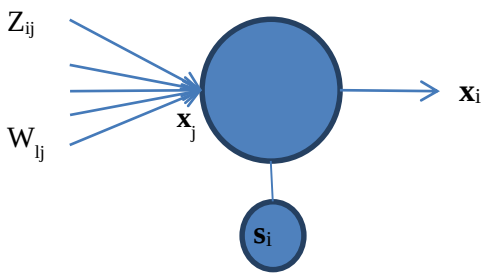

Figure 3.4. A production node structure.

3.3.5 Growth Projection

The matrix elements may be expressed as time-dependent variables if the network is dynamic temporally. For example, the growth of the economy or change in economic structure has been studied using such time-varying matrix formulation. Assuming the driving force of the network is the extraction requirement Y_{ik}, the increase in extraction requirement will increase the total production requirement $\mathbf{x}_i$ and in turn the input requirement $\mathbf{x}_j$ through the interconnections of the network. The input for the nodes $\mathbf{x}_j$ consists of Z_{ij} and W_{lj}. The ratios of the production factors, i.e. the inputs Z_{ij} and $W_{lj,}$ are assumed to have fixed ratios. This is expressed in terms of technological coefficient factors which are defined from a reference point in time:

$$A_{ij}(t=0) = Z_{ij}/\mathbf{x}_j \,|_{t=0} \qquad (3.2)$$

$$B_{lj}(t=0) = W_{lj}/\mathbf{x}_j \,|_{t=0} \qquad (3.3)$$

Therefore, the increase in inputs can be represented linearly with the input requirements as the following:

$$Z_{ij}(t) = A_{ij}(t)\,\mathbf{x}_j(t) = A_{ij}(0)\,\mathbf{x}_j(t) = A_{ij}\,\mathbf{x}_j(t) \tag{3.4}$$

$$W_{lj}(t) = B_{lj}(t)\,\mathbf{x}_j(t) = B_{lj}(0)\,\mathbf{x}_j(t) = B_{lj}\,\mathbf{x}_j(t) \tag{3.5}$$

The technical coefficients are the production conversion efficiency from raw materials to the final product, and they are related to the technological advancement. These technological advancements occur at a much slower rate than other variables, so the technical coefficients are often assumed to be constant over the years of consideration, while the time dependency is often dropped. This is especially true for ecological natural systems where the type of metabolism process stays the same. As for economic systems, the technological coefficient change would mean the use of different type of production processes. Substituting (3.4) and (3.5) to (3.2) and (3.3) respectively yields:

$$\mathbf{x}_i(t) = \Sigma_j\, Z_{ij}(t) + \Sigma_k\, Y_{ik}(t) = \Sigma_j\, A_{ij}\,\mathbf{x}_j(t) + \Sigma_k\, Y_{ik}(t) \tag{3.6}$$

This has a cyclic relation and Leontief solves this via mathematical manipulation of the matrix formulation. The LHS is multiplied with the identity matrix:

$$\mathbf{x}_i(t) = \Sigma_j\, I_{ij}\,\mathbf{x}_j(t) = \Sigma_j\, A_{ij}\,\mathbf{x}_j(t) + \Sigma_k\, Y_{ik}(t) \tag{3.7}$$

This enables the extraction term to be isolated:

$$\Sigma_j\, I_{ij}\,\mathbf{x}_j(t) - \Sigma_j\, A_{ij}\,\mathbf{x}_j(t) = \Sigma_k\, Y_{ik}(t) \tag{3.8}$$

$$\Sigma_j\, (I_{ij} - A_{ij})\,\mathbf{x}_j(t) = \Sigma_k\, Y_{ik}(t) \tag{3.9}$$

This is, in fact, a matrix multiplication of:

$$(I - A)\,\mathbf{x} = \mathbf{y} \tag{3.10}$$

$$\mathbf{x} = (I - A)^{-1}\,\mathbf{y} \tag{3.11}$$

The significance is that the amount of operation can be evaluated from any combination of the final extraction rates from the nodes. The provision required to make this requirement can be calculated from:

$$W_{lj}(t) = B_{lj}\,\mathbf{x}(t) = B\,(I - A)^{-1}\,\mathbf{y} \qquad (3.12)$$

Where W and B are the matrices for the provision of the environment. This means that any future projection of the demand can be traced back to the demand for the provision used up or provided from the environment. Note that these quantities are projected usages and production from the network.

3.3.6 Constraints on network flows

The primary issue of sustainability is the growth of economy and population requirement under the finite amount of resources available. Three constraints can be considered in the operation of the network:

(1) Constraints on the provision side of the network;

(2) Constraints on the extraction side of the network; and

(3) Constraints on the production capacity of the network nodes.

The provision side of the network can be considered as the total resource available for the operation of the network. They represent the total available for the region in which the network exists. The total available resource for the region is appropriated throughout the node. Therefore,

$$\mathbf{w}_l \leq \mathbf{w}_l^+ \tag{3.13}$$

The extraction side of the network constraint arises from two different origins. The first one being the minimum requirement for the production of the flow network. For example, in the domestic, industrial network system, there is a minimum requirement for the production of necessary goods for the livelihood of the population - this imposes the minimum constraint for the extraction rates. In the case of an economic network, another constraint is the quantity of the financial capability of the population to afford the extraction. Therefore,

$$\mathbf{y}_k^- \leq \mathbf{y}_k \leq \mathbf{y}_k^+ \tag{3.14}$$

The constraints on the node elements are imposed mainly from the level of facility assets when carrying out the throughput of network nodes. Therefore,

$$\mathbf{x}_i \leq \mathbf{x}_i^+ \tag{3.15}$$

These constraints characterise the entirety of the constraints for the operation of the network, and can be compared to the current operation level of the network, measured in $\mathbf{x}_i$.

Translation of constraints into throughput vector

The constraints in the provision side and extraction side environment can be translated into the vector equation for the throughput vector $\mathbf{x}_i$, from the vector relations.

$$\mathbf{w}_l = B_{lj}\, \mathbf{x}(t) \tag{3.16}$$

$$x = B^{-1}w \tag{3.17}$$

$$\mathbf{x} = (I - A)^{-1}\,\mathbf{y} \tag{3.18}$$

This translates into a set of linear inequations as in linear programming:

$$\mathbf{Bx} \leq \mathbf{w}_l^{+} \tag{3.19}$$

$$\mathbf{y}_k^{-} \leq (I - A)\,\mathbf{x} \leq \mathbf{y}_k^{+} \tag{3.20}$$

3.3.7 Calculation Procedure Example

Take an example of a 4-node network involving conservative flows - taking provisions from 2 external environments (say resource nodes and import), being extracted from 2 external environment nodes (say domestic consumers and export) and capital accumulation nodes for each network node. The capacities for the two provision external nodes are 400 and 500, and the minimum requirement for the domestic consumer node is growing at a constant rate. The single commodity network formulation implicitly assumes that different types of the commodities are produced from different nodes; the extraction from node 1 will be qualitatively different in comparison to the extraction from node 2.

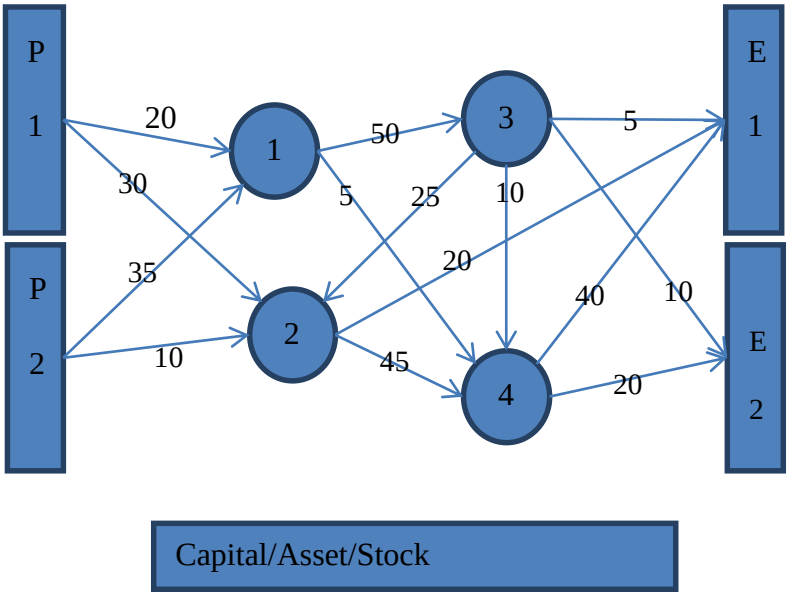

Figure 3.5. Example of conservative flow network.

The corresponding matrices that represent this open network are:

$$Z = \begin{bmatrix} 0 & 0 & 50 & 5 \\ 0 & 0 & 45 & 0 \\ 0 & 25 & 0 & 10 \\ 0 & 0 & 0 & 0 \end{bmatrix} \tag{3.21}$$

$$W = \begin{bmatrix} 20 & 30 & 0 & 0 \\ 35 & 10 & 0 & 0 \end{bmatrix} \tag{3.22}$$

$$Y = \begin{bmatrix} 0 & 0 \\ 20 & 0 \\ 5 & 10 \\ 40 & 20 \end{bmatrix}. \tag{3.23}$$

The constraints are expressed as follows, with no constraints on extraction requirement and node capacity for the time being:

$$W^{+} = \begin{bmatrix} 400 \\ 500 \end{bmatrix}, \mathrm{Y}^{-} = \begin{bmatrix} 0 \\ 0 \\ 0 \\ 0 \end{bmatrix}, \mathrm{X}^{+} = \begin{bmatrix} \infty \\ \infty \\ \infty \\ \infty \end{bmatrix} \tag{3.24}$$

For simplicity, the first extraction vector is assumed to grow linearly in time, but the second

extraction vector stays constant over time:

$$y(t) = \begin{bmatrix} 0 & 0 \\ 20 & 0 \\ 5 & 10 \\ 40 & 20 \end{bmatrix} \begin{bmatrix} mt+1 \\ 1 \end{bmatrix} \tag{3.25}$$

The throughput vector $\mathbf{x}_i$ at t=0 is calculated with a summation definition of $\mathbf{x}_i$:

$$\boldsymbol{x_i} = \sum_j Z + \sum_k Y = \begin{bmatrix} 0 \\ 0 \\ 0 \\ 0 \end{bmatrix} + \begin{bmatrix} 0 \\ 0 \\ 25 \\ 0 \end{bmatrix} + \begin{bmatrix} 50 \\ 45 \\ 0 \\ 0 \end{bmatrix} + \begin{bmatrix} 5 \\ 0 \\ 10 \\ 0 \end{bmatrix} + \begin{bmatrix} 0 \\ 20 \\ 5 \\ 40 \end{bmatrix} + \begin{bmatrix} 0 \\ 0 \\ 10 \\ 20 \end{bmatrix} = \begin{bmatrix} 55 \\ 65 \\ 50 \\ 60 \end{bmatrix} \tag{3.26}$$

Since this is a conservative flow, the magnitude of the input and output for each node must be the same. However, $\mathbf{x}_i$ and $\mathbf{x}_j$ are transposes; i.e. one is a column vector, and the other is a row vector.

$$\boldsymbol{x_j} = \boldsymbol{x_i^T} = [55 \quad 65 \quad 50 \quad 60] \tag{3.27}$$

From the throughput vector $\mathbf{x}_j$ at t=0, the technological coefficients are calculated using an element-wise division:

$$\mathrm{A} = \frac{Z_{ji}}{x_i} = \begin{bmatrix} \frac{0}{55} & \frac{0}{65} & \frac{50}{50} & \frac{5}{60} \\ \frac{0}{55} & \frac{0}{65} & \frac{45}{50} & \frac{0}{60} \\ \frac{0}{55} & \frac{25}{65} & \frac{0}{50} & \frac{10}{60} \\ \frac{0}{55} & \frac{0}{65} & \frac{0}{50} & \frac{0}{60} \end{bmatrix} = \begin{bmatrix} 0 & 0 & \frac{50}{50} & \frac{5}{60} \\ 0 & 0 & \frac{45}{50} & 0 \\ 0 & \frac{25}{65} & 0 & \frac{10}{60} \\ 0 & 0 & 0 & 0 \end{bmatrix} \tag{3.28}$$

$$B = \frac{W_{lj}}{x_j} = \begin{bmatrix} 20/55 & 30/65 & 0 & 0 \\ 35/55 & 10/65 & 0 & 0 \end{bmatrix} \tag{3.29}$$

The provision side constraints translate into throughput constraints with matrix conversion:

$$\mathbf{Bx} \leq \mathbf{w}^{+} \tag{3.30}$$

$$\begin{bmatrix} \frac{20}{55} & \frac{30}{65} & 0 & 0 \\ \frac{35}{55} & \frac{10}{65} & 0 & 0 \end{bmatrix} \mathbf{x}(\mathbf{t}) \leq \begin{bmatrix} 400 \\ 500 \end{bmatrix} \tag{3.31}$$

where the time dependent throughput increase x(t) is translated from the extraction requirement increase:

$$\mathbf{x}(\mathrm{t}) = (\mathrm{I} - \mathrm{A})^{-1}\, \mathbf{y}(\mathrm{t}) \tag{3.32}$$

$$\boldsymbol{x}(t) = \begin{bmatrix} 1 & 0 & -\frac{50}{50} & -\frac{5}{60} \\ 0 & 1 & -\frac{45}{50} & 0 \\ 0 & -\frac{25}{65} & 1 & -\frac{10}{60} \\ 0 & 0 & 0 & 1 \end{bmatrix}^{-1} \begin{bmatrix} 0 & 0 \\ 20 & 0 \\ 5 & 10 \\ 40 & 20 \end{bmatrix} \begin{bmatrix} mt+1 \\ 1 \end{bmatrix} \tag{3.33}$$

$$\boldsymbol{x}(t) = \begin{bmatrix} 32.9 & 22.1 \\ 46.6 & 18.4 \\ 29.6 & 20.4 \\ 40 & 20 \end{bmatrix} \begin{bmatrix} mt+1 \\ 1 \end{bmatrix} = \begin{bmatrix} 32.9 \\ 46.6 \\ 29.6 \\ 40 \end{bmatrix} mt + \begin{bmatrix} 55 \\ 65 \\ 50 \\ 60 \end{bmatrix} \tag{3.34}$$

Substituting this expression into the inequation from the provision constraint gives us the inequation for time.

$$B\mathbf{x}(\mathbf{t}) \leq \begin{bmatrix} 400 \\ 500 \end{bmatrix} \tag{3.35}$$

$$\begin{bmatrix} \frac{20}{55} & \frac{30}{65} & 0 & 0 \\ \frac{35}{55} & \frac{10}{65} & 0 & 0 \end{bmatrix} \begin{bmatrix} 32.9mt + 55 \\ 46.6mt + 65 \\ 29.6mt + 50 \\ 40mt + 60 \end{bmatrix} \leq \begin{bmatrix} 400 \\ 500 \end{bmatrix} \tag{3.36}$$

$$\begin{bmatrix} 33.5mt + 50 \\ 28.1mt + 45 \end{bmatrix} \leq \begin{bmatrix} 400 \\ 500 \end{bmatrix} \tag{3.37}$$

This set of inequalities is solved row-by-row for t.

$$\begin{bmatrix} mt \\ mt \end{bmatrix} \leq \begin{bmatrix} 10.4453 \\ 16.1697 \end{bmatrix} \tag{3.38}$$

This shows the solution for mt and that it should be less than 10.4, with the constraining condition at provision 1. At the constraining condition, mt=10.4, the achieved extraction, throughput, and provisions are:

$$y(t) = \begin{bmatrix} 0 & 0 \\ 20 & 0 \\ 5 & 10 \\ 40 & 20 \end{bmatrix} \begin{bmatrix} 10.4 + 1 \\ 1 \end{bmatrix} = \begin{bmatrix} 0 \\ 229 \\ 67 \\ 477 \end{bmatrix} \tag{3.39}$$

$$x(t) = (I - A)^{-1} y(t) = \begin{bmatrix} 399 \\ 552 \\ 359 \\ 478 \end{bmatrix} \tag{3.40}$$

$$W(t) = Bx(t) = \begin{bmatrix} 400 \\ 339 \end{bmatrix} \tag{3.41}$$

The main result of the procedure is the prediction of the growth parameter mt. This procedure estimated how much of the growth of the final extraction y(t) can be accommodated by constrained resource provision $\mathbf{w}^+$. As was pointed out during the calculation (equation 3.38), the provision was the bottleneck of the growth and the resulting W(t) estimation confirms this fact. Equation 3.41 shows that the system ultimately utilised 400 units of provision 1 and 339 units of provision 2 when it reached its carrying capacity. The provision 1 was utilised up to its constraint and provision 2 was under-utilised. One of the resource inputs will typically act as limiting factor for growth in constrained network flow problems. Estimation of the supportable growth level (i.e. growth carrying capacity) and identification of the limiting factor are the two key outcome of the constrained network formulation in general.

3.4 Multicommodity Network

The single commodity flow network approach has a limitation as it abstracts the transformation processes that industrial and ecological nodes perform. The purpose of the industrial and ecological nodes in an ecosystem metabolism is to transform one commodity into another. For example, the role of a plant is to convert solar energy into chemical energy in the form of carbon based macro-molecules. The natural ecosystem then transports and consumes the macro-molecules to utilise the captured energy. Similarly, industrial networks exist to convert raw resources to manufactured goods, in a form suitable for final consumption. If these transformations are aggregated into quantities of a single commodity, the action of the networks are to move the commodity from one agent to another. In reality, individuals in the ecosystem and economic system have a list of needed commodities for their survival and fitness. Each individual has a different set of chemical or dietary needs, and goods and services requirements. Also, the availability and distribution of the resources are not homogeneous. A commodity suitable for final consumption is produced from a number of different commodities. This is why a large variety of transformation nodes are needed to maintain the overall ecosystem, both in a natural and an industrial sense.

A framework that represents multi-commodity without aggregation is needed, in order investigate the action of process networks. Modelling of a multi-commodity flow network is expected to describe interesting additional laws in ecology, namely the law of minimum (Sprengel, 1828), which predicts that the growth of a community of species is limited by the most constraining nutrient. This is a general law applicable to both ecology and economics.

Research in multi-commodity network can be be found in the 1970s (Wollmer, 1970), but not

all types of multi-commodity network are considered in this thesis. Specifically, transportation optimisation networks, involving delivery of multiple types of commodities in a network of fixed capacity are not considered. The application appears in communications and disaster relief logistic problems (Melo, Nickel, & Saldanha Da Gama, 2006; Olivera, Amoza, & Testuri, 2009). In these classes of problems, multiple types of commodities whose cost for transportations are varied, and the constraints are imposed on the minimum number of packages for each type of commodity through a constrained capacity network. This type of multi-commodity network is not of interest in this thesis because they do not involve the transformation property of the nodes. The commodities from the sources are not destroyed along the transportation, and no new commodities are created during the transportation. While the majority of multi-commodity studies focused on these immutable commodity delivery networks, some studies exist on transforming network nodes. Metabolic network of system biology and industrial ecology-metabolic studies are strong examples of this, even though they do not explicitly state they are multi-commodity network problems.

3.4.1 LCI

LCI is based on what is called a unit process node, which is the building block of the matrix representation (Heijungs & Suh, 2002). The unit process takes in several commodities in and produces one or more products. Usually a unit process node will have one product, but the framework is not limited to one product output. The LCI framework distinguishes between economic commodities and environmental commodities. Economic commodities are those produced and exchanged within the network nodes while the environmental commodities are those exchanged between the internal node and the external environmental nodes (figure 3.6). Each unit process is a linearized conversion process of inputs and outputs, which means that in

order to increase an output stream by a factor of 2, all the other input and output streams have to increase by a factor of 2 altogether. In terms of the economic theory, this is equivalent to the assumption of constant returns to scale.

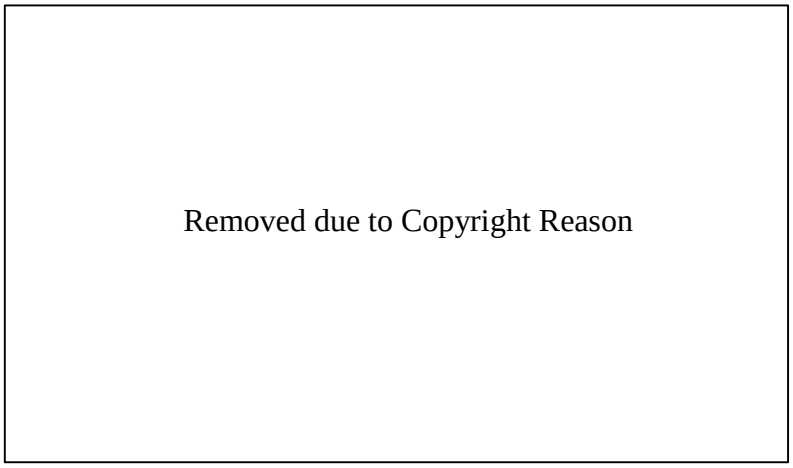

Figure 3.6. Unit process in LCI copied from (Heijungs & Suh, 2002).

A unit process is represented using a single column vector, whose entries show the technical ratios of commodity input and outputs. These vectors are stored in the form of databases (Frischknecht et al., 2005). The entries are fields measured from sample industries and typically averaged nationally or regionally (e.g. EU). Heijungs & Suh (2002) terms this vector the technical coefficient vector **p** of a unit process, whose elements are flow rates occurring within an observed unit time of operation (e.g. 1 year). This unit vector gives a direct material intensity requirement for the process. This is expressed in the following:

$$\mathbf{p} = \begin{bmatrix} \boldsymbol{a} \\ \boldsymbol{b} \end{bmatrix} = \begin{bmatrix} a_1 \\ a_2 \\ \vdots \\ a_n \\ b_1 \\ b_2 \\ \vdots \\ b_m \end{bmatrix} \tag{3.42}$$

where n and m are the numbers of economic and environmental commodity types in circulation. Heijungs & Suh (2002) uses a sign convention where output flows are positive, and the input flows are negative. This thesis will follow the same convention.

Industrial installations having a larger number of production lines using the same technology setup will have a larger throughput, although all the input and output flow rates will increase proportionally. This is expressed as the multiplication of scale factor:

$$\mathbf{Q} = \mathrm{s} \cdot \mathbf{p} = \mathrm{s} \cdot \begin{bmatrix} a_1 \\ a_2 \\ \vdots \\ a_n \\ b_1 \\ b_2 \\ \vdots \\ b_m \end{bmatrix} \tag{3.43}$$

where s is the scale factor. The scale factor can be increased by running the process longer, or by expanding the process facility of the same technology. In this thesis, the scale factor is alternatively termed as the *activity level* of the node.

Industrial and ecological systems consist a network of these unit processes, linked by the economic commodity flows. The cluster of unit processes combines together to produce a certain number of economic productions. The combined action of the cluster can be represented using a linear combination of the unit process vectors:

$$\mathbf{Q} = s_1 \cdot \boldsymbol{p_1} + s_2 \cdot \boldsymbol{p_2} + s_3 \cdot \boldsymbol{p_3} + \cdots = \begin{bmatrix} A \\ B \end{bmatrix} \begin{bmatrix} s_1 \\ s_2 \\ s_3 \\ s_4 \end{bmatrix} \tag{3.44}$$

where A and B are matrix components of the matrix formed by aligning the p-vectors column-wise. They are named the technological coefficient matrix A:

$$A = \begin{bmatrix} a_{11} & a_{12} & \cdots & a_{1n} \\ a_{21} & a_{22} & \cdots & a_{2n} \\ \vdots & \vdots & \ddots & \vdots \\ a_{n1} & a_{n2} & \cdots & a_{nn} \end{bmatrix} \tag{3.45}$$

Moreover, the environmental intervention matrix B:

$$B = \begin{bmatrix} b_{11} & b_{12} & \cdots & b_{1n} \\ b_{21} & b_{22} & \cdots & b_{2n} \\ \vdots & \vdots & \ddots & \vdots \\ b_{m1} & b_{m2} & \cdots & b_{mn} \end{bmatrix} \tag{3.46}$$

where each column represents the unit processes, and the second subscript is the index for the unit process. The total operation quantity is determined from the scaled sum of each unit.

If the desired economic commodity production output of the process cluster is given by the final demand vector **f**, where:

$$\mathbf{f} = \begin{bmatrix} f_1 \\ f_2 \\ \vdots \\ f_n \end{bmatrix}. \tag{3.47}$$

the scaled operation levels of the unit processes are determined by the following system of equation:

$$A \cdot \boldsymbol{s} = \mathbf{f} \tag{3.48}$$

$$\begin{bmatrix} a_{11} & a_{12} & \cdots & a_{1n} \\ a_{21} & a_{22} & \cdots & a_{2n} \\ \vdots & \vdots & \ddots & \vdots \\ a_{n1} & a_{n2} & \cdots & a_{nn} \end{bmatrix} \begin{bmatrix} s_1 \\ s_2 \\ \vdots \\ s_n \end{bmatrix} = \begin{bmatrix} f_1 \\ f_2 \\ \vdots \\ f_n \end{bmatrix} \tag{3.49}$$

where $\boldsymbol{s}$ is the scaling vector that defines the proper mix of the unit processes. The total environmental interactions produced is defined by the following matrix equation.

$$B \cdot \boldsymbol{s} = \mathbf{g} \tag{3.50}$$

where $\mathbf{g}$ is the total environmental intervention vector. Therefore, the technical coefficient matrix A and environmental intervention matrix B can be used directly to find the total environmental intervention from the final economic demand.

$$\mathbf{g} = B \cdot \boldsymbol{s} = B \cdot A^{-1}\mathbf{f} \tag{3.51}$$

where A^{-1} is the inverse of the technical coefficient matrix A.

This formulation appears to be mundane, but its implication enables the analysis of cyclic flow relations among the production network. Heijungs & Suh (2002, p. 13) demonstrates this with a hypothetical 2-process unit model example. Consider the production cluster including electricity generation and fuel production, whose direct material requirements are:

(1) A thermal electricity generation unit that produces 10kWh electricity with 2 L of fuel and emissions of 1kg of CO_2 and 0.1kg of SO_2

(2) A fuel production unit that produces 100 L of fuel with 50 L of crude oil, and emissions of 10kg of CO_2 and 2kg of SO_2.

Matrix A and B are defined as:

$$A = \begin{bmatrix} -2 & 100 \\ 10 & 0 \end{bmatrix} \sim \begin{bmatrix} \text{L of fuel} \\ \text{kWh of electricity} \end{bmatrix} \tag{3.52}$$

$$B = \begin{bmatrix} 1 & 10 \\ 0.1 & 2 \\ 0 & -50 \end{bmatrix} \sim \begin{bmatrix} \text{kg of } CO_2 \\ \text{kg of } SO_2 \\ \text{L of crude oil} \end{bmatrix} \tag{3.53}$$

where the columns represent the production ratios of the electricity generator unit and the fuel production unit. If the final output required in the economic system is 1000kWh of electricity

with no fuel remaining, the following economic flow criterion can be expressed (A**s**=**f**):

$$\begin{bmatrix} -2 & 100 \\ 10 & 0 \end{bmatrix} \begin{bmatrix} s_1 \\ s_2 \end{bmatrix} = \begin{bmatrix} 0 \\ 1000 \end{bmatrix} \tag{3.54}$$

The solution to this system of equation is $[s_1, s_2]^T = [100, 2]$. The environmental intervention generated from this operation level is (**g=** B**s**):

$$\boldsymbol{g} = B \cdot \boldsymbol{s} = \begin{bmatrix} 1 & 10 \\ 0.1 & 2 \\ 0 & -50 \end{bmatrix} \begin{bmatrix} 100 \\ 2 \end{bmatrix} = \begin{bmatrix} 120 \\ 14 \\ -100 \end{bmatrix} \tag{3.55}$$

This production cluster system would absorb 100 L of crude oil and emit 120 kg of CO_2 and 14 kg of SO_2 in order to produce 1000 kWh of electricity.

Solving the matrix equation for **s** is equivalent to the breakdown of the interconnected network flow problem into operations of direct inputs or outputs of individual nodes. The entire practice of LCI involves two stages of efforts. The first being the accumulation of a database of the direct requirements per unit process and the second is the synthesis calculation that brings together different unit vectors into a combined network model, facilitated by the automated LCA software. The first stage is done by LCI database vendors such as EcoInvent and the second stage is done by individual modellers using the drag-and-drop user interface provided by typical LCA software.

3.4.2 Supply-Use Table

A supply-use table is very similar to an LCI framework as it deals with a commodity-to-industry table. Figure 3.7 shows the structure of a supply-use Table. Following the convention of column-row indexing, supply table V consists of industries in the rows and products in the columns; meaning that industries are the source and the products are the destination.

Intermediate use table U and final use table Y are elements of the complete use table (figure 3.7). Transposing the supply table V orientates the table matrix in the same orientation of the technical coefficient matrix in LCI and prepares the addition of the intermediate use table U. The net production quantities of various products from the industry sectors are calculated as:

$$A = V^T - U \tag{3.56}$$

The desired final consumption of the products is the sum of the rows of the final consumption matrix Y:

$$f = \text{sum}(Y) \tag{3.57}$$

The physical environmental intervention quantities for a specific sector operation can be concatenated beneath the coefficient matrix A to form matrix B. Therefore, the direct mapping from a supply-use table to an LCI computation is possible, and the mathematical procedure used in LCI can be identically applied to the supply-use table. Further development of the theory will focus on the matrix formulation of LCI, and the application of the generalised mathematical framework in a supply-use context will be discussed in Section 3.6.

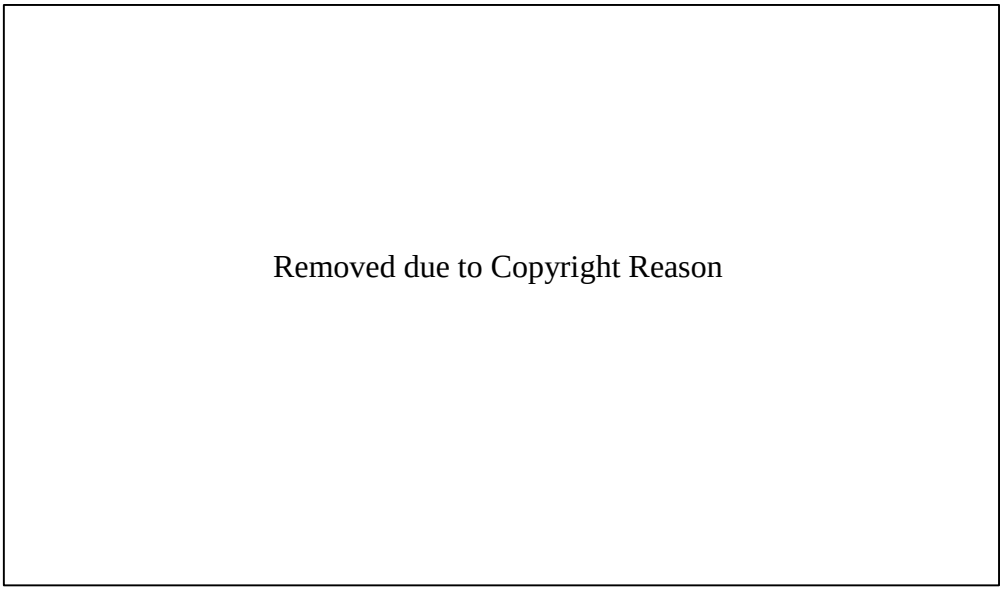

Figure 3.7. Simplified Supply-Use Table (Eurostat, 2012). Supply Table V, Intermediate Use Table U, and Final Consumption Table Y.

3.4.3 Generalisation and adding Constraint

The main usage of the LCI analysis can be summarised as to find the vector **g**, given the vector **f**. The core problem that is being addressed in this thesis is: ″is there a way to define the possible range of final product vector **f**, given the environmental constraints **g**?″ This is a reverse problem of the usual LCI problems. The core equations of the multi-commodity network framework are:

$$A \cdot \boldsymbol{s} = \mathbf{f} \tag{3.58}$$

$$B \cdot \boldsymbol{s} = \mathbf{g} \tag{3.59}$$

The solution to the formal LCI problem is to find vector **g**, given matrix A, B and vector **f**. In order to find the total external environmental impact vector **g**, scale factor vector **s** must be evaluated as an intermediate step.

The goal of a constraint-network sustainability problem is to find the feasible space for **s**, given matrix A, B, maximum levels of **g**, minimum levels of **f**, and maximum levels of **s**. Using the same numerical example from Section 3.4.1, the overall process equation for the fuel and electricity generation was:

$$P \cdot s = \begin{pmatrix} -2 & 100 \\ 10 & 0 \\ \hline 1 & 10 \\ 0.1 & 2 \\ 0 & -50 \end{pmatrix} \begin{pmatrix} s_1 \\ s_2 \end{pmatrix} = \begin{pmatrix} f_1 \\ f_2 \\ \hline g_1 \\ g_2 \\ g_3 \end{pmatrix} \tag{3.60}$$

The first and second columns represent the electricity and fuel production respectively. The rows, starting from the top, represent fuel, electricity, CO_2, SO_2 and crude oil balance. For example, if there is a limit of 1000 L/h on the maximum rate of the crude oil provision, then the crude oil supply can go as high as 1000. Since g_3 is a negative number, it can be represented by the inequality; $g_3 \geq -1000$. This imposes the restriction on the bottom part of the equation.

$$B \cdot s = g \tag{3.61}$$

More specifically,

$$\begin{pmatrix} 1 & 10 \\ 0.1 & 2 \\ 0 & -50 \end{pmatrix} \begin{pmatrix} s_1 \\ s_2 \end{pmatrix} = \begin{pmatrix} g_1 \\ g_2 \\ g_3 \end{pmatrix} \tag{3.62}$$

This poses the following inequality,

$$0s_1 - 50s_2 \geq -1000 \tag{3.63}$$

$$s_2 \leq 200 \tag{3.64}$$

Thus, the limit inequality existing in g, imposes constraints on the elements in the scale vector s, before solving the main equation. Furthermore, if the upper limit of CO_2 emission is 30 kg,

this will lead to the inequality:

$$1s_1 + 10s_2 \leq 30 \tag{3.65}$$

which should be reflected in calculating the final quantity needed. Despite the limit formulation being simple, it provides a firm mathematical foundation for the subsequent development of the societal metabolism limit. This hypothetical constrained problem is revisited with the analysis introduced in the next section in section 3.5.2.

This problem is reverse problem of the conventional LCI procedure. The conventional LCI procedure calculates the total environmental impact from the given final demand requirement. This problem defines the limits to the final demand that can be accommodated by the many environmental constraints. Each constraint is derived from considering resource availability or emission assimilation capability of the environment. The role of the environmental constraints defining the limits to the quantity of final demand products/services has not been not well recognised in conventional LCI analysis practices. This research pathway opens the way to extend the fill in the describe the system as well as

3.5 Analysis Suite

Two analysis suites provide good narratives for the absolute sustainability of the flow network system. The use of this suite is demonstrated in Chapter 6. The absolute sustainability of the networked systems is a systemic property which can be defined over the entire system. The constraints framework described in previous sections give rise to the system of inequations A**x** ≤ **b**, which results in an infeasible space with a geometric shape called convex polytope (Büeler, Enge, & Fukuda, 2000). Polytopes are the counterpart of polyhedras defined in high

dimensional space. The geometric properties of the feasible space gives rise to information about absolute sustainability involving interacting constraints.

3.5.1 Lesserre Algorithm of Feasible Volume

The resulting inequation forms a class of feasible space in the variable space of the operation levels of the nodes. This volume can be calculated and identified as a measure of absolute sustainability. The resulting volume arising from the set of linear inequations, is called convex polytope. The calculation method has also been established; Lasserre′s method is one of the exact volume calculation methods for high-dimensional polytopes (Büeler et al., 2000). It is a recursive algorithm which breaks down the high-dimensional geometric object to several lower dimensional ones.

Büeler et al. (2000) provides a review on the methods that calculate the exact volume of the feasible space generated by the polytopes. The exact volume computation is known to have a very high algorithmic complexity, and recent development has focussed on approximate solutions using statistical methods. For example, the volume of the feasible space for the biological, genetic metabolism involving hundreds of nodes was calculated using the Monte Carlo method (Braunstein, Mulet, & Pagnani, 2008).

Lasserre′s algorithm utilises a recursive method to calculate a given polytope (Büeler et al., 2000). This algorithm is based on the fact that the volume of an N-dimensional hypercone is determined with the following formula:

$$V = \frac{1}{N} Ah \tag{3.66}$$

where A is the area of the base hyperplane and h is the orthogonal height from the apex to the base hyperplane. For example, the formula for a 3D cone is V = 1/3Ah and for a 2D cone is V = 1/2Ah. For the 2D case, A is the length of the base side. For 4D cones and above, A will be the volume of hypervolumes of lesser dimensions.

A polytope is defined by a system of inequations, expressed as a matrix inequation, $A\mathbf{x} \leq \mathbf{b}$.

The polytope is defined in the span space of **x**, while the span space is $\mathbf{R}^n$. Matrix A has a size of m x n, and the row count m is equal to the number of inequations - the polytope in $\mathbf{R}^n$ has m faces. Note that this matrix A is different from the technical coefficient matrix A found in previous sections. The matrix A in this section is generalised expression of the matrix in a set of inequations. In terms of matrix formulation in previous sections, it is the combined matrix of A and B (i.e. matrix P in equation 3.60).

The core procedure of Lasserre′s algorithm is the triangulation of the given polytope. This involves the selection of an internal reference point O where the polytope is divided into m cones. The reference point can also be selected on one of the vertices of the polytope. In this case, some of the subdivided cones will have a volume of zero.

Figure 3.8. Triangulation stage of Lesserre Algorithm (Büeler et al., 2000).

Lasserre′s algorithm describes a recursive scheme that breaks down the volume of a given polytope into a sum of smaller volumes of the cones. The height b_i of the cone is the orthogonal distance to the face from point O. The calculation of the cone′s volume requires the volume of the base, which is another polytope but with dimension D-1. The base is defined by the intersection of the equation representing the face, and inequations derived from the neighbouring faces. The equation defines the infinite hyperplane that the face is in, and the inequations of neighbouring faces define the boundary of the face. The recursive procedure is described by the following equation:

$$Vol(d, A, b) = \frac{1}{d}\sum_{i=1}^{m}\frac{b_i}{\|a_i\|}Vol_i(d-1, A, b) \tag{3.67}$$

where Vol(d, A, b) = the volume of the polytope to be calculated, d = the dimension, A = the matrix representing the set of inequality, b = RHS vector, a_i = i^{th} row of A and Vol_i(d-l, A, b) = volume of the i^{th} face of dimension d-1. If the reference point O for subvolume computation is selected to be the origin, the distance to the face h becomes simplified to $b_i/|a_i|$, where |•| means the modulus.

In order to compute Vol_i(d-l, A, b), a projection scheme is used. The projection is a mathematical trick to simplify the computation since working in a subspace of V_i requires defining ~~a~~ new coordinate systems, which is burdensome to formulate. Instead, the subvolume and corresponding A and b are projected onto $\mathbf{R}^{n-1}$, with appropriate scaling. The first step is to choose which axis needs to be eliminated. The non-zero element in a_i, $a_{ij} \neq 0$ is chosen as the

pivot. The augmented matrix that represents the set of inequations [A|b] is row reduced using the pivot a_{ij}. This results in a new set of augmented matrix $[\tilde{A}|\tilde{b}]$, which defines a new system of inequations defined by $\tilde{A}\mathbf{x} \leq \tilde{b}$, but with m-1 constraints in R^{n-1}. This in effect is a projection of the subvolume V_i to R^{n-1} space where $x_j = 0$. The inequation $\tilde{A}\mathbf{x} \leq \tilde{b}$ now defines the subvolume $Vol_i(d\text{-}l, A, b)$ with a scaling factor; i.e. $Vol_i(d\text{-}l, A, b) = |a_i|/a_{ij}\ Vol(\tilde{d}, \tilde{A}, \tilde{b})$; where $\tilde{d}$ denotes $d - 1$. Substituting this scaling factor results in this recursive relation:

$$Vol(d, A, b) = \frac{1}{d}\sum_{i=1}^{m} \frac{b_i}{a_{ij}} Vol_i(\tilde{d}, \tilde{A}, \tilde{b}) \tag{3.68}$$

The recursive procedure is carried out down to the base case of $\tilde{d} = 1$, where the $Vol(\tilde{d}, \tilde{A}, \tilde{b})$ is a segment, which will be a simple intersection of $m - d + 1$ inequations of a scalar variable x; $\alpha_l x \leq \beta_l$, where α_l and β_l are the calculated coefficients by the recursive algorithm. The length of the segment is calculated by the following formula (Lasserre, 1983):

$$\max\left\{0, \left[\min_{\alpha_l>0}\left(\frac{\beta_l}{\alpha_l}\right) - \max_{\alpha_l<0}\left(\frac{\beta_l}{\alpha_l}\right)\right]\right\} \tag{3.69}$$

Lasserre′s algorithm has a very high time-complexity, in the order of O(n!) (Büeler et al., 2000), but computation of dimensions less than 100 can be done easily using the modern computer. The implementation code was written in MATLAB and is given in Appendix A.

3.5.2 Worked Example of Lesserre Algorithm Procedure

This framework can be naturally applied to the generalised framework of multi-commodity flow network with constraint. Following the introduction of the 2-stage electricity generation system in section 3.4.3, as an example, where there is a set of constraints for CO_2, SO_2 emissions and crude oil availability:

$$P \cdot s = \begin{pmatrix} -2 & 100 \\ 10 & 0 \\ \hline 1 & 10 \\ 0.1 & 2 \\ 0 & -50 \end{pmatrix} \begin{pmatrix} s_1 \\ s_2 \end{pmatrix} \begin{bmatrix} = \\ = \\ \leq \\ \leq \\ \geq \end{bmatrix} \begin{pmatrix} f_1 \\ f_2 \\ \hline g_1 \\ g_2 \\ g_3 \end{pmatrix} \quad \begin{matrix} \cdots \text{ electricity} \\ \cdots \quad \text{fuel} \\ \cdots \quad CO_2 \\ \cdots \quad SO_2 \\ \cdots \text{ crude oil} \end{matrix} \tag{3.70}$$

Let us assume hypothetically, the pollutant emissions and resource availability, CO_2, SO_2 and crude oil are subject to upper constraints, 300kg/h, 15kg/h and 1000L/h respectively. The system of inequation becomes:

$$P \cdot s = \begin{pmatrix} -2 & 100 \\ 10 & 0 \\ \hline 1 & 10 \\ 0.1 & 2 \\ 0 & -50 \end{pmatrix} \begin{pmatrix} s_1 \\ s_2 \end{pmatrix} \begin{bmatrix} = \\ = \\ \leq \\ \leq \\ \geq \end{bmatrix} \begin{pmatrix} f_1 \\ f_2 \\ \hline 300 \\ 45 \\ -1000 \end{pmatrix} \quad \begin{matrix} \cdots \text{ electricity} \\ \cdots \quad \text{fuel} \\ \cdots \quad CO_2 \\ \cdots \quad SO_2 \\ \cdots \text{ crude oil} \end{matrix} \tag{3.71}$$

The negative signs at the fifth row represents the consumptive use of the crude oil. The direction of the inequation for the fifth row was adjusted to match the inverse nature of the flow. The three constraints and the non-zero constraint form the feasible space in **s**-space (**s** = $(s_1,s_2)^T$; the level of operation for refinery and power generation plants).

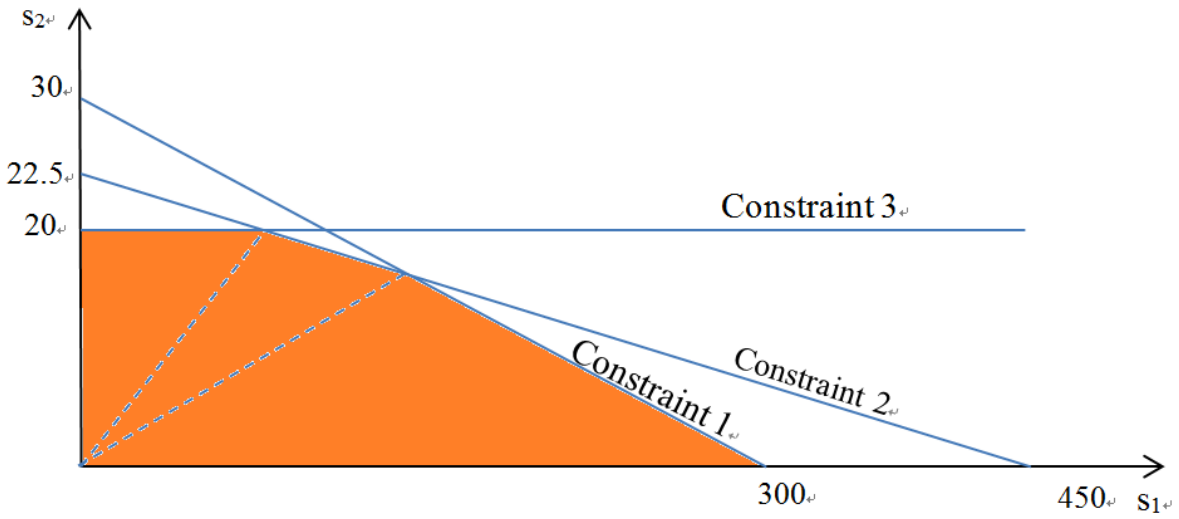

Figure 3.9. Example feasible space for 2-stage electricity generation system.

The volume of the feasible space represents the freedom of the operator to choose the operation levels of the two production nodes to match the desired outputs (in this case the electricity generation). The Lasserre algorithm recognises the problem as enclosed by 5 constraints:

$$As \leq b \tag{3.72}$$

$$\begin{pmatrix} 1 & 10 \\ 0.1 & 2 \\ 0 & 50 \\ -1 & 0 \\ 0 & -1 \end{pmatrix} \begin{pmatrix} s_1 \\ s_2 \end{pmatrix} \leq \begin{pmatrix} 300 \\ 45 \\ 1000 \\ 0 \\ 0 \end{pmatrix} \tag{3.73}$$

where the third row was multiplied by -1 so that the direction of the inequation was inverted to match the direction of the Lasserre algorithm. The fourth and fifth rows were added as the non-zero constraints (i.e. the volume must be above s_1 and s_2 axes). The algorithm first breaks the feasible space into three triangles with non-zero volume from the origin. The feasible space has dimension of d=2. Thus the equation 3.68 becomes:

$$Vol(2, A, b) = \frac{1}{2} \sum_{i=1}^{3} \frac{b_i}{a_{ij}} Vol_i(1, \tilde{A}, \tilde{b}) \tag{3.74}$$

where substitution of d=2, m=3, $\tilde{d} = 1$ were made. The summation is made for the three broken areas. When the summation symbol is expanded:

$$\begin{aligned} Vol(2, A, b) = \frac{1}{2} \frac{b_1}{a_{1j}} Vol_1\left(1, \tilde{A}, \tilde{b}\right) + \frac{1}{2} \frac{b_2}{a_{2j}} Vol_2\left(1, \tilde{A}, \tilde{b}\right) \\ + \frac{1}{2} \frac{b_3}{a_{3j}} Vol_3(1, \tilde{A}, \tilde{b}) \end{aligned} \tag{3.75}$$

Here, the b_1,b_2,b_3 are the first three entries found in the vector **b**. The entries a_{ij} are the first

non-zero entry found in i^{th} row of matrix A. For instance, the first non-zero entry for the first row of matrix A is a_{11}=1; the first non-zero entry for the second row is a_{21}=0.1; the first non-zero entry for the third row of matrix A is a_{32}=50. The a_{11},a_{21},a_{32} are used as pivot to calculate the parameters for the subspace volumes (i.e. Vol_1,Vol_2,Vol_3). Entering these values in equation 3.69 yields:

$$Vol(2,A,b) = \frac{1}{2}\frac{300}{1}Vol_1(1,\tilde{A},\tilde{b}) + \frac{1}{2}\frac{45}{0.1}Vol_2(1,\tilde{A},\tilde{b}) + \frac{1}{2}\frac{1000}{50}Vol_3(1,\tilde{A},\tilde{b}) \tag{3.76}$$

The coefficients b_i/a_{ij} contain information about the heights of the divided triangles and Vol_i containt the information about the base lengths. $\tilde{A},\tilde{b}$ for the bases are found from the row reduction with a_{11},a_{21},a_{32} regarded as pivots. For instance, row reducing A and b with a_{11} regarded as pivot yields:

pivot a_{11} $\qquad\qquad$ Ã $\quad$ b̃

$$\begin{pmatrix} 1 & 10 & 300 \\ 0.1 & 2 & 45 \\ 0 & 50 & 1000 \\ -1 & 0 & 0 \\ 0 & -1 & 0 \end{pmatrix} \rightarrow \begin{pmatrix} 1 & 10 & 300 \\ 0 & 1 & 15 \\ 0 & 50 & 1000 \\ 0 & 10 & 300 \\ 0 & -1 & 0 \end{pmatrix} \tag{3.77}$$

The subsection of the matrix is taken as the new set of A and b for the volume calculation for the base. This particular base has the dimension of d=1 and to calculate its volume, one must rely on equation 3.69 for 1-dimensional volume according to the algorithm. At this base case, the set of inequation A**s** ≤ **b** is a set of four simple inequations:

$$\begin{cases} 1s_1 \leq 15 \\ 50s_1 \leq 1000 \\ 10s_1 \leq 300 \\ -s_1 \leq 0 \end{cases} \tag{3.78}$$

The first three inequations have positive coefficients for s_1 and the last row has negative coefficient for s_1. This means that one of the first three rows define the upper bound for s_1 and the last row define the lower bound. This is why the algorithm had to distinguish between positive and negative coefficients of the matrix A for the base case. According to the equation 3.69,

$$\text{base case volume} = \max\left\{0, \left[\min_{\alpha_l>0}\left(\frac{\beta_l}{\alpha_l}\right) - \max_{\alpha_l<0}\left(\frac{\beta_l}{\alpha_l}\right)\right]\right\} \tag{3.79}$$

It uses the ratio b_i/a_i for the rows with positive a_i and the rows with negative a_i to calculate the base case volume. For the case of equation 3.78, it becomes:

$$\text{base case volume} = \max\left\{0, \left[\min_{\alpha_l>0}\left(\frac{15}{1}, \frac{1000}{50}, \frac{300}{10}\right) - \max_{\alpha_l<0}\left(\frac{0}{-1}\right)\right]\right\} \tag{3.79}$$

$$= \max\left\{0, \left[\min_{\alpha_l>0}(15,20,30) - \max_{\alpha_l<0}(0)\right]\right\} \tag{3.80}$$

$$= \max\{0, [15-0]\} = 15 \tag{3.81}$$

This is the volume for the Vol_1. Similar procedure can be performed for Vol_2 and Vol_3:

$$\text{pivot } a_{21} \qquad\qquad \tilde{A} \quad \tilde{b}$$
$$\begin{pmatrix} 1 & 10 & 300 \\ 0.1 & 2 & 45 \\ 0 & 50 & 1000 \\ -1 & 0 & 0 \\ 0 & -1 & 0 \end{pmatrix} \rightarrow \begin{pmatrix} 0 & -10 & -150 \\ 1 & 20 & 450 \\ 0 & 50 & 1000 \\ 0 & 20 & 450 \\ 0 & -1 & 0 \end{pmatrix} \tag{3.82}$$

$$\text{pivot } a_{32} \qquad\qquad \tilde{A} \quad \tilde{b}$$
$$\begin{pmatrix} 1 & 10 & 300 \\ 0.1 & 2 & 45 \\ 0 & 50 & 1000 \\ -1 & 0 & 0 \\ 0 & -1 & 0 \end{pmatrix} \rightarrow \begin{pmatrix} 1 & 0 & 100 \\ 0.1 & 0 & 5 \\ 0 & 1 & 20 \\ -1 & 0 & 0 \\ 0 & 0 & 20 \end{pmatrix} \tag{3.83}$$

The sets of inequations for Vol_2 and Vol_3 become:

$$\text{Vol}_2: \begin{cases} -10s_1 \leq -150 \\ 50s_1 \leq 1000 \\ 20s_1 \leq 450 \\ -s_1 \leq 0 \end{cases}, \quad \text{Vol}_3: \begin{cases} 1s_1 \leq 100 \\ 0.1s_1 \leq 5 \\ -1s_1 \leq 0 \\ 0s_1 \leq 20 \end{cases} \tag{3.84}$$

The volumes using the equation 3.79 become:

$$\text{Vol}_2 = \max\left\{0, \left[\min_{\alpha_l>0}\left(\frac{1000}{50}, \frac{450}{20}\right) - \max_{\alpha_l<0}\left(\frac{-150}{-10}, \frac{0}{-1}\right)\right]\right\} = 5 \tag{3.85}$$

$$\text{Vol}_3 = \max\left\{0, \left[\min_{\alpha_l>0}\left(\frac{100}{1}, \frac{5}{0.1}\right) - \max_{\alpha_l<0}\left(\frac{0}{-1}\right)\right]\right\} = 50 \tag{3.86}$$

The calculation for Vol_3 used only three ratios rather than four. The A-coefficient of the last row for Vol_3 (Equation 3.84) was zero. For this row, whatever the value s_1 was, the inequtioni would have been true. The coefficient became zero because the base of the third triangle was parallel to the s_1 axis. Whenever there are two parallel constraints, at least one of the A-coefficient at the base case becomes zero. When such incident occurs, the algorithm must check if the inequation is true or false. If the inequation containing zero A-coefficient is false, the base volume will be zero because it will make the set of inequation false. For this case, the inequation was true and the calculation can carry forward without adding the ratio from the inequation. This problem of parallel constraints were addressed in the implementation of the Lasserre algorithm in the MATLAB code. Substituting these results into equation 3.76:

$$Vol(2, A, b) = \frac{1}{2}\frac{300}{1} \cdot 15 + \frac{1}{2}\frac{45}{0.1} \cdot 5 + \frac{1}{2}\frac{1000}{50} \cdot 50 = 3875 \tag{3.87}$$

The abovementioned example had static constraints that do not evolve with time. In real life, the constraints may change as external environmental and social conditions change. For example, the crude oil prices may rise due to global reserve being depleted in a long term. If there is a fixed financial budget allocated for the 2-stage system, the crude oil constraint will

become more stringent. Worsening of global environmental condition may force local agencies to place more stringent environmental targets for CO_2 and SO_2 emissions. Mostly likely, the population growth of the region will demand higher minimum electricity generation requirement to support the growth. The case study in chapter 6 addresses the dynamics of the constraints and their implications on the feasible volumes of a networked resource flow system arrangements.

3.6 Context of Applications

The above-mentioned extension of the pre-existing matrix based flow network has potential in representing the current environmental sustainability problems arising from the constrained supply of raw materials and emission assimilation capacities. In this section, the contexts of the possible applications are only briefly described. The first two aspects (Section 3.6.1 and 3.6.2) of the application are demonstrated in the fourth paper included in the later part of the thesis. The aspects described in Section 3.6.3 are left as a future project, as they require more substantial development of the theory.

3.6.1 Multiple constraints in the same regional scale

A regional system can be modelled using input-output models. The input-output model can incorporate the quantity of the raw resources converted to economic production. The direct application of the model is to calculate the limit to the industrial and environmental productions, from the available resources for the regional system. Combined with the available technology and the investment commitment to the production system, a more accurate picture of the economic production potential of the region can be evaluated.

In order to evaluate the regional resources, the spatial database that specifically addresses a single type of resource must be utilised. Usually, the small scale resource constraints can be aggregated to a regional level sum to be entered to the mathematical framework.

3.6.2 Multiple constraints in different regional scale

Some of the resources and emissions that have high mobility may not be well associated with the region of interest, but can be for a larger spatial scope. For example, the significant impacts of CO_2 emission occur at the global planetary level, and the constraint level of CO_2 emissions only makes sense at the global level. Another example is the transboundary water resource allocation problem, where the administrative boundary (e.g. country) is smaller than the natural spatial boundary of the watershed. This requires multiple scale level modelling, involving the embedding of network models inside a larger, background model of the environmental, global model. Incorporating the spatial scale character of the networks will be left to future theory development. The approach taken will be the multi-regional input-output analysis framework.

Multi-regional application extends the multi-commodity formulation described above. A region contains an aggregate of networks. Majority of the input-output networks studied so far have had a country-level spatial scale. With the recognition of the openness of country level input-output through international trades, there is an academic trend in developing a multi-regional input-output analysis (MRIO), which may provide the basis for the multi-regional constrained network analysis (B. R. Ewing et al., 2012; C. Zhang & Anadon, 2014). This creates an opportunity to investigate the constraints that have different scales, such as the environmental constraints. Environmental constraints range from local, regional, to global scale constraints. For example, the greenhouse gas emission CO_2 has constraints that can only

be defined at the global planetary scale. Waterborne contaminant emissions are generally determined over regional watershed scales. The constraints of mined resources or solid waste emission capacities are defined by site specific studies. These constraints of different scales are expected to be integrated into the MRIO.

3.7 Concluding remarks

This chapter has developed a suite of mathematical tools for analysing the combined effect of constraints and available technology. The mathematical tool was an extension of the pre-existing environmentally extended matrix based input-output and LCI frameworks which shared the common mathematical structure to represent the flow network. While current flow network frameworks are only used to estimate or project the total raw resources and emissions created by society, this information can be compared with the constraints of resources availability, emission assimilation capacity, and productive node capacity. The inclusion of the constraints was done by imposing inequality, similar to linear programming. The resulting feasible space for the sustainable network node operation levels within the constraint conditions is known as a convex polytope, and the geometrical volume of the polytope represents the size of the decision space available for the network. Generally as the network matures, the available decision space decreases as it closely approaches the capacity allowed by the constraints. This tool is useful when it comes to investigating the effect of the combined effect of multiple resource/emission constraints and their interactions with the technological efficiency improvements of the production process (both ecological/industrial). The demonstration of how this tool could be applied in a real life situation is presented in Chapter 6 of this thesis. Future potentials and possible extensions of the tool presented in this chapter

is further discussed in the conclusion chapter of this thesis.

Chapter 4 Conceptual Model for Waiheke Island Water Resource System

Chapter 3 developed the theoretical framework of the matrix based measurement of sustainability. This framework is applied to the Waiheke Island water resource in Chapter 4,5 and 6. Chapter 4 provides the description of the application procedure and the island water resource system. The conceptual model (the network) is described, and the technical coefficients for the matrix are determined (i.e. determination of the matrix A). Chapter 5 provides the case studies that yielded the constraint values for the matrix formulation (i.e. determination of the constraint vector b; equation 3.58-59). Lastly, Chapter 6 synthesises the values determined in Chapter 4 and 5 to create the matrix description of the water resource system and demonstrates the dynamics of the sustainability measure with respect to the population growth projection of the island.

4.1 Overview of water resource problems on the island

4.1.1 Waiheke Island Overview

Waiheke Island is being utilised as a suburban residential area near Auckland which is the most populous city in New Zealand. Recent census indicate that there are 8,420 permanent residents as of year 2013 (SNZ, 2015). The main commercial operations on the island include vineyards, olive groves and other small farms as well as tourist attractions during the summer holiday. The island is a tourist destination with beautiful scenaries, and the population during summer increases up to 30,000 (Baragwanath, 2010). Along the coasts, there are non-abstractive use of

water, beaches and mussel-oyster aquaculture (WRCG Ltd, 2004). The ferry service transports passengers from downtown to the island's main wharf within 40 minutes. Electricity is connected via an undersea cable across the Tamaki Strait (Chiaroni, Hewitt, & Hailes, 2007), but no water supply main has been connected to the mainland (WRCG Ltd, 2004).

The island has a land area of 92km^2 with a rough topography, and the catchment areas are small, which is typical for small islands. Only around 14% of the island is suitable for urbanisation based on the GIS slope analysis. Many catchments do not have well-developed streams - this means construction of dams is not an appropriate option for water resource management. Streams are also intermittent due to shallow perched aquifer feeding the streams (WRCG Ltd, 2004). Low-density development favours distributed strategies over centralised options. Wastewater systems on Waiheke Island mostly rely on an onsite septic tank-irrigation system. As a result, the unit cost of water infrastructure service is more expensive than typical centralised systems in the urban area (Cape Cod Commission, 2013; Maurer, Rothenberger, & Larsen, 2005). The rough topography limits the urban expansion as well as land availability for implementation of onsite wastewater system. The island frequently experiences water shortages during the summer period (November to March) where there is little rainfall and a large number of tourists visiting the island during holiday.

4.1.2 Island-wide Hydrology

The national climate database provides the record of the daily time-series rainfall since 1 April 1914 (NIWA, 2014). The average annual rainfall for the past 20 years was 1,265mm, and the trend of annual total rainfall is increasing at a slow rate of 5.24mm/year (0.4%/year; Figure 4.1). The period starting from November to March is considered to be the dry season of the

year and the rest as a wet season (Figure 4.2).

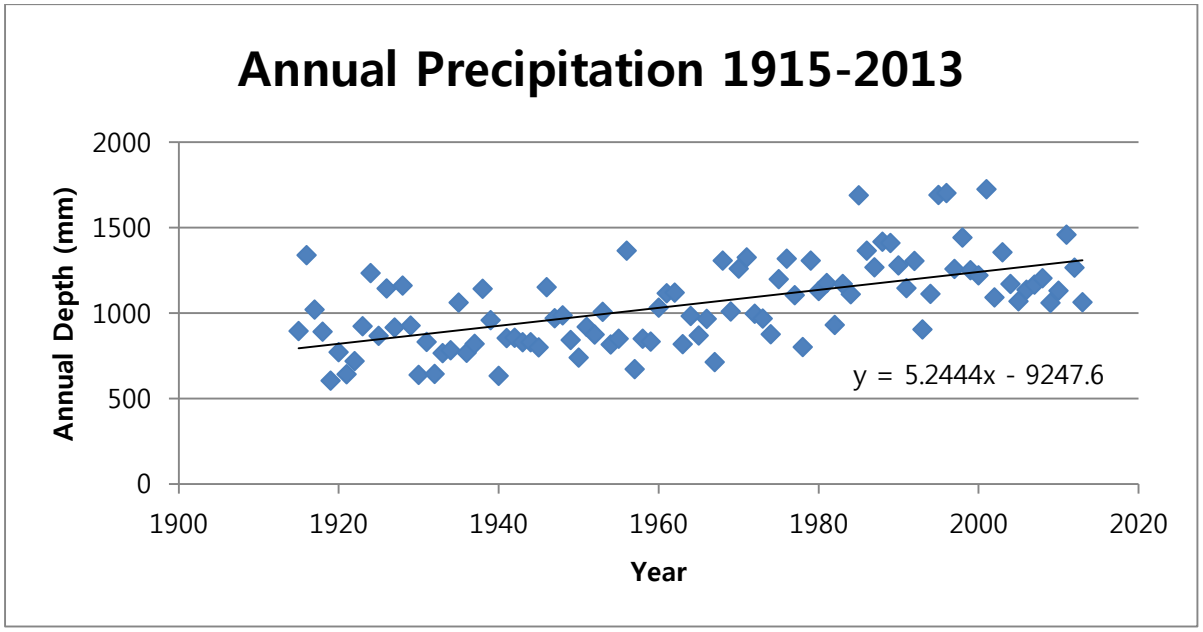

Figure 4.1 Trend in annual precipitation. The annual trend is positive, meaning the island is receiving more freshwater on average.

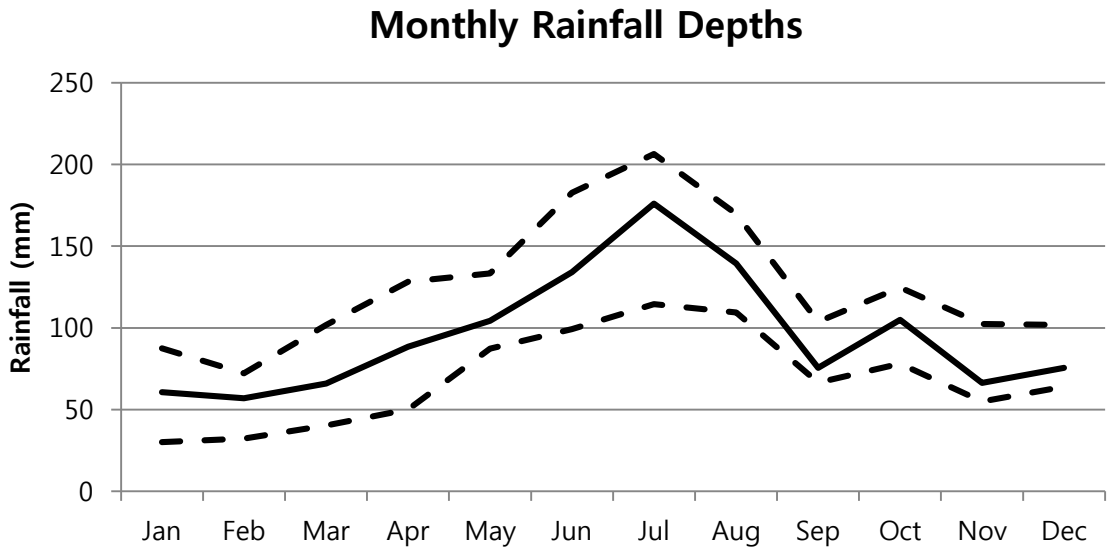

Figure 4.2. Intra-annual Rainfall Distribution. Plotted are median (solid) and quartiles (dashed) of recent 20-year monthly rainfalls. Recent 20-year average annual rainfall depth was

1265mm/year.

The statistics of annual precipitation shows a modest trend in the increase of total annual rainfall (Figure 4.1). This result is in line with the additional statistical analysis of dry-spell lengths (Figure 4.3). From the 95-year daily time series data, the frequency of dry-spell durations, which is defined as a number of consecutive days having less than 3mm daily precipitation, was counted. From the frequency counts, statistics for the return period could be obtained (Figure 4.3). The return period curve of dry-spells were obtained for the years 1914-1980 (blue) and the years 1981-2013 (red). Overall, the two curves were similar but the red curve (the recent 33 years) showed larger return periods for the 40-day to 50-day dry-spell durations. This means that the recent years experienced a smaller number of prolonged dry-spells. This finding is contrary to the common belief that the dry seasons are becoming drier, with longer days. The experiences of the water shortage during the summer period is more likely to be caused by the recent population growth than the physical climate changes. This result is only preliminary and has not undergone a more rigorous statistical test. More analysis is needed to establish solid evidence for the island's climate change trend. For the purpose of this case study, it will be assumed that there will be no significant climate change in short to mid-term time horizon (in the order of two or three decades).

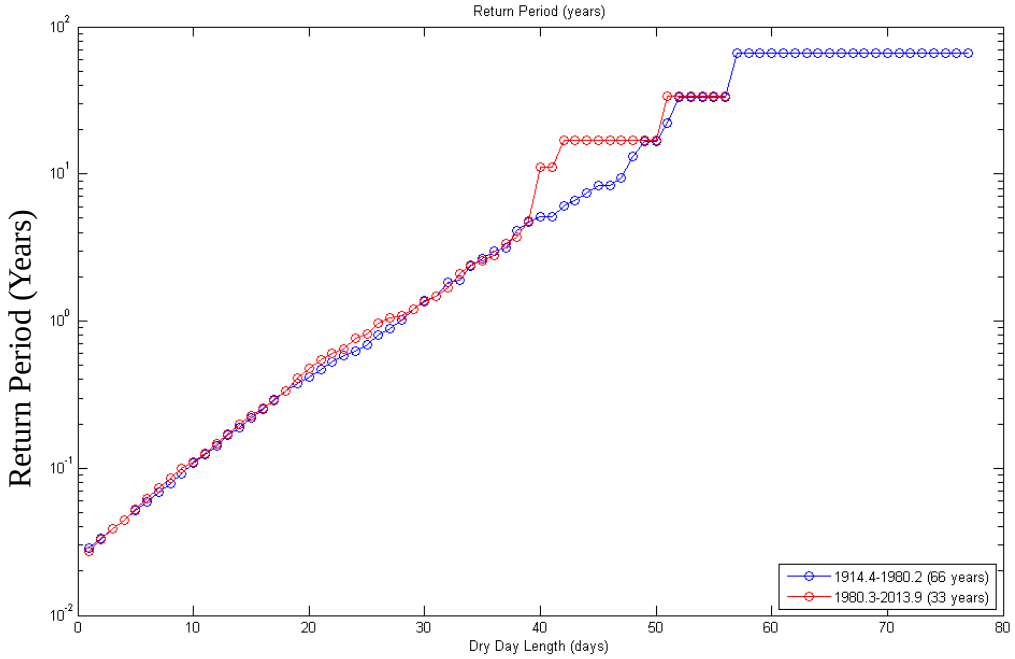

Figure 4.3 Return Period Analysis of Dry-spell Length. Long dry-spell (40-50 days long) are returning less frequently in recent year period (1980-2013) than an earlier period (1914-1979).

An island-wide water balance model (Figure 4.4) constructed from the available data from previous hydrological studies and statistics (ARC, 2008; SKM, 2007; Wujkowski, 2004) shows that the proportion of hydrological flow to the human system is only a small fraction (0.9%) of the annual rainfall. The main reason behind this is due to the rough topography prohibiting urban development in many parts of the island, while only a fraction of the western area of the island is currently developed. Current rain harvesting relies on the roof areas, and the catchment area is small compared to the overall area of the island.

The local Government (Auckland Council) regulates the abstraction of large quantities of freshwater from surface water bodies and aquifers through resource consents. Any construction

of groundwater bores with a yield greater than 5m^3/day requires a resource consent. The owners of the bores need to report the actual use volume every year. Natural hydrological component flows of infiltration rates were determined from the previous hydrogeological studies (SKM, 2007; Wujkowski, 2004). SKM (2007) reports the water balance ratio from a calibration study on a stream gauge and soil moisture time series; of the total annual precipitation, 64% was returned to the atmosphere via evapotranspiration, 31% became stream run-off, and only 5% infiltrated into the aquifer below the root zone. When the 5% infiltrate below the root zone, it does not emerge back to the surface as streams or through evapotranspiration. This proportion returns to the sea via groundwater-seawater interface mixing (Michael, Mulligan, & Harvey, 2005) and submarine groundwater discharge (Burnett, Taniguchi, & Oberdorfer, 2001).

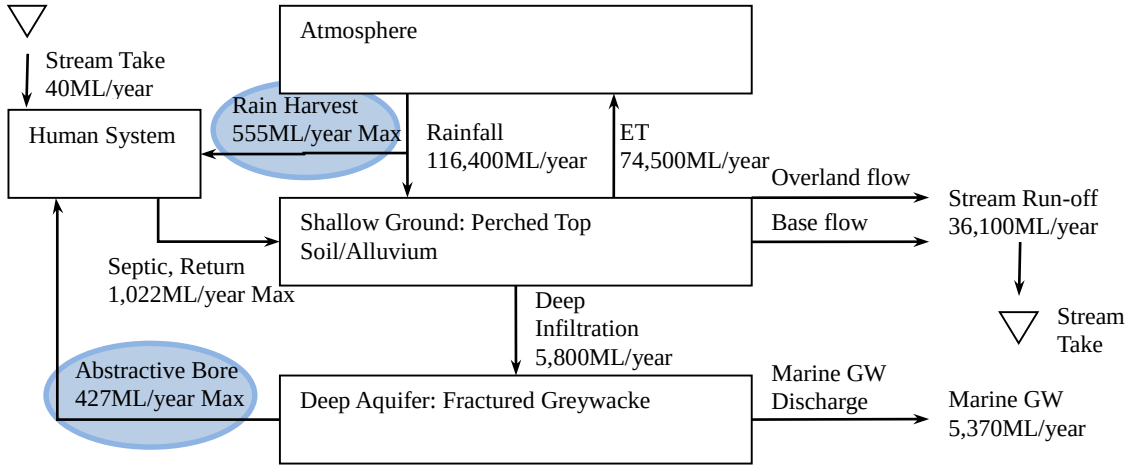

Figure 4.4. Island-wide Hydrology Components. GW=Groundwater, ET = Evapotranspiration.

4.1.3 Water Resource Issues

The water resource issues can be divided into three categories: 1) water supply, 2) wastewater and 3) SW-GW interaction issues. For most Waiheke Island residents, rooftop rainwater harvest

(RWH) is the primary source of freshwater. When this source fails, which is often the case in the dry summer, aquifer pumps supplement the water supply deficit. The island inhabitants have been experiencing troubling dry spells and shortages repeatedly in the past several years. The problem of any prolonged dry spell is compounded by the increasing summer holiday visitors, which coincide with the dry spell period. While the aquifer pumping is considered as the secondary emergency source of freshwater to supplement primary rainwater harvesting, the island aquifer is considered to be an "intensely exploited aquifer" by the Auckland Council (2008). With the island's economic and demographical growth, the stress on the aquifer pumping is expected to grow in the future. This creates concerns among the public regarding the groundwater capacity. Some of the residents have lodged complaints that their bores are beginning to produce brackish water, voicing their concerns regarding the saltwater intrusion on the island (personal communication with a groundwater consent manager of the region).

There is a debate on the island whether the transition from an onsite septic system strategy to a centralised sewer-treatment plant strategy should happen. Both centralised and distributed wastewater systems ~~have~~ both strengths and weaknesses and the consideration of which strategy to be implemented regionally depends on the financial capability and the population density of the region (U.S. EPA, 2002). Centralised and distributed wastewater systems share the common treatment concept but have a different scale, efficiency and location of the discharge. On average, the centralised system has a higher cost-to-volume ratio efficiency due to the economy of scale. However, they suffer from high capital investments and a lack of adaptability. Centralised systems are built with a high treatment capacity in advance, and a large proportion of the capacity remains idle until the population catches up to the capacity. This in effect creates an overhead from the construction lead time and the actual efficiency is

lower than anticipated (U.S. EPA, 2002). The construction and maintenance of sewers per capita are costly if the population density of the region is low. While the centralised system is a more cost effective option for high-density regions, distributed options are more cost effective and appropriate for areas with lower population growth rates and densities,

Hence it is important to question under which population desntiy is it appropriate to implement a centralised wastewater option rather than a distributed one. (U.S. EPA, 2002). The study area, Waiheke Island, is a peri-urban area that was previously considered rural and had no centralised system installed. Due to some instances of septic system failures, the regional council considered a centralised sewer option for the island. The residents strongly opposed this idea in order to protect their autonomy (URS, 2006). The expansion of the sewer collection area was postponed permanently after the initial installation on a central commercial portion of the island connected to a small size treatment plant with a servicing capacity of $80m^3$/day (URS, 2006). While the debate on whether a centralised or an onsite system strategy was to be used is mainly political in nature, it is appropriate to factor in scientific and engineering information to the discussion.

The interaction between the surface water and the deep aquifer poses important issues in groundwater management. The wastewater strategy employed by the island is an onsite septic tank irrigation system. There might be cases where a contaminant from the septic tank may pollute the aquifer, which may lead to a public health hazard. However, the aquifer is confined by a thick clay-silt layer throughout the island, effectively shielding the deep aquifer from the surface water. The implication of having this thick confining layer is the separation of the surface or near-surface hydrology and the deep confined aquifer hydrology - which works for and against the availability of groundwater. First, in terms of quantity, the recharge will be

remarkably slow leading to a sensitive hydraulic head response to pumping. However, the aquitard layer will restrict the recharge at a constant rate throughout the year, and the recharge rate is not affected by seasonal fluctuation of the precipitation. Secondly, the groundwater quality is expected to be more or less protected from surface loading due to the confining layers. However there were no formal studies carried out to confirm this contaminant shielding effect. Several groundwater quality testing results filed in the Auckland Council file room showed only trace amount of contaminants pertaining to this expectation. Ongoing monitoring of the water quality of pumped groundwater from commercial use and bores ensures the public safety of groundwater. There has been no report of a water quality problem derived from a surface contamination yet. Setback distance of bore locations from the irrigation fields is being enforced. There could be incidents where the damaged bore might introduce contaminants directly to the aquifer.

4.1.4 Human Hydrology Component

Three groups of users, residential, agricultural and commercial uses were identified. Water use intensities per activity unit and unit quantities for each use component were obtained from literature, databases, government statistics and assumptions (see Table 1 for source references). The conceptualisation of the water demanding activities was derived from the inspection of business demographic statistics, aerial photography and site visits. The current estimate of the water use has room for improvement, but it is expected that changes to estimates via refinements would be less than 10% of the current estimation levels. Despite this uncertainty, the water use model still serves as an adequate ground for building subsequent models. The resulting use component model is presented in Figure 4.6. The annual water use model (Figure 4.6) is translated into a monthly schedule of daily use rates for RWH simulation later in Chapter

5 (Table 5.5).

The water use rates of some components are relatively constant throughout the year; indoor residential uses, irrigation/livestock and commercial activities except for hotel/accommodation were considered to be steady throughout the year whereas residential outdoor uses, irrigation for vineyard, vegetables, fruits and hotel/accommodation were modelled to be varied with season. This variability reflected the seasonal vegetation requirement change and the tourism population peaking during the summer period. Due to tourism, the accommodation sector was assumed to exhibit seasonal variation. The resulting daily use rates for each month were entered to the next model, the daily-step harvest-pump simulation (see Table 5.5 for the resulting model, water use schedule).

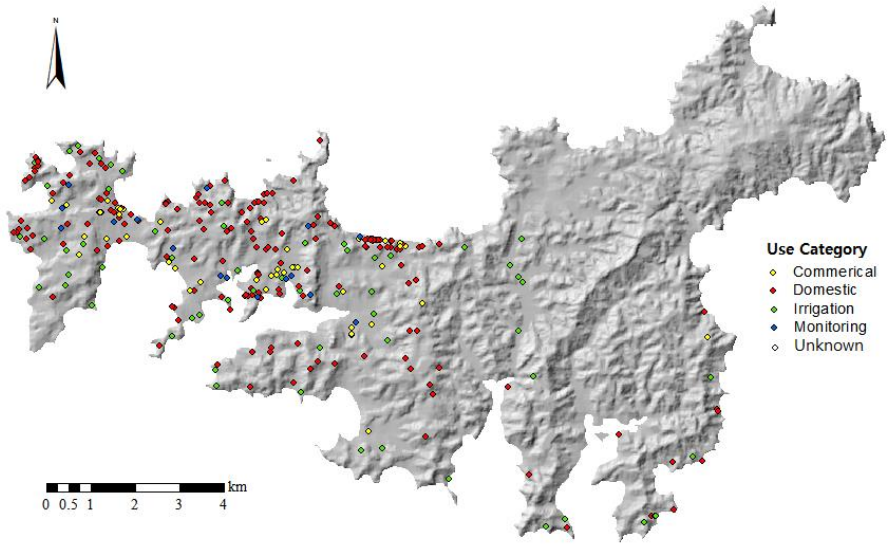

Figure 4.5. Current Bore distribution. Most developments are concentrated on the western side of the island.

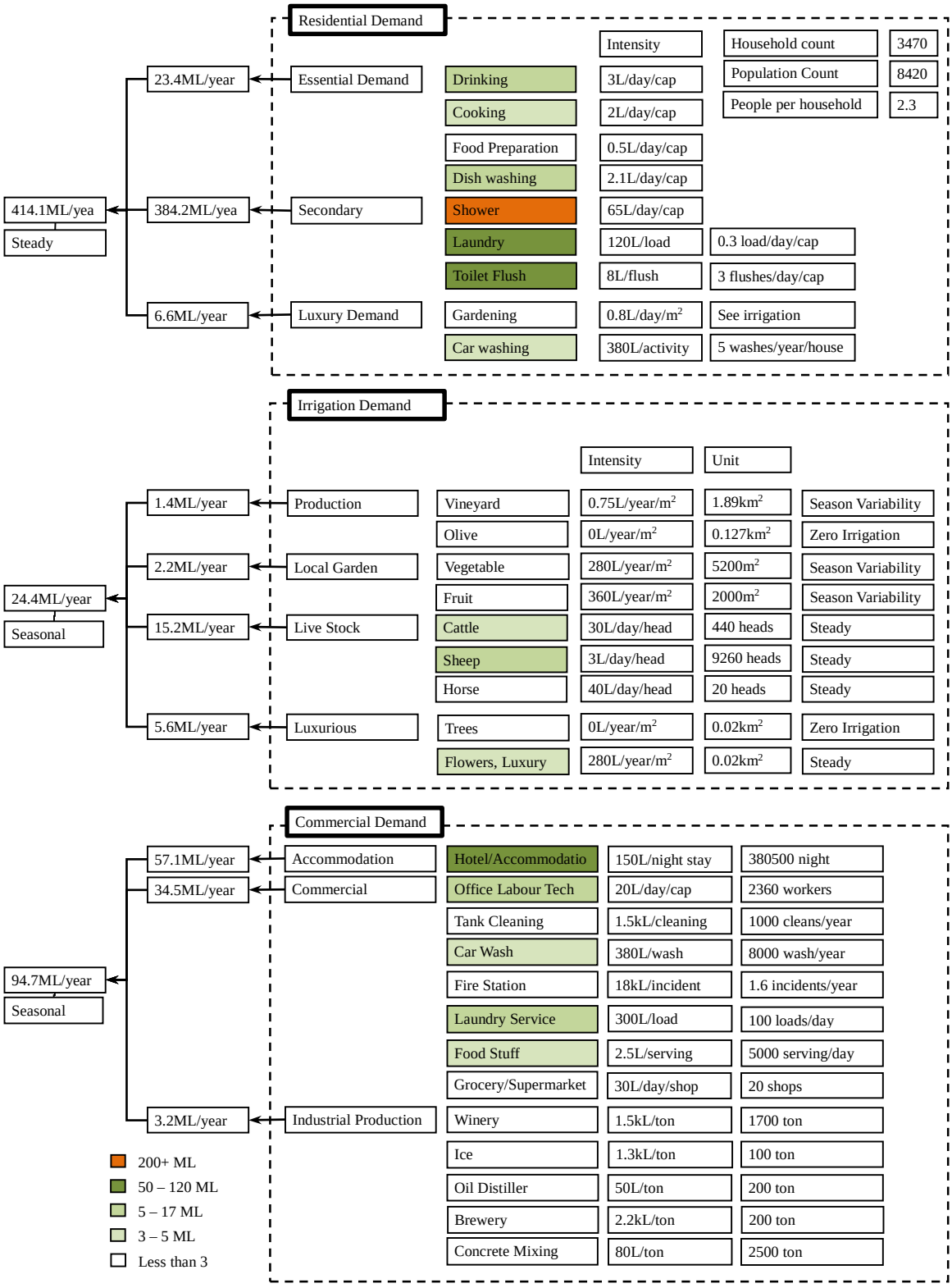

Figure 4.6. Water Use Components. The shower was the heaviest single user of the water on the island. Hotel and accommodation sector had the most drastic seasonal fluctuation. 60% of

its annual use was modeled to occur in 10 days of summer holidays at 3ML/day based on the visitor counts estimate.

4.2 Application Methodology of the Theory

To apply the theory to practice, there are suggested four stages of work to develop a systematic model of the region (Figure 4.7). The first step is to create the conceptual model in the form of a connected flow network (Section 4.3). A conceptual model includes the resource, transformation and final use nodes. The flow connection links must identify which commodity the flow link represents, while the resource and final use nodes need to identify the types constraints they are subject to. The second step is the data collection of the technical coefficients for matrix A (Section 4.4). Dataset from LCI, National/Regional Input-output table, Bill of Building Materials or data from the various field/desktop studies can be utilised to compile the matrix coefficients. The third step is the estimation of constraints for vector b (Chapter 5). At the moment, there is no established dataset for resource or demand constraints – only case studies of individual resource types exist in literature. For most cases, the studies of constraints must be conducted by the investigators to determine the level of constraints for the resource and final use nodes. These constraints can be determined from various studies including environment models, social acceptance surveys, toxicology threshold studies, economic analyses, feasibility studies of infrastructure projects. In the final step, the data collected in step 2 and 3 are combined in the matrix framework and mathematical analysis is conducted (Chapter 6). The analysis involves the sustainability measure identified by the feasible space volume which is defined by the constraints. The dynamics of the sustainability measure in terms of population growth or the sustainability measures for different development strategies can be compared. The usage of the sustainability measure is demonstrated in detail

in Chapter 6.

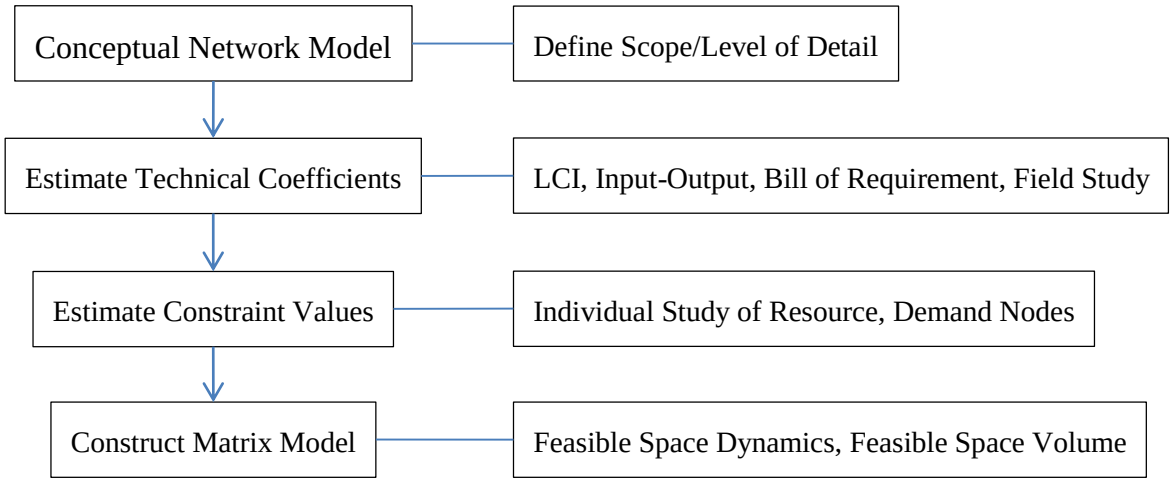

Figure 4.7. Application Procedure of the Matrix Framework.

The computational analysis that comes after the construction of matrix model consists of drawing the feasible space defined by the system of equation and inequation. For the lower dimensional case with ~~a~~ fewer transformation nodes, geometric analysis of the feasible space can be done visually on the graph. However, for the high dimensional case, where there are many transformation nodes (number of nodes > 3), visualisation is not possible. This is where the volume computation algorithm, Lasserre algorithm, is useful (Section 3.5.1 for the framework, Chapter 6 for demonstration). The graph of the feasible space volume (i.e. the sustainability measure) against population growth shows qualitative change where there is a phase transition or shift in dominant technology utilised in the network system.

4.3 Conceptual Model for Waiheke Island Case Study

The Waiheke Island water resource system uses multiple technologies at the same time (Duchin & Levine, 2011). The nodes on the left column in Figure 4.8 are the resource nodes, the nodes

in the middle column are the transformation nodes and the nodes on the right column are the final use nodes. Aquifer and rainwater nodes provide groundwater and collected rainwater to the pumps and RWH units respectively. The electricity node provides power to all transformation nodes. RWH and onsite septic systems use the land area for their operation. All transformation nodes are constructed and maintained with financial costs. The pump, desalination and RWH provide a flow of freshwater to the water consumption node while the greywater node produce greywater that is used for the non-potable purpose, which in effect ~~it~~ reduces the consumption of freshwater usage through non-potable uses (e.g. toilet flush, gardening). After the water use in the consumption node, the water returns to the septic tank for disposal or to greywater if the greywater system is installed. The water consumption node acts as resource node for greywater systems. Therefore, the greywater availability is determined from amount of greywater produced after the water consumption. Lastly, the onsite septic tank system provide wastewater assimilation service to the population.

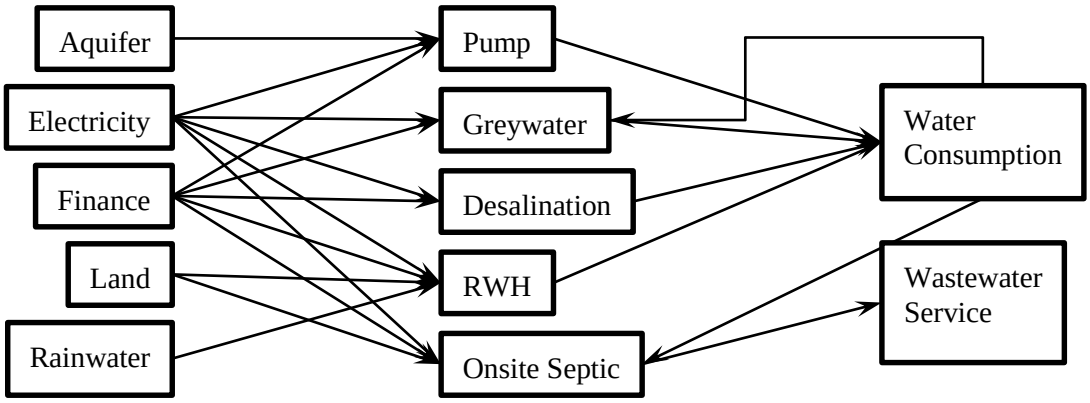

Figure 4.8. The Concept Network. Interaction of 5-Technologies.

4.4 Technical Coefficients

The technical coefficient matrix A is the conversion coefficient of the water infrastructure

options. They are obtained from various literature sources and the characteristics of the sizes of infrastructure assets typically used in Waiheke Island. A literature search was the primary means of obtaining these coefficients. Informal consultation with the local dealers and installers, brochures, catalogue, previous studies were also searched to determine the mostly commonly installed items for the island. The coefficients to be listed in matrix A are the resource requirements and quantity of the final product for a year. Assets of different technology have different life-years of effective operation. To compare the services they provide, annualised costs and resource uses were calculated while ongoing maintenance was calculated on an annual basis. The construction costs and resource uses were divided by the expected life-time of the assets.

The technological efficiency was assumed to stay constant over the years of operation. This assumption of fixed matrix coefficients A is typically used for most input-output analyses, but it may not be valid over a long-term period. This is because the installed assets may degrade over time resulting in a reduction of efficiency. Secondly, newer technology with higher efficiency may be introduced for the particular class of technology, for example a more energy-efficient desalination units. For the purpose of demonstrating the use of the matrix framework, the assumption of constant efficiency will be regarded as a sufficient approximation of reality. Considering the typical life-time of ~~the~~ water resource assets being around 20-50 years, the pace of implementation of efficient technologies will be slow even if they are introduced to the island. Ongoing maintenance and replacements of the assets will maintain the efficiency of the existing installations. Due to short to medium-term time horizons being similar to the life-time of the assets, the assumption of a fixed A will be valid. Another advantage of having this assumption is that the framework can assess the sustainability of the region with the current

technological efficiency projected into the future. It can be beneficial to identify the limits of the current level of technology in achieving sustainability.

4.4.1 Rainwater Harvesting System (RWH)

Rainwater harvesting requires a roof catchment area, a water tank, plumbing and a water treatment unit. The operation would require the pumping to the hydraulic pressure for in-house distribution and the cleaning of the tanks. The availability of harvested rainwater is limited by the area of the roof. When the stored water in the RWH tank gets used up, the household often call water tanker service to refill the tank. The water tanker services obtain the water from their groundwater bore, which in effect makes the aquifer pumping the secondary source of freshwater in case of an emergency during summer.

The resource intake of the RWH is broken down to the tank installation, small-scale treatment (e.g. filtering and collection plumbing), and a small pump to create the pressure required for indoor use. In a typical installation, the pressure is maintained with the secondary storage placed 2-3m higher than the water taps. The electricity usage for the small pump can be calculated by $E = mgh/e = \rho Vgh/e$, where ρ = density of water, V = volume of water, h = height, and e = mechanical efficiency of pump. The model assumes 50% efficiency and 2.5m height for the secondary storage. To pump $1m^3$ of water to this auxiliary storage, it can be calculated by : 1000 kg/m^3 x $1m^3$ x 9.8 N/kg x 2.5m / 0.5 = 30.6 kJ = 0.0085 kWh. The retail residential electricity rate in New Zealand is 27 NZc/kWh, which gives a unit cost of 0.0085 kWh/m^3 and 0.23c/m^3. The average water use rate was found to be $144m^3/y$ (Section 5.4) and the corresponding electricity usage will be 1.2 kWh/y. The annual electricity charge will be 33c/y.

The unit cost for the storage tank was calculated from the average value obtained from

brochures of New Zealand water storage tank retailers. The average household tank size used in Waiheke Island was 15,400 L (WRCG Ltd, 2004). The average price of a similar tank size was $2500 from the inspection of the catalogues of various suppliers. The labour cost for the installation was approximated to be a three day work with three laborers ($20/hr/person) and was estimated to cost $1440. Total cost for plumbing and pump costs were also estimated to be around $1000. Therefore, the total estimated installation cost was about $4940 per household unit.

Maintenance includes cleaning of the tank and filter replacement every three years. The local service provider charges $200 for a standard tank cleaning service. Other replacement and repair costs were estimated to be $70/year and the cleaning was estimated to take around six hours. Simple maintenance such as leaf gutter cleaning is estimated to take around 2 hours per year, performed by household members. Therefore, the total labour required for maintenance work was estimated to be 4 hours per year, and the total maintenance cost being $137/year. With the expected lifetime of a RWH system being nearly thirty years, the annual cost is estimated at $301/y/unit.

4.4.2 Aquifer Pump

A groundwater bore installation requires drilling of the bore, installation of the pump, water treatment and plumbing; the operation requires electrical energy and maintenance. The quantity pumped from the aquifer will be limited by the bore yields, which is in turn is determined by the transmissivity of the aquifer at the bore's location.

Robinson (2002) provides the details of the material and cost breakdown of a bore construction. However, these were the values for a high-yield aquifer; bores with more than 10,000m^3/day

yield. Robinson's details (2002) were used as a guidance of the items to be included in the cost estimation. The actual estimates were made using the unit quote appeared on a website of a drilling company (Synergy Boreholes and Systems Ltd., 2011). With the exchange rate of around £1=$2 as of Aug 2013 between British Pound (GBP) to New Zealand Dollar (NZD), the cost estimates of a bore construction can be converted to New Zealand Dollars.

- **Drilling:** £60-100/m drilled = $200/m drilled
- **UV and filtration equipment:** £1500~3000 = $4500
- **Extras**: £2000 = $4000 (e.g. labor, survey, consenting, plumbing)

On average, the bores had a screen depth of around 70m. The cost to construct a 70m bore, based on the unit quote above, was estimated by adding the three cost components: $200/m x 70m + $4500 + $4000 = $22,500 per bore. Assuming the bore will last 50 years, annualised construction cost was $450/y.

The electricity requirement for the pump is calculated with the same formula as the pump electricity usage of the RWH system, with the difference of the water being modeled to be pumped from 50m below the ground elevation. For every $1m^3$ pumped, 1000 kg/m^3 x $1m^3$ x 9.8 N/kg x 50m / 0.5 = 610 kJ = 0.17 kWh of energy is required using 50% conversion efficiency from the electricity. Thus, the unit electricity cost was 0.17 kWh/m^3 pumped or 4.6c/m^3. For a typical annual pump rate of $150m^3$/y, the annual energy cost will be 25.5 kWh/y or $6.90/y. Specification of a typical 100W UV lamp treatment unit with a flow rate of 60L/min gives an unit electricity use of 0.028 kWh/m^3 treated. The annual cost of a UV filter treatment for $150m^3$ will be 4.2 kWh/y or $1.13/y. Therefore, the total electricity usage for the modeled pump system will be 29.7 kWh/y or $8.02/y of electricity.

The maintenance cost was small compared to the construction cost, with a 5-year UV lamp replacement for $40, a 10-year replacement of the pump for $200 and general repair maintenance of $10/y. Total maintenance cost was estimated to be $38/y.

The labour requirement for the bore installation varies from site to site but the installation procedure is assumed to take 4 full working days with a 3-man crew, which is the average value taken from the contractor (private communication with Kiwi Drilling Ltd). This means 4 days x 8 hours/day x 3 men = 96 man-hours. Bores are only occasionally used as supplementary measures and do not require as much cleaning as RWH systems. The maintenance activity includes the repairs and replacement of consumables. The time taken for maintenance was is estimated to be 0.5 hours for a UV lamp replacement, 4 hours for a pump replacement and 1 hour per year for general repair. These give annual maintenance labour requirement of 1.5 man-hour/y. Assuming 50 years expected life-year of the bore, the total annualised cost for the groundwater pump was estimated to be $488/y/unit.

4.4.3 Septic Tank

Components of the conventional septic tank system consist of a septic tank, distribution box, distribution trench lines and the effluent irrigation field. From a detailed review of the land area required for the septic tank operation (Section 5.5), the land area requirement per septic tank was found to be around the $1000m^2$/septic tank to avoid any significant environmental contamination. The typical capacity of the septic tank considered in this estimation is the average household septic tank that produces around $150m^3$ of wastewater per year.

The construction costs of a typical septic tank system has a broad range (On-Site NewZ, 2010):

- Traditional septic tank and trench systems $6,000 to $10,000
- Modern septic tank and ETS or Mounds $7,000 to $15,000
- Aerated treatment plant and driplines $9,000 to $12,000
- Modern septic tank packed bed filter and driplines $10,000 to $15,000

From this, the estimation of the construction cost was decided to be in the upper end of the price range, which will include the transportation costs to the island; it was assumed $15,000 to be the construction cost for the island. The typical domestic septic tank pump is rated at 300W, and it was assumed to operate around 10% of the time (Onsite Sewage Treatment Program, 2011). 0.3 kW x 10% x 24hr/day x 365 day/y = 263 kWh/y - this translates to $70/y. This is considerably higher than the water supply components because the irrigation system uses thin pipes to distribute the effluents to the irrigation field. The pressure required to push the effluents continually to the network of pipes require more energy than pumping water occasionally to the storage tanks.

A major maintenance of septic tank system includes the pumping out of sludge that has accumulated over time. It is recommended that the septic tank be pumped out every three years. The model used in this case study used a 2.5-year pump out frequency for the septic tank. The cost to pump out a septic tank was estimated at around $500, which results in a $200/y maintenance cost. Assuming that the septica tank will last around 30 years, the total annualised cost for septic tank system comes out to be $770/y/unit.

4.4.4 Greywater Reuse

The reuse of greywater has gained attention in water-scarce regions. The basic strategy is to reuse relatively good quality wastewater to reduce the total water usage (Ghunmi, Zeeman,

Fayyad, & Van Lier, 2011). Although there are reclamation methods for combined sewages in general, household greywater reuse modeled in this case study is specific to the systems that reuse collected greywater from the shower, baths and laundry. Greywater can be used for non-potable, non-human contact uses, such as toilet flushing and landscaping. Health related issues are the most serious concerns in the reuse of grewater (Chaillou, Gérente, Andrès, & Wolbert, 2011). The greywater is generally contaminated with microbes, soaps, grease and solids. Therefore greywater reuse system without treatment components are recommended for outdoor subsurface irrigations only (Yu, DeShazo, Stenstrom, & Cohen, 2014). Aboveground uses including toilet flushes are recommended to have treatment units to remove infections. The treatment units are expensive and range from 13,000 to 15,000 USD, with a maintenance cost of up to 500 USD per year (Yu et al., 2014). However, simple uses of bucketing to flush the toilet are also exercised in dry areas without any treatment to save water (Dougherty & Murphy, 2012).

There was a household water use breakdown study done in a region similar to Waiheke Island. A pilot household water meter study was conducted in Kapiti Coast to obtain the average household water use breakdown statistics from 12 sample households (Matthias Heinrich, 2007) and again from 51 sample households in the Auckland region (Matthias Heinrich, 2008). These two coastal regions, while having similar climates to the Waiheke Island served as a guideline for the availability of greywater for onsite household installations (Table 4.1).

Table 4.1. Household Water Use Division (Auckland Region, Heinrich 2008)

	Total use (%)		Indoor use (%)		Average (l/p/d)	
	Summer	Winter	Summer	Winter	Summer	Winter
Tap	11.9	13.5	15.6	15.5	24.3	22.7
Shower	22.2	26.7	29.8	30.5	45.3	44.9

Washing machine	20.5	23.7	27.4	27.1	41.8	39.9
Toilet	17.4	18.6	22.9	21.3	35.5	31.3
Dishwasher	1.3	1.2	1.8	1.4	2.7	2.1
Bathtub	1.5	3.3	2	3.8	3.1	5.5
Miscellaneous	0	0.4	0	0.5	0	0.8
TOTAL INDOOR	74.22	87.5	100	100	151.3	147.1
Outdoor	21.7	8.3			44.2	13.9
Leaks	3.3	4.2			6.7	7
TOTAL USE	100	100			203.9	168.1

The scale of greywater reuse system varies from onsite household installation to large multistory building applications. Gardels (2011) performed a life cycle cost analysis of onsite greywater systems for household scales. The greywater modules are designed to tap into various degrees of connections, where an increase in connection to grewater sources correlated to an in increase in cost. Gardels (2011) suggests three levels of complexity in the connection members. Cheapest option being the connection to the washing machine only for US$400-800, the connection to all greywater sources with a low technology for US$1000-1500 and the connection to all greywater sources with a treatment capability to augment potable supply for US$2500-5000. The typical discharge rate of the household washing machine was estimated at 320-380 L/person/week and the total greywater source potential at 164 L/person/day (Gardels, 2011). To meet the non-potable greywater quality guideline, membrane bio-reactor and aerators had to be used in the work of Gardels (Gardels, 2011).

The model system adopted the cheap option for simple collection and flush uses, which will be the case for the dry Waiheke Island. The cost estimate for the greywater was chosen to be in the middle range of US$1500; the exchange rate of NZ$1=US$0.7 was used. Four people was used for this estimation. Greywater reuse serves a dual purpose, generating freshwater and wastewater service simultaneously. This is because it reduces the amount of freshwater needed

and reduces the amount of wastewater that would have ended up in a septic tank. The hydrological efficiency of 80% was assumed - the remaining quantity is lost through overflow and evaporation in the plumbing lines. Greywater pump was assumed to have same power rating as the RWH pump. Greywater coefficients are comparable to the data from the study done by Christova-Boal (Christova-Boal, 1995).

4.4.5 SeaWater Reverse Osmosis (SWRO)

Seawater desalination plants are often constructed at a large scale, and it requires a large amount of energy. The reverse osmosis provides a cost effective way of providing freshwater from the sea. Reverse osmosis desalination uses semi-permeable membranes to filter out the solute from the water using high-pressure differential. Without the need to heat water, the process uses considerably lower energy than traditional desalination processes (Ghaffour, Missimer, & Amy, 2013). The global capacity of the reverse osmosis plant has overcome the traditional MFS or distillation plant capacity since the year 2000 (Ghaffour et al., 2013). The size of SWRO plants varies from small portable units for boats or camping applications to huge desalination plants for industrial or municipal water supply (Bross, Kochanowski, & El Maraghy, 2005).

The cost of SWRO has been dropped in the period of 1980s to early 2000s, but the unit cost has been stabilized at around US$0.75 per m^3 (Zhou & Tol, 2004). Gude & Nirmalakhandan (2010) estimates the specific energy requirement for the RO system is 120 kJ/kg freshwater produced, which is 33 kWh/m^3 of freshwater produced. The recent recovery ratio of the SWRO desalination is around 45% in a single stage (Reddy & Ghaffour, 2007). The membrane costs have fallen by 86% between 1990 and 2005 (Reddy & Ghaffour, 2007), which reduced the unit

cost of water production. The trend of the cost of SWRO plants have been falling fast in the 1980s to 1990s and stabilized during the early 2000s at an average around 1 US$/$m^3$, with the minimum being 0.5 US$/$m^3$ (Zhou & Tol, 2004). The trendline shows that the average coefficient of SWRO plant construction cost is about US$800 per m^3/day capacity (Reddy & Ghaffour, 2007).

The reference SWRO plant used in the future scenario model is a commercially available 500m^3/day capacity unit, which is packaged in two shipping containers (Figure 4.9; MakWater, 2014). This capacity can support up to 3000 people, with a 160L/day/person consumption rate. The 500m^3/day twin container unit was priced at AU$ 450,000 for purchase or alternatively AU$20,000 for a 6-month hire (personal communication with MakWater, 2014), excluding the delivery and installation costs. For the costs associated with installation, a cost study of a RO plant construction and operation was used (Wateruse Association Desalination Committee, 2010). The construction cost of the RO plant itself typically took up only 31% of the total life cycle cost. Another 30% was used for project design, permitting, pretreatment construction and intake & discharge construction. Operation and Management (O&M) costs 39% of the total life cycle cost over its 20-30 year life span of operation (26% for power, 6% for parts replacement and 7% for others). The replacement of parts included regular membrane replacements every 2-3 years. By scaling the unit container cost with the ratios obtained from the statistics, the O&M costs excluding power (13%) could be estimated at AU$190,000 over the 25 years of its useful life span, which estimates the annualised O&M cost at AU$7600/y. With an exchange rate of 1 AUD = 1.1 NZD as of June 2014, the annualised O&M cost is estimated at NZ$8400/y.

The operation level of the twin SWRO unit was assumed to be 80% of its full capacity over the

year. The annual production will be up to 150,000m^3/y of freshwater without seasonal variability. From the freshwater recovery rate of 45% (MakWater, 2014), the seawater intake for the production would be 330,000m^3/y, and the brine emission would be 180,000m^3/y. The electricity usage for RO plants was reported to be 4kWh/m^3 of freshwater production (Ghaffour et al., 2013; MakWater, 2014). The estimated annual electricity consumption was 600,000kWh/y and the retail electricity rate for residents is 27c/kWh, making the annual electricity cost NZ$162,000/y. Assuming a life-span of 25 years for the unit, the total annualised construction and operation cost will be NZ$188,400/y. Unit cost is estimated to be $1.26/$m^3$ freshwater produced for the unit. Considering that Watercare, the urban water provider of Auckland region, charges $1.30/$m^3$ (Watercare, 2014), the unit price of a SWRO system is already a competitive option for the island's water supply. However, the cost estimates did not count the distribution costs; if it was included it may have impacted the final calculation. The labour required to operate the plant is known to not change much with the plant size. However, for the sake of the model, the number of people required for the maintenance has been set to change linearly depending on the installed capacity of the desalination plant.

Figure 6.9. A Photograph of a Commercial 500m^3/day SWRO plant housed in a Sea Container (MakWater, 2014).

4.3.6 Summary Table of Conversion Coefficients

The collection of data obtained from literature, field visits and supplier contacts were summarised in Table 4.2. The columns of the table were utilised as entries for matrix A, the resource conversion coefficients in the constrained network framework in Chapter 6. Each technological option has a different set of resource usage to produce a set of final products. The technical coefficients are the efficiency of water production using a particular type of technology. The unit cost is estimated by adding the annual operating cost and amortised capital cost for implementation. This table provides the basis for the matrix entries used in Chapter 6.

Table 4.2. Technical Coefficient Matrix. RWH, bore pump and greywater reuse were estimated for a single household unit, and SWRO is estimated for a single plant. The values are annualised based on the life cycle cost/inventory and the expected lifetime of the assets.

Resource	**Roof Rain Harvest**	**Bore Pump**	**Desalination: Reverse Osmosis (RO)**	**Greywater Recycling**	**Septic Tank**
Rainwater (m^3/y)	144	0	0	0	0
Aquifer (m^3/y)	0	160	0	0	0
Seawater (m^3/y)	0	0	330,000	0	0
Grey water (m^3/y)	0	0	0	30	0
Wastewater (m^3/y)	0	0	0	30	164
Installation Cost ($)	5,000	22,500	450,000	1,440	32,000
Maintenance Cost ($/y)	70	38	8,400	10	300
Electricity (kWh/y)	1.2	29.7	600,000	0.25	263
Installation Labour (man-hr)	72	96	28,000	12	500
Operation labour (man-hr/y)	4	1.5	40	1	5
Potable water (m^3/y)	115.2	150	150,000	0	0
Non-potable water (m^3/y)	0	0	0	30	0
Evaporation/Loss (m^3/y)	20	10	9,600	0	0
Purchase of electricity ($/y)	0.33	8	162,000	0.07	70
Land Area Needed (m^2)	120	0	0	0	60
Life Year	30	30	25	30	30
Annualised Total Cost ($/y)					
Total Unit Cost ($/$m^3$)	2.06	5.31	1.26	1.95	8.76

4.4 Conclusion

This chapter described the workflow associated with applying the matrix theory into practice. With Waiheke Island's recent population increase, water supply and wastewater issues arose. Waiheke Island's water resource system was chosen as our case study to demonstrate the matrix framework for the sustainability metric. As the first step of this application, the conceptual model of the water resource system was outlined, and the preliminary conversion coefficients were collated based on the publicly available data on the technologies associated with water resource systems. Studies regarding the constraints are reported in Chapter 5 followed by mathematical analysis in Chapter 6. Even though the current conceptual model only included 5 technologies in the water resource technology mix, additional technologies may be added simply by extending the table of bill of requirements (Table 4.2) when the relevant data become available. The technical conversion coefficients are almost independent to the location of implementation, and thus the data can be accumulated and reused in different studies.

Chapter 5 Constraints Estimation for the Waiheke Island Water Resource System

5.1 Significance of Constraints Estimation in Matrix Theory

The matrix framework models the multicommodity flow and describes the interactions of the various constraints that society and infrastructure systems encounter during growth. These constraints interact through sharing common resources or by utilising common production nodes. During the conceptualisation phase of a workflow (Section 4.2), the investigator chooses which industrial or infrastructure nodes are to be included in the model. The choice inevitably determines which types of resource uses and the waste/pollution emissions are to be included in the model. The investigator must then follow up by studying the constraint conditions for each resource use and pollution emission type. The constraints may arise from a limited resource endowment (physical, financial and social), or the tolerance levels of wastes/pollutant emission (public acceptance, legal, ecological, environmental).

Evaluating constraint values can be more challenging than finding the technical coefficients for the production nodes because they need to be studied for each type of resources/waste/emission, individually. The technical coefficients are universal, in the sense that they do not depend on where the production technology or infrastructure technology is employed. Therefore they are often documented well in categorised databases or reports. On the other hand, the constraints that affect regional development and growth are subject to the specific condition of the region. Therefore, studies of the constraints are relatively lacking compared to the technical coefficients. The constraint data for Waiheke Island must be

estimated before going into the mathematical analysis of the framework. Each constraint is estimated from a single case study so that it can be substituted into the RHS entries of the matrix inequation.

5.2 Constraint Elements in Waiheke Island

The conceptual model (Figure 4.8 and Table 4.1) identified that the water resource system for Waiheke Island operates upon five resources to produce two final products and one waste emission.

- **Resources:** (1) freshwater from rainfall, (2) freshwater from groundwater, (3) land area, (4) electricity, and (5) finance;
- **Final Products:** (1) potable water, (2) non-potable water; and
- **Waste:** (1) wastewater

The subsequent sections help estimate the constraints for each of the category above. Section 5.3 and 5.4 focusses on the constraint on the freshwater potential of groundwater and rainfall respectively. Section 5.5 focusses on the land area capacity of the onsite wastewater treatment for septic tank-irrigation technology adopted by the island community. Section 5.6 considers the potential of the greywater reuse system in terms of the availability of greywater. Section 5.7 considers the other constraints including the financial capacity, the land available for development, and the electricity grid capacity for the island.

5.3 Groundwater Potential

All groundwater ultimately originates from surface recharge by precipitation (Fetter, 2001). A

well-known criteria for groundwater sustainability is the *safe yield*, which is the amount of annual recharge. An over-extraction beyond the recharge rate results in the decline in water table depth. The decline in water table depth is known to cause ground subsidence (Galloway, Jones, & Ingebritsen, 2005; Hu, Yue, Wang, & Wang, 2004), and a loss of seepage to wetlands and springs (Ministry for Environment, 2009). There is a more strict safety guideline for groundwater exploitation, called *sustainable yield*. This is the extraction rate that will not cause any negative damage to the environment. Safe yield only considers the net balance of recharge and extraction. However, some recharge must be reserved as environmental and ecological flows, in order maintain the environmental and ecological features of the region.

For island aquifers, the saltwater intrusion is the most important issue that requires the reservation of recharge. In coastal aquifers, saltwater from the sea, and freshwater from inland recharge form an interface, which has a sharp change in concentration (Figure 5.1(b)). The freshwater flow rate maintains the geometry of the freshwater zone by providing hydraulic pressure to push the interface seaward. The reduction of the flow rate by an interception through groundwater pumping, shrinks the freshwater zone. For example, a cluster of pumps will reduce the hydraulic head of the affected region (Figure 5.1(a)). This leads to shifting in the saltwater-freshwater interface landward, which affects the aquifer along the coastal line. This is called saltwater intrusion, and coastal bores are affected by the increase in salt concentration in their pumped water. Because the position of the interface is maintained by the continual flow of freshwater by recharge, some recharge must be reserved for the hydraulic pressure that maintain the geometry. Therefore, the groundwater extraction rate must be kept less than the recharge.

A general rule of thumb is that 15% of the regional recharge is to be left unused for the hydraulic

pressure on the saline-freshwater interface (Wujkowski, 2004). The quantity will be determined by numerical simulation in the subsequent sections. It is not possible to determine how much recharge must be reserved through a simple water balance model but can be done through a hydraulic simulation of the aquifer system.

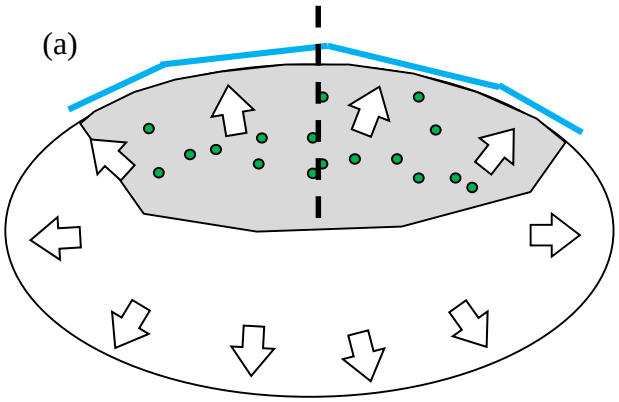

(b)

Removed due to Copyright Reason

Figure 5.1. (a) Aquifer Hydraulic Pressure on a Hypothetical Island. The general direction of hydraulic pressure is outward (arrows). The dots represent bores. Capture zones of the bores experience decreased aquifer pressure and discharge thus elevating the saline intrusion risk along the corresponding portion of the coastline. Aquifer cross section along the dotted line is shown in (b). **(b) Vertical Cross-Section.** Continuous outward flow to sea preserves the geometry of the freshwater-saline water interface. Decreased discharge (arrows) due to pumping retracts freshwater-saline interface inland. This may cause some come in contact with the saline water of the sea. This event is called saline intrusion. Cross-section source: OzCoast (2010).

5.3.1 Geologic Background and Conceptual Model

The geological origin of the island dates back to the Jurassic era greywacke, the most prevalent and old metamorphic bedrock in New Zealand. Throughout history, the bedrock of Waiheke

Island has undergone intense geological action. Bending, faulting, and fracturing has occurred to the bedrock leading to a thick weathered greywacke layer on top of the fracture networks in the bedrock's fresh layer. At some places, the outcrops of the bedrock show a 70^{o} strike angle, indicating severe geologic stresses that the bedrock has undergone (Wujkowski, 2004).

The island consists of low-yielding bedrock aquifer that exists due to the fractured greywacke. The fractured aquifer layer is overlain with a less permeable silt-clay layer originating from the weathered greywacke. The overlain confining layer from the weathered greywacke ranges from 1m to 30m thick depending on the location based on the interpolation of the stratigraphy obtained from the drillers' bore logs. Typically the locations with high elevation had a thinner overlain layer, which is expected for the sediments. The overlain material behaves as an aquitard that limits the infiltration of rainfall into the fractured aquifer. According to the previous soil moisture and catchment water balance study in Waiheke Island, the regional recharge rate was only 4% of the incoming rainfall, which was at 48mm/year (SKM, 2007). Therefore, careful use of the delicate aquifer is essential. The previous pump tests showed a storativity value in the order of 10^{-4}, which signifies that the aquifer behaves as confined aquifer (WRCG Ltd, 2004).

The model was constructed as an unconfined aquifer with an aquitard as the top layer. The model used four slice surfaces to represent a 3-layer aquitard-aquifer model. The upper most layer was the aquitard, consisting of weathered greywacke. The aquifer geometry was modelled using a 5m Digital Elevation Model (DEM), island boundary, simplified streamlines, and the stratigraphy information from 174 bore drill logs. The resulting finite element contained 4739 nodes. There were no previous research on the depth of impermeable aquifer bed thus the depth was assumed to be located at 150m below the sea level.

Recharge occurs throughout the island surface through the small surface impermeable layer of the clay-silt overlain material. Previous studies indicate that there is no special recharge mechanism but there was surface recharge throughout the island area (SKM 2007). The unconfined modelling mechanism allows for seepage modelling, which added more realism in the contour of the hydraulic pressure. The SKM report only studied the hydraulic head distribution change in the case of pumping scenarios at the centre of the island, and did not go into the saltwater intrusion event assessments.

The model described the upper aquitard so that it can represent the surface recharge in a more realistic way. FEFLOW features a seepage surface option when the user chooses to model an unconfined aquifer. With movable phreatic surface mode (Slice Type option in Table 5.2), FEFLOW allows the 3D finite elements to be partially saturated if the hydraulic head is between the elevation of the top and bottom of the element. The element is considered to have partial conductivity based on the saturation level that is defined by the water table level (DHI-WASY 2010). For the finite elements of the top layer, the typical hydraulic head will be lower than the elevation of the ground, making the elements partially saturated. Seepage is expected when the hydraulic head of any finite element volume exceeds the elevation. This simulates the natural occurrence of a spring and stream, which is included for the realism of the model. The initial uniform recharge over the aquitard layer was assumed to be 48 mm/year from an earlier surface water balance study (SKM, 2007).

Figure 5.2. Partially saturated cell. (User Manual FEFLOW 6.0; DHI-WASY 2010)

For the effect of the terrain to be simulated, an interesting feature of FEFFLOW called seepage surface option is chosen. The water table depth and the ground surface elevation do not coincide in general. When the elevation of the water table height is lower than the predefined ground elevation, the simulated 3D cell is considered partially saturated in the form as shown in Figure 5.2. When the water table height is below the ground level elevation, the FEFLOW models the cell as partly filled and the fluid conduction is calculated by collapsing the cell to match the water table level (the cell is called partially saturated cell). If the water table level goes beyond any computational step, a subroutine is run so that the ground level acts as an upper limit (similar to fixed hydraulic head constraint) that the water level cannot rise against. The excess water that emerges from the ground level is summed up as seepage volume.

There were other approximations and assumptions that simplified the modelling procedure and computation complexity of the optimisation:

- **Assumption:** The impermeable bedrock was assumed to exist at 150m below sea level. There was no study done to find the extent of the fracture networks in the bedrock. This was the depth of the deepest bore drilled in the island. The hydraulic head required

to prevent the saltwater wedge to come in contact with the impermeable bedrock was 150m/40 = 3.75m. Therefore, as a first approximation, if the hydraulic head is less 3.75m at the location of the proposed bores, saltwater intrusion will occur.

- **Approximation III:** The sharp interface model was used for the saltwater intrusion event. This means that the salt concentration was not considered in the model. Only the hydraulic head was computed for the given pumping scenarios. The determination of saltwater intrusion event was based on the depth of the interface at the node location. If the depth of the saltwater-freshwater interface was less than 150m at the location of the node, the node was recognised as experiencing ~~the~~ saltwater intrusion and the bore near the node were considered to be affected.

5.3.2 Method

The objective was to calculate the maximum pump rate achievable from the plausible pump sites without causing saltwater intrusion. To achieve this, a calibrated groundwater simulation was created for scenario analysis. Groundwater software package, FEFLOW was used because it can model 3D groundwater flow and can import complex island geometry from the GIS database.

There have been a number of optimisation studies estimating the maximum pump rates subject to saltwater intrusion constraints in literature. Abarca et al. (2009) provide a brief review of optimisation case studies (both analytical and numerical) and find that most studies are demonstrative using hypothetical aquifer conditions. Javadi et al. (2008) demonstrated a coupled simulation-optimization model to compare the effectiveness of three different management strategies on an already intruded aquifer – the abstraction of brackish water,

recharge of freshwater, and a combination of abstraction and recharge. Mantoglou & Papantoniou (2002) demonstrated the simulation-optimization technique (S/O) that links the optimization routine with the simulation subroutine to find the best locations for the well location under the constraint condition of saltwater intrusion. Mantoglou & Papantoniou (2002) linked a genetic algorithm that passed variables of the location and pump rates (x_i,y_i,p_i) to the simulation subroutine, which returned performance scores. The performance score was O = sum(p_i) + penalty, where the penalty of the largest negative number was added when saltwater intrusion occurred. This type of penalty function has discontinuity (i.e. infinite derivative) near the desired optimal coordinate and such performance scores are impossible to be used by derivative based optimisers. Mantoglou & Papantoniou had to use a global optimiser, which converges to the optimal solution at a much slower rate. Mantoglou & Papantoniou stated that it took several hours to reach the global optimum using only four pumping bores in their work.

Optimising the regional pump distribution requires optimising hundreds or even thousands of bore pump rates. It was necessary to reduce the complexity of the problem; two approximations were introduced to simplify the method used by Mantoglou & Papantoniou achieved (2002):

- **Approximation I:** The locations of groundwater pumping were assumed to be on the finite element nodes of the FEFLOW model. While Mantoglou & Papantoniou (2002) optimised both coordinates of the pumps and pump rates, the pump locations were fixed, and only the pump rates were optimised in this work. When a new bore is drilled, the driller conducts a simple drawdown pump test to determine the maximum pump rate. The maximum pump rates of the simulated nodes were determined by the sum of maximum yields of the closest bores to the nodes. There were around 4000 nodes in the finite element geometry. Therefore, the set of decision variables are reduced to

4000 pump rates. The nodes that do not have any bores nearby were assigned to have a 30m^3/day maximum yield based on the average yields of the bores found on the island.

- **Approximation II:** The hydraulic effect of the salt wedge was ignored for the model. Near the coastline, the freshwater-saltwater interface will close off the flow pathway of freshwater to the sea. This creates an effective decrease in transmissivity, increasing the hydraulic head for the nodes near the coast. This approximation overestimates the occurrence of saltwater intrusion, and provides a conservative safety factor. More research is needed if one wish to include the hydraulic modification of the saltwater wedge along the coastline where the freshwater exits to the ocean. However, it is expected that the magnitude of the effect is small.

The coastal nodes were modelled to have a 0m hydraulic head. The effective bulk porosity of the fractured greywacke was assumed to be similar to the fractured igneous rocks (Table 5.1). The assigned porosities for topsoil, clay, and fractured greywacke were 0.55, 0.6, and 0.25 respectively. An average of $6x10^{-4}$ compressibility (i.e. storativity) was used from 4 recorded pump tests around the island.

Table 5.1. The typical porosity of rocks and sediments and Greywacke (TUGRUL & ÜNDÜL, 2006). Greywacke is in the middle of metamorphic compaction. Thus, the porosity is much less than the other types of rocks (only 2%). However, the bulk porosity of the fractured greywacke layer is more than this, as the fractures contribute to the effective porosity.

Type	Porosity	Average

Soil	55%	0.55
Gravel & Sand	20-50%	0.35
Clay	50-70%	0.60
Sandstone	5-30%	0.17
Limestone	10-30%	0.20
Fractured igneous rocks	10-40%	0.25
Fresh Greywacke	0.95-3.66%	0.023
Weathered Greywacke	8.47-10.23%	0.094

Hydraulic conductivity of the aquitard and aquifer layers were manually calibrated against the static water levels recorded in the 174 bore drilling logs with an assumption of uniform and isotropic parameter throughout either layer. The horizontal conductivity was assumed to be ten times the vertical conductivity. The resulting model parameters are given in Table 5.2.

Table 5.2. Modelled Parameters.

Parameter		Value
Nominal Resolution		6,000
Actual Node per slice		4,739
No of Slices		4
Elevation	Slice 1	Interpolated from DEM
	Slice 2	Interpolated from Bore Log Data
	Slice 3	-75m (observation slice)
	Slice 4	-150 m
Problem Type		Saturated media, Unconfined Aquifer
Slice Type	Slice 1	Free & movable
	Slice 2	Unspecified
	Slice 3	Unspecified
	Slice 4	Fixed
Free Surface Constraint	Falling Dry at bottom	Unconstrained
	Touching the top surface	Constrained as seepage
Hydraulic head BC		0m around the island boundary
Material properties	In/outflow on top/bottom	48 mm/y
	Porosity	0.2
	Isotropic Hydraulic Conductivity (Aquitard)	0.0004 m/d
	Isotropic Hydraulic Conductivity (Aquifer)	0.004 m/d
	Compressibility	6.00E-04

Two pumping scenarios were added to find the maximum achievable pump rate to the calibrated model that represented the reference, the non-pumping scenario. The first scenario simulated the case where only the current pump locations were utilised for pumping without additional drilling (Section 5.3.2.2). The current bore locations were registered in a GIS layer provided by the Auckland Council. The GIS layer included the maximum yield for every drilled bore. The pumping rate for the nodes was optimised within the maximum nominal yield. If all bores were pumped at their maximum yield, saltwater intrusion would occur in many locations around the island. The maximum yield achievable without saltwater intrusion was less than the maximum nominal yield. The main results obtained from the simulation runs are (1) the hydraulic head distribution and (2) the water balance account. Three simulation runs were presented in this section:

- Calibrated solution with no pumping;
- Maximum pumping rate using only current bore locations and their yields as a limit; and
- Maximum pumping utilising all regions of the island, simulating the ultimate upper limit of the regional pumping without causing saltwater intrusion event.

The second scenario simulated the case where the aquifer development was spread out throughout the island, while trying to pump out as much water as possible while avoiding saltwater intrusion event (Section 5.3.2.3). With a 150m aquifer base depth, 3.75m minimum hydraulic head constraints were assigned to every node except for the ones situated on the coastline (termed internal nodes). Nominal pump rate of $30m^3/d$ was assigned to each of the internal nodes.

The objective function was the island-wide pump rate. The optimisation routine utilised the steady state routine of FEFLOW. The steady state solution routine in FEFLOW was an optimisation routine that incrementally approaches an optimal solution until it finds the closest solution to the given boundary conditions. If the well boundary for pumping nodes are set to a large negative value, the FEFLOW steady state solver routine will try to find the steady state solution that maximises the pump rate. There is an option called the minimum hydraulic head constraint to the well boundary. If this value is specified along with a high nominal pump rate, the solver will try to find the solution that maximises the pump rate while keeping the hydraulic head above the specified minimum. This is the optimisation that this investigation is trying to achieve. For an aquifer base with a depth of 150m below sea level, the minimum hydraulic head to keep saltwater intrusion from occurring is 3.75m (Section 5.3.2). This was the value entered in the minimum hydraulic head constraint for the well boundary condition. The

quantity for the nominal pump rate varied according to the simulated scenarios (Section 5.3.4).

FEFLOW reports the water balance account for each simulation run. Along with the visual representation of the hydraulic head distribution of the simulation result, the water balance account forms the next primary source of analysis. It reports input-output flows through five types of boundaries in the model. The Dirichlet BC accounts for the water flow across the fixed hydraulic head boundary. The Dirichlet BC balance is the sum of the flow across the island coastline. The most important variables in the water balance report are the Wells BC flow and Distributed Sources/Sinks. The Well BC balance accounts for the water flow through the pumps and injections. The Distributed Sources/Sinks accounts for the areal recharge from the surface of the ground. Sometimes, steady state solutions resulted in some well boundaries with injection values (positive water balance). This means in order to satisfy the constraint conditions in preventing saltwater intrusion; injection is required for some bores to create extra pressure to maintain the hydraulic balance. When such positive water balance occurs, the overall pump rate achieved were calculated as the net water balance of the Well BC report.

5.3.2 Results

5.3.2.1 Calibrated Solution, without any pumping

The steady state solution without any pumping is shown in Figure 5.3. Even in the natural state, there were locations where the hydraulic head was less than 3.75m. These locations were the river mouth, low-lying areas, and wetlands. These locations would have required the net injection balance of well boundary nodes for the pump scenarios (i.e. artificial recharge needed to meet the 3.75m goal). The water balance report showed the standard budget for the non-pumped natural state on a steady state recharge condition. No flow across the Well BC is

observed, and Neumann BC flows were implicitly generated by FEFLOW algorithm to include the net mass balance of water in the simulation.

FEFLOW reports the total water balance at the boundary of the simulation after achieving the convergence in the solution. There were three types of boundaries in the model: (1) fixed hydraulic head boundary along the coastline, (2) ground surface boundary that represent constant recharge and seepage calculation, and (3) well boundary for those nodes with pumping. For the location of the well boundary, the pumping was set to occur at the deepest node of the location, while the vertical hydraulic conductivity was set to a very high value in the simulation. The flow across the boundaries formed the main output of the simulation.

- Surface Infiltration: 12169.3m^3/d
- The water re-emerged as the surface seepage (i.e. stream baseflow): 7356.42m^3/d
- Net recharge to the aquifer: 4818.11m^3/d
- Water emerged to the coastline: 4818.08m^3/d

In this scenario without any pumping, the simulation showed that around 60% of the total surface infiltration emerged back to the stream flow. The remaining 40% resulted in seaward groundwater flow along the coastline.

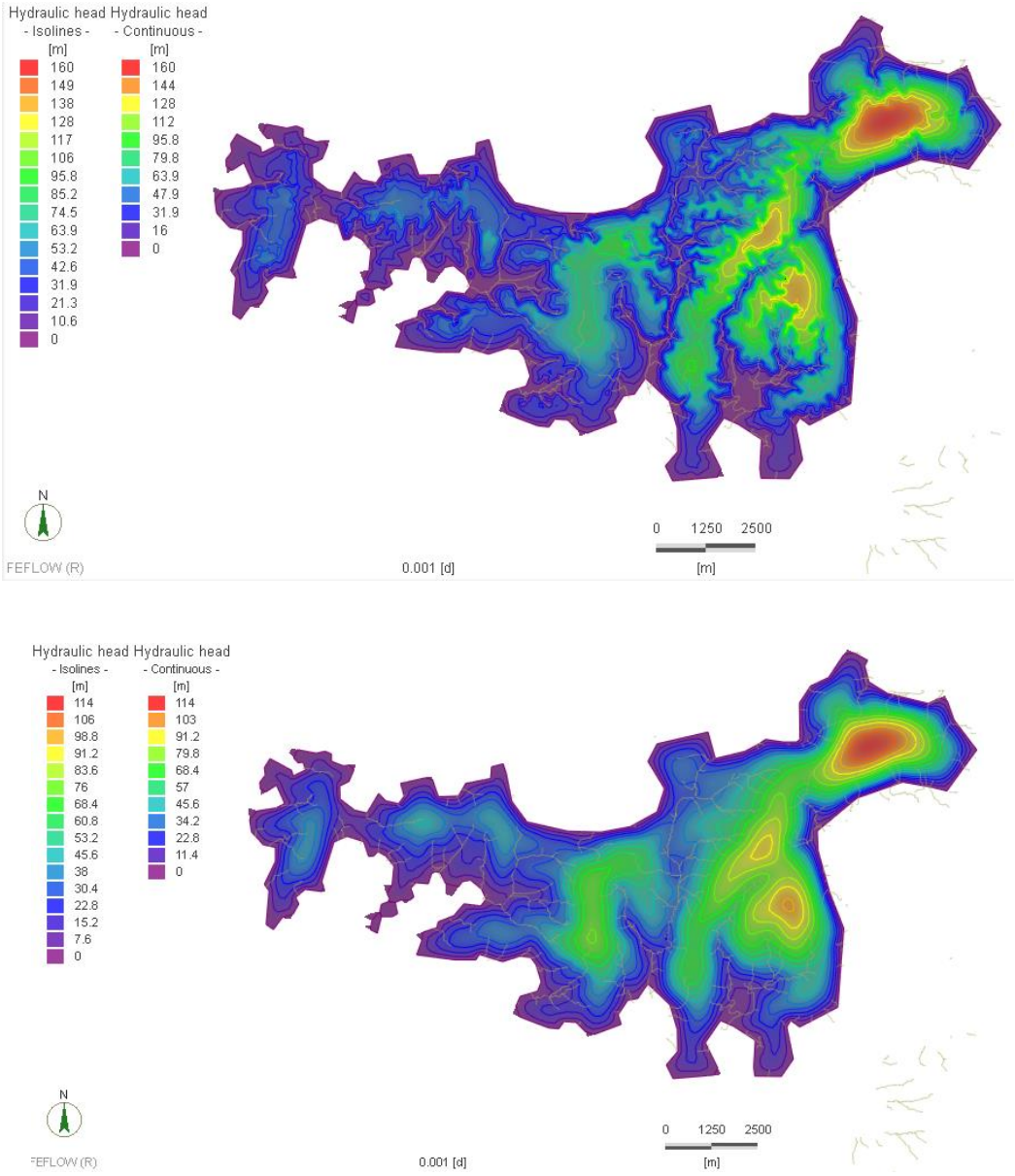

Figure 5.3. Hydraulic Head Distribution for No Pumping Scenario. (Top) Hydraulic Head Distribution for the ground elevation slice. It clearly shows the influence of the ground topography and seepage constraint to the hydraulic head. **(Bottom)** Hydraulic Head Distribution at the observation slice at 75m below sea level. In the aquifer, the hydraulic head distribution is smoother.

5.3.2.2 Total Bore Installations Capacity

Most of the population live in the western half of the island and correspondingly, most bores

were located there. The major decline in water table height was observed when bores were operated at maximum intensity while avoiding saltwater intrusion. On the eastern half of the island, draw-down cones for isolated locations are observed (Figure 5.4). The total installation capacity of the bore production is not determined by the sum of individual bore yield. At most locations, the pump rate did not reach the nominal pump rate determined from the sum of bore yields. The water balance report showed that the maximum regional pump rate achieved, while only using the current pump locations, was 1,861 m^3/d. This amounts to approximately 15% of the island-wide recharge. The maximum value was larger than expected because the bores are mostly concentrated on the western side of the island.

- Surface Infiltration: 12169.3m^3/d
- The water re-emerged as the surface seepage (i.e. stream baseflow): 5963.91m^3/d
- Net recharge to the aquifer: 6205.39m^3/d
- Water emerged to the coastline: 4357.89m^3/d
- Bore: 1861.26m^3/d

In the case of localised pumping at current bore locations, 49% of surface infiltration emerged back to stream flows, and 51% recharged into the aquifer. Of the recharge, 31% has been pumped out for regional use when the current constructed bores were utilised to the maximum without causing saltwater intrusion.

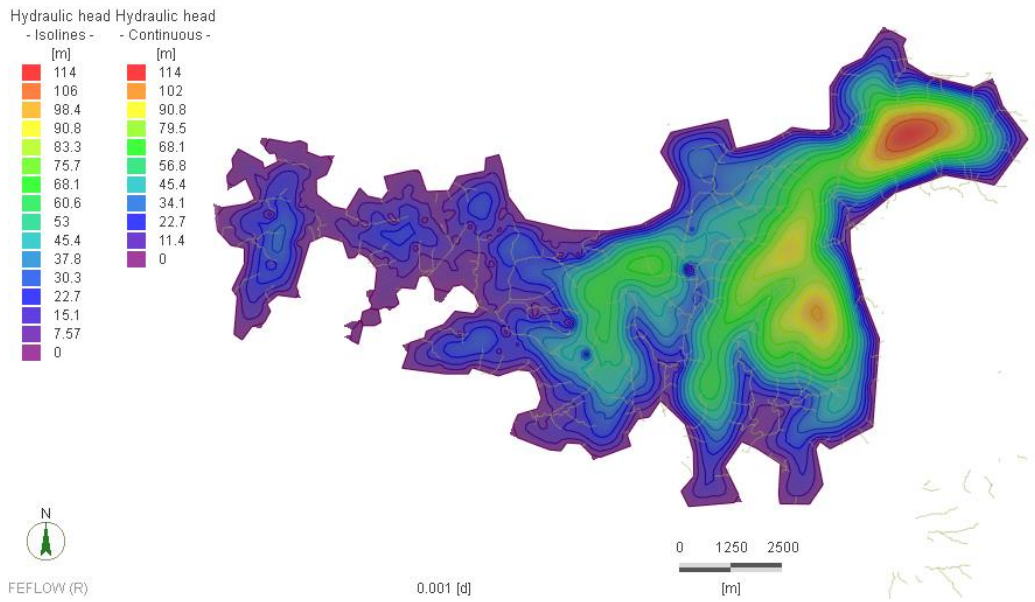

Figure 5.4. Hydraulic Head Distribution for the maximum operation of current pump capacity. Slice 3 observation slice.

5.3.2.3 The maximum regional Pump Capacity

When all internal nodes were assigned with a high nominal pump rate with the minimum hydraulic head of 3.75m, the FEFLOW solver found the solution that had a 3.75m minimum hydraulic head for all internal nodes (Figure 5.5). The maximum pump achievable was 9,881 m^3/d, which amounts to 81% of the recharge. This means that at least 19% of recharge must be reserved for the hydraulic push to prevent the saltwater intrusion wedge to advance to the location of the pump nodes. However, this pumping rate will never be realised because the economic and technical feasibility of developing the bores in remote locations needs to be considered first. If the bore location is too far away from the residential or commercial zones where the water is used, the construction and transportation cost for the water may be prohibitively large.

The regional water budget report from the simulation run showed:

- Surface Recharge: 12169.3m^3/d
- The water re-emerged as the surface seepage (i.e. stream baseflow): 0m^3/d
- Net recharge to the aquifer: 12169.3m^3/d
- Water emerged to the coastline: 2288.21m^3/d
- Bore: 9881.1m^3/d

The problem with this case is that there is no stream flow. Even though most of the streams on Waiheke Island is intermittent, the ecology that depends on the stream flow will get damaged if there is no stream flow allocated as in this scenario.

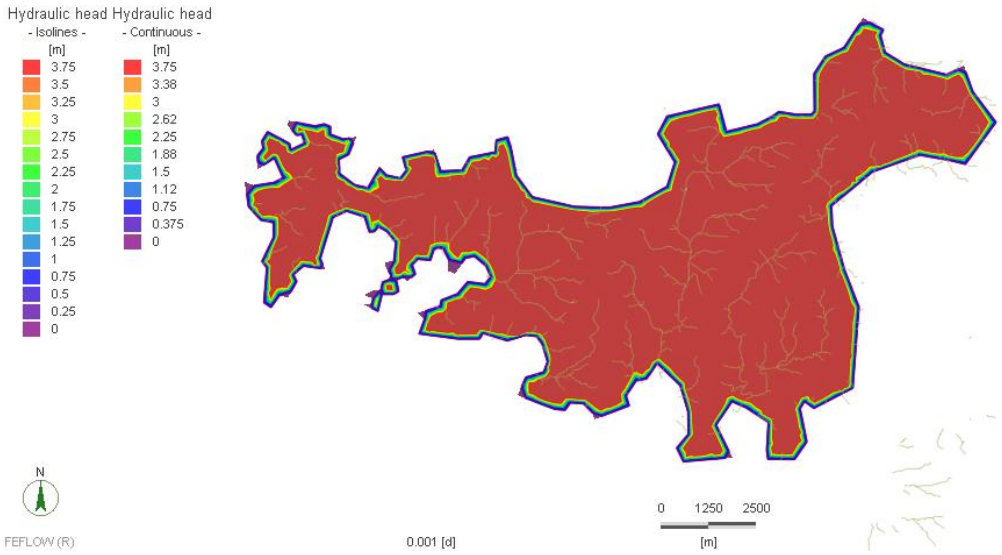

Figure 5.5. Hydraulic Head Distribution for Maximum Bore Development throughout the island.

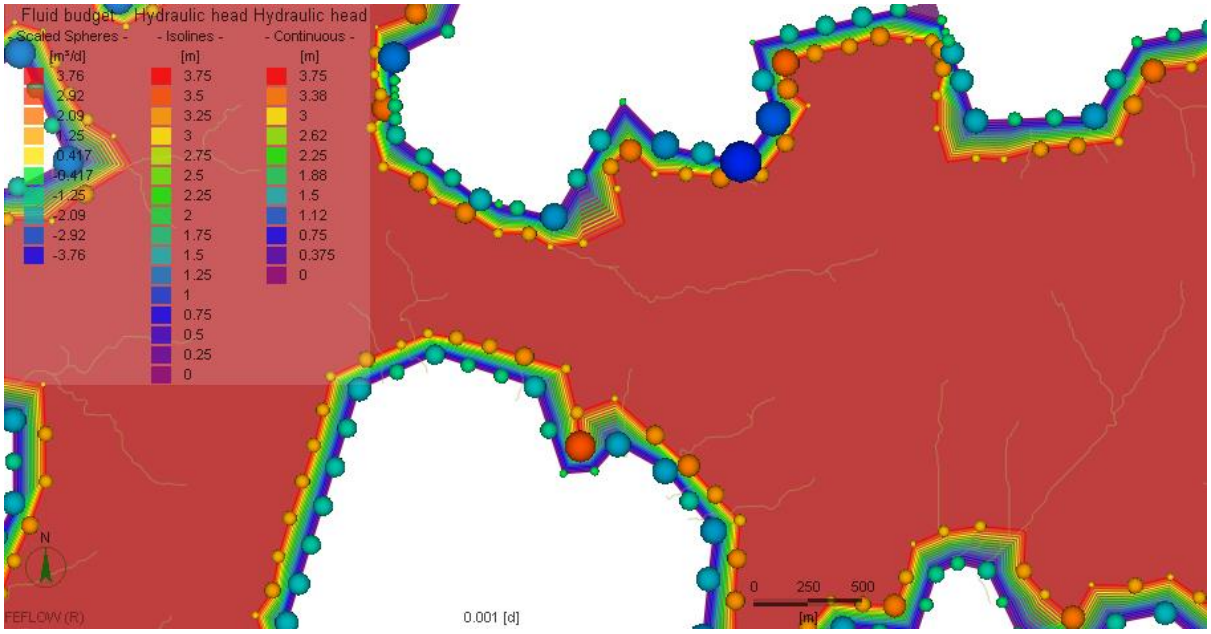

Figure 5.6. Pump Rates to maintain the hydraulic head pattern.

The spheres on the FEFLOW result in Figure 5.6 show the fluid budget on the nodes (i.e. pump or injection rates). The size of the sphere represents the quantity of the flow. Most of the pump and injection management must be performed along the near-coast lines. Positive numbers represent pumping, while the negative numbers represent injection. The green-blue spheres along the coastlines are the discharge to the sea. The majority of the pumps occur at the nodes immediately next to the coastline. More pumping should be undertaken at the capes than the bays in order to achieve the maximum regional pump rates, while the pumps should be arranged along the coastline to capture the outward flow to the sea. In the actual implementation, it would be necessary to monitor the change in the hydraulic head to alter the water production. Since the aquifer is confined and the recharge is expected not fluctuate throughout the seasons, constant production of water will be best.

5.3.2.4 Sensitivity analysis

The data used in the assessment of the fractured groundwater used the limited availability of geologic data. Thus, the uncertainty of the estimation remains and is expected to be large. Sensitivity analysis was performed to determine which parameters influenced the estimates of the maximum pump rates the most, and to what extent. The sensitivity analysis provides the most influential parameter used in the calibrated model so that future investigations may focus on getting the accurate data on the most influential parameter. Seven parameters were calibrated for the steady state FEFLOW problem; (1) recharge to the aquifer, (2-3) hydraulic conductivity of the aquifer and aquitard, (4-5) porosity of aquifer and aquitard, (6) compressibility, and (7) the aquifer base depth. For each scenario, the seven parameters were increased and decreased independently, and the resulting water balance was recorded. Bedrock depth was changed from the calibrated value of 150m to 100m and 200m. All other parameters were changed to 75% and 125% to observe the maximum flow achieved through the well boundary (Figure 5.7).

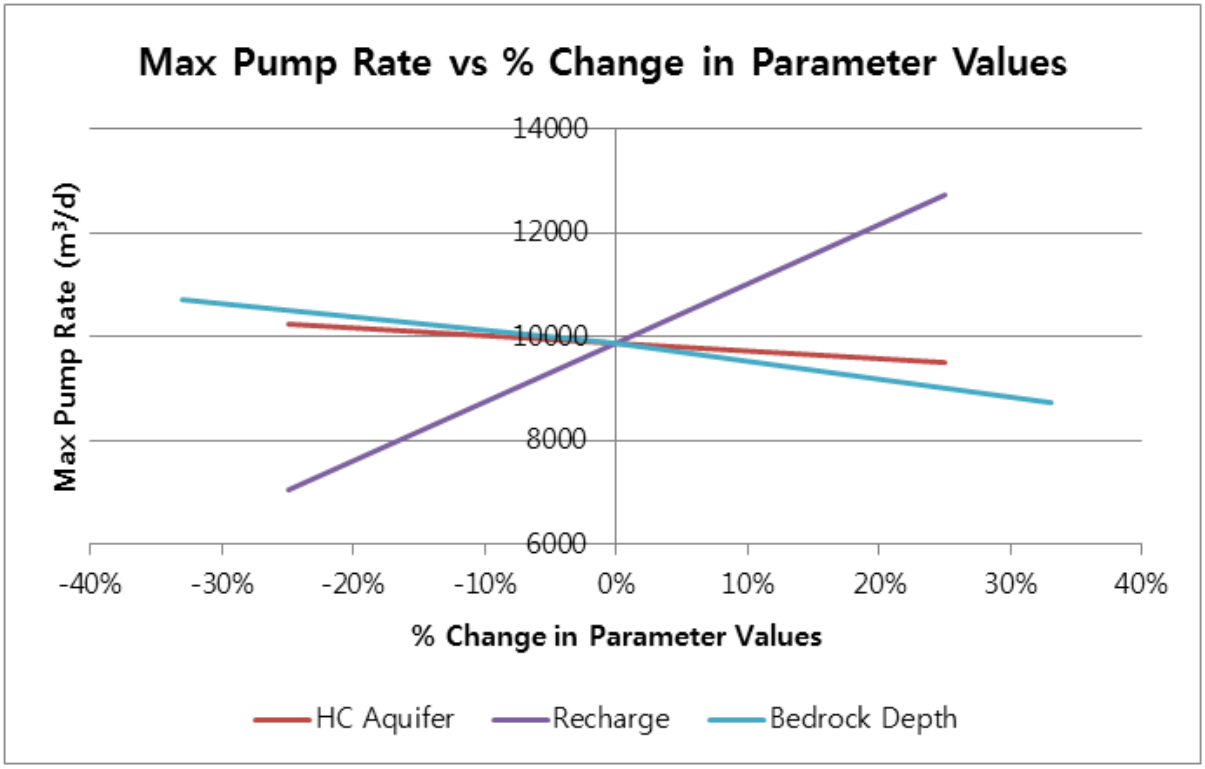

Figure 5.7. Sensitivity Analysis Results. Only three parameters showed a significant change in max pump rate achieved.

Table 5.3 Sensitivity Gradient

Parameter	Gradient (m^3/d per +10% change)
Bedrock Depth	-298
HC aquifer	-147
Recharge	+1136

The sensitivity gradient was defined as the change of achieved pump rate expected with a 10% change to the parameter of interest. From the analysis (Figure 5.7 and Table 5.3), an increase in bedrock depth and hydraulic conductivity of aquifer had a negative impact on the maximum pump rate while avoiding saltwater intrusion. The increase in recharge had a positive impact on the maximum pump rate achieved as expected. Recharge parameter was found to be

the most influential parameter in determining the maximum pump rate achieved on the island while porosity and compressibility had zero influence on the objective function. The depth of the aquifer base ranked second. Therefore, studies that can reduce uncertainties in surface recharge rates and aquifer base depth are recommended to refine the estimates.

5.3.3 Conclusion

This section investigated the groundwater constraint for the aquifer. The limit identified in the regional authority GIS database was 427ML/year (7% of recharge). The physically possible limit of using active bores without creating saltwater intrusion was 679ML/year (11% of recharge). Maximal limit considering further groundwater development throughout the island was 3,600ML/year (81% of recharge). This estimation was obtained solely from the hydraulic point of view that will prevent saltwater intrusion. Not all areas of the island can be developed with bores with high densities. Some highlands and rural areas that are too far away from society will not have economic feasibility due to the cost associated with the transport of water. This is linked with the rough topography of the island, which renders a large portion of the island unsuitable for high-density urban development. The groundwater potential constraint used for the matrix based constraint modelling in chapter 6 is the physically possible limit, 11% of the island-wide recharge, 679,000m^3/year.

5.4 RWH constraint

Rainwater systems are considered as the primary source of freshwater when there is no centralised supply through reticulation (Gabe, Trowsdale, & Mistry, 2012). They are adopted in many rural areas. They are cheap and easy to maintain compared to the reticulated

counterparts. About 10% of the New Zealand population relies on collected rainwater supply (Abbott, Caughley, & Douwes, 2004). Rainwater harvesting systems has a large variety of materials, arrangements and scales (Mishra, 2006). Alternative rainwater harvesting setups share the same functional component arrangement: collection catchment, treatment, storage and distribution. The major criterias for the RWH constraint are the catchment area and the storage volume capacity. A good combination of the roof area and storage volume is essential for optimal design operation of RWH. Enough storage volume is needed to prevent the overflow of the collected rainwater. The relationship between the roof area and the storage volume is dependent on the rainfall pattern, where the prolonged, concentrated seasonal rainfall will create an overflow from the storage tank.

5.4.1 Background of the Region

In Waiheke Island, roofs of most buildings are equipped with a water collection unit. GIS building footprint layer provided by Auckland Council was used to estimate the total roof area utilised as a catchment surface (see Table 5.4). Roof areas of auxiliary buildings such as garages and water storage tanks are not connected to the storage tanks. It was assumed that 80% of the island-wide building roof surfaces were actively collecting rainwater. A nominal 80% collection efficiency of these collection surfaces was assumed, which was used as a rough guideline in rainwater tank design manuals. In Section 5.4.3, the collection efficiency will be determined using a collection simulation model. The annually harvested volume was then calculated with the following equation:

$$V = PAe_1e_2 \quad (5.1)$$

where P is precipitation depth (m), A is total roof area (m^2), e_1 is connection rate, and e_2 is the

collection efficiency.

Using the 80% collection efficiency, the island-wide capacity of rainwater harvest was 554ML/year (= Rainfall depth x Total connected roof area x efficiency) based on the GIS measurement of island-wide total roof area of 847,000m^2, the total building footprint area. Not all roof areas are connected for collection. 80% of the footprint was assumed to be connected for the rainwater collection (i.e. e_1=0.8). The collection efficiency was obtained from preliminary simulation results (Section 3.2), and it was 65% (i.e. e_2=0.65). The building footprint measurement included auxiliary structures such as small garages and rainwater tanks which do not contribute to the collection.

The total island-wide annual acquisition capacity with the current level of infrastructure was 1,022ML/year. This is only 2.4% of the annual island-wide renewed freshwater volume, 41,900ML/year (= Rainfall – Evapotranspiration; UNESCO (2009) reports this quantity as the total renewable water resource available for a basin). The island's utility rate of the annually renewed freshwater volume was very low because only the western part of the island was being utilised for freshwater collections. The annually renewed freshwater volume of 41,900ML/year is the absolute upper limit for a regional water availability. This value is the budget that all entities on the island (human and environmental) must share.

Table 5.4. Input data sources for the model

Component	Data Sources
Household Uses	
Population and Household Count	Statistics New Zealand (2006, 2007)
Drinking, Cooking, Food Prep.	WHO (2006).
Dishwashing, Shower	Heinrich (2007).
Toilet, Laundry	Use the scenario set to match Heinrich (2007).
Car Washing	Assumption.
Irrigation use	
Agricultural Categories	Agriculture business with a large share of employee counts (Statistics New Zealand, 2010).
Vineyard Irrigation Rate	Logan (2009).
Vineyard Area	Digital Aerial Photo supplied by Auckland City Council (2009).
Olive Irrigation Rate	Olives Australia (2009) and FAO Water (2010).
Olive Area	Digital Aerial Photo supplied by Auckland City Council (2009).
Animal Water-use Rate	Stewart & Rout (2007).
Animal Count	Stringleman (2005) for cattle and sheep. Assumption for horses.
Other Crops Irrigation Rate	Australian farm stats (Queensland Goverment, 2009).
Other Crops Plantation Area	Assumption.
Commercial uses	
Commercial Categories	Intensive water user businesses (Statistics New Zealand, 2010).
Visitor Count	Season visits scenario based on Waiheke Community Board (2008).
Office & Workforce	Assumption - 2 flushes+2 hand washes + drinks per worker for a working day. 300 working days per year.
Fire Station	Scion (2007) and Cote (2003, p. 374).
Wine Production per year	Scaled from national stats (NZ Wine Growers Association, 2010).
Concrete Water use rate	Portland Cement Association (2010).
Concrete Mixing per year	Scaled from national stats (Gaimster, 2009).
Others	Assumptions.
Collection Instruments	
Rainfall Data	NIWA (2014).
Roof area	Auckland City Council GIS layer
Water Balance Ratio	Calibration study by SKM (2007).
Roof connection rate	Assumption. 80%.
Rainwater Tank	Average tank volume 15400L (WRCG Ltd, 2004).
FF Diverter	0.14ML temp store volume in proportion to collection roof area. Assumption of 0.07ML/day drip rate (Texas Water Development Board, 2005).
Collection Efficiency	Simulation result in Section 3.2.
Pump Count	Auckland Regional Council GW Consent Files
Pump Yield	Scenario built based on water resource allocation report (ARC, 2008).

5.4.2 Current Installed Capacity of RWH

To estimate the limit of the water collectable from the roof rainwater harvesting system, under seasonal variability, a daily time-step rainfall capture-storage-use simulation was constructed. A two-stage tank model was used (Figure 5.8). The raw rainwater from the roof is initially collected to the smaller tank, the first flush diverter (FFD), which traps the initial run-off with a high level of contaminant from the roof (Texas Water Development Board, 2005). The FFD has a limited storage volume, and an overflow is generated during an intense rain event. The overflow gets stored in the main, second stage storage tank. During an extreme storm event, even the main storage may experience overflow. When the overflow occurs, the water is lost to the environment and the harvesting system will experience inefficiency (Equation 5.9). The rainwater harvesting system over the whole island was aggregated to a single system with total daily use rates, roof area, and tank storage volumes at a island-wide level. The 95-year daily-step rainfall time series was used to drive the model (1915-2010; NIWA, 2014).

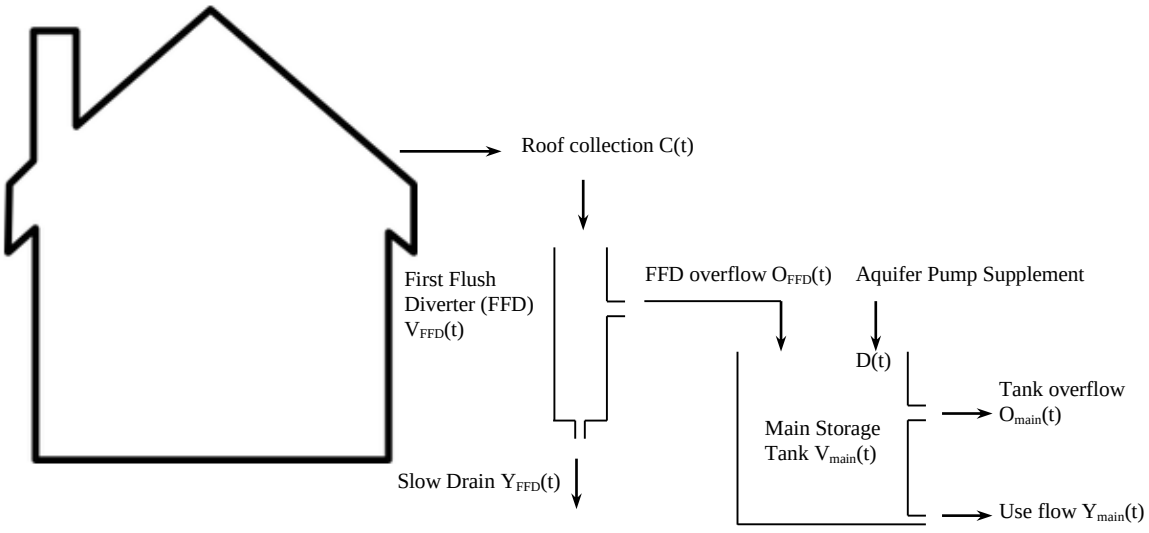

Figure 5.8. Rainwater Harvesting Simulation Structure. Two tank model. The definition of the mathematical symbols is given in the text.

Table 5.5. Daily Water Use Rate Schedule. Unit=ML/day.

Month	Days	Residential Steady	Residential Seasonal	Irrigation Steady	Irrigation Seasonal	Hotel	Commercial	Workforce	Total Daily
Jan	31	1.116	0.044	0.057	0.024	0.707	0.065	0.039	2.052
Feb	28	1.116	0.044	0.057	0.024	0.248	0.065	0.039	1.593
Mar	31	1.116	0.044	0.057	0.024	0.085	0.065	0.039	1.430
Apr	30	1.116	0.000	0.057	0.000	0.015	0.065	0.039	1.292
May	31	1.116	0.000	0.057	0.000	0.015	0.065	0.039	1.292
Jun	30	1.116	0.000	0.057	0.000	0.015	0.065	0.039	1.292
Jul	31	1.116	0.000	0.057	0.000	0.015	0.065	0.039	1.292
Aug	31	1.116	0.000	0.057	0.000	0.015	0.065	0.039	1.292
Sep	30	1.116	0.000	0.057	0.000	0.015	0.065	0.039	1.292
Oct	31	1.116	0.000	0.057	0.000	0.015	0.065	0.039	1.292
Nov	30	1.116	0.044	0.057	0.024	0.015	0.065	0.039	1.360
Dec	31	1.116	0.044	0.057	0.024	0.707	0.065	0.039	2.052
Year Total (ML)		407.5	6.6	20.8	3.6	57.1	23.6	14.2	533.4

The Yield-After-Spillage (YAS) method is a more accurate daily-time step representation of the simulation for rainwater harvest process than the Yield-Before-Spillage (YBS) method (Fewkes & Warm, 2000; Ward, Memon, & Butler, 2010). The yield here means the withdrawal of stored water for use and it is computed after the overflow has been calculated. Daily step rainfall time series, P(t), was used to calculate the collected volume, C(t), where t is the index for the days. The fluctuation of the volume in FFD component, $V_{FFD}(t)$, was simulated according to equation (5.2) to (5.5), and the overflow from FFD, OFFD(t), was used as an input volume time series for the main tank storage.

$$C(t) = P(t)Ae \tag{5.2}$$

$$V_{FFD}(t) = MIN(S_{FFD}, V_{FFD}(t-1) - Y_{FFD}(t-1) + C(t)) \tag{5.3}$$

$$O_{FFD}(t) = MAX(V_{FFD}(t-1) - Y_{FFD}(t-1) + C(t) - S_{FFD}, 0) \tag{5.4}$$

$$Y_{FFD}(t) = MIN(V_{FFD}(t), Y_{FFD,nominal}) \tag{5.5}$$

The volume of water in the main tank, $V_{main}(t)$, was simulated with equations (5.6) to (5.8).

The additional equation was added to account to meet the daily water demand D(t). At the regional level, D(t) is the amount that has to be supplied by secondary means, i.e. the aquifer pumping (equation 5.9).

$$V_{main}(t) = MIN(S_{main}, V_{main}(t-1) - Y_{main}(t-1) + O_{FFD}(t)) \quad (5.6)$$

$$O_{main}(t) = MAX(V_{main}(t-1) - Y_{main}(t-1) + O_{FFD}(t) - S_{main}, 0) \quad (5.7)$$

$$Y_{main}(t) = MIN(V_{main}(t), U(t)) \quad (5.8)$$

$$D(t) = MIN(Y_{main,nominal} - Y_{main}(t), 0) \quad (5.9)$$

The initial conditions and the parameter values are in Table 5.6.

Table 5.6. Parameters for the simulation.

Parameter	Description	Value
$V_{FFD}(0)$	Initial volume in FFD	0
$V_{main}(0)$	Initial volume in the main tank	0
A	Aggregate Roof Area used for collection	847,500m^2
E	Collection Efficiency	0.8
S_{FFD}	Storage Capacity of FFD	0.14m^3
$Y_{FFD,nominal}$	Nominal slow drain rate for FFD	0.07m^3/d
S_{main}	Storage Capacity of the main tank	54.479m^3
U(t)	Water use Demand	Table 5.5

The output time series of the simulation that were of particular interest were $O_{main}(t)$ and D(t), which were further analysed to assess the two performance measures of the current rainwater harvesting setup in the island. The total annual overflow, $O_{main}(t)$, is associated with the efficiency of the collection-storage design. Installation level of the main storage volume must match the collection capacity from the roof area so that the seasonal rainfall during the wet period is carried over to the dry period. If the storage volume is insufficient for the collection capacity, overflow will occur, resulting in inefficiency due to a parameter mismatch. This system inefficiency was measured by comparing the annual overflow to the annually collected volume from the roof catchment. The overflow quantity has a complementary relationship with

the total annual yield (i.e. actual water used):

$$\text{System Efficiency} = \frac{\sum Y_{main}(t)}{\sum C(t)} = 1 - \frac{\sum O_{main}(t)}{\sum C(t)}, \text{ for each year} \quad (5.10)$$

The monthly total of the yield deficit D(t) is associated with the volume of aquifer pump needed to support the exceeding water demand for the dry seasons. This quantity was compared to the maximum pump capacity, which has been estimated from a bore consent database provided by the council. The D(t) were aggregated for each month so that the pump operation percentage can reflect the seasonal fluctuation of the water stress:

$$\text{Pump Operation \%} = \frac{\sum D(t)}{\text{Pump capacity}} \text{ x } 100\%, \text{ for each month} \quad (5.11)$$

If this quantity for a particular month exceeds 100%, this means that the water requirement for the month cannot be covered by the pump capacity allocation defined by the council. It is highly likely that the residents would have experienced water shortage issues. When such incidents occur, on the time series, the water supply system (consisting of rainwater harvest and aquifer pump system) was considered to have failed for the month.

The identification of failed months was extended to define statistical water supply reliability. Of the 95-year time series generated from the simulation, the highest monthly operation levels for each year were recorded. Then, the probability of an exceedance curve for the pump operation levels percentage was constructed at a yearly level. Based on the probability of the exceedance curve, reliability could be estimated:

$$\text{Reliability} = \frac{\text{no.of failed years}}{95} \quad (5.12)$$

where the failed year was defined as any year that had a pump operation level exceeding 100%

for at least one month in a particular year.

A key output of the daily time-step simulation was the pump operation level (Equation 5.11). In summer days, the population demands pump supply as their rain tanks start to run out by prolonged dry days. The daily pump capacity allocated by the regional council was 1.17ML/day (=427ML/365; Section 4.1.2), and it formed a constraint for aquifer pumping. Figure 5.9 shows the simulation result of the monthly pump operation level percentage for the recent 10-year to demonstrate the pattern of water scarcity in the recent years. The result showed the seasonal pattern of increased pump operations during the summer as expected - peak pump operations occurred in either January or February. The peak operation level approaching 100% indicates the risk of water supply failure for the year. The pump operation level required in Feb 2010 finally exceeded 105%, and this suggests that the year would have experienced water shortage even with pump operation at its maximum throughout the month. Indeed, during the summer of 2010, the island residents had to queue for the water tank suppliers' delivery and wait for weeks without water.

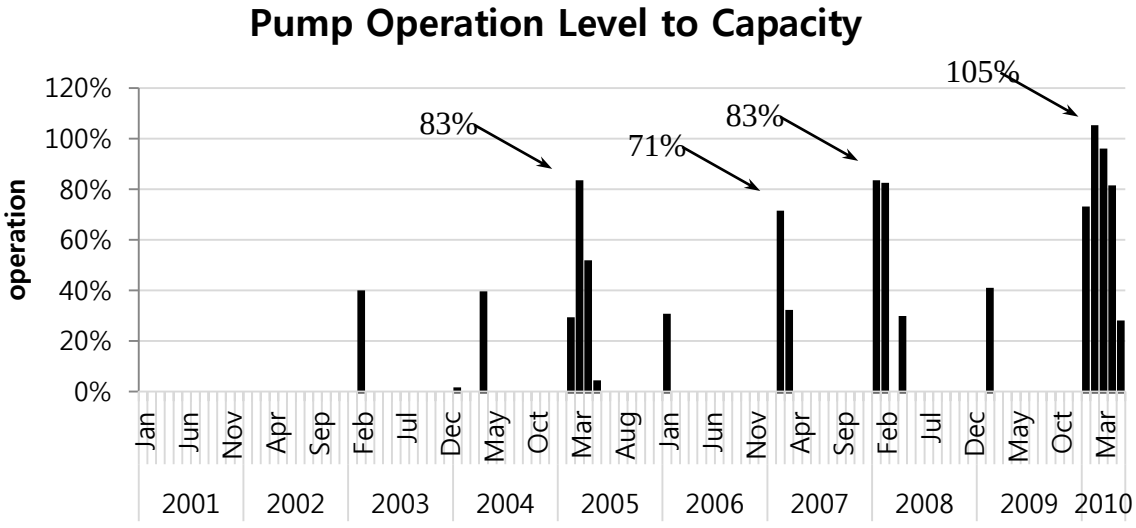

Figure 5.9. Seasonal Operation of Pumps.

The simulation output of yearly operation levels for the last 95 years was used to create the probability of an exceedance curve (Figure 5.10). Out of the 95 simulated years, 22 years showed the water supply failure condition under current infrastructure capacity and population level. This corresponds to a 4.3-year (=95/22) return of water supply failure rate. In the recent years, more frequent water shortage events were reported, and this was mainly due to the population increase. The rainfall pattern more or less stayed the same over the last century, but the water demand has increased for the island due to population growth.

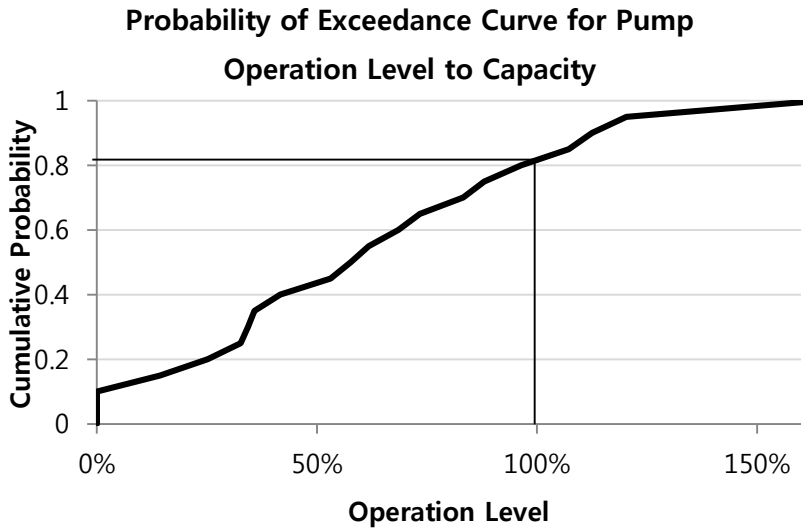

Figure 5.10. Historic Pump Operation level to capacity. Rain-Harvest-Pump simulation run over 95-year historic rainfall data revealed that the current setup would fail around 20% under the historic intra-annual rainfall variation. This means that the current water supply system capacity fails once every 5-years on average if this historic rainfall pattern continues in the future.

Consistent 35% losses of harvested volume due to overflow during the wet seasons were observed in the simulation (Figure 5.11). This indicates the potential for rapid increases in

water availability using rain tank extension via retrofit. The simulation indicated that the loss due to the first flush diverter was only 2% of the harvested volume.

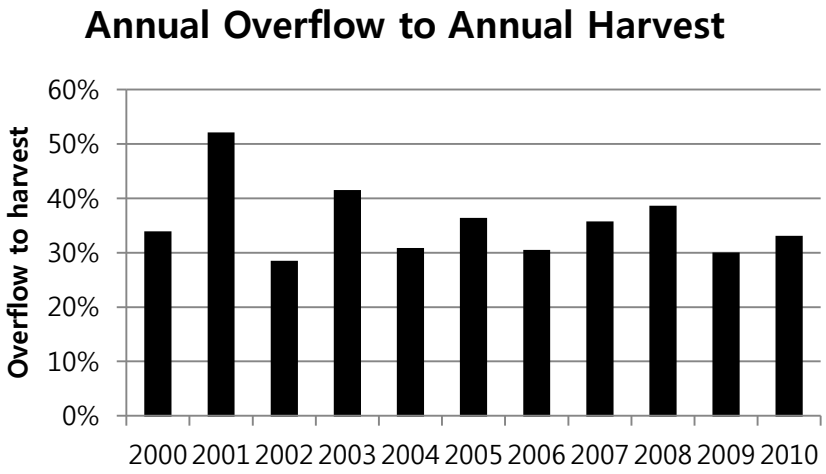

Figure 5.11. Simulated Overflows. A consistent 30% loss of the roof collected volume was observed in the simulation. The rain-harvesting system is running inefficiently because of the tank volume design that inadequately matches the roof area for the collection.

It is commonly accepted that 95% reliability is to be achieved for the urban water supply system (reliable against 20-year drought). The simulation showed that the current system reliability was only 76% (=22/95x100%) for the rainfall pattern for the past 95 years. This shows that the current infrastructure setup (RWH and pumping) does not have sufficient capacity for the water demand of the island. It will be beneficial to link the water supply carrying capacity to the water supply infrastructure upgrades. This was the purpose of the following extension of the investigation.

The simulation model was modified to incorporate the population change by implementing the daily use rate response to the population growth described in the previous paragraph. Several

simulation runs with different population inputs were performed until the simulation achieved a drought reliability of 95%. The population at which the current system achieves 95% reliability was 6,730. This population count is the sustainable population for the freshwater acquisition system.

5.4.3 RWH Extension Capacity

The growth of the infrastructure will ultimately be bound by the physical constraints of the island. The criteria for the physical constraints were researched from literature and measurements obtained from a GIS (Section 4.3). The sustainable population was estimated for each maximum infrastructure growth scenario using the same method above.

Since RWH requires installation material from outside of the island, the financial capability and land area becomes the critical issue. This technology relies on the catchment area and thus, the expansion capacity is ultimately determined by the expansion capacity of the rainfall catchment area. For the onsite strategy of RWH, the roof top is used as the primary catchment area. The roof area is somewhat dependent on the population. Over time the pressure of population growth on the island will increase, which will lead to multi-story buildings in the future; this means the change of the roof area density per population. The roof area will be very dependent on the population growth of the island because the island will most likely be used as a residential satellite centre for the Auckland CBD. The roof area will grow with the population. In the end, the physical limitation of the roof area construction will be limited by the land area available for the urban development. According to the slope suitability assessment for urbanisation, most of the suitable areas are already occupied in a building. The building footprint analysis of some urban centres revealed that the densest urbanised area did not exceed

50% of building footprint to the urban area covered. This means that the MUL boundary of Waiheke Island can be used to estimate the approximate limit to the roof area. The MUL boundary for urban development is 6km^2. From the slope suitability analysis for urban development in Section 5.5.2, the urban area can be grown up to 8.9km^2. With 50% maximum intensification of urbanisation, a maximum of 3km^2 roof area can be achieved for Waiheke Island. Compared with the current roof area of 890,000m^2, the maximum roof area possible is around three times the current area. The water collection capability can only grow up according to that amount. With water collection efficiency increase via the increase in storage volume, the amount can increase by around 30% at maximum. If the land area is going to be fully utilised by providing the roof area for collection only, the potential for improvement will be 3.9 times the current capacity.

The actual carrying capacity will not be as much as the estimated above because not all land area is used for water supply. The land area is shared with the onsite wastewater strategy which is utilised by the island community. Therefore, not all the 6km^2 available area is going to be used to sustain the population in terms of water resources services. The full answer considering the interaction will be described in Chapter 6.

5.4.3 Conclusion

The sustainable population capacity of the current Waiheke freshwater acquisition system is 6,730 and is susceptible to a peak season failure of a 4.3-year return drought. With respect to the matrix model, the rainwater collection constraints are defined by two aspects. The first is the land area needed to collect the rainwater. The maximum land area available was identified as 6km^2 in this investigation, which is equal to the current urban limit. This land area will be

shared among roading, reserves, building footprints and others. The next is the collection volume itself. The amount is directly proportional to the rainfall depth and the total building footprint of the region. The collection efficiency can be improved by installing more tank volume to carry the excess precipitation during the wet season, and 90% was estimated to be the maximum for a moderate-to-high cost for tank volume. With the island-wide total roof area being 847,500m^2, a rainfall depth of 1.21m/y and 90% collection efficiency estimates the maximum rainwater potential to be 922,000m^3/y. This value is used in Chapter 6 for further investigation of the sustainability measure of the water resource infrastructure system.

5.5 Onsite Wastewater constraint

In rural areas, the majority of wastewater treatment is done through irrigation involving the septic tanks. The wastewater is discharged directly to the soil through leach fields, and this relies on the attenuation and assimilation capacity of the soil. As the population density increases, there is a risk of cumulative impact on the onsite systems. A regional assimilation capacity of the soil for Waiheke Island's septic wastewater could be estimated using Geographical Information System (GIS) data and parameters obtained from the literature. The assimilative capacity of wastewater is one of many constraints of population increase on Waiheke Island.

5.5.1 Background

Wastewater is the largest outflow of material from human settlement to the environment, and it is excluded in the standard material flow analysis due to its sheer mass. In a well-developed residential urban centre, most indoor use of water is non-consumptive and becomes wastewater.

Auckland, the most populous city in New Zealand, had a residential water supply of 180L/person/day (Auckland Water Group, 2008). Watercare, the provider of water supply and sewer services, estimated that the wastewater volume of around $30m^3$/person/year is generated in the Auckland region (Auckland Water Group, 2008). Sewer systems are utilised to collect wastewater in centralised treatment plants before being discharged into the environment. In rural areas, onsite wastewater treatment systems are used, and septic tank and irrigation systems are the primary options. The Auckland region has approximately 45,000 households and numerous businesses in unsewered areas, which relies on onsite sewage treatment and disposal systems (Ormiston, Floyd, & Gunn, 2004).

The region-wide carrying capacity of wastewater assimilation is defined from the regional assimilation rate:

$$TR = AR_A \quad (5.14)$$

where TR = Region-wide assimilation rate, A = Area available for assimilation and R_A = Rate assimilated per land area. The carrying capacity is multiplied by the per person wastewater production and the assimilation rate.

$$CC = TR/P \quad (5.15)$$

where CC = carrying capacity, TR = Region-wide assimilation rate and P = Per capita wastewater generation. These equations show that the parameters, A, R_A and P, need to be evaluated to estimate the carrying capacity provided by the onsite wastewater treatment strategy for the island. Section 5.5.2 provides an account of the land area available (A) for the strategy. Section 5.5.3 provides an account of the efficiency of the onsite septic tank strategy in terms of the required land area (R_A). Section 5.5.4 concludes with the estimation of the

carrying capacity by bringing these parameters together.

5.5.2 Available Land area for Treatment

The first factor that determines the constraint for onsite wastewater treatment strategy is the limited land area. The land area for the strategy is limited by two reasons:

(1) Not all land on the island can be developed for residential and commercial purposes

(2) Not all section of the property can be utilised for onsite wastewater treatment purposes

Waiheke Island has a rough topography and only a small proportion of the island land area is suitable for urban development. The Municipal Urban Limit (MUL) defined by the land use plan of the regional council reflects the suitable land for the development. The area enclosed by the municipal urban limit had 5,485 property subdivisions and a total area of 8.90km^2 as according to the 2013 GIS data (Figure 5.12). The average size of the property boundary was 1,300m^2. These property subdivisions are used for shops, public facilities, farms and residential houses. Some subdivisions are vacant, and some public facilities may have a larger number of septic tanks. Areas outside of the urban limit have a rough topography and have a low probability of being developed into the densely populated area in the foreseeable future. Even within the current MUL, some property sections were reported to be unsuitable for building residential houses because of unstable slopes (Rawson, 2006); this illustrates the difficulty of a sprawl for the island. The primary land area limit for the onsite wastewater strategy is the MUL for urban development. There are properties with houses outside the MUL but they are constructed at such low density that they do not add significant proportion to the final carrying capacity. Wastewater generated within the MUL cannot be transported outside.

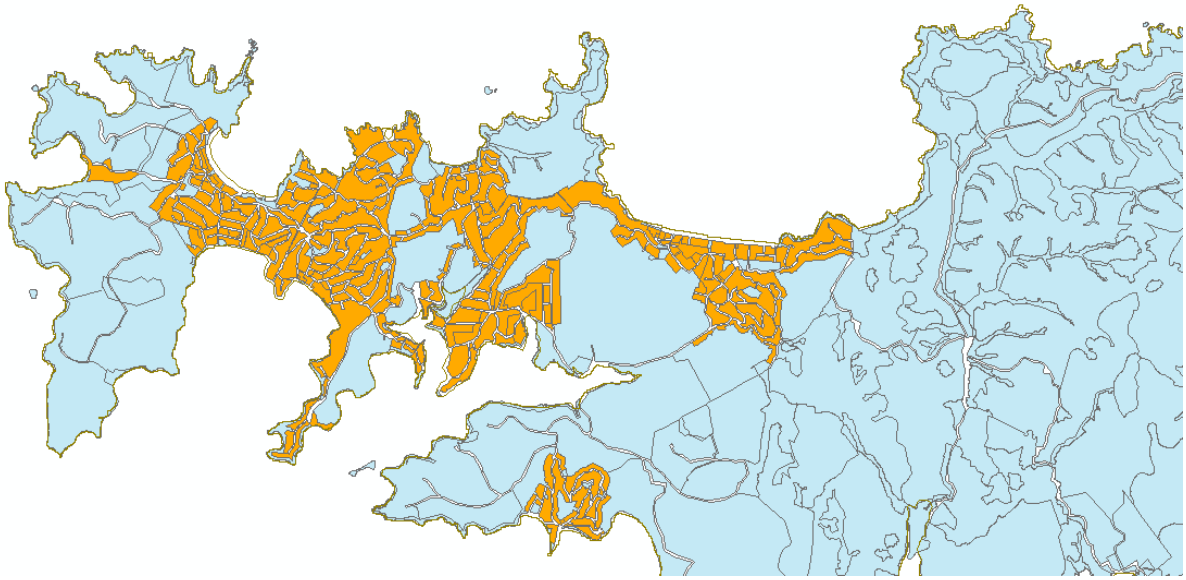

Figure 5.12. The current council plan for Dense Development. Orange Areas are allowed to undergo subdivisions for residential development. These areas have a high density of septic tanks.

Within the urban limit, some areas cannot be used for onsite wastewater systems, constraining the available area for the potential septic tank system installations even further. They are impervious areas including roads and buildings, highly sloped areas, crop fields, sensitive waterbodies such as streams and wells. The available land area for the septic tank system on Waiheke Island was estimated from the GIS data and buffer method. Six GIS layers were obtained from the council for the analysis: 5m Digital Elevation Model (DEM), property boundary, planning Information, the development plan area, building outlines, streamlines, and the island outline. The technical design guideline employed by the council (Ormiston et al., 2004) requires that a minimum offset distance of 3m is to be observed from any building outlines, impervious roads, and horticultural farming areas.

Buffer tool was used to identify the exclusion zones where onsite systems cannot be installed

(Figure 5.13). As shown in the figure, the areas that fall within 3m from the building boundary, property boundary, and sensitive structures (e.g. wells) were excluded. The crème coloured areas are the available land for the septic tank-effllluent irrigation system. Onsite wastewater disposal takes up the land use exclusively, meaning if the land is used for onsite disposals, the land is not available for other uses, such as building or farming because of the hydraulic, and health and safety reasons. This left a narrow strip of the land available for the septic effluent application (the crème coloured areas).

The available areas from the GIS analysis were added up to give the island-wide available area for the assimilation of wastewater. The sum of the available area of urban areas is only 3,362,102m^2. The total available area within for the urban limit excluding roading and stream buffers was 7,554,566m^2. This means only 45% of the urban lands are available for septic tank assimilation because of the exclusion areas due to buildings, streams, wells and roads.

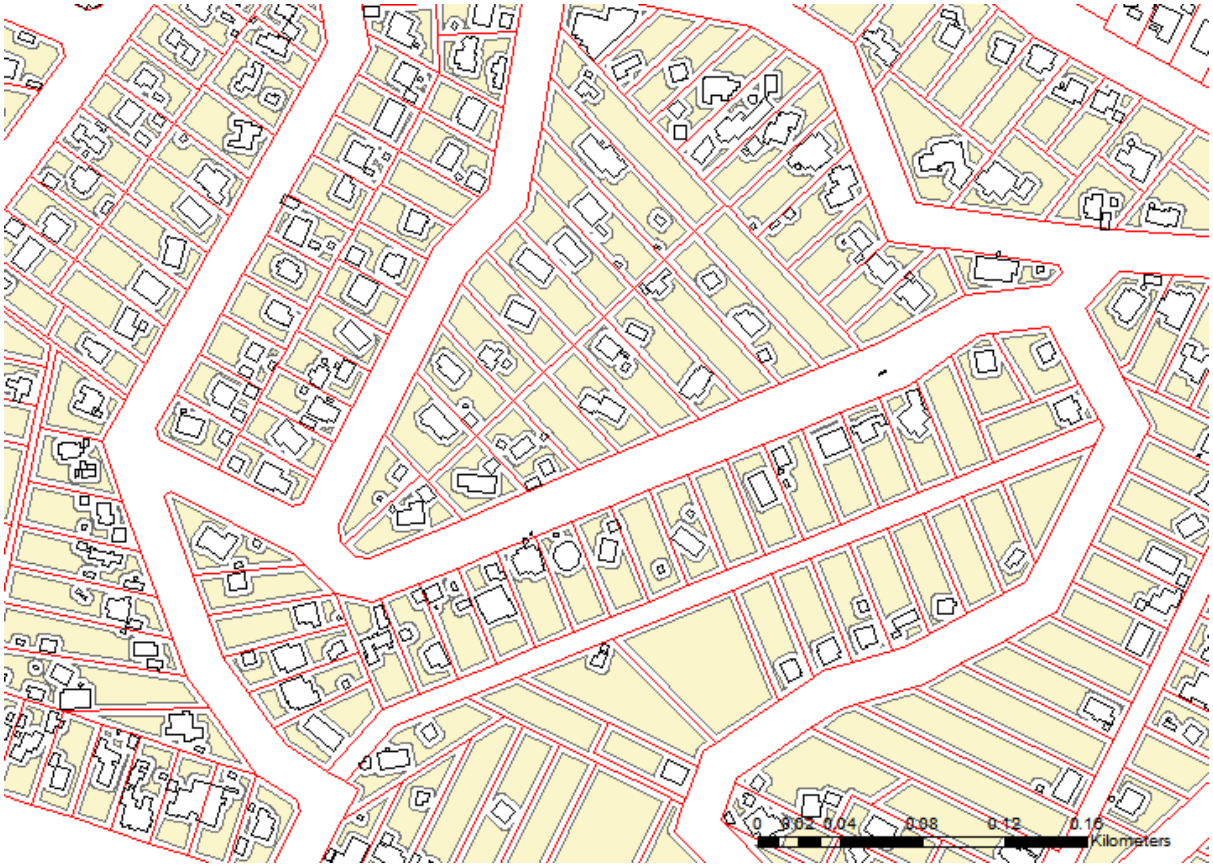

Figure 5.13. An example of the buffering process. The black and red outlines are buildings and property boundary respectively. The white areas that are outside the property boundary are roads and reserves for the utility purposes. 3m buffers are applied to those exclusive objects. The remaining areas noted as cream colours are the available areas for the septic system installations.

5.5.3 Land use efficiency of Septic tank

The rate of assimilation parameter R_A is reflected in the regional septic tank management policy in many different parts of the world. Many local governments view lot size (or area division within property boundary) as an indicator of the septic tanks density threshold. Auckland Council recognises that the appropriate density threshold is 7.0 property per ha, which

corresponds to a lot size of 1400m^2, based on health risk assessment (WRCG Ltd, 2004). Many municipalities in the United States require the minimum lot size to be maintained during urban development to avoid environmental and public health risks from the dense outflow of residential wastewater contaminants. These minimum lot sizes typically range from ½ to 1 acre, which is attributed to Yates (1985). The Washington State Department of Health (2002) underwent a literature review on the origin of the minimum lot size requirements, and they were attributed to several other studies along with Yates (1985); for example, Perkins (1984) presented three mathematical models to predict lot size for limiting nitrate-nitrogen concentrations in groundwater. From these models, the recommended minimum lot size to provide minimum reasonable protection was 0.5 to l.0 acre based on reported data, and 0.75 to l.0 acre based on models. The second controlling consideration is the technical factors such as setback distance requirements between sensitive receptions such as wells and septic tanks, minimum percolation rates, and/or absorption field sizing requirements to provide adequate dilution and attenuation of chemical and biological contaminants, thus preventing contamination of ground water and drinking water supplies (Perkins, 1984; Yates, 1985). These criteria for the lot size threshold for septic tank capacity give a preliminary estimation of maximum population density achievable with the septic tank systems approach. The design parameter of septic tanks for an average household of 3 was 150L/person/day (Ormiston et al., 2004), the average household wastewater generation volume is 450L/septic tank/day.

The septic density guidelines used by various local governments are comparable with the early threshold estimates obtained from considering the dilution process of the nitrates. It is likely that the commonly used values for planning decision were following the guidelines of the early estimation efforts and publications. US septic tank density guidelines of minimum lot sizes are

based on a mass balance model of nitrates. Consider a conceptual box of soil system of lateral land area A and depth h. When contaminants enter the soil system box via leach field application, contaminants undergo dilution with the infiltration of rainfall and lateral flow of fresh (or lower concentration) groundwater. With fast mixing assumption, in which contaminant concentration is homogenous throughout the box and is updated instantaneously, the mass balance relation can be expressed as the following:

$$C_t V_t = C_s V_s + C_r V_r + C_g V_g + \Delta \quad (5.16)$$

where C and V are concentrations of contaminants and volume, the subscripts t, s, r and g represent total, septic, rain and groundwater flow respectively, and Δ is the mass loading/removal from biochemical contributions. For the scenario of the dilution via infiltration, the mass balance terms V_g and Δ are assumed to be zero (i.e. horizontal water table with no lateral flow and no biochemical breakdown removal). This leaves the dilution between the septic tank and the rainwater. Inclusion of this is achieved by dividing the mass balance equation by area:

$$C_t V_t/A = C_s V_s/A + C_r V_r/A \quad (5.17)$$

where A is the lateral area of the conceptual box. The regional contribution from septic tank V_s can be expressed as:

$$V_s = nV' \quad (5.18)$$

where n is the number of septic tanks installed over the conceptual box and V' is the average effluent volume production per septic tank. The quantity of interest is the area density of septic tanks, D septic tanks per km^2 (D=n/A). The volume of infiltration is expressed as:

$$V_r = (1\text{-}R)PA \quad (5.19)$$

where R is the runoff coefficient, P is the annual rainfall depth rate, and A is the lateral area of the conceptual box. V_r is the portion of the rainfall that participates in the dilution process. The total infiltrated volume V_t is the sum of the two infiltration components, V_s and V_r:

$$V_t = nV' + (1\text{-}R)PA \quad (5.20)$$

Substituting the expressions of V_t, V_s and V_r into equation 5.17 yields:

$$C_t\, nV'/A + C_t\,(1\text{-}R)P = C_s\, V'\, n/A + C_r(1\text{-}R)P \quad (5.21)$$

This equation can be rearranged to make the desired quantity n/A subject of the equation:

$$[C_t\, V' - C_s\, V']\, n/A = [C_r - C_t](1\text{-}R)P \quad (5.22)$$

$$n/A = [C_r - C_t]\,(1\text{-}R)P \,/\, [(C_t - C_s)V'] \quad (5.23)$$

The area septic tank density is dependent on the nitrate concentration of the rain and septic tank effluent, runoff coefficient, precipitation depth and septic tank effluent production volume. As a quick guideline, Porter et al. (2000) estimated that the total nitrogen concentration of rainfall in semiurban areas was 1.2 mg/L in Eastern US. An estimation found for a UK semiurban area (Conolly et al., 2010) agreed with this estimate, 1.3 g/m^3 for UK (i.e. C_r = 1.2 gN/m^3). Typical residential septic effluent has a nitrate concentration of 100gN/m^3 (Ormiston et al., 2004). The drinking water quality targets for nitrate and nitrite in US are 10 g N/m^3 and 1 g N/m^3; this makes the total nitrogen target C_t = 11gN/m^3. The runoff coefficient for suburban residential areas is 0.25-0.40 (Akan, 1993; R=0.3 used for calculation). For a typical subtropical climate, the rainfall depth rate P is around 1200mm/year (P = 1.2 m/yr). A typical 3-people household has the design effluent volume rate V' of 450L/day (i.e. V' = 164m^3/yr). Putting these data into

the equation gives n/A = 0.000564 septic tanks/m^2 = 564 septic tanks/km^2. The dilution process of rainfall with background nitrate concentration can reduce the concentration of the nitrate down to drinking water quality, from septic tank densities up to 564 septic tanks per km^2. This number is close to the threshold of degraded environmental quality due to high septic tank density observed in Yates (1985).

The highest septic tank density recommended by Yates (1985) was 1/4 acre per septic tank (988 septic tanks/km^2). Many states of US follow this recommendation with the regulatory requirement of minimum size for a subsection of the rural land. New Zealand and Australia do not regulate septic tank densities but Auckland Council began to consider one dwelling per 3000m^2 lot size (333 septic tanks/km^2) as the threshold for high septic risk which requires rigorous regional strategy placed for onsite system management. The current average lot size for Waiheke Island is around 1300m^2 (769 septic tanks/km^2). The prediction made by the dilution from rainfall alone can account for the thresholds utilised by the regional authorities. Although not explicitly stated, the regional authorities are using the result of the rainwater dilution factor for setting the policy limit. This simple calculation demonstrates that the rainfall dilution process contributes to the bulk of the treatment power required to bring down the contaminant load concentration from septic tanks to a safe water quality level. The septic tank density thresholds from different considerations ranges from 333 to 988 septic tanks per km^2.

This estimation is a conservative underestimation since it does not take into account the attenuation process of the soil-aquifer system (the term Δ in Equation 5.16). The inclusion of the biochemical degradation term Δ will decrease the concentration of the effluent in the subsurface environment over time, and the actual threshold density of the septic tanks will be higher than what was estimated above. However due to the large uncertainty involved with the

attenuation rate estimation for Waiheke Island, it is premature to include the attenuation factors in the threshold calculation. The current thresholds used by the regional authorities are conservative figures that allow for a safety factor. With the large uncertainty and variability involved in the biochemical process rates, it is advised to use the current estimation parameters appearing in the technical guideline. This thesis adopted the upper end of the threshold ranges (i.e. 333-988 septic tanks per km^2), 1000 septic tanks per km^2, considering the effect of the biochemical processes. This is the value suggested by the Yates (1985) and this translates to a $1000m^2$ minimum land area needed per septic tank.

5.5.4 Carrying Capacity by Onsite Wastewater Technology

The constraints identified in section 5.5.2 and 5.5.3 can be combined to estimate the population capacity provided by the onsite wastewater treatment strategy (Equation 5.14 and 5.15). Section 5.5.2 estimated the available land area for septic tank installation to be $3,362,102m^2$. Section 5.5.3 estimated the land requirement per septic tank installation to be in the range of 333 to 988 septic tanks per km^2. Assuming each lot can accommodate three people, the population density achievable through using the septic tank strategy ranges from 3,400 to 10,000. The population on the island in 2013 was 8,262 (SNZ, 2015), which indicates that the capacity threshold in terms of the septic tank strategy has been exceeded or is close to being exceeded. Considering the effect of biochemical assimilation in increasing the allowed septic tank density, it is likely that the threshold is on the upper end of the estimated range (subject to further research). The land area requirement per septic tank of $1000m^2$/septic was used in the subsequent chapter.

The abovementioned carrying capacity estimation assumed a certain scenario for the allocation

of land use. Of the 8.9km^2 land area enclosed by MUL, 3.36km^2 was considered to be available for the septic tank use. In reality, the land area is dynamically shared with regional development with the building footprint for RWH. It is difficult to distinguish how the land area suitable for urban development is going to be allocated beforehand. When estimating the carrying capacity, the effect of sharing land resource with another water resource technology must be considered. How the interaction is addressed is demonstrated in Chapter 6.

5.6 Greywater Reuse Potential

The capacity for greywater is constrained by the installation rate and the availability of greywater feed. It is assumed that a fixed proportion of the household water use becomes greywater. Greywater is the wastewater collected from faucets, showers, and washing machines, whose effluents contain less amounts of organic matter. According to a sampled monitoring study of 51 houses in the Auckland region (Matthias Heinrich, 2008), the proportions of the water usage suitable for greywater feed during summer and winter were 44.2% and 53.7% respectively (Table 5.7), while the proportion of the water usage suitable to use the collected greywater during summer and winter were 39.1% and 26.9% respectively. On average, 51% of the residential potable water use end up as greywater. This is the availability for greywater. Therefore, the total greywater availability grows with the population and the total water supply. Since each person is modeled to use 54m^3 of water per year, the total greywater production potential is around 24m^3/person. This means that the total available greywater quantity for the island grows with population. Other constraints such as costs and electricity are shared with other water infrastructure technology. Greywater reuse systems may not be suitable for public facilities such as commercial buildings due to public health issues, hence the model assumes

that only households will implement greywater reuse systems.

Table 5.7. Household Water Use division (Auckland Region, Heinrich 2008). Category suitable to feed greywater are Shower, Washing Machine, Bathtub. Category suitable to use greywater are Toilet and outdoor.

	Total use (%)		Indoor use (%)		Average (l/p/d)	
	Summer	Winter	Summer	Winter	Summer	Winter
Tap	11.9	13.5	15.6	15.5	24.3	22.7
Shower	22.2	26.7	29.8	30.5	45.3	44.9
Washing machine	20.5	23.7	27.4	27.1	41.8	39.9
Toilet	17.4	18.6	22.9	21.3	35.5	31.3
Dishwasher	1.3	1.2	1.8	1.4	2.7	2.1
Bathtub	1.5	3.3	2	3.8	3.1	5.5
Miscellaneous	0	0.4	0	0.5	0	0.8
TOTAL INDOOR	74.22	87.5	100	100	151.3	147.1
Outdoor	21.7	8.3			44.2	13.9
Leaks	3.3	4.2			6.7	7
TOTAL USE	100	100			203.9	168.1

5.7 Other Non-hydrological Constraints

There are other constraints apart from the hydrological constraints. The constraints for the water resource infrastructure system include electricity usage, financial costs, human resources, and the land area needed to install and operate the infrastructures.

5.6.1 Financial Cost

Affordability is measured to be the 5% of the household income. The affordability threshold value is based on the water poverty threshold indicator used in OECD and other development NGOs. The average income of a Waiheke household is NZ$38,725 per household. This means NZ$1,936 per house per year can be used as the maximum to sustain a system of water supply

and wastewater. A 3% affordability threshold of average income was used (Hutton, 2012).

All infrastructure costs money. Ultimately the services provided for the island community have to be paid back by the residents and the commercial entities. The financial capacity is calculated from the water poverty threshold concept, which states that the expenses for the water supply and sanitation must be less than 3-5% of the income (World Bank 2002). The average income for the residents in the Waiheke Island is reported to be $23,500 per person. 3% threshold was used as the financial constraint for the water infrastructure. This means that as the population grows the fund for the water infrastructure grows as well. At the current population level of 8200, $5.8M can be spent on water infrastructure annually. The available fund is assumed to increase linearly with population. The financial capacity allocation for the water resource systems on Waiheke Island was modeled to be 23500N, where N is the population of the island. Therefore, the financial constraint also grows with the population.

5.6.2 Land Area

Land area is another constraint for the water resources and urban development. The land area is used for building and the septic tank irrigation. The septic tank irrigation system will be installed in the lot area. The land is allocated with planning and the planning is undertaken with regards to the slope analysis of the region. The slope analysis shows that Waiheke Island has a more hilly topography than the rest of Auckland. The proportion of the area suitable for urbanisation is less than the rest of Auckland. As was discussed in Section 5.5.2, the total land area for the urbanisation is limited by the MUL, and it was estimated that the land area covered by the MUL was 8.9km^2. Within the area covered by the MUL, the total available area within for the MUL excluding roading and stream buffers was 7,554,566m^2. This area is shared

between buildings and septic tank systems in Chapter 6.

5.6.3 Electrical Grid Supply

Waiheke is connected to the national electricity network by twin 33 kV undersea cables, which crosses the Tamaki Strait (Vector Ltd, 2012). The capacity of this line along with the zone substation is reported to be 2x12.5MVA (Vector Ltd, 2012), while the capital cost of building zone substation is estimated to be around $3M. The maximum electricity volume capacity per year that the transmission line can deliver is 219 GWh/year if operated at its 100% capacity all the time.

The estimated current electricity usage of the island is 10.7% of this capacity. Annual domestic electricity usage for New Zealand in 2004 was 11,723,124 MWh (SKM, 2005) and the NZ population in 2004 was 4.06 million. This gives us a 2,880 kWh/person domestic electricity usage. There is no formal study of the total island power usage but assuming they use the same level of usage with other New Zealanders, scaling down the national domestic electricity usage to 8262 population would use a volume of 23.6 GWh/year, which is 10.7% of the current capacity.

5.8 Summary of Constraint Estimates

The development of the water resource system on Waiheke Island is subject to several constraints. The possible configuration of the water resource system on the island was conceptualised as a network of five technologies in the previous chapter (Section 4.3). This chapter reviewed what elements may constrain the implementation of the water resource technologies. The constraints arise from capacity limits of the physical, environmental, and

financial resources that support the operation of the technologies. Some resources are associated with technology in a one-to-one relationship (e.g. aquifer system – groundwater pump). Many other resources are shared among different water resource systems (e.g. electricity, finance, land area) and identifying the capacity for these resources do not clearly define the limit to the growth of a single technology implementation. A system-wide representation of the constraint must be developed for the entire network of technology implementation to have proper effect of the resource constraints reviewed in this chapter. The estimated constraint values are fed into the matrix model development in Chapter 6. Thus the role of this chapter was to create a list of estimated constraint values to be inserted in the right hand side column vector **g** of the matrix formulation developed in Chapter 3.

$$A\mathbf{x} = \mathbf{f} \quad (5.24)$$

$$B\mathbf{x} \leq \mathbf{g} \quad (5.25)$$

where matrices A and B are the technological coefficients estimated in Chapter 4, and the vectors **f** and **g** are final demand and resource constraints as defined in Chapter 3.

As identified in the conceptual network model in Section 4.3, there were six resources that support the overall water resource network system: (1) Rainwater, (2) Aquifer, (3) Electricity, (4) Finance, (5) Land Area, and (6) Greywater. The modelling and literature review efforts in this chapter can be summarised as six entries to be placed in vector **g,** which are listed in Table 5.8.

Table 5.8. Summary of Constraint Values and Causes.

Constraining Resource	Value	Causes of Constraint
Rainwater Collection	922,000m^3/year	Collection Roof Area, Rainfall depth
Groundwater Potential	679,000m^3/year	Saltwater Intrusion, Location of Wells

Electricity	200,000,000kWh/year	Capacity of Substation, Capacity of Undersea Power Cable
Finance	$705N per year where N = Population	Total Income of the Region, Water Poverty Threshold Index
Land Area	$7.554km^2$	Suitable Land Area for Urbanisation, Land used for roading, Buffer for streams and other sensitive items.
Greywater Availability	$29m^3$ x N per year	Greywater Production Limit from Households

Note. Financial Capacity and Greywater Availability grows with population.

Chapter 6 Application of Matrix Model to the Waiheke Island Water Resource System

6.1 Introduction

This chapter brings together the technical coefficients (Chapter 4) and constraints (Chapter 5) identified for the island within the matrix framework developed in Chapter 3. The volume of feasible region given by the constraints gives a measure of sustainability (Section 3.5.1). With the development of the regional system, the constraint for the demand grows whereas resource constraints diminish - as a result, the volume of feasible space reduces over the course of development. Ultimately, the demand constraint will exceed the allowed resource constraints thus making the volume of feasible space zero. This is when the system cannot be sustained using the modeled technology adoption alone. The population level can be found using the graphs plotted using the Lasserre algorithm when the volume of feasible space becomes zero. This workflow can be utilised to estimate the ultimate sustainable population achieved using the selected technology.

Although the capacity estimation for individual technologies can be found in literature frequently (Cohen-Tanugi, McGovern, Dave, Lienhard, & Grossman, 2014; Jamrah, Al-Futaisi, Prathapar, & Harrasi, 2008; Y. Zhang, Chen, Chen, & Ashbolt, 2009), the estimation of a system-wide capacity of many technologies is novel to literature.

This chapter begins with the application of the framework to the current development strategy, which relies on rainwater harvest, a groundwater aquifer pump and a distributed septic tank-

irrigation technology for the wastewater treatment systems. Scenarios involving additional technologies were then applied to observe the effectiveness of introducing the technologies on the behaviour of the sustainability measure.

6.2 Current Infrastructure Setup

Before going into the hypothetical scenarios, the validity of the method is checked against the known parameters of the island. The sustainability metric found in this section is cross-checked with the constraints considerations and sustainable population discussed in Chapter 5.

6.2.1 Water Supply: 2-Tech Arrangement

The current water supply system on Waiheke Island consists of Rainwater Harvesting (RWH), low yielding bedrock aquifer pumping, and onsite septic tank systems for wastewater treatment (Figure 6.1). This section applies the matrix theory to the two simplest technology systems for water supply. This gives an opportunity to observe the behaviour of the constraints with respect to population growth with the visualisation of feasible space in 2D.

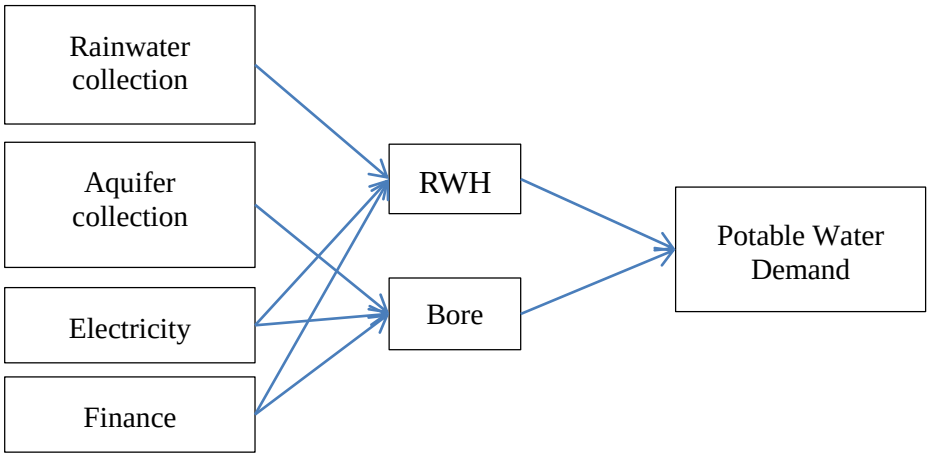

Figure 6.1 The conceptual network for 2-technology system.

The unit process input and output ratios for RWH and aquifer pumping are given with the following vector based on the conversion coefficient found in section 4.3.2:

$$\mathrm{v}_1 = \mathrm{RWH} = \begin{bmatrix} 115.2 \\ 144 \\ 0 \\ 0.0085 \\ 237 \end{bmatrix}, \mathrm{v}_2 = \mathrm{Bore} = \begin{bmatrix} 150 \\ 0 \\ 160 \\ 29.7 \\ 796 \end{bmatrix} \begin{matrix} \cdots \text{ Potable Water (m}^3\text{)} \\ \cdots \text{ Rain Captured (m}^3\text{)} \\ \cdots \text{ Aquifer (m}^3\text{)} \\ \cdots \text{ Electricity (kWh)} \\ \cdots \text{ Unit Cost (\$)} \end{matrix} \tag{6.2}$$

All values are calculated for the yearly production of potable water. The total potable water demand is 54N (m^3) where N is the population of the island. With the lack of a large-scale potable water storage, the produced amount will be the same as the demand. There will be no deposit in the potable water production seen in the time frame. Thus, the potable water constraint will be in the form of equality:

$$115.2s_1 + 150s_2 = 54N \tag{6.3}$$

The constraints of the resources (i.e. captured rain, aquifer pump limit, electricity and finance) will be in the form of inequality because not all resources will be utilised to their potential at a given time. The constraining condition can be expressed in vector form:

$$\begin{bmatrix} 144 & 0 \\ 0 & 160 \\ 0.0085 & 29.7 \\ 237 & 796 \end{bmatrix} \begin{bmatrix} s_1 \\ s_2 \end{bmatrix} \leq \begin{bmatrix} 922000 \\ 679000 \\ 200 \times 10^6 \\ 235N \end{bmatrix} \begin{matrix} \cdots \text{ Rain Captured (m}^3\text{)} \\ \cdots \text{ Aquifer (m}^3\text{)} \\ \cdots \text{ Electricity (kWh)} \\ \cdots \text{ Unit Cost (\$)} \end{matrix} \tag{6.4}$$

The constraints were obtained from the results found in Chapter 5. The volume computation was carried out using the matlab code outlined in Appendix A - the matlab code is shown in Tech 2. The code utilises the function subvol4.m, which is the fourth version of the feasible space volume calculation code. First, the Gaussian elimination was carried out using equation

6.3, then the feasible space formed by the reduced space of single variable was conducted; the resulting graph is Figure 6.2. The graph shows three distinctive regimes with population growth - ultimately the feasible space volume becomes zero at N=25400. The current population is 8240 and the projected supportable population by RWH and aquifer pumping combined is around three times the current population, given that rainfalls are captured and utilised at maximum efficiency.

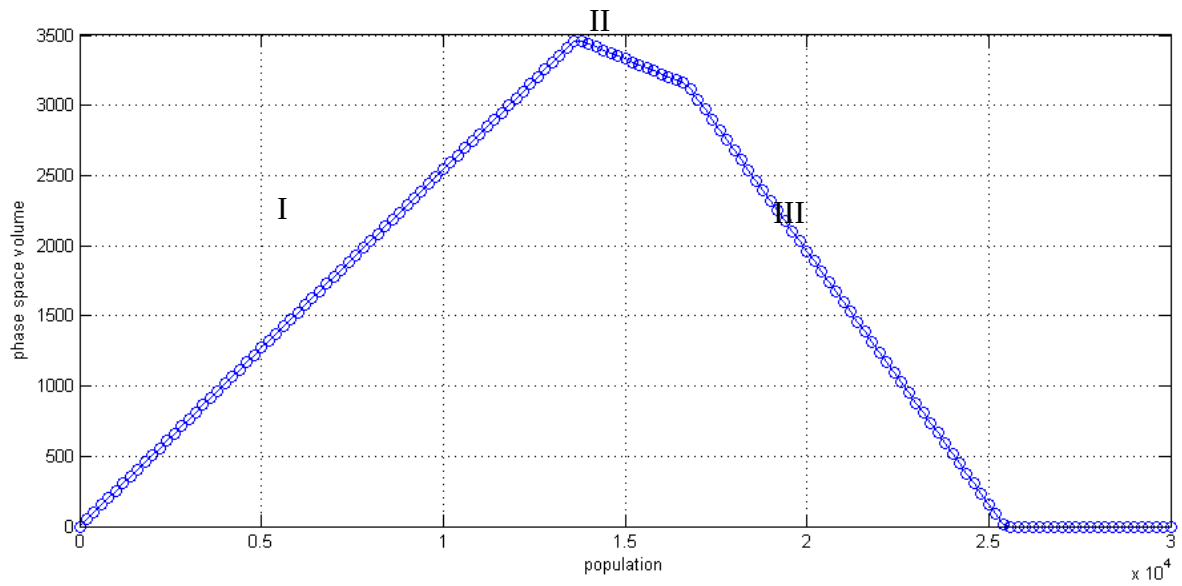

Figure 6.2. Feasible Space Volume versus the Population. The size of feasible space grows initially with the population but declines to zero as population grows beyond carrying capacity. The Roman numerics (I,II,III) represent the different regimes of constraints that the system experiences as the population grows.

The feasible space undergoes a phase transition, in terms of the topology constraints that touches the feasible space. The feasible space segment and the cost constraint shift towards the upper right with the population growth N at the rates determined by the right hand side of the equation and inequation (i.e. 54N and 235N in Equation 6.3 and 6.4). As demand increases

with population, the most constraining resource changes:

- **Regime I:** For $N \leq 13660$, the feasible space is constrained by the cost. With the increase of population, more finance is available for the population at a faster rate than the growth in potable water demand. People have larger freedom in choosing what type of water supply infrastructure they are going to utilise. This is reflected in the increase in feasible space volume.
- **Regime II:** For $13660 \leq N \leq 17250$, the feasible space is constrained by the rainwater potential and financial cost constraints. The growing financial capacity and system reaching the rainwater collection capacity, competes and results in a slow decline of feasible space volume.
- **Regime III:** For $17250 \leq N \leq 27020$, the feasible space is constrained by the aquifer limit from above and the RWH limit from below. The increase in financial budget availability is no longer important because the cost limit line lies beyond the aquifer potential line. At this regime, the feasible space volume decreases at a fast rate, as the system is growing to become saturated to the maximum capacity of water supply system.
- **Unsustainable Regime:** For $N > 27020$, there is no feasible space and the water supply demand cannot be supported by a combination of any two technologies. The population reaches the ultimate end-point of unsustainability, N = 27,024. This is where the size of feasible space becomes zero.

The reason for the phase change can be visualised using the phase space of two decision variables, s_1 and s_2 (Figure 6.3 and 6.4). The intersection of the constraints results in a 1-dimensional region represented as a thick segment. For this case, the feasible space size is the

length of the segment, even though it is called ‘volume’. For higher dimensional systems, where the feasible space has a dimension greater than 2, the terminology makes more sense - this case is demonstrated in a later section. Figure 6.3 shows the snapshot of the relative locations of the constraints at the current population of N=8200. There are static constraints that do not change with population growth. However, the cost and potable water demand constraints change their locations with population growth because the growth of the financial capability and demand changes with population growth. They cause the change in topology among the constraints and thus the change in the rate of growth of the feasible space size.

At the current population of N=8200, the feasible space is constrained by the cost (N=8200 line in Figure 6.3). The actual usage levels of either technology will be a point lying on the feasible space shown as a thick segment (shown as black dots). The length of the feasible space on the N=8200 line represents the freedom of choice of the residents on how much of the water will be withdrawn from the RWH (s_1) and the aquifer (s_2) to meet the demand. The population increase will shift the feasible space to the upper right due to the increase in the water demand. Examples of the locations of demand constraint line are shown in Figure 6.3.

The movement of cost and demand constraints are further visualised with the help of a matlab graphing tool (Figure 6.4; code in Appendix A). The constraints location of N=8200, 15000, 20000 are shown as the typical examples of the growth Regimes I, II and III respectively. The domain and range of the graphs were chosen to be equal to the rectangular region contained by the RWH and bore constraints (grey area in Figure 6.3). The result shows the clear topological change in which constraints are touched by the two ends of the feasible space segment.

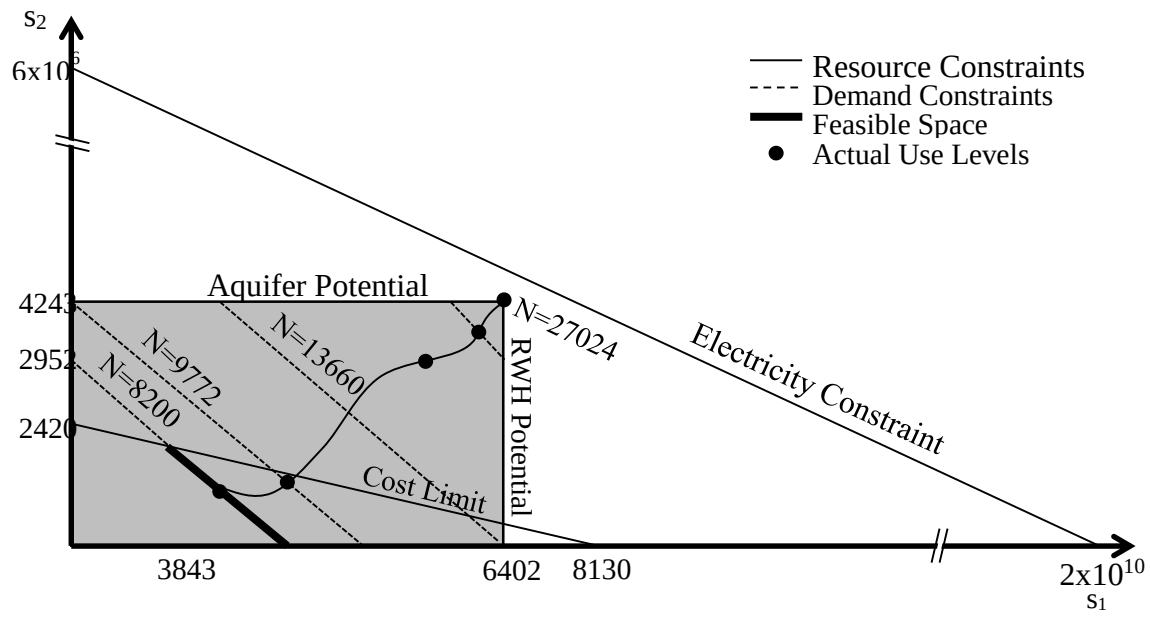

Figure 6.3. The feasible space of the design parameter. The feasible space, in this case, is 1D because of the water supply demand constraint being an equation. The designs must be made within the rectangle confined by the Aquifer and RWH limits.

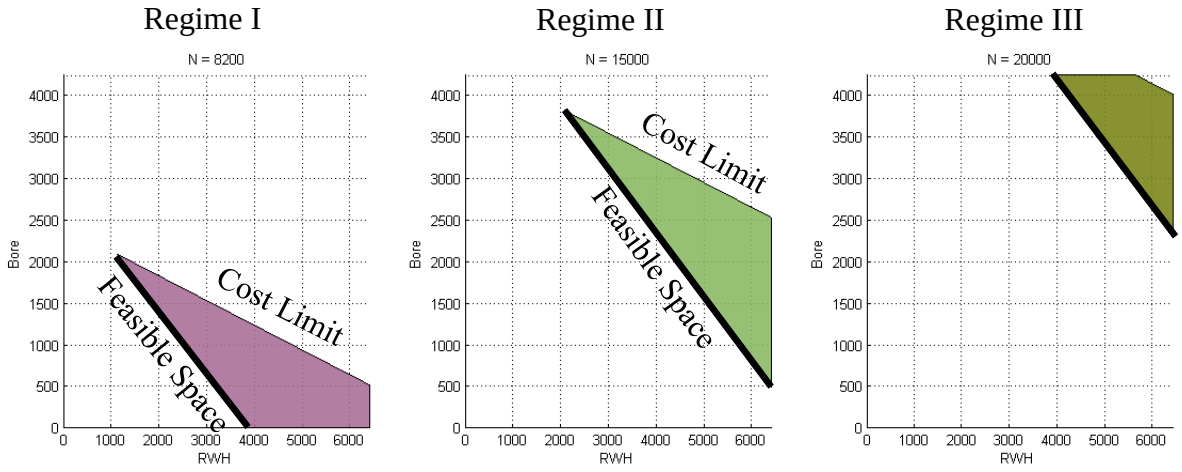

Figure 6.4. The feasible space evolution with population (For N=8200,15000,20000). Regime I: Feasible space is touching the cost limit and zero Bore line. **Regime II:** Feasible space is touching the Cost Limit and maximum RWH potential line. **Regime III:** Feasible space is touching the maximum Bore potential and RWH line.

6.2.2 Supply-Wastewater System (3-Tech)

The current water resource system on Waiheke Island includes wastewater components. The wastewater technology must be included in the framework to assess the population capacity of the technology that are currently implemented. The infrastructure network now consists of 3 major technology nodes that utilise five resource nodes to produce two final demand products. The network diagram is presented in Figure 6.5.

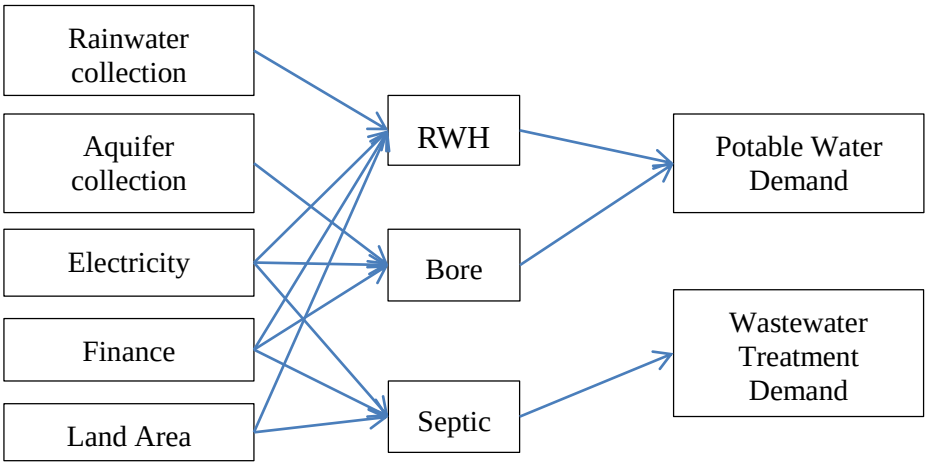

Figure 6.5 The conceptual network for 3-technology system.

The resources to form the infrastructure network, financial cost, electricity and land area, must be shared among the technology nodes. The annual resource and production budget for the septic tank technology (v_3) is summarised by the following vector using the technical coefficients found in Section 4.4:

$$v_1 = \begin{bmatrix} 115.2 \\ 0 \\ 144 \\ 0 \\ 0.0085 \\ 237 \\ 120 \end{bmatrix}, v_2 = \begin{bmatrix} 150 \\ 0 \\ 0 \\ 160 \\ 29.7 \\ 796 \\ 0 \end{bmatrix}, v_3 = \begin{bmatrix} 0 \\ 164 \\ 0 \\ 0 \\ 263 \\ 1437 \\ 1000 \end{bmatrix} \begin{matrix} \cdots \text{Potable Water } (m^3) \\ \cdots \text{Wastewater } (m^3) \\ \cdots \text{Rain Captured } (m^3) \\ \cdots \text{Aquifer } (m^3) \\ \cdots \text{Electricity (kWh)} \\ \cdots \text{Unit Cost (\$)} \\ \cdots \text{Land Area Used } (m^2) \end{matrix} \quad (6.11)$$

The first two rows show the coefficients of the production of services for the community. The coefficients for the supply systems remain the same as the 2-technology supply case study in Section 6.2.1. An additional row of resource, land area was added in the coefficient vectors because the septic irrigation systems use the extensive land area to treat the wastewater. Section 5.5 estimated that the threshold density of the septic system is 1000m^2 per septic tank. The RWH and septic systems use the land area exclusively because the RWH requires building footprint to collect rain and also because the building cannot be built on a septic irrigation field. The total land area used by the water management system is the sum of the areas used for the RWH and septic tank technology. With the population increase, the density of development is expected to increase because of the limited urbanisable land present on the island. An increase in the intensity of the competition of land use is expected with population growth. The septic tank system uses more electricity because of the pump needing to create continous pressure for the seepage pipe system. The capital cost of the septic system is higher than the supply systems. The coefficient is the annualised cost spread throughout the expected life year of the infrastructure (Section 4.4.1).

The final service demand constraints for potable water supply and wastewater treatment volume are expressed as equations (Equation 6.12-6.13). Wastewater treatment is supported with only one technology; the septic tank-irrigation system (s_3) at the moment:

$$b_1 = 115.2s_1 + 150s_2 = 54N \tag{6.12}$$

$$b_2 = 164s_3 = 54N \tag{6.13}$$

The subsequent five rows form the system of five inequations of resource capacity:

$$\begin{bmatrix} 144 & 0 & 0 \\ 0 & 160 & 0 \\ 0.0085 & 29.7 & 263 \\ 237 & 796 & 1437 \\ 120 & 0 & 1000 \end{bmatrix} \begin{bmatrix} s_1 \\ s_2 \\ s_3 \end{bmatrix} \leq \begin{bmatrix} 922000 \\ 679000 \\ 200 \times 10^6 \\ 705N \\ 7.554 \times 10^6 \end{bmatrix} \tag{6.14}$$

The land capacity for the building area and septic tank is assumed to be 7.554km^2 based on the suitability analysis for urban development using GIS (Section 5.5.3). There are three decision variables, and the phase space is positioned in $\mathbf{R}^3$. The dimension of the feasible space will be 1D because there are two equations that eliminate two decision variables. Similar to the 2-technology water supply case, Gaussian elimination was conducted and the matlab code that implements the Lasserre algorithm was carried out under the changing population parameter N. The resulting feasible space volume plot shows a similar pattern to the 2-technology water supply system, but there was an additional phase transition caused by the land area constraint (Figure 6.6). Figure 6.7 demonstrates the interactions of the constraints on the RWH-bore plain (s_1-s_2 axis) of the $\mathbf{R}^3$ phase space. The topology of the constraints look the same in regimes I, II and III, but regime IV shows the effect of the land area constraint which shifts the RWH potential constraint (vertical boundary on the right) to the left. As the population growth increases, this transition of I to III occurs for the same reason as the 2-technology water supply system case. The last phase transition from phase III to IV occurs because the septic-irrigation system has used up the land and it is constraining the building footprint area needed for the RWH collection. The transition from regime III to IV occurs when the population reaches N=20610. The system becomes unsustainable when the population becomes N=21320.

The estimated maximum sustainable population was N=21320 when both the water supply and wastewater treatment systems are considered. This was less than the estimate when the water supply was considered alone, where N=27020. This shows that the water resource carrying capacity for the island population will be determined by the limitation of the land used for the wastewater systems rather than the water supply potential by the two collection methods. This idea is carried forward into the next section when future scenarios are considered to solve these two constraining issues.

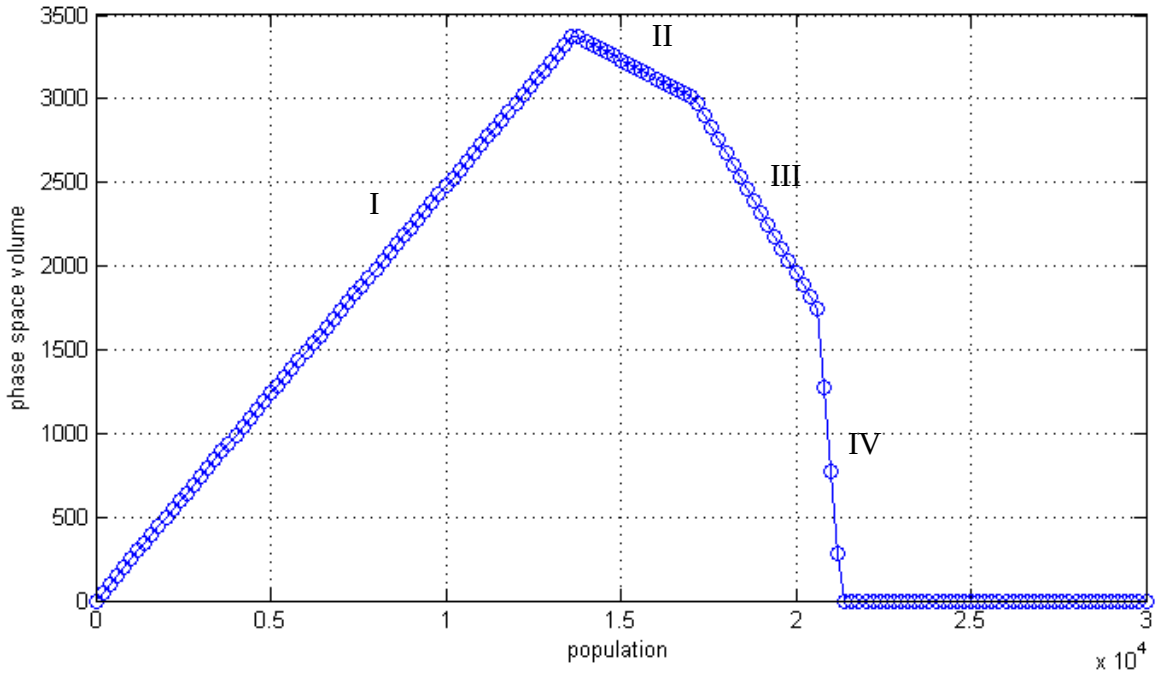

Figure 6.6. Tech-3 Feasible Space Volume Change with the population. The sudden drop off of the feasible space volume is caused by the land area constraint. This resulted in a maximum habitable population using the septic tank strategy which is around N=21310.

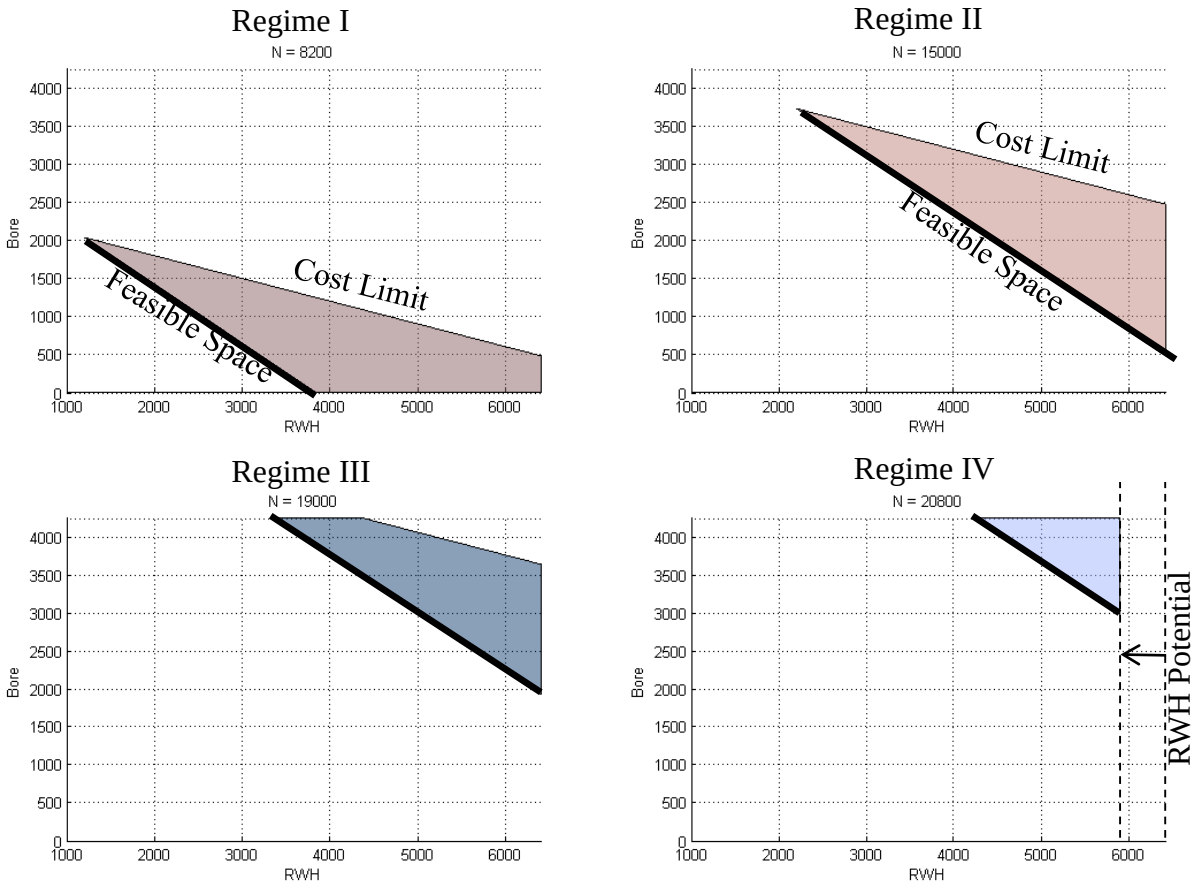

Figure 6.7. Feasible space analysis for the system including the septic tank. Regime I: Feasible space is touching the cost limit and the zero bore line. **Regime II:** Feasible space is touching the cost limit and maximum RWH potential line. **Regime III:** Feasible space is touching the maximum Bore potential and RWH potential line. **Regime IV:** Feasible space is touching the maximum bore potential and RWH potential line, but the RWH line is shifted to the left from the usual value.

6.3 Future Scenarios

The utilisation of the three technologies considered above is the island's current water resource infrastructure strategy. There are many water resource technologies and strategies that can

increase the maximum sustainable population and also alleviate the water shortage issues and environmental concerns experienced even today at the population level of N=8200. This section considers the effectiveness of implementing two additional technologies as hypothetical scenarios for future development of the island: (1) desalination and (2) greywater reuse. The effectiveness is assessed in terms of how they change the feasible space volume along with the population and the maximum population that alternative strategies can achieve. Desalination technology has advanced over the years to reduce the cost to compete with the conventional technology of water production while greywater reuse has been considered as an attractive low-tech option to augment water shortage conditions in dry regions. For example, the modular Seawater Reverse Osmosis (SWRO) desalination units are available for sale or hire. The coefficients for SWRO were obtained from a small scale modular ($250m^3$/day) model of SWRO which is packaged in shipping containers (Section 4.4.3). The technical coefficients and constraining factors used in this section were discussed and estimated in Section 4.4.2-4.4.3 and Section 5.6/5.7.3 respectively for the two systems.

This section is organised to compare the effectiveness between SWRO and greywater reuse in Section 6.3.1 and 6.3.2. The performance of the combined implementation of SWRO and greywater reuse system at an island wide setting is in Section 6.3.3.

6.3.1 4-Technology Systems: SWRO

The mathematical formulation of adding SWRO to the current system is done by adding an additional column vector to the matrix equation. The technical coefficient of SWRO is summarised as the following:

$$v_4 = SWRO = \begin{bmatrix} 150000 \\ 0 \\ 0 \\ 0 \\ 600000 \\ 243000 \\ 0 \end{bmatrix} \begin{matrix} \cdots \text{ Potable Water } (m^3) \\ \cdots \text{ Wastewater } (m^3) \\ \cdots \text{ Rain Captured } (m^3) \\ \cdots \text{ Aquifer } (m^3) \\ \cdots \text{ Electricity (kWh)} \\ \cdots \text{ Cost (\$)} \\ \cdots \text{ Land Area } (m^2) \end{matrix} \quad (6.15)$$

Since it draws water from the seawater inlet, the production quantity is not limited to the freshwater availability within the island. The key environmental impact, apart from the energy use, is the brine emission pumping back to the sea (Lattemann & Höpner, 2008). With a typical permeate recovery rate of 40% (MakWater, 2014), the salt concentration of emitted brine is around 1.67 times the original seawater concentration. It is likely that the dilution process is accompanied before the emission of the brine. The small scale of the plant considered in this thesis is likely to have a negligible environmental impact and will be of future study. The vector shows the potable water production and resource use per yearly operation of the stand-alone full-container size, which is 250m^3/d SWRO unit (MakWater, 2014). Comparing it with the current island-wide water demand of around 1200m^3/d, installation of several SWRO units are sufficient to cover the entire island's potable water demand. High installation cost and electricity consumption has been a prohibitive factor for this technology traditionally.

The final demand for the potable water and wastewater treatment volume are expressed as an equation as in the previous section. The resource capacity is represented with a set of inequations as in the previous section but with the additional column vector for SWRO technology:

$$\begin{bmatrix} 115.2 & 150 & 0 & 150000 \\ 0 & 0 & 164 & 0 \\ 144 & 0 & 0 & 0 \\ 0 & 160 & 0 & 0 \\ 0.0085 & 29.7 & 263 & 600000 \\ 237 & 796 & 1437 & 243000 \\ 120 & 0 & 1000 & 0 \end{bmatrix} \begin{bmatrix} s_1 \\ s_2 \\ s_3 \\ s_4 \end{bmatrix} \begin{bmatrix} = \\ = \\ \leq \\ \leq \\ \leq \\ \leq \\ \leq \end{bmatrix} \begin{bmatrix} 54N \\ 54N \\ 922000 \\ 679000 \\ 200 \times 10^6 \\ 705N \\ 7.554 \times 10^6 \end{bmatrix} \begin{matrix} \cdots \text{ Potable Water } (m^3) \\ \cdots \text{ Wastewater } (m^3) \\ \cdots \text{ Rain Captured } (m^3) \\ \cdots \text{ Aquifer } (m^3) \\ \cdots \text{ Electricity (kWh)} \\ \cdots \text{ Cost (\$)} \\ \cdots \text{ Land Area } (m^2) \end{matrix} \quad (6.16)$$

The same algorithm was applied to find the feasible space volume change with population growth as in the previous section. Gaussian elimination was performed to reduce the number of decision variables using the two equations. Then the matlab function subvol4.m was applied to the resulting matrix inequation to find the feasible space volume for changing the population from 0 to 30000. The resulting feasible space volume plot was Figure 6.8. A noticeable feature of the graph is that it has curved regions; these curves arise mainly due to geometric reasons. Since the feasible space has a dimension of 2, we can have a more felxible combination of technology uses. The topological interactions among constraints have become more complex - another key observation is the sharp cut-off past population N=20000 (Regime V). With this feature, the maximum population is not much different from that of Figure 6.6. This sharp cut-off is caused by the land area constraint. Even if the water supply potential is increased, if the technological problem in wastewater sector is not resolved, the carrying capacity will not increase much (Max pop: N=22950).

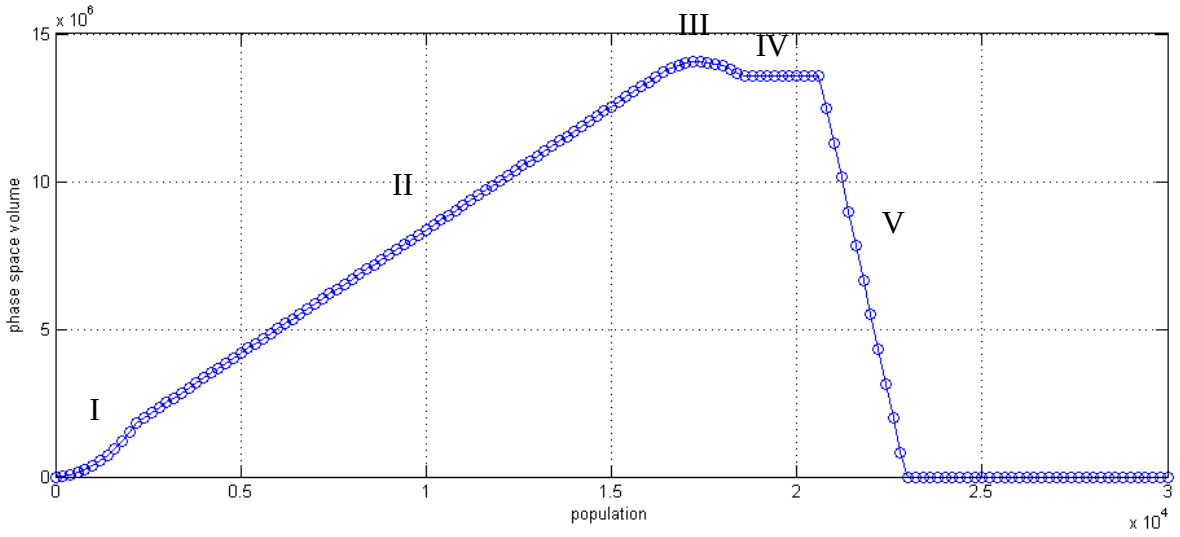

Figure 6.8. Feasible Space Volume Change with Population growth for Tech-4 Scenario with SWRO only.

The changes in the slope pattern are associated with the topological configuration among the constraints. Since there are four decision variables, the dimension of the hypersurface will be 3D while the overall feasible space geometry is 4D. Visualising the geometry as itself is difficult. It is necessary to eliminate decision variables to reduce the dimension of the feasible space plot. Using the Gaussian elimination technique, the decision variable s_3 was eliminated to create feasible space plots in a reduced dimensional space for the visualisation of constraint relations. A slight increase in maximum population is observed which is caused by the slight reduction in reliance in RWH for potable water production.

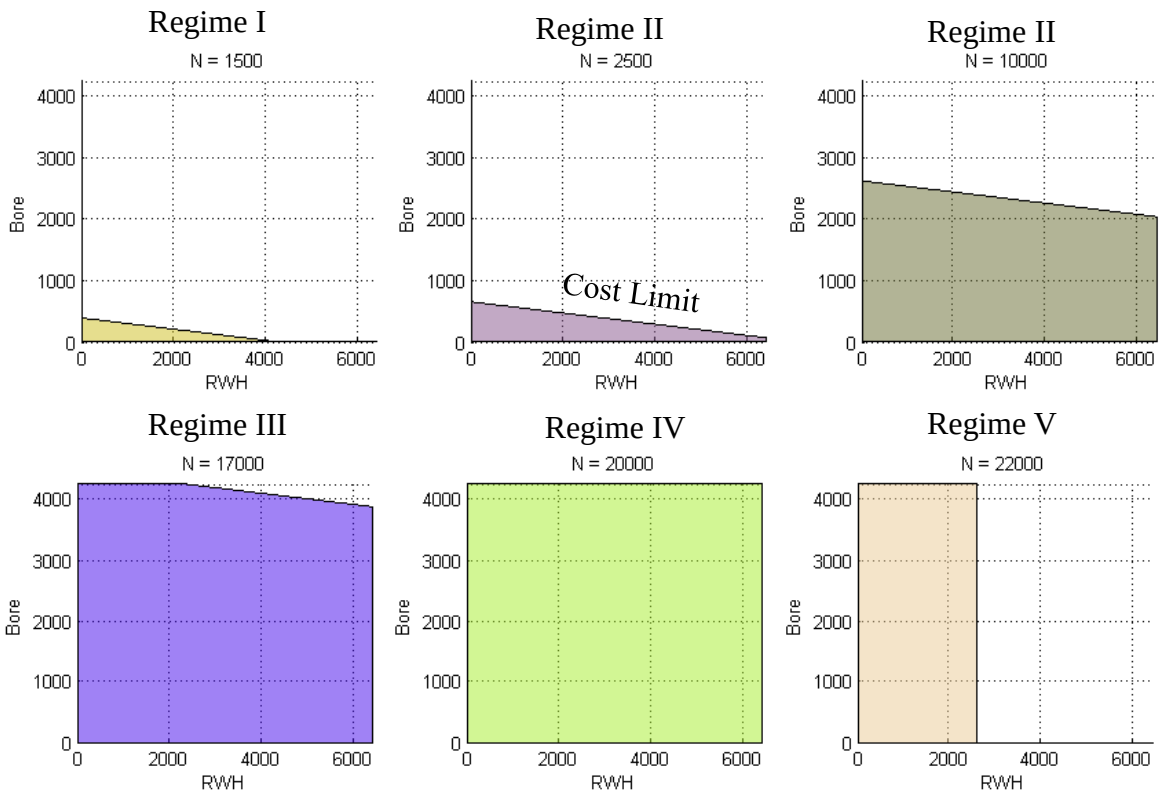

Figure 6.9. 4 Technology with SWRO Feasible Space Topology with population growth. **Regime I:** Feasible space is constrained by the Cost Limit only. **Regime II:** Feasible space expanded to touch the maximum RWH potential line. **Regime III:** Feasible space grew to touch the maximum Bore potential. **Regime IV:** Feasible space is no longer confined by the Cost Limit. Due to the fixed RWH and Bore limit, the size of the feasible space does not change in this regime with population growth. **Regime V:** The land area constraint is beginning to affect the feasible space, which effectively reduces the land area available for RWH thus reducing RWH potential.

6.3.2 4-Technology Systems: Greywater reuse

Review of the household water use in Auckland region shows that 40% of the residential water use results in greywater from washing machines and showers (Section 4.4.2). From this

estimate, it is expected that 29m^3 of greywater will be generated per person over the year, given a 54m^3 annual use per person. The greywater availability is thus population dependent. The technical coefficient for the greywater system has been compiled in Section 4.4.2, and the vector is outlined as in Equation 6.17.

$$v_5 = \begin{bmatrix} 30 \\ 16.6 \\ 0 \\ 0 \\ 30 \\ 0.0085 \\ 58.4 \\ 0 \end{bmatrix} \begin{matrix} \cdots \text{ Potable Water (m}^3\text{)} \\ \cdots \text{ Wastewater (m}^3\text{)} \\ \cdots \text{ Rain Captured (m}^3\text{)} \\ \cdots \text{ Aquifer (m}^3\text{)} \\ \cdots \text{ Greywater (m}^3\text{)} \\ \cdots \text{ Electricity (kWh)} \\ \cdots \text{ Cost (\$)} \\ \cdots \text{ Land Area (m}^2\text{)} \end{matrix} \tag{6.17}$$

The constraint for the island-wide greywater availability will be directly proportional to N:

$$30s_5 \leq 29N \tag{6.18}$$

The greywater reuse does not directly provide potable water. However, it provides for the non-potable uses, which would have been supplied by potable water. This in effect reduces the potable water burden and can be considered as an addition the potable water supply. The equations for the potable water and wastewater constraints are:

$$115.2s_1 + 150s_2 + 150000s_4 + 30s_5 = 54N \ \cdots \text{ Potable Water (m}^3\text{)} \tag{6.19}$$

$$164s_3 + 16.6s_5 = 54N \cdots \text{ Wastewater (m}^3\text{)} \tag{6.20}$$

As before, Gaussian elimination was performed to reduce the number of decision variables using the 2 equations and matlab function subvol4.m to plot how the size of the feasible space changes with population growth from 0 to 30000 (Figure 6.10). A more curved pattern resulted for greywater reuse, possibly because of the cyclic, thus more complicated, dependence of the

greywater reuse system to the rest of the components. For example, the cusp found for the population range N~19000 resulted from the transition of the dominant cost constraint to the land area constrained system (N=19500 instance in Figure 6.11). Another key observation is that the sharp cut-off caused by the land area limit (N>20000 in cases without greywater reuse) disappears. The transition towards non-sustainability point is now smooth, and there was a significant increase in the maximum supportable population (Max pop: N=31920). The resulting feasible regions are shown in Figure 6.11 and 6.12. The island water supply can support a higher population even without the use of SWRO. There is feasible region available in case of a zero SWRO utilisation level. Previously, the end-point came about at around N=22950; the maximum supportable population is now N=31920.

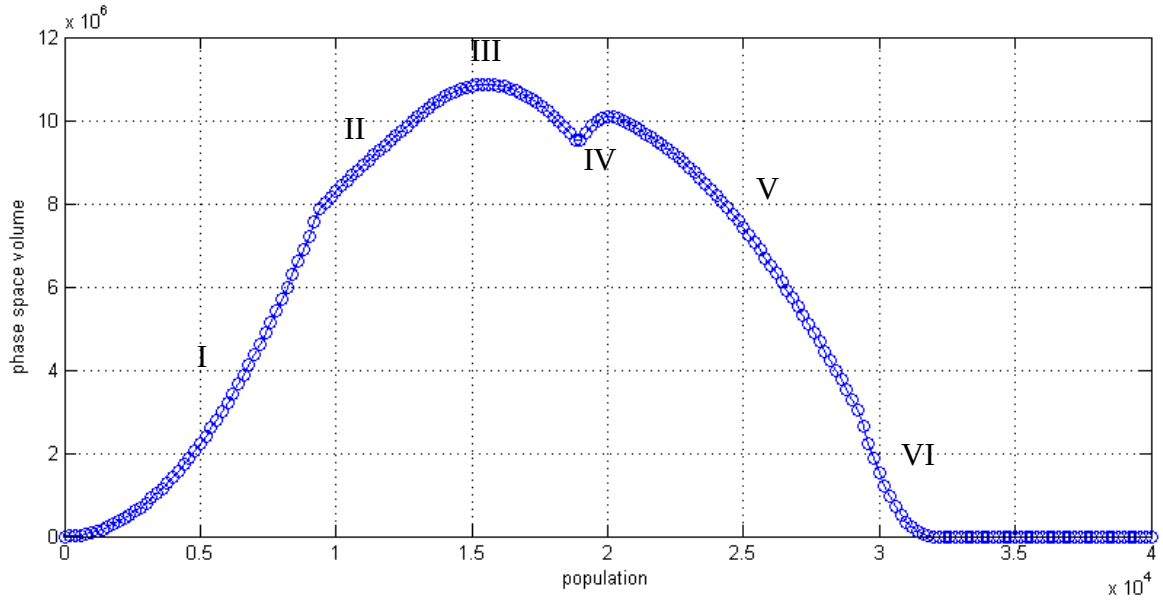

Figure 6.10. Feasible Space Volume Evolution for Tech 4 with Greywater Reuse.

The phase transition caused by the topology change of the constraint plains are demonstrated by looking at the geometry of the feasible spaces at the sample population (Figure 6.11). The

outline of the transition is described in the following:

- **Regime I:** For 0< N < 9000, bound by greywater availability on the lower left and cost limit from the upper right.
- **Regime II:** For 9000 < N < 13600, increase in cost limit now reaches the RWH constraint on the right.
- **Regime III:** For 13600 < N < 19000, further increase in cost limit now reaches the maximum bore potential constraint on the right.
- **Regime IV:** For 19000 < N < 20600, transition from cost limit to land area constraint on the upper right.
- **Regime V:** For 20600< N < 22500, the transition to the land area constraint completes and the land area constraint grows. The impact of land area constraint not as big as before.
- **Regime VI:** For 29400 < N < 31920, constraints for the greywater availability and the land area touches and the size of the feasible space decreases rapidly to zero.

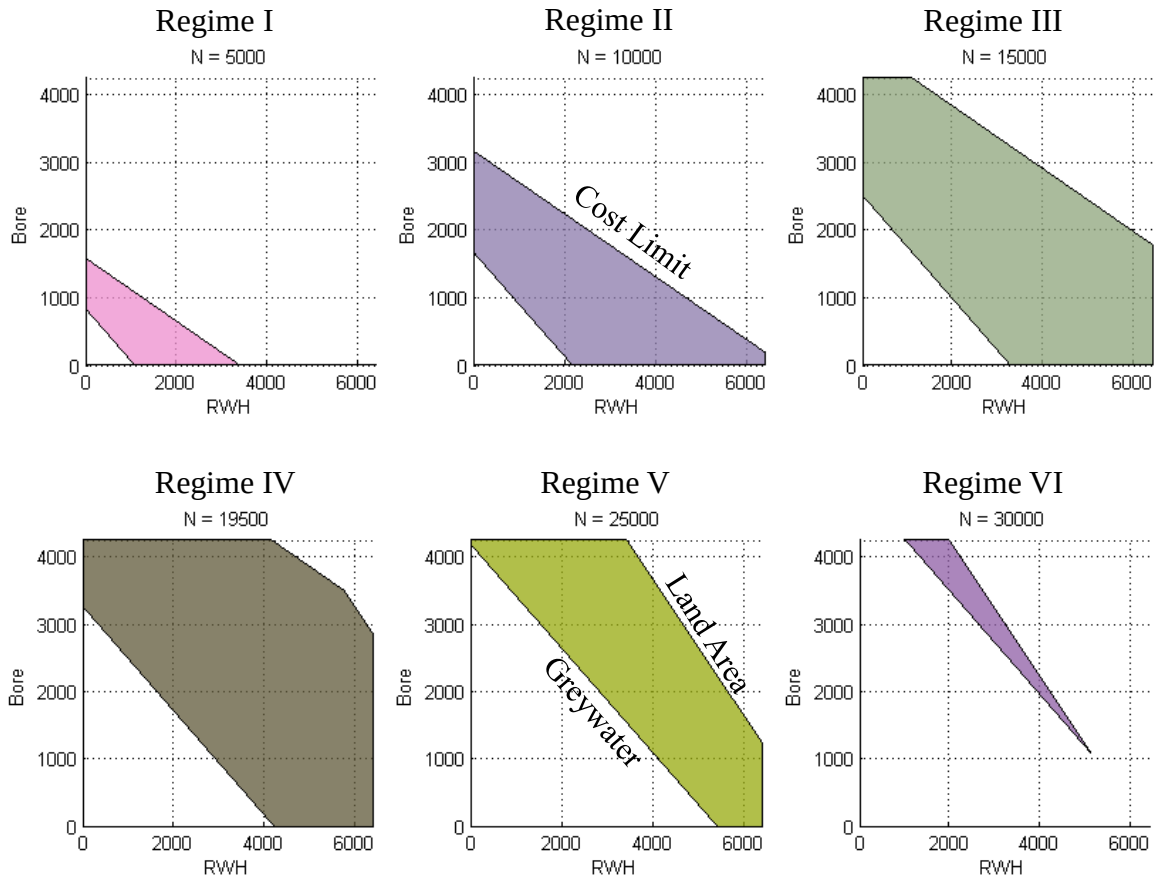

Figure 6.11. Feasible Space Topology for Tech 4 with Greywater Reuse.

6.3.3 5-Technology System: Putting all together

In an actual regional development, many different technologies will be employed at the same time. Assessing combined effect of the mixed use of the technology is more relevant than finding the best technological option for the region. The conceptual network for the combined use of the five technologies analysed in the previous sections is represented in Figure 6.12.

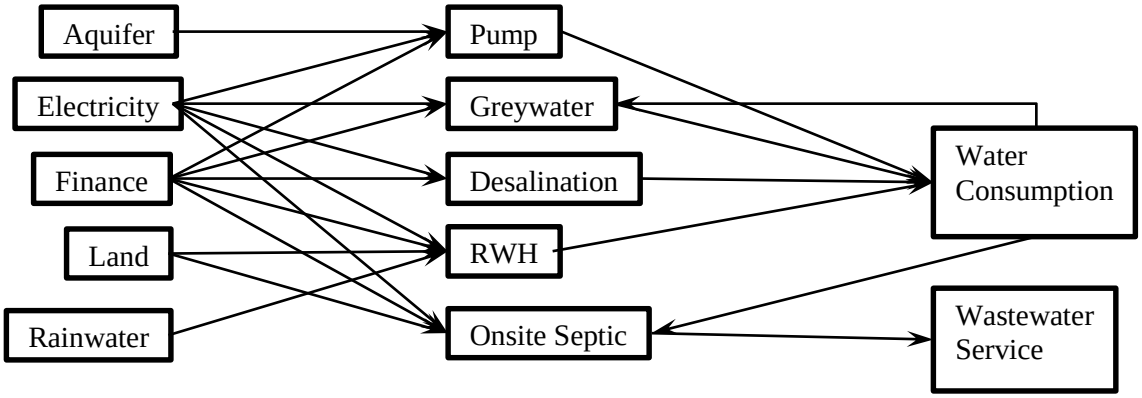

Figure 6.12 The conceptual network for 5-technology system.

The mathematical formulation for this case was expressed in Equation 6.21. For the case of a 5 technology system, there are five decision variables and two equations that reduce the number of dimension for the feasible space. The feasible space has the dimension of 3.

$$\begin{bmatrix} 67.2 & 150 & 0 & 150000 & 30 \\ 0 & 0 & 164 & 0 & 16.6 \\ 84 & 0 & 0 & 0 & 0 \\ 0 & 160 & 0 & 0 & 0 \\ 0 & 0 & 0 & 0 & 30 \\ 0.0085 & 29.7 & 263 & 600000 & 0.0085 \\ 237 & 796 & 1437 & 243000 & 58.4 \\ 120 & 0 & 1000 & 0 & 0 \end{bmatrix} \begin{bmatrix} s_1 \\ s_2 \\ s_3 \\ s_4 \\ s_5 \end{bmatrix} \begin{bmatrix} = \\ = \\ \leq \\ \leq \\ \leq \\ \leq \\ \leq \\ \leq \end{bmatrix} \begin{bmatrix} 54N \\ 54N \\ 537800 \\ 679000 \\ 29N \\ 200 \times 10^6 \\ 705N \\ 6 \times 10^6 \end{bmatrix} \begin{matrix} \cdots \text{Potable Water (m}^3\text{)} \\ \cdots \text{Wastewater (m}^3\text{)} \\ \cdots \text{Rain Captured (m}^3\text{)} \\ \cdots \text{Aquifer (m}^3\text{)} \\ \cdots \text{Greywater (m}^3\text{)} \\ \cdots \text{Electricity (kWh)} \\ \cdots \text{Cost (\$)} \\ \cdots \text{Land Area (m}^2\text{)} \end{matrix} \quad (6.21)$$

The change of the feasible space volume shows a complex pattern (Figure 6.13). The phase change of the constraints topology is reflected in the feasible space volume plot. There were eight distinct regimes of water resource system evolution if five technologies were to be employed.

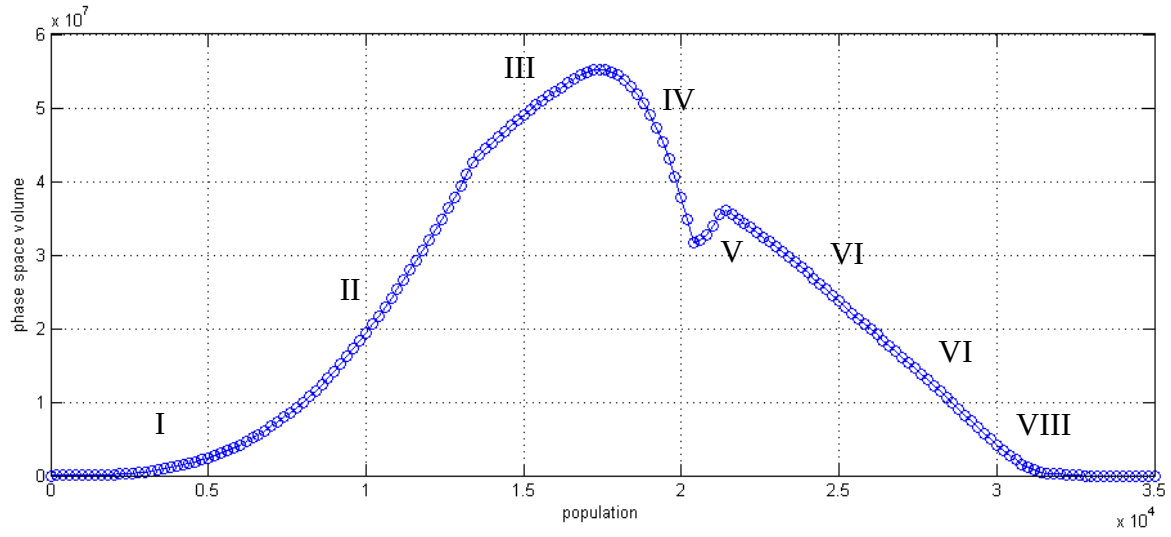

Figure 6.13. Change of feasible space volume with respect to population. The 5 Technology scenario shows a more complicated behaviour as it has more complicated dynamics among the constraint surfaces, as shown in Figure 6.11.

Similar to the previous scenarios, the changes in the growth pattern of feasible space volume were related to the topological shifts in constraints:

- **Regime I:** For $0 \leq N \leq 6850$, the cost constraint is the limiting factor and the volume increases as the cost constraint shifts outward from the origin. The feasible space is constrained by the non-zero constraints, greywater availability (smaller triangular surface near the origin; N=3000; Figure 6.14) and cost constraint (larger triangular surface; N=3000; Figure 6.14).
- **Regime II:** For $6800 \leq N \leq 13600$, the RWH potential begins to take effect (see triangular surface emerging at right end corner; RWH=6402 surface; N=12500; Figure 6.14).

- **Regime III:** For $13600 \leq N \leq 16200$, the Aquifer potential begins to take effect (see triangular surface emerging at left end corner; Bore=4244 surface; N=15000; Figure 6.14).
- **Regime IV:** For $16200 \leq N \leq 18800$, the land area constraint begins to take effect from N=16200 (additional surface appearing next to cost constraint surface; N=19000; Figure 6.14). At N=18800, the land area constraint surface touches the SWRO=0 surface, separating the connection between the cost constraint and RWH potential constraint surfaces. N=19000 plot was used because it shows the land area constraints clearly.
- **Regime V:** For $18800 \leq N \leq 21400$, the land area constraint surface grows larger and the cost constraint becomes no longer influential on the feasible space at N=21400 (see N=21000; Figure 6.14).
- **Regime VI:** For $21400 \leq N \leq 25200$, the land area constraint shifts inwards towards the origin (0,0,0) slowly and the greywater constraint shifts outwards from the origin so that the greywater constraint begins to touch the aquifer potential constraint (see left corner of N=25000; Figure 6.14). At this population regime, the feasible space volume decreases almost at a constant rate.
- **Regime VII:** For $25200 \leq N \leq 29400$, because of the outward shift of the greywater constraint, the feasible space becomes smaller and smaller, eliminating the aquifer constraint and RWH constraint from the picture.
- **Regime VIII:** $29400 \leq N \leq 31400$, the land area constraint and the greywater constraint gets close together reducing the feasible space volume. At N=31400, the

volume becomes zero. This signifies the maximum population level that these five technologies can support.

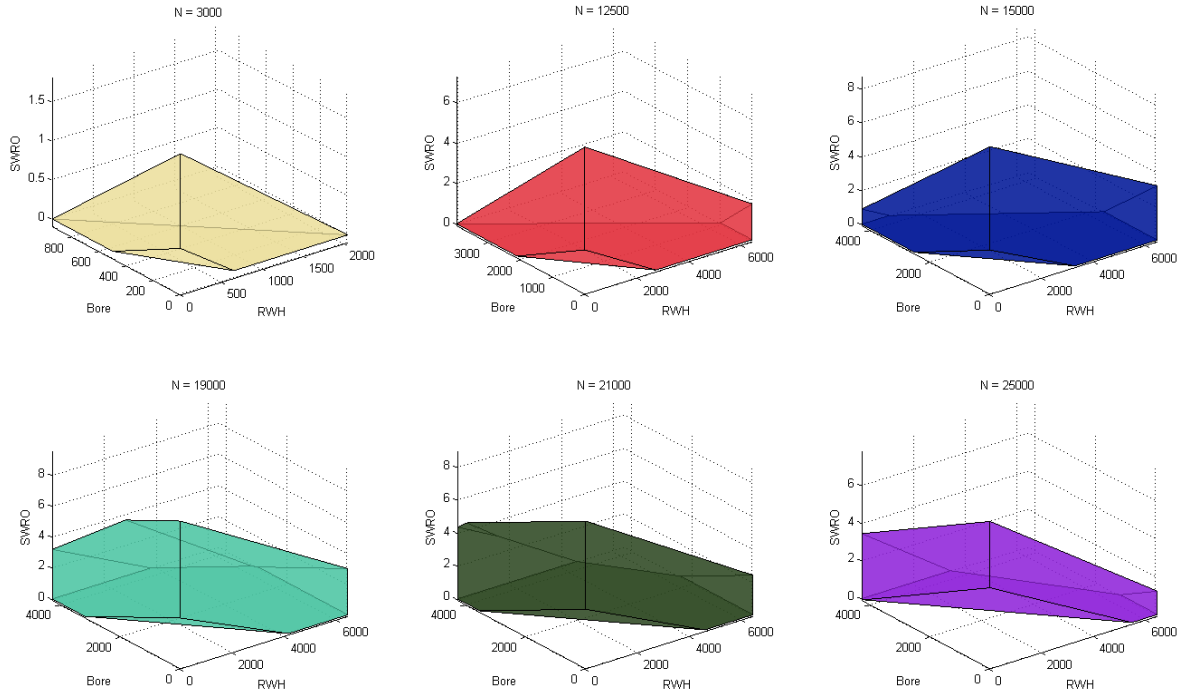

Figure 6.14. Feasible region for the design options. The inclusion of SWRO and greywater augmentation dramatically increases the supportable population by providing another axis for the feasible region to manifest.

6.4 Discussion

6.4.1 The effect of adding different technologies

The common technological arrangement adopted by the Waiheke Island residents is the 3-tech configuration as discussed in Section 6.2.2, which consists of RWH, bore, and septic tank irrigation system for the water supply and wastewater treatment. At the current population level

of N=8200, the most constraining element comes from the financial capacity of the residents (Regime I; Section 6.2.2). The optimal population level with this configuration, which is associated with the population level with largest feasible space volume, is N~13600. At this population level, the availability of the fund will allow for a larger freedom of choice for the residents to build and maintain the infrastructure to sustain themselves. When the population increases past that point, the degree of freedom for the infrastructure choice option decreases because of the technical potentials of RWH and bore collection. The maximum achievable population using the current choice of 3-tech arrangement was N_{max}=21300.

The maximum sustainable population increases when additional technologies are introduced to the region. The introduction of an appropriate technology that addresses the most constraining resource will have the largest effect in increasing the maximum sustainable population. SWRO systems have great potential for being a reliable water supply source in an island context because it does not depend on small and variable freshwater availability of the island; the limited development-suitable land area was the defining constraint for the island, however. SWRO systems do not address this issue, so it did not have a large impact in increasing maximum sustainable population for the island (N_{max}=23000). On the other hand, the introduction of greywater reuse strategy was effective in this regard (N_{max}=31900) because the greywater system alleviated the land area requirement by assisting in wastewater service without the need for extra land. However, due to the fact that greywater can only be used once, there was a limit to greywater availability.

An interesting observation throughout all the scenarios was that the feasible space volume increases initially with population growth. This is contrary to common belief that the increase in population will lead to the exploitation of the island resource that results in decreased

sustainability. This is indeed the case for a high population regime where the population is reaching the island's "carrying capacity" for various resource constraints. However, for the small population cases, the limiting factor for the development is the financial capability of the residents. The investment for the infrastructure is a critical factor in the initial development when there is a small population for the region.

There is an optimal population level where there are enough financial resources while the system is reaching saturation in terms of constraining physical resources - this is signified as the population regime that has largest feasible space volume (i.e. at the peaks of the feasible space volume plots; Figure 6.2, 6.6, 6.8, 6.10, 6.13). At this optimal point of population, the level of economic burden of the water infrastructure no longer becomes significant to the residents and the level of resource base constraints are yet to appear. At this level, design options for infrastructure are more broad which means more flexibility and choices on how residents can carry out activities on the island (both business and residential). The positive impact of introducing SWRO systems to the region was that it shifted the population peak higher. Although it did not contribute to the maximum population, the optimal population level certainly increased from N_{opt}=14000 range to N_{opt}=20000 range. Greywater reuse system, on the other hand, did not shift the peak as much (i.e. N_{opt}=15000). Introducing both SWRO and greywater technology has an effect of increasing the optimal population (N_{opt}=18000) and maximum sustainable population (N_{max}=32000) for the region.

6.4.2 Significance and Limitation of the Calculation

The present methodology provides a useful way of integrating different types of technologies to evaluate the "Limits to Growth". It is possible to extend the model to include additional

technologies of very different background, as long as the technology is presented with the technical coefficient vectors. The methodology exploits the power of concurrent modelling of matrix computations. The matrix methodology provides a system level modelling framework by abstracting the complex inner-workings of model components to technical coefficient vectors and the corresponding constraint value of the resources that the technology relies on. Extending the model is easy; once the technical coefficient vector of the technology is established, it can simply be added as an additional column of the matrix. When the data on the additional resource constraint is identified, it can be added as an additional row of the matrix.

Although the framework is a promising integrative tool for the multidisciplinary modeling of the regional system, it has several limitations, the first being the current lack of easily accessible data. Few quantitative studies exist for the constraints for regional development. This will be solved by efforts to accumulate the knowledge of the various constraints at a regional level. There are some statistical studies on global reserves of critical resources. The data on resource constraints are especially lacking. The technical conversion coefficient data can be derived from the national and regional input-output table statistics; established LCI database table can also help. However, the problem with finding the constraint values at the regional level is difficult, not because they are technically infeasible but due to the lack of attention for the regional data and methodology. Until now there were no combining frameworks that utilise the individual studies of ecological, economical, social constraints of a region - thus, no need for the development of data. However with the utility framework developed in this thesis, only time and investment of the individual studies can accumulate with the proper systematic framework. They often involve the environmental impact assessment and the threshold studies of sensitive natural environments such as estuaries, waterbodies and the soil.

Another limitation of the matrix based methodology is the linearity of the approach. Non-linearity may arise from three sources. First is the economy of scale involved with the choices of technology. Mass production always leads to more efficient production per final production quantity. With a high number of system installed throughout the region, the overall system will be more efficient. This can be addressed within the linear methodology proposed here by introducing piecewise linearisation of coefficients (Lin, Carlsson, Ge, Shi, & Tsai, 2013). If a certain technology is affected by the economy of scale (non-linearity), the technology is broken down to several technology category based on their installation sizes. Non-linearity arising from the technical coefficient change in the size of implementation can be addressed by treating the different size of installation as different technology. The non-linearity arising at the constraint side such as threshold and tipping point behaviour, is already included in the subsystem analysis that give rise to the estimation of the constraints. The constraint values are the product of the non-linear consideration of the tipping point and threshold behaviour of the complex system that the subsystem components have.

Despite these limitations, the methodology provides a novel way of defining the sustainability metric and a solid estimation mechanism for optimal population size and maximum population size that can be accommodated within given regional resource endowments, both ecological and economical. These are based on the efficiency of the operational technology on how to utilise the endowed resources to service the growing population's demand. With the additional accumulation of support data for the framework, the framework will grow to be an essential tool for strategically assessing the sustainability for future regional growth**.** It will also encourage the adoption of an appropriate technology for the region resulting in the proper choice of the technological introduction for regional development. The accumulation of the

various technology in the form of a database of resource conversion coefficients and categories will help choose best arrangement of the different technologies for regional development.

Being a matrix theory, the theory describes behaviour of the linear systems. Non-linearity may arise in two areas, the LHS of the inequation and RHS of the inequation. Non-linearity in the LHS may arise because of the economy of scale. Typically it will be a positive economy of scale, where the larger system implementation of the same technology will have a higher conversion efficiency of the node due to the shared use of an overhead. Mathematically, with increase in the vector s entry will result in decrease in some entries in matrix A. If that is the case, step-wise modeling can be utilised, where you separate a same sector or technology into a small, medium to large implementation technology so that they have different conversion coefficients. Non-linearity occurring in RHS may be due to the many different non-linear threshold behaviours in the subsystems. The subsystem constraints are caused by many threshold and tipping point behaviours of the subsystems and the constraint value summarises the non-linear behaviour of the complex subsystems. These complex behaviours are already taken into account in the constraint value evaluation step.

6.5 Conclusion

This synthesis chapter applied the matrix theory in Chapter 3 to the Waiheke water resource case. The volume (length, area in case of 1D, 2D case) of the feasible space was regarded as a quantitative measure of sustainability. The volume of the feasible space is identical to the idea of accessible space in the literature (Bossel, 1999). The changes of the sustainability measure with respect to 4 different population growth scenarios were considered in this chapter. With the growth of the population, the available options for water resource system and its

sustainability measure increased to an optimal level because of the growing financial capability of the community. As the population grew past the optimal point, the physical resource constraints for the growth began to take effect, and ultimately the sustainability measure became zero. The population level when the sustainability measure becomes zero, was defined as the maximum sustainable population for the island.

Two types of graphs were used to analyse the geometric behaviour of the feasible space with population growth: (1) feasible space volume plot and (2) feasible space diagram. The feasible space volume plot was the primary means of estimating the maximum sustainable population and optimal population level for the island. The feasible space volume plot showed several regime changes to the behaviour of sustainability measure when the population increased. The phase change was caused by the change in topological relations among the constraint plains. These topological changes at the phase change population levels were confirmed by the feasible space diagram. The regime changes identified in the feasible volume plots is a useful guide in identifying the critical population level that regional planners must be aware of; when the population level goes beyond these critical levels, the focus of the regional growth strategy must shift towards addresing the different challenges that the modelled system might face.

At the moment, establishing constraint values in order to enter the mathematical framework is the most difficult part in regard to applying the theory to real-life cases. It will become easier by using an accumulated database of constraints in the future. This database may be kept by the regional authorities by identifying more of the constraining elements of their regions for their environmental planning efforts.

Chapter 7 Conclusion

7.1 Major findings and Contributions

This thesis developed a simple yet versatile extension of the matrix-based industrial ecology framework, shared by the input-output analysis and LCI framework. The existing input-output and LCI framework focus on calculating the size of the environmental impacts (resource required and emissions produced) created throughout the life-cycle of a product, basket of products or even by the metabolism of a region. By adding constraints to the flow network, the extended framework provides a mathematical link between the constraints science and the existing input-output LCI framework. The thesis identified the matrix based input-output and LCI frameworks as variations of multi-commodity network flows involving transformation nodes (i.e. transmuting nodes that convert several input-commodity-streams to output commodity streams). The project involved two hierarchical layered modelling; a system-level top layer that models the overarching flow-constraint relationship and a supportive bottom layer involving detailed models of the individual resource components that result in constraint/threshold values. The upper system-level model was summarised as a matrix algebra and geometric interpretations arising from an equation-inequation system.

The framework provided a way to modularise a complex interconnected system via an open systems approach. The theory was deliberately formulated as open network flows in order for the models to have extension capabilities, ready to be incorporated into a greater spatial or sectoral system organisation. For instance, the ‘Waiheke Island water resource system’ case study can be used as an enclosed component in the greater material and financial flows of

Auckland regions and above. It can also be extended to different sectors of industry or the infrastructure channel; for example, the interaction between energy, commercial and agricultural systems. The extended regional model can be further extended to be a part of the greater spatial and sectoral systems (e.g. global trade flow system).

Being a generic flow model, the model can be applied in a large variety of sectors incorporating flow network features. Unlike typical network optimisation problems such as transport routing, the nodes in the thesis involve the transformation feature that enables the linking of flows of different commodities. This feature enables the coupling of networks whose flows are of different commodities, which are previously studied separately. The immediate applications will be in the energy-water nexus, financial-infrastructure nexus, and ultimately involve the overall economy-physical coupling.

The case study revealed that intensive modelling and data gathering effort are required to populate the matrix entries for production efficiencies and constraints. There is a direct relationship between a matrix entry and a subsystem constraint model. This is a common problem in bottom-up data-driven approaches – rather, this challenge presents a research opportunity of establishing a database for constraints of critical subsystems of society. The establishment of a such database will become an indispensable reference for sustainability-aware policies and decision-making. The matrix framework developed in this thesis can be used to identify which critical subsystems need modelling for constraint computations.

The final model utilised the system of equation-inequation. The analysis of the modeled system would take the form of the geometric analysis of the feasible space defined by the equation-inequation. The geometric analysis included the topological relationship between the

constraints and the change of feasible space volume with respect to the growth of population. In general it was identified that the feasible space decreases as the population grows because of the increased demand while diminishing the environmental conditions. Surprisingly, the modeled case study showed an initial increase of the feasible space volume with the population, meaning an increase in population increases the freedom of choosing the strategy that meets the resource requirement. With the initial increase of sustainability measure, there was a peak but this diminished as the eventual demand increased. Also, the initial increase of feasible space volume was caused by the population's increasing financial capability. Indeed in the development scenario, the regional development is initially constrained by social capability and at a later stage, the development will be limited by the physical and environmental constraints imposed to the region.

As a case study, the growth limit of the Waiheke Island water resource system was estimated, based on the hydrological, financial and technological limits. Waiheke Island is the driest location in the Auckland region and is known to experience several seasonal water resource problems - supply shortages during dry summer, island saltwater intrusion issues, and water quality standard breaches due to stormwater during the wet months. The study revealed that the current onsite approach of water management utilising rainwater harvest, bore pumping, and septic tank can sustainably support a population up to 23,000. The greatest limitation for the carrying capacity was the land area requirement for the septic tank system with little room for urban expansion due to the rough topography. Even a hypothetical adoption of micro-scale seawater desalination plants and the implementation of greywater reuse practice will not increase the carrying capacity much. Greywater reuse was found to be more effective in increasing the carrying capacity up to 30,000 by assisting the wastewater treatment requirement

through rerouting some of the wastewater. Seawater desalination plants did not have much effect on the ultimate carrying capacity, but shifted the optimal population level by providing a cheap alternative source of freshwater. Allowing for more flexible options increases the optimal population level according to the feasible volume analysis demonstrated by the analytical tool proposed in the thesis.

7.2 Significance of Sustainability Research Context

This research addresses the gap between the heavily empirical field of industrial ecology modelling and the conceptual/theoretical constraint science field. Industrial ecology focuses on modelling and data acquisition methodologies for resource flow relations between industrial processes, fostering resource efficiency and cleaner production technologies, and assessment methodologies in order understand the impact of technological improvements. The focus on efficiency improvements is a result of the relative sustainability philosophy, where the foundation is based on the precautionary principle. Early sustainability discussions revolved around the concept of carrying capacity for the human race. Discussions related to the capacity and constraints belong to the realm of absolute sustainability philosophy, an emphasis which faded over the years due to the complex and descriptive nature of the topic (Faber et al., 2005). The complexity and the large scope of the systems have prevented empirical studies from burgeoning because of its sheer data requirement. With the emergence of high-resolution environmental databases on a global scale, absolute sustainability initiatives are becoming more and more viable. However, there is still a gap between the data-driven modellers' community and theory-driven constraint/threshold ecologists group. The open system framework in this thesis demonstrated how the gap between these two groups could be bridged.

The current research direction of the data-driven modellers' community, i.e. industrial ecologists, is the material flow itself. Keywords in this direction are "interconnectedness" and "indirect impacts". Various empirical methods developed in the industrial ecology field share a similar mathematical structure, and the empirical methods are being integrated by exploiting the similarity (in particular, integration of input-output framework and LCA). On the other hand, the empirical science of constraints, namely sustainable yields, peak-resources, thresholds and tipping points, have not yet developed sufficient momentum for integration; this is because these topics are large and complex enough to be topics on their own, whereas individual toolsets are still under development. Developing the combined effect of two or more constraints will require more time. An insight from this thesis shows that the flow-based matrix model developed from the industrial ecology perspective, can provide an excellent integrative framework to bind individual constraint studies. Industrial ecologists will benefit from a widened scope of the matrix based tools, where their tools can now address the issues of constraints and absolute sustainability on top of relative efficiency aspects of the system.

7.3 Shortcomings and Limitations

The framework developed in this thesis is far from being complete. It has opened up a new research approach that may work as an integrative framework for many related datasets. Before going into the future directions and research opportunities, this section provides a critique of the approaches and methods undertaken in this project. Due to the time constraint and the level of expertise that could be developed within the given time, the research could only be made within the domain of the water resource sustainability of a small region. As the framework can also be applied to a more general case and complex network configuration, naturally, the next

step would be to seek a case study with a higher geographical coverage with a more complex network connectivity. However, it was demonstrated that even with a simple five node network system, it created many interesting behaviours in terms of topological phase transitions and measurement of feasible space volume with population growth. A more intricate node network would produce a much more complex analysis. The simple case study provided several basic features to look out for in the analysis of the evolution of feasible space geometry with the population.

Linearity is the largest shortcoming of the approach. Industrial processes typically have positive economies of scale, which results in a change of efficiency as the production capacity gets larger. This means that the entries of the conversion efficiency matrix A and B must change with the growth of the vector **s**. Matrix representation is excellent in the parallel processing of large quantities of data, but it can only model linear systems. This short-coming is shared with all variants of IO analysis and LCA, which are all matrix based frameworks. This issue of non-linearity is addressed in LCA occasionally, but no definite solutions could be found in the literature (Karimuribo, Chenyambuga, Makene, & Mathias, 2011). In the future, efforts in how to incorporate non-linearity in flow network modelling will an important for both the practical sustainability assessment perspective and in the field of the mathematics of network modelling.

7.4 Future Research Directions

The immediate extension of the framework will be the application of this network to the sustainability of industrial network utilising the LCI database. This will provide a wide application arena for the already established database. The difficulty faced in this application will be identifying the constraints for the many resource inputs and emission outputs that the

LCI computation calculates. Identifying the appropriate constraint values for individual inputs and emissions will be a large task where the workload will be almost identical to that of establishing the LCI database itself. Trying to create a systematised methodology to establish the constraint values more efficiently, rather than having to manually investigate through modeling and literature search, will be an interesting direction to take as well.

Appendix A MATLAB code

Lassere Algorithm is a recursive algorithm. The mathematical details of the algorithm is given in section 3.5. This appendix provides the implementation codes for the computation used in Chpater 6. This appendix is organised in three sections. Section A.1 contains the MATLAB function code implemeting the recursive Lassere Algorithm. Section A.2 lists some simple test scripts that calls Lassere function. Section A.3 lists the actual computation code used for Chpater 6.

A.1 Lasserre Algorithm

The implementation was created using Matlab function.

```
% Lassere Algorithm that finds volume of polytope
% The polytope is defined with as the intersection of half-spaces
% This is defined by system of inequation Ax <= b
% d_original = original dimension of the problem
% This parameter is used to identify the touching surfaces.
% Touching surfaces will have subvol ~= 0
% This version traces the division of the volumes
% Outputs the individual volumes: 1-2-3-4-5:6 = 47634
% Added data structure for debug purpose, additional column at the end of
% Ab to trace the row number
% enter branch as empty matrix when use
% Input Parameters
% (1) A
% (2) B
% (3) tag = []
% (4) branch = []
% (5) d_original = dimension of the problem, number of columns in A
% (6) report_level = the level of detail of the reporting. Range:
% -2 ~ d_original. Special input: -10 => shows the connectivity only. -20
% => shows only adjacency matrix
function [volume,sa_return] =
subvol4(A,b,tag,branch,d_original,report_level,surface_adajacency)
disp('Im in')
d = size(A,2);
stab = [];

for i = 1:(d_original-d+1)
    add = '    ';
    stab = [stab add];
end
% report_level
% d_original
```

```
% d
if report_level >= (d_original - d)
    disp([stab,'d = ',num2str(d)])
end
if d == d_original
    tag = (1:size(A,1));
    surface_adajacency = zeros(size(A,1));
    if report_level >= (d_original - d)
        disp([stab,'tag set [',num2str(tag),']'])
    end
end
% base case
if d == 1
    branch
    Ab = [A b];
    A_neg = Ab(find(Ab(:,1)<0),:); % extract the negative aij subject to maximum
    A_pos = Ab(find(Ab(:,1)>0),:); % extract the positive aij subject to minimum
    volume = max(0, min(A_pos(:,2)./A_pos(:,1)) - max(A_neg(:,2)./A_neg(:,1)));
    tag_neg = tag(find(Ab(:,1)<0));
    tag_pos = tag(find(Ab(:,1)>0));
    [c1,i1] = min(A_pos(:,2)./A_pos(:,1));
    [c2,i2] = max(A_neg(:,2)./A_neg(:,1));

    if report_level >= (d_original - d) || report_level == -10
        if volume == 0
            disp([stab,'**** base [',num2str(branch),'] = ',num2str(volume)])
        else
            disp([stab,'**** base [',num2str(branch),']
',num2str(tag_neg(i2)),':',num2str(tag_pos(i1)),' = ',num2str(volume)])
            A_pos(:,2)./A_pos(:,1)
            A_neg(:,2)./A_neg(:,1)
        end
    end
    if volume ~= 0 && d_original > 2
        surface_adajacency(branch(1),branch(2)) = 1;
    end
    sa_return = surface_adajacency;
    return
end

% pivot operation, utilising i,j
m = size(A,1);
n = size(A,2);

base_volumes = zeros(m,1);
distances = zeros(m,1);

if report_level >= (d_original - d)
    disp([stab,'open loop at d = ',num2str(d)])
end

for i = 1:m
    if report_level >= (d_original - d)
        disp([stab,'i = ',num2str(i),' Tag = [',num2str(tag),'] Branch =
[',num2str(branch),']'])
    end

    % calculating the pivoting procedure
    % locate suitable j
    j = find(A(i,:) ~= 0);
    j = j(1); % I need error check but not doing it this time of drafting the code

    distances(i) = b(i)/abs(A(i,j));
```

```
% do the row reduction
pivot = A(i,j);

% Eliminate any parallel surface
% parallel surface have the parallel normal vector. thus the dot
% product will be zero.
% carried out only when d >= 3
if report_level >= (d_original - d)
    disp([stab,'in elim section'])
end

% Find parallel
[p_index, np_index] = find_parallel(A,A(i,:));
if report_level >= (d_original - d)
    disp([stab,'Parallel detected: [',num2str(tag(p_index)),']'])
end
% if the current parallel plain is not feasible, then the volume will be zero.
% The feasibility is calculated by comparing with other parallel surfaces.
% This check is done only when the size of p_index is bigger than 1.
if (length(p_index) > 1)
    % Find the parallel surfaces other than the current surface
    parallels_to_check = p_index(p_index ~= i);

    % Select one point from the current surface and check the
    % iequality of other surfaces. If any surface says not feasible,
    % the base volume will be zero, being infeasible.
    sample_coord = [zeros(1,size(A,2)-1) b(i)/A(i,end)]';
    if ~all(A(parallels_to_check,:)*sample_coord <= b(parallels_to_check))
        base_volumes(i) = 0;
        disp('infeasible parallel')
        continue;
    end
end


% Or if the current parallel plain is feasible, carry on with the
% calculation.
to_remain = sort([np_index i],'ascend');
i_augmented = find(to_remain == i);
A_elim = A(to_remain,:);
b_elim = b(to_remain,:);
m_elim = length(to_remain);
tag_elim = tag(to_remain);

Abar = zeros(m_elim,n);
bbar = zeros(m_elim,1);
tag_bar = tag_elim;

% Gaussian reduction calculation
for k = 1:m_elim
    Abar(k,:) = A_elim(k,:) - (A_elim(k,j)/pivot)*A_elim(i_augmented,:);
    bbar(k) = b_elim(k) - (A_elim(k,j)/pivot)*b_elim(i_augmented);
end

branch_bar = [branch tag_bar(i_augmented)];
if report_level >= (d_original - d)
    disp([stab,'removing ',num2str(tag_bar(i_augmented))])
end

% Remove pivot row, column
Abar = delete_row_column(Abar,i_augmented,j);
bbar = delete_row(bbar,i_augmented);
```

```
    tag_bar = delete_column(tag_bar,i_augmented);

    % order the sub volume calculations
    if report_level >= (d_original - d)
        disp([stab,'subvol4(Abar,bbar,[',num2str(tag_bar),'],[',num2str(branch_bar),
'],',num2str(d_original),')'])
    end

    % recursive call
    [base_volumes(i),surface_adajacency] =
subvol4(Abar,bbar,tag_bar,branch_bar,d_original,report_level,surface_adajacency);


    % Reporting phase of the code
    % This part of the code does not deal with the computation.
    % This part outputs the each subvolume calculated in the iteration

    if report_level >= (d_original - d)
        disp([stab,'next'])
    end
end
if report_level >= (d_original - d)
    disp([stab,'close loop at d = ',num2str(d)])
end
volume = 1/d*sum(distances.*base_volumes);
disp('distances .* base_volumes')
disp([distances,base_volumes])
if report_level + 1 >= (d_original - d)
    disp([stab,'**** volume Branch = [',num2str(branch),'] = ',num2str(volume)])
end

if d == d_original
    if report_level >= (d_original - d) || report_level == -10
        disp(' ')
        disp(' ')
        disp('Guide: **** base [1] 3:2 = 60 : lower bound = surface 3 & upper bound
= surface 2')
        disp(' ')
        disp(' ')
        disp('Surface Adjacency Matrix')
        disp(' ')
        disp(surface_adajacency)
    end
    if report_level == -20
        disp(' ')
        disp(' ')
        disp('Surface Adjacency Matrix')
        disp(' ')
        disp(surface_adajacency)
    end
end

sa_return = surface_adajacency;

return

% Identify the parallel rows
% Returns the row indices of the parallel rows.
% Input: matrix A, row vector x
% Return: index = row vector containing indices
% Return: n_index = index of rows that are not parallel
function [index,n_index] = find_parallel(A,x)
    tol = 1e-15;
```

```
    n = size(A,1);
    index = [];
    n_index = [];
    for i = 1:n
        thisTime = A(i,:);
        % find if the position of zeros are the same
        if length(find(thisTime==0)) == length(find(x==0))
            if all(find(thisTime==0) == find(x==0))
                % remove zeros and do detailed analysis
                a = thisTime(find(thisTime~=0));
                b = x(find(x~=0));
                c = a./b; % the resulting ratios
                d = c/c(1); % are they all ones?
                if all(similar(d,1,tol))
                    index = [index i];
                else
                    n_index = [n_index i];
                end
            else
                n_index = [n_index i];
            end
        else
             n_index = [n_index i];
        end
    end

return

% Helper function
% delete the ith row and jth column of the matrix A
function A_reduced = delete_row_column(A,i,j)
    A_reduced = delete_column(delete_row(A,i),j);
return

% Helper function
% delete the ith row of the matrix A
function A_reduced = delete_row(A,i)
    [m,n] = size(A);
    if i == 1
        A_reduced = A(2:end,:);
    elseif i == m
        A_reduced = A(1:end-1,:);
    else
        A_reduced = [A(1:i-1,:); A(i+1:end,:)];
    end
return

% Helper function
% delete the jth column of the matrix A
function A_reduced = delete_column(A,j)
    [m,n] = size(A);
    % find the submatrix of size (m-1,n-1); remove the pivot row and column
    if j == 1
        A_reduced = A(:,2:end);
    elseif j == n
        A_reduced = A(:,1:end-1);
    else
        A_reduced = [A(:,1:j-1) A(:,j+1:end)];
    end
return

function answer = isThereZeroRow(A)
    answer = false;
```

```
    for i = 1:size(A,1)
        if length(find(A(i,:)~=0)) == 0
            answer = true;
        end
    end
return

function t = similar(a,b,tolerance)
    t = (abs(a-b)/(abs(a)+abs(b))) < tolerance;
return
```

A.2 Codes used in Chapter 6

A.2.1 2-Technology system

```
%% 2 Technology reduced volume plot (Figure 6.2)
z = -1*eye(1);
bz = zeros(1,1);
d = 1;

vol = [];
N_choice = 0:200:30000;

tic
disp('------ begin ------')
for N = N_choice
    A = [115.2 150 54*N; 144 0 922000; 0 160 679000; 0.0085 29.7 200e6; 237 796
235*N];
    A1 = pivot(A,1,1);
    A2 = A1(2:end,[2 3]);

    A3 = [A2(:,1); z];
    b = [A2(:,2); bz];
    vol = [vol subvol4(A3,b,[],[],d,-1)];
end
disp('------- end -------')
toc

figure(2)
plot(N_choice, vol, 'o-')
xlabel('population')
ylabel('phase space volume')
grid on

Tech2_volume = vol;

%% 2 Tech phase space plot (Figure 6.4)
figure(1)

count = 1;
for N = [8200 15000 20000]
    A = [-115.2 -150 -54*N; 144 0 922000; 0 160 679000; 0.0085 29.7 200e6; 237 796
235*N];
    A1 = pivot(A,1,1);
```

```
    A2 = A1(2:end,[2 3]);

    A1 = [A2(:,1:end-1); z];
    b = [A2(:,end); bz];

    subplot(1,3,count)
    count = count + 1;

    plotregion(-A(:,1:2),-A(:,3),[0 0],[922000/144 679000/160]);
    title(['N = ',num2str(N)])
    xlabel('RWH')
    ylabel('Bore')
    grid on

    axis([0 922000/144 0 679000/160])
end
```

A.2.2 3-Technology System (Conventional)

```
%% 3 Technology population volume plot: Reduced inequation (Figure 6.6)
z = -1*eye(1);
bz = zeros(1,1);
d = 1;

vol = [];
N_choice = 0:200:22500;

tic
disp('------ begin ------')
for N = N_choice
    A = [115.2 150 0 54*N; 0 0 164 54*N; 144 0 0 922000; 0 160 0 679000; 0.0085 29.7
263 200e6; 237 796 1437 705*N; 120 0 1000 7.554e6];
    A1 = pivot(A,1,1);
    A2 = A1(2:end,2:end);
    A3 = pivot(A2,1,2);
    A4 = A3(2:end,[1 3]);
    A5 = A4(:,2)./A4(:,1);

    A1 = [A4(:,1); z];
    b = [A4(:,2); bz];
    vol = [vol subvol4(A1,b,[],[],d,-1)];
end
disp('------- end -------')
toc

figure(2)
plot(N_choice, vol, 'o-')
xlabel('population')
ylabel('phase space volume')
grid on

Tech3_volume = vol;

%% 3 Technology reduced (Figure 6.7)
figure(1)
clf
count = 1;
for N = [8200,15000,19000,20800];
```

```
    v3_2 = [263; 1437; 1000];
    s3_req = 54*N/164;
    A1 = [115.2 150];
    b1 = N*54;
    A = [0.0085 29.7; 237 796; 120 0];
    b = [200e6; 705*N; 7.554e6] - v3_2*s3_req;
    subplot(2,2,count)
    count = count + 1;
    plotregion([A1; -A],[b1; -b],[0 0],[922000/144 679000/160]);
    title(['N = ',num2str(N)])
    xlabel('RWH')
    ylabel('Bore')
    axis([1000 922000/144 0 679000/160])
    grid on
end
hold off
```

A.2.3 4-Technology (SWRO+Conventional)

```
%% Tech 4 Reduced (Figure 6.8)
% with SWRO only
clear
d = 2;
z = -1*eye(d);
bz = zeros(d,1);

vol = [];
N_choice = 0:200:30000;

tic
disp('------ begin ------')
for N = N_choice
    A = [115.2 150 0 150000 54*N; ...
        0 0 164 0 54*N; ...
        144 0 0 0 922000; ...
        0 160 0 0 679000; ...
        0.0085 29.7 263 600000 200e6; ...
        237 796 1437 243000 705*N; ...
        120 0 1000 0 7.554e6];
    A1 = pivot(A,1,4);
    A2 = A1(2:end,[1:3 5]);
    A3 = pivot(A2,1,3);
    A4 = A3(2:end,[1 2 4]);

    A1 = [A4(:,1:end-1); z];
    b = [A4(:,end); bz];
        disp('Part 1')

    vol = [vol subvol4(A1,b,[],[],d,4)];
end
disp('------- end -------')
toc


figure(2)
plot(N_choice, vol, 'o-')
xlabel('population')
ylabel('phase space volume')
grid on
```

```
figure(3)
plot(diff(vol), 'o-')

Tech4_no_grey_volume = vol;

%% 3D feasible space plot: 4 Technology reduced with SWRO only (Figure 6.9)
count = 1;
d = 3;
z = -1*eye(d);
bz = zeros(d,1);
choice = 2;

for N = N_choice

    A = [-115.2 -150 0 -150000 -54*N; ...
        0 0 -164 0 -54*N; ...
        144 0 0 0 922000; ...
        0 160 0 0 679000; ...
        0.0085 29.7 263 600000 200e6; ...
        237 796 1437 243000 705*N; ...
        120 0 1000 0 7.554e6];

    if choice == 2
        d = 2;
        z = -1*eye(d);
        bz = zeros(d,1);
        A1 = pivot(A,1,4);
        A2 = A1(2:end,[1:3 5]);
        A3 = pivot(A2,1,3);
        A4 = A3(2:end,[1 2 4]);

        A1 = [A4(:,1:end-1); z];
        b = [A4(:,end); bz];

    elseif choice == 3
        A1 = pivot(A,2,3);
        A2 = A1([1 3:end],[1:2 4:5]);

        A1 = [A2(:,1:end-1); z];
        b = [A2(:,end); bz];

    elseif choice == 4
        A1 = pivot(A,1,4);
        A2 = A1(2:end,[1:3 5]);

        A1 = [A2(:,1:end-1); z];
        b = [A2(:,end); bz];
    end

    figure(1)

    subplot(2,3,count)
    count = count +1;
    plotregion(-A1,-b,zeros(1,d),[]);
    title(['N = ',num2str(N)])
    xlabel('RWH')
    ylabel('Bore')
    zlabel('SWRO')

    grid on

    axis([0 922000/144 0 679000/160 0 6])
```

```
end
```

A.2.4 4-Technology (Greywater+Conventional)

```
%% Tech 4 Reduced with Greywater only (Figure 6.10)
% with Greywater reuse only
clear
d = 2;
z = -1*eye(d);
bz = zeros(d,1);

vol = [];
N_choice = 0:200:40000;

tic
disp('------ begin ------')
for N = N_choice
    A = [115.2 150 0 150000 30 54*N; ...
        0 0 164 0 16.6 54*N; ...
        144 0 0 0 0 922000; ...
        0 160 0 0 0 679000; ...
        0 0 0 0 30 29*N; ...
        0.0085 29.7 263 600000 0.0085 200e6; ...
        237 796 1437 243000 58.4 705*N; ...
        120 0 1000 0 0 7.554e6];
    A = A(:,[1:3 5:6]);
    A1 = pivot(A,1,4);
    A2 = A1(2:end,[1:3 5]);
    A3 = pivot(A2,1,3);
    A4 = A3(2:end,[1 2 4]);

    A1 = [A4(:,1:end-1); z];
    b = [A4(:,end); bz];

    vol = [vol subvol4(A1,b,[],[],d,4)];

end
disp('------- end -------')
toc


figure(2)
plot(N_choice, vol, 'o-')
xlabel('population')
ylabel('phase space volume')
grid on

figure(3)
plot(diff(vol), 'o-')

Tech4_no_grey_volume = vol;


%% 3D feasible space plot: 4 Technology reduced with Greywater only (Figure 6.11)
count = 1;
d = 3;
z = -1*eye(d);
bz = zeros(d,1);
choice = 2;
```

```
for N = N_choice

    A = [115.2 150 0 150000 30 54*N; ...
        0 0 164 0 16.6 54*N; ...
        144 0 0 0 0 922000; ...
        0 160 0 0 0 679000; ...
        0 0 0 0 30 29*N; ...
        0.0085 29.7 263 600000 0.0085 200e6; ...
        237 796 1437 243000 58.4 705*N; ...
        120 0 1000 0 0 7.554e6];
    A = A(:,[1:3 5:6]);

    if choice == 2
        d = 2;
        z = -1*eye(d);
        bz = zeros(d,1);
        A1 = pivot(A,1,4);
        A2 = A1(2:end,[1:3 5]);
        A3 = pivot(A2,1,3);
        A4 = A3(2:end,[1 2 4]);

        A1 = [A4(:,1:end-1); z];
        b = [A4(:,end); bz];

    elseif choice == 3
        A1 = pivot(A,2,3);
        A2 = A1([1 3:end],[1:2 4:5]);

        A1 = [A2(:,1:end-1); z];
        b = [A2(:,end); bz];

    elseif choice == 4
        A1 = pivot(A,1,4);
        A2 = A1(2:end,[1:3 5]);

        A1 = [A2(:,1:end-1); z];
        b = [A2(:,end); bz];
    end

    figure(1)
    subplot(2,3,count)
    count = count +1;
    plotregion(-A1,-b,zeros(1,d),[],[922000/144 679000/160 10e10]);
    title(['N = ',num2str(N)])
    xlabel('RWH')
    ylabel('Bore')
    zlabel('SWRO')

    grid on

    axis([0 922000/144 0 679000/160])% 0 6])

end
```

A.2.5 5-Technology (Greywater+SWRO+Conventional)

```
%% 5 Technology reduced volume plot (Figure 6.13)
clear
d = 3;
z = -1*eye(d);
bz = zeros(d,1);

vol = [];
N_choice = 0:200:35000;

tic
disp('------ begin ------')
for N = N_choice
   A = [115.2 150 0 150000 30 54*N; ...
       0 0 164 0 16.6 54*N; ...
       144 0 0 0 0 922000; ...
       0 160 0 0 0 679000; ...
       0 0 0 0 30 29*N; ...
       0.0085 29.7 263 600000 0.0085 200e6; ...
       237 796 1437 243000 58.4 705*N; ...
       120 0 1000 0 0 7.554e6];
   A1 = pivot(A,1,5);
   A2 = A1(2:end,[1:4 6]);
   A3 = pivot(A2,1,3);
   A4 = A3(2:end,[1 2 4 5]);

   A1 = [A4(:,1:end-1); z];
   b = [A4(:,end); bz];
   vol = [vol subvol4(A1,b,[],[],d,-1)];
end
disp('------- end -------')
toc

figure(2)
plot(N_choice, vol, 'o-')
xlabel('population')
ylabel('phase space volume')
grid on

figure(3)
plot(diff(vol), 'o-')

Tech5_volume = vol;

%% 3D feasible space plot: 5 Technology reduced (Figure 6.14)
figure(1)
clf
count = 1;
for N = [3000 12500 15000 19000 21000 25000]
   A = [115.2 150 0 150000 30 54*N; ...
       0 0 164 0 16.6 54*N; ...
       144 0 0 0 0 922000; ...
       0 160 0 0 0 679000; ...
       0 0 0 0 30 29*N; ...
       0.0085 29.7 263 600000 0.0085 200e6; ...
       237 796 1437 243000 58.4 705*N; ...
       120 0 1000 0 0 7.554e6];
   A1 = pivot(A,1,5);
   A2 = A1(2:end,[1:4 6]);
   A3 = pivot(A2,1,3);
   A4 = A3(2:end,[1 2 4 5]);

   A1 = [A4(:,1:end-1); z];
   b = [A4(:,end); bz];
```

```
    subplot(2,3,count)
    count = count + 1;
    plotregion(-A1,-b,[0 0 0],[],[922000/144 563000/160 10e10]);
    title(['N = ',num2str(N)])
    xlabel('RWH')
    ylabel('Bore')
    zlabel('SWRO')
    grid on

end
```

Reference

Abbott, S., Caughley, B., & Douwes, J. (2004). The microbiological quality of roof-collected rainwater of private dwellings in New Zealand. Institute of Food Nutrition and Human Health, Massey University, New Zealand. Retrieved 12 Aug, 2015, from http://greywateraction.org/wp-content/uploads/2014/11/roofwater-quality.pdf

Akan, A. Osman. (1993). Urban stormwater hydrology : a guide to engineering calculations. Lancaster, Pa.: Technomic Pub. Co.

Albert, Réka, & Barabási, Albert-László. (2002). Statistical mechanics of complex networks. *Reviews of Modern Physics*, *74*(1), 47-97.

Andersson, B. A., Azar, C., Holmberg, J., & Karlsson, S. (1998). Material constraints for thin-film solar cells. *Energy*, *23*(5), 407-411.

ARC. (2008). TR 2008/011 State of the Environment Monitoring Auckland Water Quantity Statement, 2006/07: Auckland Regional Council.

Archer, Cristina L., & Jacobson, Mark Z. (2005). Evaluation of global wind power. *Journal of Geophysical Research: Atmospheres, 110*(D12), n/a-n/a. doi: 10.1029/2004JD005462

Auckland City Council. (2009). ALGGi Map Portal. Auckland, New Zealand. Retrieved 10 July, 2010, from http://alggi.auckland.govt.nz/mapportal.htm

Auckland Water Group. (2008). Auckland water industry Annual Performance Review 2007/08 Retrieved 24 Jan, 2011, from http://www.northshorecity.govt.nz/Services/WaterServices/AssetManagement/Documents/awg-performance-reveiw-final-report-2007-2008.pdf

Ayres, Robert U., & Ayres, Leslie. (2002). *A handbook of industrial ecology*. Cheltenham, UK ; Northampton, MA: Edward Elgar Pub.

Büeler, Benno, Enge, Andreas, & Fukuda, Komei. (2000). Exact Volume Computation for Polytopes: A Practical Study. In G. Kalai & G. Ziegler (Eds.), *Polytopes — Combinatorics and Computation* (Vol. 29, pp. 131-154): Birkhäuser Basel.

Baharumshah, Ahmad Zubaidi, & Lau, Evan. (2007). Regime changes and the sustainability of fiscal imbalance in East Asian countries. *Economic Modelling, 24*(6), 878-894. doi: DOI: 10.1016/j.econmod.2007.03.002

Balat, M. (2006). Current geothermal energy potential in Turkey and use of geothermal energy. *Energy Sources, Part B: Economics, Planning and Policy, 1*(1), 55-65.

Baragwanath, Lucy. (2010). The Waiheke Project. Overview of tourism, wine and development on Waiheke Island. School of Environment. The University of Auckland. Retrieved 21 July,

2015, from http://www.waihekewine.co.nz/images/resources/pdfdocs/Waiheke%20Report.pdf

BEA. (2010). Input-Output Accounts Data. Bureau of Economic Analysis. United States of America. Retrieved 7 Jan, 2012, from http://www.bea.gov/industry/io_annual.htm

Behrens, A., Giljum, S., Kovanda, J., & Niza, S. (2007). The material basis of the global economy. Worldwide patterns of natural resource extraction and their implications for sustainable resource use policies. *Ecological Economics, 64*(2), 444-453.

Benham, B. L., Baffaut, C., Zeckoski, R. W., Mankin, K. R., Pachepsky, Y. A., Sadeghi, A. M., . . . Habersack, M. J. (2006). Modeling bacteria fate and transport in watersheds to support TMDLs. *Transactions of the Asabe, 49*(4), 987-1002.

Benn, S., Dunphy, D., & Griffiths, A. (2006). Enabling change for corporate sustainability: An integrated perspective. *Australasian Journal of Environmental Management, 13*(3), 156-165.

Bertani, R. (2012). Geothermal power generation in the world 2005-2010 update report. *Geothermics, 41*, 1-29.

Biswas, W. K. (2009). Life cycle assessment of seawater desalinization in Western Australia. *World Academy of Science, Engineering and Technology, 56*, 369-375.

Borah, D. K., Yagow, G., Saleh, A., Barnes, P. L., Rosenthal, W., Krug, E. C., & Hauck, L. M. (2006). Sediment and nutrient modeling for TMDL development and implementation. *Transactions of the Asabe, 49*(4), 967-986.

Bossel, H. (1999). Indicators for Sustainable Development: Theory, Method, Applications. A Report to the Balaton Group: International Institute for Sustainable Development (IISD).

Boustcad, I. (1996). LCA - How it came about the beginning in the U.K. *International Journal of Life Cycle Assessment, 1*(3), 147-150.

BP. (2014). BP Statistical Review of World Energy June 2014. Retrieved 28 Aug, 2014, from http://www.bp.com/content/dam/bp/pdf/Energy-economics/statistical-review-2014/BP-statistical-review-of-world-energy-2014-full-report.pdf

Braunstein, A., Mulet, R., & Pagnani, A. (2008). Estimating the size of the solution space of metabolic networks. *BMC bioinformatics, 9*, 240.

Bross, S., Kochanowski, W., & El Maraghy, N. (2005). SWRO-core-hydraulic-system: First field test experience. *Desalination, 184*(1-3), 223-232.

Brunner, P. H. (2011). Urban mining a contribution to reindustrializing the city. *Journal of Industrial Ecology, 15*(3), 339-341.

Burnett, W. C., Taniguchi, M., & Oberdorfer, J. (2001). Measurement and significance of the direct discharge of groundwater into the coastal zone. *Journal of Sea Research, 46*(2), 109-116.

Cape Cod Commission. (2013). Regional Wastewater Management Plan: Understanding the Cost Factors of Wastewater Treatment and Disposal. Retrieved 22 July, 2015, from http://www.capecodcommission.org/resources/RWMP/RWMP_costs_comparative.pdf

Chaillou, Katell, Gérente, Claire, Andrès, Yves, & Wolbert, Dominique. (2011). Bathroom Greywater Characterization and Potential Treatments for Reuse. *Water, Air, & Soil Pollution, 215*(1-4), 31-42. doi: 10.1007/s11270-010-0454-5

Chiaroni, L., Hewitt, J.E., & Hailes, S. F. . (2007). Tamaki Strait: Marine benthic habitats, ecological values and threats. A Report prepared for Auckland Regional Council. National Institute of Water & Atmospheric Research Ltd Retrieved 21 July, 2015, from http://www.aucklandcouncil.govt.nz/EN/planspoliciesprojects/reports/technicalpublications/Documents/tr2010038tamakistraitmarinebenthichabs.pdf

Christova-Boal, Diana. (1995). *Installation and Evaluation of Domestic Greywater Reuse Systems.* (Master of Engineering), Victoria Universtity of Technology, Victoria, Australia.

Cohen-Tanugi, David, McGovern, Ronan K., Dave, Shreya H., Lienhard, John H., & Grossman, Jeffrey C. (2014). Quantifying the potential of ultra-permeable membranes for water desalination. *Energy & Environmental Science, 7*(3), 1134-1141. doi: 10.1039/C3EE43221A

Conolly, C., Lawrence, H., Vincent, K., Donovan, B., Davies, M., & Colbeck, C. (2010). UK Eutrophying and Acidifying Atmospheric Pollutants (UKEAP) Annual Report 2010. . Retrieved 15 Aug, 2014, from http://nora.nerc.ac.uk/14299/

Costanza, R., D'Arge, R., De Groot, R., Farber, S., Grasso, M., Hannon, B., . . . Van Den Belt, M. (1997). The value of the world's ecosystem services and natural capital. *Nature, 387*(6630), 253-260.

Cote, Arthur E. (2003). *Operation of Fire Protection Systems*. Quincy, Massachusetts: National Fire Protection Association, Inc. .

Cucek, L., Klemes, J. J., & Kravanja, Z. (2012). A review of footprint analysis tools for monitoring impacts on sustainability. *Journal of Cleaner Production, 34*, 9-20.

Cumberland, J.H. (1966). A Regional Interindustry Model for Analysis of Development Objectives. *Papers, Regional Science Association, 17*, 65-94.

Daily, Gretchen C., & Ehrlich, Paul R. (1992). Population, Sustainability, and Earth's Carrying Capacity. *BioScience, 42*(10), 761-771.

Daly, H. (1968). On Economics as a Life Science. *Journal of Political Economics, 76*, 392-406.

Daly, H. (1996). Beyond growth : the economics of sustainable development. Boston: Beacon Press.

Daniels, P. L., Lenzen, M., & Kenway, S. J. (2011). The ins and outs of water use - a review of multi-region input-output analysis and water footprints for regional sustainability analysis and policy. *Economic Systems Research, 23*(4), 353-370.

Dougherty, Elizabeth, & Murphy, Michael. (2012). Evaluation of Potential Best Management Practices: Graywater Use in California Single and MultiResidential Units. Prepared for The California Urban Water Conservation Council. Retrieved 28 July, 2015, from http://cuwcc.org/Portals/0/Document%20Library/Resources/Publications/Potential%20BMP%20Reports/2012%20PBMP%20for%20Graywate%20Use%20in%20California.pdf

Duchin, F., & López-Morales, C. (2012). DO WATER-RICH REGIONS HAVE A COMPARATIVE ADVANTAGE IN FOOD PRODUCTION? IMPROVING THE REPRESENTATION OF WATER FOR AGRICULTURE IN ECONOMIC MODELS. *Economic Systems Research, 24*(4), 371-389. doi: 10.1080/09535314.2012.714746

Duchin, F., & Levine, S. H. (2011). Sectors may use multiple technologies simultaneously: The rectangular choice-of-technology model with binding factor constraints. *Economic Systems Research, 23*(3), 281-302. doi: 10.1080/09535314.2011.571238

Dwyer, L., Forsyth, P., & Spurr, R. (2005). Estimating the impacts of special events on an economy. *Journal of Travel Research, 43*(4), 351-359.

Ehrlich, Paul R., & Holdren, John P. (1971). Impact of Population Growth. *Science, 171*(3977), 1212-1217. doi: 10.1126/science.171.3977.1212

Ercin, A. Ertug, & Hoekstra, A. Y. (2012). Carbon and Water Footprints. Concepts, Methodologies and Policy Responses. WWDR4 Side Publication Series 04. United Nations World Water Assessment Programme. UNESCO. Retrieved 29 Oct, 2012, from http://unesdoc.unesco.org/images/0021/002171/217181e.pdf

Eurostat. (2012). Building the System of National Accounts - supply and use tables. Retrieved 28 Oct, 2013, from http://epp.eurostat.ec.europa.eu/statistics_explained/index.php/Building_the_System_of_National_Accounts_-_supply_and_use_tables

Ewing, B. R., Hawkins, T. R., Wiedmann, T. O., Galli, A., Ertug Ercin, A., Weinzettel, J., & Steen-Olsen, K. (2012). Integrating ecological and water footprint accounting in a multi-regional input-output framework. *Ecological Indicators, 23*, 1-8.

Ewing, B., Reed, A. , Galli, A., Kitzes, J., & Wackernagel, M. (2010). Calculation Methodology for the National Footprint Accounts, 2010 EditIon. Retrieved 2 Nov, 2010, from http://www.footprintnetwork.org/images/uploads/National_Footprint_Accounts_Method_Paper_2010.pdf

Faber, N., Jorna, R., & Van Engelen, J. (2005). The sustainability of "sustainability" - A study into the conceptual foundations of the notion of "sustainability". *Journal of Environmental Assessment Policy and Management, 7*(1), 1-33.

FAO Water. (2010). Crop Water Information: Olive. Retrieved 5 July, 2010, from http://www.fao.org/nr/water/cropinfo_olive.html

Farooq, U., Hardy, J. L., Gao, L., & Siddiqui, M. A. (2008). Economic impact/forecast model of intelligent transportation systems in Michigan: An input output analysis. *Journal of Intelligent Transportation Systems: Technology, Planning, and Operations, 12*(2), 86-95.

Fetter, C. W. (2001). *Applied hydrogeology* (4th ed.). Upper Saddle River, N.J.: Prentice Hall.

Fewkes, A., & Warm, P. (2000). Method of modelling the performance of rainwater collection systems in the United Kingdom. *Building Services Engineering Research and Technology, 21*(4), 257-265.

Finnveden, G., Hauschild, M. Z., Ekvall, T., Guinée, J., Heijungs, R., Hellweg, S., . . . Suh, S. (2009). Recent developments in Life Cycle Assessment. *Journal of Environmental Management, 91*(1), 1-21.

Fischer-Kowalski, M., Krausmann, F., Giljum, S., Lutter, S., Mayer, A., Bringezu, S., . . . Weisz, H. (2011). Methodology and indicators of economy-wide material flow accounting: State of the art and reliability across sources. *Journal of Industrial Ecology, 15*(6), 855-876.

Fluri, Thomas P. (2009). The potential of concentrating solar power in South Africa. *Energy Policy, 37*(12), 5075-5080. doi: http://dx.doi.org/10.1016/j.enpol.2009.07.017

Forrester, Jay W. (1969). *Urban dynamics*. Cambridge, Mass.,: M.I.T. Press.

Frischknecht, R., Jungbluth, N., Althaus, H. J., Doka, G., Dones, R., Heck, T., . . . Spielmann, M. (2005). The ecoinvent database: Overview and methodological framework. *International Journal of Life Cycle Assessment, 10*(1), 3-9.

Fthenakis, V. (2009). Sustainability of photovoltaics: The case for thin-film solar cells. *Renewable and Sustainable Energy Reviews, 13*(9), 2746-2750.

Gabe, J., Trowsdale, S., & Mistry, D. (2012). Mandatory urban rainwater harvesting: Learning from experience. *Water Science and Technology, 65*(7), 1200-1207.

Gaimster, Rob. (2009). Cement and Concrete demand: Activity and trends, November 2009: CCANZ Industry Report. Cement & Concrete Association of New Zealand (CCANZ).

Galli, A., Kitzes, J., Wermer, P., Wackernagel, M., Niccolucci, V., & Tiezzi, E. (2007). An exploration of the mathematics behind the ecological footprint. *International Journal of Ecodynamics, 2*(4), 250-257.

Galli, A., Wiedmann, Thomas, Ercin, Ertug, Knoblauch, Doris, Ewing, Brad, & Giljum, Stefan. (2012). Integrating Ecological, Carbon and Water footprint into a "Footprint Family" of

indicators: Definition and role in tracking human pressure on the planet. *Ecological Indicators, 16*(0), 100-112. doi: http://dx.doi.org/10.1016/j.ecolind.2011.06.017

Gallopín, Gilberto. (2003). A systems approach to sustainability and sustainable development. Sustainable Development and Human Settlements Division. ECLAC/ Government of the Netherlands Project NET/00/063. "Sustainability Assessment in Latin America and the Caribbean". Santiago, Chile, March, 2003. Retrieved 1 Feb, 2011, from http://www.eclac.org/publicaciones/xml/8/12288/lcl1864i.pdf

Galloway, Devin, Jones, David R., & Ingebritsen, S.E. (2005). Land Subsidence in the United States. U.S. Geological Survey Circular 1182. Retrieved 10 Jun, 2011, from http://pubs.usgs.gov/circ/circ1182/

Gardels, Derek J. (2011). *Economic Input-Output Life Cycle Assessment of Water Reuse Strategies in Residential Buildings and Communities.* (Master of Science, Civil Engineering), University of Nebraska-Lincoln. Retrieved from http://digitalcommons.unl.edu/civilengdiss/18

Ghaffour, N., Missimer, T. M., & Amy, G. L. (2013). Technical review and evaluation of the economics of water desalination: Current and future challenges for better water supply sustainability. *Desalination, 309*, 197-207.

Ghunmi, L. A., Zeeman, G., Fayyad, M., & Van Lier, J. B. (2011). Grey water treatment systems: A review. *Critical Reviews in Environmental Science and Technology, 41*(7), 657-698. doi: 10.1080/10643380903048443

Gilau, A. M., & Small, M. J. (2008). Designing cost-effective seawater reverse osmosis system under optimal energy options. *Renewable Energy, 33*(4), 617-630.

Giljum, Stefan, Dittrich, Monika, Lieber, Mirko, & Lutter, Stephan. (2014). Global Patterns of Material Flows and their Socio-Economic and Environmental Implications: A MFA Study on All Countries World-Wide from 1980 to 2009. *Resources, 3*(1), 319-339.

Goodland, R. (2002). Sustainability: Human, Social, Economic and Environmental. In R. E. Munn (Ed.), *Encyclopedia of global environmental change*. Chichester ; New York: Wiley.

Goodland, R., & Daly, H. (1996). Environmental sustainability: Universal and non-negotiable. *Ecological Applications, 6*(4), 1002-1017.

Graedel, T. E., & Voet, E. van der. (2010). *Linkages of sustainability* (pp. xiii, 532 p.). Retrieved from http://site.ebrary.com/lib/auckland/Doc?id=10359390

Gude, V. G., & Nirmalakhandan, N. (2010). Sustainable desalination using solar energy. *Energy Conversion and Management, 51*(11), 2245-2251.

Guinée, J. B. (2002). *Handbook on life cycle assessment operational guide to the ISO standards Eco-efficiency in industry and science v. 7* (pp. xi, 692 p.). Retrieved from

http://site.ebrary.com/lib/auckland/Doc?id=10067324

Guinee, J.B. , & Heijungs, R. (1993). A proposal for the classification of toxic substances within the framework of Life Cycle Assessment of products. *Chemosphere, 26*(10), 1925-1944.

Hák, Tomáš, Moldan, Bed rich, & Dahl, Arthur L. (2007). *Sustainability indicators : a scientific assessment*. Washington, DC: Island Press.

Haberl, Helmut, Erb, K. Heinz, Krausmann, Fridolin, Gaube, Veronika, Bondeau, Alberte, Plutzar, Christoph, . . . Fischer-Kowalski, Marina. (2007). Quantifying and mapping the human appropriation of net primary production in earth's terrestrial ecosystems. *Proceedings of the National Academy of Sciences, 104*(31), 12942-12947. doi: 10.1073/pnas.0704243104

Hallegatte, S. (2008). An adaptive regional input-output model and its application to the assessment of the economic cost of Katrina. *Risk Analysis, 28*(3), 779-799.

Hang, Qu, Jun, Zhao, Xiao, Yu, & Junkui, Cui. (2008). Prospect of concentrating solar power in China—the sustainable future. *Renewable and Sustainable Energy Reviews, 12*(9), 2505-2514. doi: http://dx.doi.org/10.1016/j.rser.2007.06.002

Heijungs, Reinout. (2001). A theory of the environment and economic systems : a unified framework for ecological economic analysis and decision-support. Cheltenham, UK ; Northampton, MA: Edward Elgar Pub.

Heijungs, Reinout, & Suh, Sangwon. (2002). *The computational structure of life cycle assessment*. Dordrecht ; Boston: Kluwer Academic Publishers.

Heinrich, Matthias. (2008). Water Use in Auckland Households: Auckland Water Use Study (AWUS) Final Report EC1356: BRANZ Ltd. Judgeford, City New Zealand.

Heinrich, Matthias (2007). Water End Use and Efficiency Project (WEEP) - Final Report. BRANZ Study Report 159 (Vol. 2010): BRANZ Ltd, Judgeford, New Zealand.

Hoekstra, A. Y. (2009). Human appropriation of natural capital: A comparison of ecological footprint and water footprint analysis. *Ecological Economics, 68*(7), 1963-1974. doi: 10.1016/j.ecolecon.2008.06.021

Hoekstra, Arjen Y., Chapagain, Ashok K., Aldaya, Maite M., & Mekonnen, Mesfn M. (2011). *The Water Footprint Assessment Manual: Setting the Global Standard*. London, Washington, DC: Earthscan.

Hoekstra, Arjen Y., & Mekonnen, Mesfin M. (2012). The water footprint of humanity. *Proceedings of the National Academy of Sciences, Upcoming Issue*. doi: 10.1073/pnas.1109936109

Hoekstra, R., & van den Bergh, J. C. J. M. (2006). Constructing physical input-output tables for environmental modeling and accounting: Framework and illustrations. *Ecological Economics, 59*(3), 375-393.

Holling, C.S. (1996). Engineering Resilience versus Ecological Resilience In P. C. Schulze (Ed.), *Engineering within ecological constraints* (pp. 31-44). Washington, D.C.: National Academy Press.

Horan, Richard D., Fenichel, Eli P., Drury, Kevin L. S., & Lodge, David M. (2011). Managing ecological thresholds in coupled environmental–human systems. *Proceedings of the National Academy of Sciences*. doi: 10.1073/pnas.1005431108

Hu, R. L., Yue, Z. Q., Wang, L. C., & Wang, S. J. (2004). Review on current status and challenging issues of land subsidence in China. *Engineering Geology, 76*(1-2), 65-77.

Huang, H., & Yan, Z. (2009). Present situation and future prospect of hydropower in China. *Renewable and Sustainable Energy Reviews, 13*(6-7), 1652-1656.

Huang, R., Liu, J., & Li, L. (2012). Water resources carrying capacity of Xianyang City based on system dynamics. *Paiguan Jixie Gongcheng Xuebao/Journal of Drainage and Irrigation Machinery Engineering, 30*(1), 57-63. doi: 10.3969/j.issn.1674-8530.2012.01.012

Huang, S. L., & Chen, C. W. (2009). Urbanization and Socioeconomic Metabolism in Taipei. *Journal of Industrial Ecology, 13*(1), 75-93. doi: 10.1111/j.1530-9290.2008.00103.x

Hubacek, K., & Giljum, S. (2003). Applying physical input-output analysis to estimate land appropriation (ecological footprints) of international trade activities. *Ecological Economics, 44*(1), 137-151.

Hunt, R. G., & Franklin, W. E. (1996). LCA - How it Came about - Personal Reflections on the Origin and the Development of LCA in the USA. *International Journal of Life Cycle Assessment, 1*(1), 4-7.

Hutton, Guy. (2012). Monitoring "Affordability" of water and sanitation services after 2015: Review of global indicator options. A paper submitted to the United Nations Office of the High Commission for Human Rights. Retrieved 21 May, 2015, from http://www.wssinfo.org/fileadmin/user_upload/resources/END-WASH-Affordability-Review.pdf

IEA. (2013). Key World Energy Statistics 2013. International Energy Agency. Retrieved 28 Aug, 2014, from http://www.iea.org/publications/freepublications/publication/KeyWorld2013.pdf

Isard, W. (1968). Some Notes on the Linkage of Ecological and Economic Systems. *Papers, Regional Science Association, 22*, 85-96.

ISO. (2013). ISO/TS 14067:2013 Greenhouse gases -- Carbon footprint of products -- Requirements and guidelines for quantification and communication. International Organization for Standardization. Retrieved 30 Aug, 2014, from http://www.iso.org/iso/catalogue_detail?csnumber=59521

Jamrah, Ahmad, Al-Futaisi, Ahmed, Prathapar, Sanmugan, & Harrasi, AliAl. (2008). Evaluating greywater reuse potential for sustainable water resources management in Oman. *Environmental Monitoring and Assessment, 137*(1-3), 315-327. doi: 10.1007/s10661-007-9767-2

Jerneck, A., & Olsson, L. (2008). Adaptation and the poor: Development, resilience and transition. *Climate Policy, 8*(2), 170-182.

Karimuribo, E. D., Chenyambuga, S. W., Makene, V. W., & Mathias, S. (2011). Characteristics and production constraints of rural-based small-scale pig farming in Iringa region, Tanzania. *Livestock Research for Rural Development, 23*(8).

Kemp, R., & Rotmans, J. (2005). The management of the co-evolution of technical, environmental and social systems *Towards Environmental Innovation Systems* (pp. 33-55).

Kennedy, C., Steinberger, J., Gasson, B., Hansen, Y., Hillman, T., Havranek, M., . . . Mendez, G. V. (2010). Methodology for inventorying greenhouse gas emissions from global cities. *Energy Policy, 38*(9), 4828-4837. doi: 10.1016/j.enpol.2009.08.050

Kenway, S., Gregory, A., & McMahon, J. (2011). Urban water mass balance analysis. *Journal of Industrial Ecology, 15*(5), 693-706.

Kim, S. S., Chon, K., & Chung, K. Y. (2003). Convention industry in South Korea: An economic impact analysis. *Tourism Management, 24*(5), 533-541.

Kinzig, A.P., Ryan, P., Etienne, M., Allison, H., Elmqvist, T., & Walker, B.H. (2006). Resilience and regime shifts: assessing cascading effects. *Ecology and Society, 11*(1), 20.

Kitzes, J., & Wackernagel, M. (2009). Answers to common questions in Ecological Footprint accounting. *Ecological Indicators, 9*(4), 812-817.

Krausmann, Fridolin, Erb, Karl-Heinz, Gingrich, Simone, Haberl, Helmut, Bondeau, Alberte, Gaube, Veronika, . . . Searchinger, Timothy D. (2013). Global human appropriation of net primary production doubled in the 20th century. *Proceedings of the National Academy of Sciences, 110*(25), 10324-10329. doi: 10.1073/pnas.1211349110

Lade, Steven J., Tavoni, Alessandro, Levin, Simon A., & Schlüter, Maja. (2013). Regime shifts in a social-ecological system. Centre for Climate Change Economics and Policy Working Paper No. 125. Retrieved 8 Oct, 2013, from http://www.lse.ac.uk/GranthamInstitute/publications/WorkingPapers/Papers/100-109/WP105-regime-shifts-socio-ecological-system.pdf

Lancker, Elly, & Nijkamp, Peter. (2000). A policy scenario analysis of sustainable agricultural development options: a case study for Nepal. *Impact Assessment and Project Appraisal, 18*(2), 111-124. doi: 10.3152/147154600781767493

Lasserre, J. B. (1983). An analytical expression and an algorithm for the volume of a convex polyhedron in Rn. *Journal of Optimization Theory and Applications, 39*(3), 363-377.

Lattemann, Sabine, & Höpner, Thomas. (2008). Environmental impact and impact assessment of seawater desalination. *Desalination, 220*(1–3), 1-15. doi: http://dx.doi.org/10.1016/j.desal.2007.03.009

Lave, Lester B., Cobas-Flores, Elisa, Hendrickson, Chris T., & McMichael, Francis C. (1995). Using input-output analysis to estimate economy-wide discharges. *Environmental Science & Technology, 29*(9), 420A-426A. doi: 10.1021/es00009a003

Lenton, T. M., Held, H., Kriegler, E., Hall, J. W., Lucht, W., Rahmstorf, S., & Schellnhuber, H. J. (2008). Tipping elements in the Earth's climate system. *Proceedings of the National Academy of Sciences of the United States of America, 105*(6), 1786-1793. doi: 10.1073/pnas.0705414105

Lenton, T. M., & Williams, H. T. P. (2013). On the origin of planetary-scale tipping points. *Trends in Ecology and Evolution, 28*(7), 380-382. doi: 10.1016/j.tree.2013.06.001

Lenzen, M., Wood, R., & Wiedmann, T. (2010). Uncertainty analysis for multi-region input - output models - a case study of the UK'S carbon footprint. *Economic Systems Research, 22*(1), 43-63.

Lenzen, Manfred. (2000). Errors in Conventional and Input-Output—based Life—Cycle Inventories. *Journal of Industrial Ecology, 4*(4), 127-148. doi: 10.1162/10881980052541981

Leontief, Wassily W. (1936). Quantitative Input and Output Relations in the Economic Systems of the United States. *The Review of Economics and Statistics, 18*(3), 105-125.

Leontief, Wassily W. (1970). Environmental Repercussions and the Economic Structure: An Input-Output Approach. *Review of Economics and Statistics, 52*, 262-271.

Lin, Ming-Hua, Carlsson, John Gunnar, Ge, Dongdong, Shi, Jianming, & Tsai, Jung-Fa. (2013). A Review of Piecewise Linearization Methods. *Mathematical Problems in Engineering, 2013*, 8. doi: 10.1155/2013/101376

Llop, M. (2008). Economic impact of alternative water policy scenarios in the Spanish production system: An input-output analysis. *Ecological Economics, 68*(1-2), 288-294. doi: 10.1016/j.ecolecon.2008.03.002

Logan, Gerard (2009). [Waiheke Wine Laboratory Water Use].

MakWater. (2014). Product Data Sheet. Sea Water Reverse Osmosis (SWRO) Desalination. MakWater. Australia. Retrieved 21 May, 2015, from http://d335hnnegk3szv.cloudfront.net/wp-content/uploads/sites/899/2014/08/PDS-SWRO-170614.pdf

Maurer, M., Rothenberger, O., & Larsen, T. A. (2005) Decentralised wastewater treatment technologies from a national perspective: At what cost are they competitive? *: Vol. 5. Water Science and Technology: Water Supply* (pp. 145-154).

Mayer, A. L. (2008). Strengths and weaknesses of common sustainability indices for

multidimensional systems. *Environment International, 34*(2), 277-291.

Meadows, Donella H. (1972). The Limits to growth; a report for the Club of Rome's project on the predicament of mankind. New York,: Universe Books.

Meadows, Donella H., Randers, Jørgen, & Meadows, Dennis L. (2004). *Limits to growth : the 30-year update*. White River Junction, Vt: Chelsea Green Publishing Company.

Melo, M. T., Nickel, S., & Saldanha Da Gama, F. S. (2006). Dynamic multi-commodity capacitated facility location: A mathematical modeling framework for strategic supply chain planning. *Computers and Operations Research, 33*(1), 181-208.

Michael, Holly A., Mulligan, Ann E., & Harvey, Charles F. (2005). Seasonal oscillations in water exchange between aquifers and the coastal ocean. *Nature, 436*(7054), 1145-1148. doi: http://www.nature.com/nature/journal/v436/n7054/suppinfo/nature03935_S1.html

Miller, Shepherd. (2002). Total Maximum Daily Load for Dissolved Zinc in Little Cottonwood Creek. Retrieved 20 Feb, 2011, from http://www.waterquality.utah.gov/TMDL/Little_Cottonwood_Creek_TMDL.pdf

Ministry for Environment. (2009). National environmental standard on ecological flows and water levels. Retrieved 4 May, 2011, from http://www.mfe.govt.nz/laws/standards/ecological-flows-water-levels/index.html

Mishra, Archana. (2006). Water harvesting : ecological and economic appraisal. Delhi: Authorspress.

Moore, D., Cranston, G., Reed, A., & Galli, A. (2012). Projecting future human demand on the Earth's regenerative capacity. *Ecological Indicators, 16*, 3-10.

Moors, E. H. M. (2006). Technology strategies for sustainable metals production systems: a case study of primary aluminium production in The Netherlands and Norway. *Journal of Cleaner Production, 14*(12-13 SPEC. ISS.), 1121-1138.

Moriguchi, Y., Hondo, Y., & Shimizu, H. (1993). Analyzing the life cycle impact of cars: the case of CO_2. *Industrial and Environment, 16*, 42-45.

Natural Habitats. (2009). The Differences between Sustainability and Environmentalism. Retrieved 25 Aug, 2014, from http://natural-habitats.com/en/blog/the_differences_between_sustainability_and_environmentalism/

Ness, B., Urbel-Piirsalu, E., Anderberg, S., & Olsson, L. (2007). Categorising tools for sustainability assessment. *Ecological Economics, 60*(3), 498-508.

Niccolucci, V., Tiezzi, E., Pulselli, F. M., & Capineri, C. (2012). Biocapacity vs Ecological Footprint of world regions: A geopolitical interpretation. *Ecological Indicators, 16*, 23-30.

NIWA. (2014). The National Climate Database, New Zealand., from http://www.niwa.cri.nz/services/clidb

Niza, S., Rosado, L., & Ferrao, P. (2009). Urban Metabolism Methodological Advances in Urban Material Flow Accounting Based on the Lisbon Case Study. *Journal of Industrial Ecology, 13*(3), 384-405. doi: 10.1111/j.1530-9290.2009.00130.x

NZ Wine Growers Association. (2010). New Zealand Winegrowers Statistical Annuals. Retrieved 10 July, 2010, from http://www.nzwine.com/statistics/

Olivera, Alfredo, Amoza, Franco Robledo, & Testuri, Carlos E. (2009). A GRASP algorithm for a capacitated, fixed charge, multicommodity network flow problem with uncertain demand and survivability constraints. Retrieved 8 Mar, 2012, from http://www.fing.edu.uy/~aolivera/papers/olivera08grasp.pdf

Olives Australia. (2009). Water Requirements for Olive Orchards. Retrieved 5 July, 2010, from http://www.oliveaustralia.com.au/Olifax_Topics/Water_Requirements/water_requirements.html

Olivier, Jos G.J., Janssens-Maenhout, Greet, Muntean, Marilena, & Peters, Jeroen A.H.W. (2013). Trends in Global CO2 Emissions. 2013 Report. PBL Netherlands Environmental Assessment Agency. Retrieved 28 Aug, 2014, from http://edgar.jrc.ec.europa.eu/news_docs/pbl-2013-trends-in-global-co2-emissions-2013-report-1148.pdf

On-Site NewZ. (2010). ON-SITE WASTEWATER SYSTEMS SELECTING A SYSTEM FOR YOUR PROPERTY: An Information Booklet for Homeowners. Retrieved 24 July, 2015, from http://www.concretetanks.co.nz/files/pdfs/on-site-wastewater-systems.pdf

Onsite Sewage Treatment Program. (2011). Section 9 Pumping System. In Onsite Sewage Treatment Program (Ed.), *Manual for Septic System Professionals in Minnesota*: Water Resource Center, University of Minnesota.

Ormiston, A. W., Floyd, Robyn E., & Gunn, Ian. (2004). *On-site wastewater systems : design and management manual* (3rd ed.). [Auckland, N.Z.]: Auckland Regional Council.

OzCoasts. (2010). Saline intrusion, OzCoast Australian Online Coastal Information. Retrieved 14 July, 2010, from http://www.ozcoasts.org.au/indicators/saline_intrusion.jsp

Pedersen, O. G., & De Haan, M. (2006). The system of environmental and economic accounts-2003 and the economic relevance of physical flow accounting. *Journal of Industrial Ecology, 10*(1-2), 19-42.

Perez, L. P. Y., & Barreiro-Hurle, J. (2009). Assessing the socio-economic impacts of drought in the Ebro River Basin. *Spanish Journal of Agricultural Research, 7*(2), 269-280.

Perkins, R. J. (1984). Septic tanks, lot size and pollution of water table aquifers. *Journal of Environmental Health, 46*(6), 298-304.

Perrings, Charles, & Vincent, Jeffrey R. (2003). *Natural resource accounting and economic development : theory and practice*. Cheltenham, UK: Edward Elgar.

Porter, Ellen, Tonnessen, Kathy, Sherwell, John, & Grant, Richard. (2000). Nitrogen in the Nation's Rain. Retrieved 3 Jul, 2013, from http://nadp.isws.illinois.edu/lib/brochures/nitrogen.pdf

Portland Cement Association. (2010). Concrete Basics. Retrieved 10 July, 2010, from http://www.cement.org/basics/concretebasics_concretebasics.asp

Postel, S. L., Daily, G. C., & Ehrlich, P. R. (1996). Human appropriation of renewable fresh water. *Science, 271*(5250), 785-788.

Potschin, M., & Haines-Young, R. (2008). Sustainability impact assessments: Limits, thresholds and the sustainability choice space *Sustainability Impact Assessment of Land Use Changes* (pp. 425-450).

Queensland Goverment. (2009). Rural water use statistics, Queensland, Australia. Retrieved 10 July, 2010, from http://www.derm.qld.gov.au/rwue/statistics.html

Rawson, Peter. (2006). Waiheke Residential Land Use Survey - 2005/06. Auckland: Auckland City Council.

Rebitzer, G., Ekvall, T., Frischknecht, R., Hunkeler, D., Norris, G., Rydberg, T., . . . Pennington, D. W. (2004). Life cycle assessment Part 1: Framework, goal and scope definition, inventory analysis, and applications. *Environment International, 30*(5), 701-720.

Reddy, K. V., & Ghaffour, N. (2007). Overview of the cost of desalinated water and costing methodologies. *Desalination, 205*(1–3), 340-353. doi: http://dx.doi.org/10.1016/j.desal.2006.03.558

Rees, William E. (1992). Ecological footprints and appropriated carrying capacity: what urban economics leaves out. *Environment and Urbanization, 4*(2), 121-130. doi: 10.1177/095624789200400212

Resilience Alliance. (2014). Thresholds Database. Retrieved 15 July, 2014

Richardson, H. W. (1985). Input-output and economic base multipliers: looking backward and forward. *Journal of Regional Science, 25*(4), 607-661.

Robinson, D.W. (2002). Construction and Operating Costs of Groundwater Pumps for Irrigation in the Riverine Plain. Technical Report 20/02. CSIRO Land and Water.

Retrieved 24 July, 2015, from http://www.clw.csiro.au/publications/technical2002/tr20-02.pdf

Rockström, J., Steffen, W., Noone, K., Persson, A., Chapin Iii, F. S., Lambin, E., . . . Foley, J. (2009). Planetary boundaries: Exploring the safe operating space for humanity. *Ecology and Society, 14*(2).

Rose, A., & Liao, S. Y. (2005). Modeling regional economic resilience to disasters: A computable general equilibrium analysis of water service disruptions. *Journal of Regional Science, 45*(1), 75-112.

Schandl, H., & Eisenmenger, N. (2006). Regional patterns in global resource extraction. *Journal of Industrial Ecology, 10*(4), 133-147.

Scheffer, M., Bascompte, J., Brock, W. A., Brovkin, V., Carpenter, S. R., Dakos, V., . . . Sugihara, G. (2009). Early-warning signals for critical transitions. *Nature, 461*(7260), 53-59. doi: 10.1038/nature08227

Scheffer, M., Carpenter, S., Foley, J. A., Folke, C., & Walker, B. (2001). Catastrophic shifts in ecosystems. *Nature, 413*(6856), 591-596.

Schellnhuber, H. J. (2010). Tipping elements in the Earth System (vol 106, pg 20561, 2009). *Proceedings of the National Academy of Sciences of the United States of America, 107*(3), 1254-1254. doi: 10.1073/pnas.0914246107

Scion. (2007). Auckland Region Fire Returns 1991/92 to 2006/07, Scion Research New Zealand. . Retrieved 5 July, 2010, from http://www.scionresearch.com/__data/assets/pdf_file/0012/4503/Auckland-Region-Append.pdf

Sheppard, S. C. (2002). Three approaches to define the ecotoxicity threshold for atmospheric ammonia. *Canadian Journal of Soil Science, 82*(3), 341-354. doi: 10.4141/S01-029

Singh, Rajesh Kumar, Murty, H. R., Gupta, S. K., & Dikshit, A. K. (2009). An overview of sustainability assessment methodologies. *Ecological Indicators, 9*(2), 189-212. doi: DOI: 10.1016/j.ecolind.2008.05.011

SKM. (2005). Auckland's Electrical Demand Characteristics and Applicability of Demand Management. (Vol. 2015). Auckland, NZ: Sinclair Knight Merz (SKM).

SKM. (2007). Waiheke Island - Extended Groundwater Model: Sinclair Knight Merz (for Auckland Regional Council).

SNZ. (2007). Supply and Use Tables for the Year Ended March 2007. Retrieved 29 Oct, 2010, from http://www.stats.govt.nz/browse_for_stats/economic_indicators/NationalAccounts/s

upply-use-tables-yr-end-mar-07.aspx

SNZ. (2012). National Accounts input-output tables: year ended March 2007. Statistics New Zealand. Retrieved 16 Oct, 2013, from http://www.stats.govt.nz/browse_for_stats/economic_indicators/NationalAccounts/input-output%20tables.aspx

SNZ. (2015). New Zealand Census 2013. Retrieved 21 May, 2015, from http://www.stats.govt.nz/Census/2013-census.aspx

Sorrell, S., Speirs, J., Bentley, R., Brandt, A., & Miller, R. (2010). Global oil depletion: A review of the evidence. *Energy Policy, 38*(9), 5290-5295. doi: 10.1016/j.enpol.2010.04.046

Sporri, C., Borsuk, M., Peters, I., & Reichert, P. (2007). The economic impacts of river rehabilitation: A regional Input-Output analysis. *Ecological Economics, 62*(2), 341-351.

Sprengel, C. (1828). Von den Substanzen der Ackerkrume und des Untergrundes. *Journal fur Tecnische und Okonomische Chemie, 2*, 423-474.

Statistics New Zealand. (2006). Census 2006 Meshblock Dataset. Retrieved 5 Feb 2010, from http://www.stats.govt.nz/Census/2006CensusHomePage/MeshblockDataset.aspx

Statistics New Zealand. (2007). Population Projections Tables: Area Unit Population Projections. Retrieved 1 July, 2010, from http://www.stats.govt.nz/methods_and_services/access-data/TableBuilder/population-projections-tables.aspx

Statistics New Zealand. (2010). Table Builder: Businesses Statistics. Retrieved 29 June, 2010, from http://www.stats.govt.nz/methods_and_services/access-data/TableBuilder/business-statistics.aspx

Stewart, Gordon , & Rout, Robert (2007). Reasonable Stock Water Requirements. Tauranga and Hamilton: AQUAS Consultants Ltd & Aqualinc Research Ltd (for Horizons Regional Council).

Stringleman, H. (2005, 17 May). Foot and Mouth Fright Hits Farmers at Low Ebb, *The New Zealand Farmers Weekly*. Retrieved from http://www.nzfarmersweekly.co.nz/article/3460.html

Suh, S., & Huppes, G. (2005). Methods for life cycle inventory of a product. *Journal of Cleaner Production, 13*(7), 687-697.

Suh, S., Lenzen, M., Treloar, G. J., Hondo, H., Horvath, A., Huppes, G., . . . Norris, G. (2004).

System Boundary Selection in Life-Cycle Inventories Using Hybrid Approaches. *Environmental Science and Technology, 38*(3), 657-664.

Suh, Sangwon. (2005). Theory of materials and energy flow analysis in ecology and economics. *Ecological Modelling, 189*(3-4), 251-269. doi: DOI: 10.1016/j.ecolmodel.2005.03.011

Suh, Sangwon, & Kagawa, Shigemi. (2005). Industrial ecology and input-output economics: an introduction. *Economic Systems Research, 17*(4), 349 - 364.

Synergy Boreholes and Systems Ltd. (2011). How much will it cost? Retrieved 24 July, 2015, from http://www.synergyboreholes.co.uk/water_boreholes/index/cost/

ten Raa, T., & Shestalova, V. (2015). SUPPLY-USE FRAMEWORK FOR INTERNATIONAL ENVIRONMENTAL POLICY ANALYSIS. *Economic Systems Research, 27*(1), 77-94. doi: 10.1080/09535314.2014.922461

Texas Water Development Board. (2005). The Texas Manual on Rainwater Harvesting. Third Edition. Retrieved 6 July, 2010, from http://www.twdb.state.tx.us/publications/reports/RainwaterHarvestingManual_3rdedition.pdf

Trinh, Bui, Kobayashi, Kiyoshi, & Kim, Kwang Moon. (2012). The Supply and Use tables: The approach for conversion to input-output table *Advances in Management & Applied Economics, 2*(2), 83-89.

TUGRUL, ATIYE , & ÜNDÜL, ÖMER. (2006). *Engineering geological characteristics of Istanbul greywackes, Turkey, IAEG2006 Paper number 395*. Paper presented at the The 10th IAEG International Congress, Nottingham, United Kingdom. http://www.iaeg.info/iaeg2006/PAPERS/IAEG_395.PDF

Tukker, Arnold, Poliakov, Evgueni, Heijungs, Reinout, Hawkins, Troy, Neuwahl, Frederik, Rueda-Cantuche, José M., . . . Bouwmeester, Maaike. (2009). Towards a global multi-regional environmentally extended input-output database. *Ecological Economics, 68*(7), 1928-1937. doi: DOI: 10.1016/j.ecolecon.2008.11.010

U.S. EPA. (2002). Onsite Wastewater Treatment Systems Manual. Office of Water. Office of Research and Development. U.S. Environmental Protection Agency. Retrieved 5 May, 2011, from http://www.epa.gov/nrmrl/pubs/625r00008/html/625R00008.htm

Ulanowicz, Robert E. (2004). Quantitative methods for ecological network analysis. *Computational Biology and Chemistry, 28*(5-6), 321-339. doi: DOI: 10.1016/j.compbiolchem.2004.09.001

UN. (1992). Agenda 21. United Nations Conference on Environment & Development Rio de Janerio, Brazil, 3 to 14 June 1992. Retrieved 5 Oct, 2013, from http://sustainabledevelopment.un.org/content/documents/Agenda21.pdf

UN. (2008). System of National Accounts 2008. Retrieved 14 Oct, 2010, from http://unstats.un.org/unsd/nationalaccount/SNA2008.pdf

UNEP. (2007). Global Environment Outlook 4 (GEO4): Environment for Development. Retrieved 24 Jan, 2011, from http://www.unep.org/geo/geo4.asp

UNEP. (2012). GEO-5. Global Environment Outlook. 5th edition. Retrieved 5 Oct, 2013, from http://www.unep.org/geo/geo5.asp

UNESCO. (2009). World Water Assessment Programme. 2009. The United Nations World Water Development Report 3: Water in a Changing World. Paris: UNESCO, and London: Earthscan.

URS. (2006). Owhanake Wastewater Treatment Plant, Waiheke Island - Designation of Land for Reticulated Wastewater Treatment and Disposal Purposes. Supporting Information and Assessment of Effects on the Environment. Prepared for Auckland City Council. New Zealand. Retrieved 31 Aug, 2014, from http://www.aucklandcity.govt.nz/council/documents/hgi/docs/hgis32supporting.pdf

Vadenbo, C., Hellweg, S., & Guillén-Gosálbez, G. (2014). Multi-objective optimization of waste and resource management in industrial networks - Part I: Model description. *Resources, Conservation and Recycling, 89*, 52-63. doi: 10.1016/j.resconrec.2014.05.010

Vaithianathan, R. (2009). Economic Impact of Super City Amalgamation on Peripheral Councils (Manukau, Waitakere, Rodney, North Shore, and Franklin). Retrieved 29 Oct, 2010, from http://blog.labour.org.nz/wp-content/uploads/2009/06/economic-impact-of-super-city.pdf

Vector Ltd. (2012). Electricity Asset Management Plan 2012 – 2022. Retrieved 7 Aug, 2014, from http://vector.co.nz/documents/101943/102874/Vector+-+Electricity+AMP+-+2012.pdf/9d8b2baa-42eb-4c00-a4b8-870ae83cff2f

Verheijen, F. G. A., Jones, R. J. A., Rickson, R. J., & Smith, C. J. (2009). Tolerable versus actual soil erosion rates in Europe. *Earth-Science Reviews, 94*(1-4), 23-38.

Victor, P.A. (1972). *Economics of Pollution*. London: Macmillan.

Waiheke Community Board. (2008). *Waiheke Community Board's Submission to the Regional Governance Commission*. Retrieved from http://www.royalcommission.govt.nz/rccms.nsf/0/CC2573E80010C73BCC25742F00831548/$file/Waiheke%20Community%20Board%20Regional%20Governance%20Submission.doc.

Wang, P., & Keller, A. A. (2009). AgInput: An Agricultural Nutrient and Pesticide Source Model. *Environmental Modeling and Assessment, 14*(3), 391-403.

Ward, S., Memon, F. A., & Butler, D. (2010) Rainwater harvesting: Model-based design evaluation. *Vol. 61. Water Science and Technology* (pp. 85-96).

Washington State Department of Health. (2002). Rule Development Committee Issue Research Report. Wastewater Management Program. . Retrieved 15 Jun, 2015, from http://www.doh.wa.gov/Portals/1/Documents/Pubs/337-101.pdf

Watercare. (2014). Annual Report 2013. Watercare, Ltd. Retrieved 26 July, 2014, from http://www.watercare.co.nz/SiteCollectionDocuments/AllPDFs/Publications/Annual%20Report%202013.pdf

Wateruse Association Desalination Committee. (2010). Seawater Desalination Costs. White Paper. Wateruse Association Desalination Committee. Retrieved 30 July, 2015, from https://www.watereuse.org/sites/default/files/u8/WateReuse_Desal_Cost_White_Paper.pdf

WCED. (1987). *Our common future*. Oxford ; New York: Oxford University Press.

WHO. (2006). Minimum Water Quantity Needed for Domestic Uses. Retrieved 5 July, 2010, from http://www.who.or.id/eng/contents/aceh/wsh/water-quantity.pdf

Wiedmann, T. (2009a). A first empirical comparison of energy Footprints embodied in trade - MRIO versus PLUM. *Ecological Economics, 68*(7), 1975-1990.

Wiedmann, T. (2009b). A review of recent multi-region input-output models used for consumption-based emission and resource accounting. *Ecological Economics, 69*(2), 211-222.

Wollmer, Richard D. (1970). Multicommodity Supply and Transportation networks with Resource Constraints: The Generalised Multicommodity Flow Problem

Memorandum. RM-6143-PR. RAND Corporation. Retrieved 8 Mar, 2012, from http://www.rand.org/pubs/research_memoranda/2009/RM6143.pdf

WRCG Ltd. (2004). DRAFT Water & Sanitary Services Assessments - Hauraki Gulf Islands, Part A Waiheke Island: WRCG, Ltd. (for Auckland City Council).

Wujkowski, Peter. (2004). *Characterisation of a fractured bedrock aquifer, Waiheke Island, New Zealand.* (Thesis (MSc), Geology)--University of Auckland, 2004.

Yates, M. V. (1985). Septic-Tank Density and Groundwater Contamination. *Ground Water, 23*(5), 586-591.

Yu, Zita L.T., DeShazo, J.R., Stenstrom, Michael K., & Cohen, Yoram. (2014). Cost-Benefit Analysis of Onsite Residential Graywater Recycling – A Case Study: the City of Los Angeles.

University of California, Los Angeles. Retrieved 28 July, 2015, from http://innovation.luskin.ucla.edu/sites/default/files/Cost-Benefit%20Analysis%20of%20Onsite%20Residential%20Graywater%20Recycling.pdf

Zhang, C., & Anadon, L. D. (2014). A multi-regional input-output analysis of domestic virtual water trade and provincial water footprint in China. *Ecological Economics, 100*, 159-172.

Zhang, Changkuan, Tang, Hongwu, & Park, Dooho. (2009). The Economic Impacts of Water Shortage During a Drought in Korea: Using Intraregional I-O Analysis *Advances in Water Resources and Hydraulic Engineering* (pp. 326-332): Springer Berlin Heidelberg.

Zhang, Y., Chen, D., Chen, L., & Ashbolt, S. (2009). Potential for rainwater use in high-rise buildings in Australian cities. *Journal of Environmental Management, 91*(1), 222-226.

Zhou, Yuan, & Tol, Richard S. J. (2004). Implications of desalination for water resources in China — an economic perspective. *Desalination, 164*(3), 225-240. doi: http://dx.doi.org/10.1016/S0011-9164(04)00191-2

Zou, Y., Wang, S., Mizunoya, T., Yabar, H., & Higano, Y. (2014). Research on environmental tax with emphasis on developing renewable energy in Beijing, China. *Journal of Sustainable Development, 7*(2), 78-88. doi: 10.5539/jsd.v7n2p78